The ontogeny and heterogeneity of Fcγ receptor bearing cells in the human placenta and fetal membranes.

by

Nicholas Alexander Bright.

A thesis submitted for the degree of Doctor of Philosophy at the University of Leicester.

Department of Pre-Clinical Sciences,
Faculty of Medicine,
University of Leicester,
University Road,
Leicester, LE1 9HN.

June 1994.

UMI Number: U540874

UMI U540874

ProQuest LLC
789 East Eisenhower Parkway
P.O. Box 1346
Ann Arbor, MI 48106-1346

DEDICATION.

I dedicate this thesis to my mother, Mrs. J. A. Goodchild, and father, Mr. W. Bright, who simply asked me to 'do my best' in education. I also dedicate this work to Miss Katie M^{C}Allister whose love got me through it.

DECLARATION.

I declare that all the work recorded in this thesis is original unless otherwise acknowledged in the text. None of the work has been submitted for another degree in this, or any other, University.

Signed.

Nicholas Bright

Date.

1/06/94.

ACKNOWLEDGEMENTS.

CONTENTS.

CHAPTER 3: Clathrin.

CHAPTER 4: Immunoglobulin G.

CHAPTER 5: Fcγ receptors.

CHAPTER 6: Ultrastructural immunocytochemistry.

CHAPTER 7: General Discussion

ABSTRACT.

The human fetus is donated passive immunity, via the placenta, in the form of maternal IgG class antibodies. This provides protection against pathogens while the fetus is immunologically immature.

Immunocytochemistry has been performed on placental tissues to localise endogenous IgG and three subtypes of IgG receptor designated FcγRI (CD64), FcγRII (CDw32) and FcγRIII (CD16). Ultrastructural immunocytochemistry has been used to investigate the subcellular distribution of IgG.

FcγRI is expressed by mesenchymal cells of term and first trimester placentae. FcγRII is expressed by endothelial cells and FcγRIII is expressed by syncytiotrophoblast. Endogenous IgG is restricted to the syncytiotrophoblast in first trimester villi indicating that transport is inhibited in early stages of gestation. At term IgG is associated with extracellular matrix, serum, endothelial cells, mesenchymal cells and syncytiotrophoblast suggesting that it is efficiently transported across the trophoblast. Ultrastructural observations of IgG distribution indicate that it is taken up by receptor-mediated endocytosis into the syncytiotrophoblast and reaches an endosome-like compartment.

In term amniochorion FcγRI, FcγRII and FcγRIII are expressed by leucocytes in the maternal decidua and heterogeneous populations of mesenchymal cells in the fetal connective tissues suggesting that they possess an immunoregulatory role. Endogenous IgG is restricted to the extracellular matrix and cells possessing Fcγ receptors. Cytotrophoblast and amniotic epithelial cells, which do not possess Fcγ receptors, contain no endogenous antibodies.

The hypothesis is proposed that cytotrophoblast cells are a barrier to IgG transmission across the placenta. This accounts for the paradox that there are low levels of transport in the first trimester when the syncytiotrophoblast expresses Fcγ receptors. Cytotrophoblast cells form an almost continuous layer underlying the syncytiotrophoblast in the first trimester which becomes attenuated as the placenta matures. Furthermore, IgG may diffuse non-specifically between cytotrophoblast cells of the amniochorion and thus contribute to the acquisition of passive immunity. These data suggest that IgG is transmitted across the vascular system of the placenta and is not acquired via amniotic fluid.

CHAPTER 1: General Introduction.

GENERAL INTRODUCTION.

The human placenta is a versatile organ that is capable of performing a diversity of biological functions which sustain and protect the developing fetus. In addition to transporting water and nutrients to the fetus the placenta is capable of removing waste products and of gaseous exchange. The placenta also secretes steroid (Ryan, 1959; Zander, 1964) and peptide (Jones et. al., 1943; Midgely and Pierce, 1962) hormones responsible for the maintenance of pregnancy. A further, vitally important role of the placenta is to maintain the immunological integrity of the fetus. The aim of the work presented in this thesis is to investigate the mechanism by which maternal passive immune IgG is acquired by the human fetus.

1.1 The acquisition of passive immunity by the fetus: a review.

The human fetus is protected against deleterious infectious agents by a number of mechanisms. Immunological integrity is contributed to by an intact placental barrier, by the fetal membranes and enclosed amniotic fluid, and by its own successively developing immunocompetance. Furthermore, *in utero* the human fetus is donated maternal passive immunity. The newborn is suddenly exposed to many new antigens and its own immune system usually begins to synthesize antibodies after birth. The immature immune system of the infant is compensated for by maternally derived, transplacentally transmitted, IgG class antibodies directed against currently prevalent pathogens (Figure 1.1). Subsequently, other immunoglobulin classes in colostrum reinforce protection after birth (Nevard et. al., 1990).
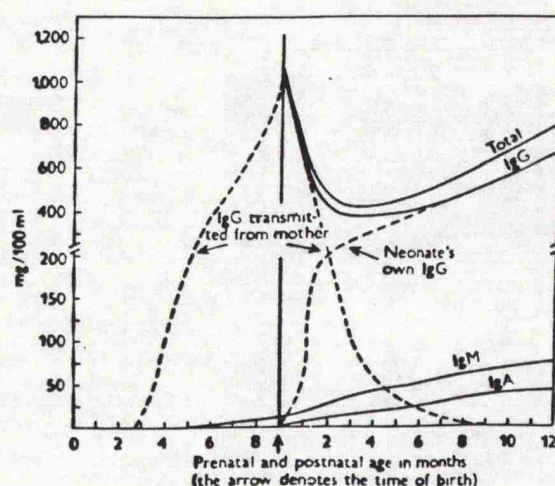
Figure 1.1. Serum immunoglobulin (IgG, IgM and IgA) levels in the human fetus and infants up to the age of 1 year (from Stiehm, 1975). Note that IgG is the only transplacentally transmitted antibody class.

Close attention will be paid to the mechanism and kinetics of the transplacental transmission of IgG molecules since it is one of the vitally important defence mechanisms ensuring that the fetus is provided with adequate antibody immunity in the critical postnatal period.

1.1.1 Historical aspects.

It is well established clinical experience in paediatrics that certain infections, such as measles, chickenpox and hepatitis A, seldom occur in infants aged up to 6 months; and when scarlet fever and diphtheria were common childhood diseases, they were likewise less frequent during the first months of life. Conversely, infections caused by staphylococci, pathogenic strains of E. coli and certain respiratory viruses are both commoner and severer in the postnatal period than in older children. The differences in the susceptibility of newborn and older infants to these infections are determined by the type of immunoglobulins which are formed by the mother in response to these pathogens. The decisive factor is whether these immunoglobulins belong to the IgG class since these are capable of crossing the placental barrier.

Antibodies to influenza virus (Mantyjarvi et. al., 1970), small pox (Kempe and Benenson, 1953), diphtheria antitoxin (Neill et. al., 1932; Barr et. al., 1949; Osborn et. al., 1952) and tetanus antitoxin (Ten Broek and Bauer, 1923; Chandra, 1976) have all been detected in fetal serum. Many studies demonstrate that this humoral immunity is derived passively, that is, of maternal origin. Good and Zak (1956) documented the finding that a child born of an agammaglobulinaemic mother was also agammaglobulinaemic at birth and during the neonatal period. However, by the second month the child was capable of synthesizing its own gammaglobulins since it had not inherited its mothers genetic defect. These authors also noted that in areas of high endemic rates of infectious diseases that infants have elevated immunoglobulin levels at birth. In a further study these authors were able to correlate differences in concentrations between pairs of maternal and cord sera (Zak and Good, 1959) whilst Grubb and Laurell (1956) and Linnet-Jepson et. al. (1958) demonstrated that allotypes of IgG in maternal and newborn serum are identical. More recently, convincing evidence has been contributed by Sorensen et. al. (1984) who demonstrated that cord-blood levels of IgG were above the expected low levels when hypogammaglobulinaemic mothers were treated intravenously with immune globulin during pregnancy.

1.1.2 Transmission of IgG subclasses.

Immunoglobulins belong to one of 5 different structural classes: Immunoglobulin G (IgG), IgA, IgD, IgE and IgM. However, IgA (Allansmith and Buell, 1964; Fulginiti et. al., 1966; Stiehm and Fudenberg, 1966), IgD (Leslie and Swate, 1972), IgE (Ishizaka and Ishizaka, 1967) and IgM (Franklin and Kunkel, 1958; Stiehm and Fudenberg, 1966; Usategui-Gomez et. al., 1967) are only found in trace amounts in fetal cord serum and Loke (1978) attributes this to low levels of fetal synthesis. In contrast, the concentration of IgG in cord serum is often up to twice the concentration found in maternal serum (Figure 1.2; Pitcher-Wilmott et. al., 1980; Kohler and Farr, 1966; Virella et. al., 1972) which indicates that IgG is actively transported across the human placenta (Gitlin et. al., 1964b; Kohler and Farr, 1966; Allansmith et. al., 1968). Active transport of immunoglobulin across the placenta has also been demonstrated in rhesus monkeys. Bangham et. al. (1958) showed that the transport of immunoglobulins exceeded that of albumin by 15-20 times, despite the fact that the immunoglobulin molecule is twice the molecular weight of albumin.
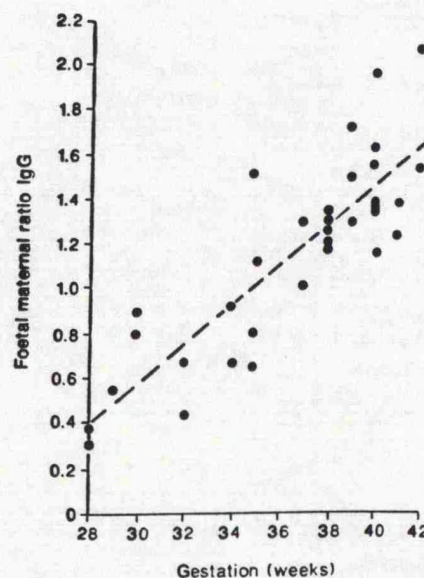
Figure 1.2. The transfer of IgG across the human placenta. The ratio of fetal to maternal IgG is plotted against the period of gestation. Note that beyond 36 weeks of gestation there is a greater concentration of IgG in fetal blood which indicates that active transport occurs against a concentration gradient (from Pitcher-Wilmott et. al., 1980).

The immunoglobulin G molecule is composed of four peptide chains, two light and two heavy, linked by intra and interchain disulphide bonds. The IgG class of molecule may further be divided into subclasses, IgG_1, IgG_2, IgG_3 and IgG_4, based upon structural heterogeneity of the heavy peptide chains (Grey and Kunkel, 1964; Terry and Fahey, 1964a; 1964b).

All four IgG subclasses are transported across the placenta although they are transported to different degrees. The majority of IgG transported at 16 weeks of gestation is IgG_1, but by 22 weeks of gestation all subclasses cross the placenta, although the transmission of IgG_2 appears to be less efficient (Chandra, 1976). Further studies indicate that IgG_2 and IgG_4 are transported less efficiently (Wang et. al., 1970; Hay et. al., 1971; Virella et. al., 1972) and evidence that IgG_2 in particular is discriminated against was provided by Pitcher-Wilmott et. al. (1980). Data from Morell et. al. (1970) implies that the low levels of IgG_2 are not a consequence of different rates of catabolism since IgG_3, in fact, has the shortest half-life.

Transport across the human placenta appears to increase substantially beyond 22 weeks of gestation. Gitlin and Biasucci (1969), on the basis of a detailed study of IgG levels in fetal blood in different phases of gestation, found a sudden (as they describe it 'dramatic') increase in transmission in the 22nd week such that by the 26th week of gestation the IgG level in fetal serum was the same as in maternal serum (Figure 1.3). The authors attributed this phenomenon to a sudden change in the permeability of the placenta for IgG or to the activation of a carrier mechanism of the transport of IgG molecules. These conclusions are in agreement with the earlier results of Vahlquist et. al. (1950) who demonstrated that fetal serum, in the 16th-22nd week of gestation, contained low antistreptolysin titres and that most of these antibodies were transmitted in the latter stages of gestation. In the mouse placenta Morphis and Gitlin (1970) attribute this phenomenon to a rapid increase in the activity of the syncytiotrophoblast rather than an increased rate of non-specific diffusion. Transport across trophoblast in early gestation does not appear to be rate-limited by a lack of receptors specific for IgG (Gitlin and Gitlin, 1976).
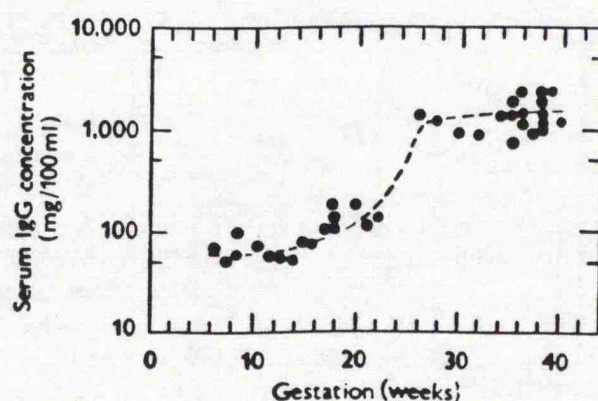
Figure 1.3. IgG levels in human fetal serum at different stages of gestation (from Gitlin and Biasucci, 1969). Note that these authors observed a sudden increase in transport rate beyond 22 weeks of gestation.

1.1.3 Animal models.

Studies on animals have shown that IgG transmission may be mediated in a number of ways (Figure 1.4). Transport of IgG is accomplished via the yolk sac in the rabbit and guinea pig (Brambell, 1966; 1970) whilst in rats and mice this transfer appears to take place prior to birth via the yolk sac and post-natally via the milk. In primates passive immunity is conferred via the chorioallantoic placenta. From these models the initial uptake of IgG appears to be via receptor-mediated endocytosis into micropinocytic vesicles. However, the precise ultrastructural route subsequently taken by the IgG during transcytosis has not been determined.
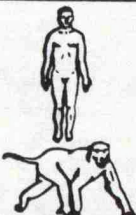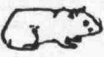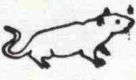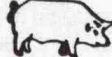
	Before Birth	After Birth
	chorioallantoic placenta	
	chorioallantoic placenta	
	yolk sac	
	yolk sac	
	yolk sac	neonatal small intestine
	yolk sac	neonatal small intestine
		neonatal small intestine
		neonatal small intestine
		neonatal small intestine
		neonatal small intestine

Figure 1.4. Schematic illustration demonstrating the various methods of passive immune IgG transfer. The different species employ the chorioallantoic or yolk sac placenta prior to birth, or the preclosure proximal small intestine after birth (from Nevard et. al., 1990).

A number of models for the transport process have been proposed. Brambell (1966) postulated a simple model based upon the results of animal studies. His hypothesis was that proteins became selectively adsorbed to specific cell surface

receptors on the walls of pinocytic vesicles. These vesicles subsequently pinched off and were transported across the cell. Brambell suggested that as a consequence of the attachment of the protein to the receptor within the vesicle that it was afforded protection from lysosomal degradation. This model proposed that it was the macropinocytic vesicles that were the vehicle for protein transport. However, if this were the case, one would expect to find enzymes associated with the vesicles at the basement membrane where the contents of these vesicles are released. Results from a study of a common proteolytic enzyme, cathepsin D, associated with macropinocytic vesicles showed that the enzyme is not present within or below the basement membrane (Wild, 1976). On the basis of this evidence Wild proposed another model which predicted that selection of specific proteins occurred at the cell surface and involved binding of proteins to receptors over selective areas of the cell. These areas, Wild proposed, then invaginated to form coated micropinocytic vesicles, which subsequently transported IgG to the basal aspect of the cell. Wild suggested that the coating on the cytoplasmic surface of these vesicles prevented them from fusing with lysosomes and thus prevented degradation of the bound ligand. Any protein not bound by a receptor would be pinocytosed into macropinocytic vesicles which would fuse with a lysosome, resulting in the degradation of the enclosed contents.

An alternative model for IgG transport was proposed by Hemmings and Williams (1976). Experimental results obtained using ferritin markers and ^{125}I-labelled IgG failed to reveal any conjugates attached to the periphery of vesicles. Their results indicated the presence of the probe lying free in the cytoplasm and they proposed a transport mechanism in which proteins diffuse freely across the cell cytoplasm.

1.1.4 Transmission of IgG in the human.

Due to the variation in strategy between animals and humans it is difficult to extrapolate the results from animals to the mechanism of maternofetal transmission of immunoglobulins in man. Some studies have been performed on human subjects (Dancis et. al., 1961) but the risk to mother and child prevents extensive experimentation. As a consequence, research upon the mechanism of IgG transmission in man is largely limited to the study of post-delivery placentae.

There are two possible anatomical pathways by which maternal immunological protection may be conferred upon the human fetus. The first is via the vascular system of the chorioallantoic placenta and the second is across the fetal membranes, via the amniotic fluid and, as a consequence of the fetus swallowing

amniotic fluid, across the fetal gut endothelium (Figure 1.5). Steigman and Lipton (1958), Wild (1960), Usategui-Gomez and Stearns (1969), Gadow et. al. (1974) and Monif and Mendenhall (1970) have demonstrated the presence of IgG in amniotic fluid. However, clinical observations by Wasz-Höckert et. al. (1956) indicate that this second pathway is not likely to contribute to IgG transport since infants born with oesophageal atresia, a condition preventing the fetus from swallowing amniotic fluid, did not possess significantly decreased levels of anti-diptheria toxin antibodies. Thus IgG transport in the human, it would appear, is largely accomplished via the vascular system of the placenta, although a small amount, mainly IgG_2, is thought to be transported post-natally via colostrum (Ogra et. al., 1977; Nevard et. al., 1990).
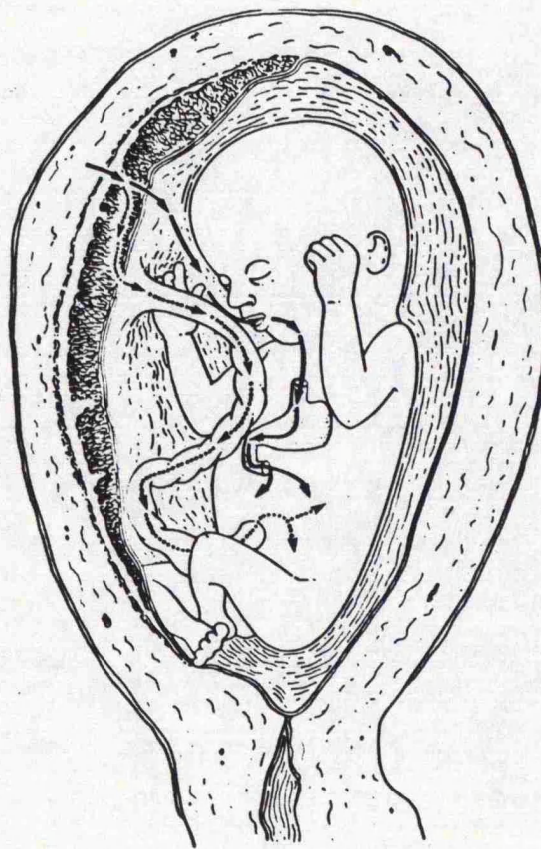
Figure 1.5. Diagram illustrating the alternative theoretical transport routes by which passive immune IgG may reach the human fetus. The route via the amniotic fluid has been shown to be insignificant (from Ockleford and Dearden, 1984).

The latter stages of transport from the connective tissue cores of chorionic villi into the capillary lumen have rarely been investigated. There are alternative theoretical routes. Firstly, IgG may be transported across the endothelial cells surrounding the capillary lumen by a process of transcytosis and secondly IgG may gain access to the fetal circulation by penetration between the endothelial cells. However, autoradiographic uptake studies (Ockleford and Clint, 1980; Dearden and

Ockleford, 1983) demonstrate labelling over the entire circumference of sectioned capillaries. These observations suggest that the intercellular transport route is not likely since you would expect localised strips of silver grains over regions of endothelial cell-cell contacts. Indeed transport between endothelial cells appears to be restricted by tight junctions on the basis of charge and size (Professor J. A. Firth, personal communication). These findings imply that a transcytoplasmic route is responsible for mediating IgG transport from the connective tissue stroma, across the capillary endothelium and into the fetal blood circulation.

1.1.5 The role of the Fc fragment of IgG.

Investigation of the phenomenon of transplacental transport has been undertaken using whole IgG molecules and fragments produced using enzyme digestion. Cleavage of IgG by the enzyme papain yields 3 fragments (Porter, 1959). Two of these are identical and are the univalent antigen-binding or Fab fragments (Fragment antigen binding). The third fragment does not combine with antigen and is known as the Fc fragment (Fragment crystallisable). Brambell assumed that the IgG molecule was bound to a cell surface receptor by its Fc fragment. The role of the Fc fragment of the IgG molecule and of cell surface receptors for this fragment have been the subject of a number of variously conceived studies. Brambell et. al. (1959) and Kaplan et. al. (1965) found that when IgG was digested by the enzyme pepsin, yielding a divalent $F(ab')_2$ fragment, its ability to be transmitted from mother to fetus in rabbits was severely reduced. The latter authors further demonstrated that the Fc fragment of rabbit IgG passed into the rabbit fetus in larger amounts than the intact molecule and, conversely, that transmission of the $F(ab')_2$ fragment was minimal. Still earlier Hartley (1951) had arrived at similar results in human subjects using heterologous (equine) serum digested by pepsin. Börner et. al. (1974) confirmed these results by injecting women in the 40th week of pregnancy with the purified $F(ab')_2$ fragment of IgG containing anti-tetanus toxin antibodies. Parturition took place 32-185 hours after the injection and determination of antibodies in cord serum showed the occurrence of transplacental transmission only in cases in which the mothers were injected with the original, intact IgG preparation. Balfour and Jones (1976) found that radio-iodinated Fc portions of IgG bound to human placental membranes to a much greater extent than Fab fragments.

According to this data, therefore, active transplacental transmission of IgG is mediated by a binding site localised on the Fc fragment of the molecule. Gitlin and his colleagues (Gitlin et. al., 1964a) administered papain digested ^{125}I-labelled Fab and Fc fragments of IgG intravenously to pregnant women and found that the concentration of Fc fragments in fetal blood after delivery was 4-10 times that of the

Fab fragments. However, in further experiments (Gitlin et. al., 1964b) in which relative amounts of catabolism were taken into consideration, they found that both Fc and Fab fragments were transported and concluded that parts of the molecule located on the Fab fragment also participated in the mechanism of transmission. Indeed, further evidence also suggests that there may be receptor sites for more than one region of the immunoglobulin molecule since Gitlin and Gitlin (1976) have demonstrated the binding of Bence-Jones proteins to human placental membranes. These proteins are immunoglobulin light chains and thus lack an Fc fragment.

The discovery and direct demonstration of the existence of receptors for the Fc fragment of IgG was an important step forwards. Matre et. al. (1975) demonstrated that erythrocytes sensitized with IgG (human, rabbit and guinea-pig) adhered firmly to cryostat sections of human placenta whilst cells sensitized with $F(ab')_2$ fragments did not. The binding of IgG-sensitized cells could be blocked completely by adding either intact IgG or its Fc fragment. IgG binding to purified vesicles from syncytiotrophoblast plasma membrane has also been investigated. These purified vesicles were shown to agglutinate IgG-coated erythrocytes: this agglutination was specific since Fab, IgA and IgM did not inhibit agglutination whereas IgG did (Van der Meulen et. al., 1980). These authors further demonstrated that intact IgG_1 and IgG_3 and their fragments inhibited agglutination more efficiently than IgG_2 and IgG_4. IgG from dog, guinea pig, mouse and rabbit was increasingly effective at inhibiting agglutination whereas IgG from sheep, goat and cow did not inhibit which suggests that there may be Fc domain cross-reactivity with these receptors in some species. Jenkinson et. al. (1976) demonstrated receptors for the Fc fragment on human trophoblast and chorion cells. They showed that isolated placenta syncytiotrophoblast and chorion cells formed rosettes in vitro with human erythrocytes (group O Rh^+) with bound anti-D on their surface (EA rosettes). Rosette formation in this system is determined by interaction of the Fc receptor on the surface of the test cell with the Fc part of the antibody molecule bound to the erythrocyte. Balfour and Jones (1976) claim to have demonstrated a single population of membrane receptors which bind all four subclasses of IgG and McNabb et. al. (1976) showed saturable and displaceable binding of labelled IgG on placental membranes. In their experiments IgG_1 and IgG_3 bound with equal affinity, IgG_4 showed less affinity than IgG_1 and IgG_3, and IgG_2 possessed least affinity. These findings correlate with the transport studies in which IgG_2 and IgG_4 were found to be transported less efficiently than the other subclasses of IgG (Wang et. al., 1970; Hay et. al., 1971; Virella et. al., 1972).

Fc receptors for IgG (FcγR) have subsequently been demonstrated on trophoblast cells (Matre and Haugen, 1978), fetal endothelial cells (Matre, 1977;

-11-

Johnson et. al., 1975; 1976; Matre et. al., 1981) and on placental macrophages known as Hofbauer cells (Moskalewski et. al., 1975). It has been suggested that the receptors on these cells may function to prevent immune complexes (formed by the reaction of maternal antibodies with incompatible fetal antigens) from entering the fetal circulation. Thus the fetus is afforded further protection from deleterious maternal antibodies by the placenta. Neizgodka et. al. (1981) have partly characterised a human placental Fc receptor. They isolated a water soluble glycoprotein fraction from human placental membrane using lithium diiodosalicylate. This fraction retained the ability to bind labelled IgG.

Human leucocytes of the immune system have been shown to express three subtypes of receptor on the cell surface that are specific for the Fc region of IgG (see review: Anderson and Looney, 1986). These receptor subtypes designated FcγRI, FcγRII and FcγRIII have different molecular weights and affinities for human complexed and monomeric subclasses on leucocytes. Recently, Kristoffersen et. al. (1990) and Kameda et. al. (1991) have demonstrated the presence of these three subtypes of receptor on cells of the human placenta using a panel of monoclonal antibodies. Their immunohistochemical analyses revealed the presence of FcγRI on Hofbauer cells, FcγRII on Hofbauer cells and the endothelium of term placental vessels and FcγRIII on trophoblast cells. The significance of these receptors is not yet established.

As previously described, it is almost certain that the acquisition of passive immunity by the human fetus is not conferred via the amniotic fluid (Wasz-Höckert et. al., 1956; Gitlin et. al., 1972). Experiments designed to assess the importance of the amniochorion, which surrounds the amniotic fluid, in the immunological protection of the fetus have largely been neglected. Intra-uterine infections are often accompanied by the infiltration of microorganisms and their proliferation in the amniotic fluid. Utilisation of amniocentesis in obstetric practice greatly increases the risk of infection of the amniotic fluid. Furthermore it is evident that the fetal membranes, bearing a large surface area, are in direct juxtaposition with the maternal uterine decidua and are thus likely to be subject to antigenic stimulation.

Amnitoic fluid has been shown to contain IgG (Monif and Mendenhall, 1970; Gadow et. al., 1974; Usategui-Gomez et. al., 1967) of maternal origin as demonstrated by the Gm allotype (Cederqvist et. al., 1972). Binding sites for the Fc fragment of the IgG molecule have been demonstrated in the human amniochorion (Wood et. al., 1983; Stone et. al., 1987). These studies claim to reveal Fcγ binding sites in cells of the amniotic epithelium, the trophoblast layer and 'stromal macrophages' using fluorescein-conjugated IgG on frozen sections of the membrane. However the

subtypes of receptor in this tissue have not been investigated and it is not yet apparent how maternal IgG gains access to the amniotic fluid.

1.1.6 Coated vesicles.

The models suggested for the mechanism of transplacental protein transport indicate that coated vesicles may have an important role, particularly in receptor-mediated uptake. Coated vesicles were first described as mediators of protein transport by Roth and Porter (1964) in the transmission of yolk protein in the mosquito oocyte. Coated vesicles are now known to occur in most cells and it has been shown using one-dimensional peptide mapping that the major component of coated vesicles, the protein clathrin, is highly conserved between several species (Pearse, 1976; 1978). There are now a great many systems in which the evidence indicates that coated vesicles are involved in protein uptake. For example α_2 macroglobulin (Maxfield et. al., 1978), ferritin (King and Enders, 1970), transferrin (Bliel and Bretscher, 1982), asialoglycoprotein (Wall et. al., 1980), low density lipoprotein (Anderson et. al., 1977; 1978), insulin (Pilch et. al., 1983) and Semliki Forest Virus (Marsh and Helenius, 1981) are all internalised into cells after first becoming associated with coated pits.

In some systems coated vesicles mediate the whole of transepithelial protein transport. For example, in neonatal suckling rat jejunum (Rodewald, 1980), rat yolk sac (Huxham and Beck, 1981), rabbit yolk sac (Moxon et. al., 1976) and guinea pig placenta (King and Enders, 1970) coated vesicles have been found in apical, midcytoplasmic and basolateral regions. They have also been found to associate with the Golgi where they may play a part in the transport of secretory proteins.

Further studies have demonstrated that the contents of coated vesicles appear to be delivered to large membrane-bounded structures about 600nm in diameter. These have been termed the receptosome by Willingham and Pastan (1980) and are very similar in morphology to the multivesicular bodies discovered by Martin and Spicer (1973). However, they do not appear to contain lysosomal enzymes (Willingham and Pastan, 1981). The structure of coated pits and vesicles is well documented (see review: Ockleford, 1982). Placental coated vesicles are similar in structure to those isolated from other sources. They have a thickened glycocalyx on their luminal surface and a polygonal lattice of the protein clathrin on their cytoplasmic surface. The size of these vesicles ranges from approximately 60-200nm. Their size is dependent upon the ratio of the number of polygons in the lattice. These are usually five or six-sided (Ockleford et. al., 1977a) but heptagons may occur temporarily during curvature induction (Heuser, 1980). Clathrin is the major protein

component of coated vesicles and has a molecular weight of 180 000. Other proteins with molecular weights of 100 000, 45 000, and 32 000 have also been isolated (Ockleford and Whyte, 1977; Pearse, 1978). In other systems these molecules have been shown to be associated with trimers of clathrin to form an 8.4S lattice subunit. The trimeric subunit is known as the triskelion (Ungewickell and Branton, 1981). Each triskelion is apparently associated with two different types of light chain structures.

Because coated vesicles are responsible for the transport of many different molecules it is not surprising that they contain more than one type of molecule. Huxham (1982) carried out a dual-labelling study in rat yolk sac, using IgG and ferritin conjugated to different sized particles of colloidal gold. He found both sizes of colloidal gold probe located in the same coated vesicle. In neonatal rat jejunum, IgG binds to Fc receptors on the luminal side of the enterocyte (pH 6-6.5). Receptors are localised in coated pits and are internalised in coated vesicles (Rodewald, 1976; 1980). Vesicle contents are transferred rapidly through an endosome-like compartment (pH 4.8-6) and released at the basolateral surface (pH 7.4). The affinity of this receptor (Ka = $2x10^7M^{-1}$) is maintained at pH 4.8-6 and lost at pH 7.4, which may be a factor contributing to the binding and subsequent release of the ligand (Jones and Waldmann, 1972).

In humans, a similar receptor-mediated uptake into coated vesicles may mediate transmission across the syncytiotrophoblast. Ockleford (1976) and Ockleford and Whyte (1977) demonstrated large numbers of coated vesicles located at the apical cell surface. Furthermore, Lin (1980) discovered IgG in micropinocytotic vesicles, using immunoperoxidase, which correlated in size with coated vesicles. Ockleford and Clint (1980) identified tritiated IgG in an isolated fraction enriched in coated vesicles and, using electrophoresis, Pearse (1982) identified IgG 'heavy chains' in a highly purified sample of coated vesicles from human placenta. Booth and Wilson (1981) were not able to identify IgG in their isolates but these were mainly coated vesicle lattices. It is not clear if a subpopulation of coated vesicles mediate transport to the basolateral surface as asserted by King (1982a) since they are observed more rarely deep to the maternally-orientated surface (Ockleford, 1976). Studies with radiolabelled IgG by Ockleford and Dearden (1984) indicated that coated vesicles discharge some contents into large endosome-like compartments. The antibody may then be uncoupled from its receptor, intracellularly sorted or the receptor recycled. Observations by Lin (1980) suggest that it is from these compartments that IgG is released onto the basolateral side although this latter stage has not been visualised ultrastructurally.

1.2 The pathology of IgG transport.

A pertinent reason for investigating the transmission of immunoglobulins is that, since receptors recognise the Fc domain of the IgG molecule, the transport machinery is not capable of discriminating between helpful and deleterious antibodies. It is conceivable that maternal antibodies, raised against allotypic fetal antigens, are transported across the placenta. This has profound consequences causing fetal and neonatal diseases such as rhesus isoimmunisation (Rote, 1982), systemic lupus erythematosus (Bresnihahn et. al., 1977), thyrotoxicosis (Kitzmiller, 1978), thrombocytopenia (Jones, 1979; Kelton et. al., 1980) and heart block (Scott et. al., 1983).

1.3 Aims.

The aims of this thesis were twofold: i) to discern the anatomical, histological and ultrastructural route by which the extraembryonic membranes confer passive immunity on the human fetus and ii) to investigate the distribution of molecules that may be important in the immunological protection of the developing neonate.

1.4 Experimental strategy.

To achieve these aims the technique of immunocytochemistry was employed to localise endogenous tissue components. The goal of immunocytochemistry, conceived by A. H. Coons et. al. (1941), is to determine the cellular location of biochemically defined antigens. This technique combines a unique mix of biochemistry and immunochemistry, which provide high affinity antibodies, with the field of microscopy (including anatomy, cell biology and pathology) to determine whether a particular target molecule is associated with a certain tissue, cell or organelle (Polak and Van Noorden, 1983; Bullock and Petrusz, 1982, 1983, 1985; Ockleford, 1990).

In this study immunocytochemical techniques were applied to investigate the localisation of endogenous IgG, clathrin and specific receptor molecules for the Fc domain of IgG in the human placenta and fetal membranes from various gestational ages. Furthermore, techniques for reliably conserving the immunological properties of proteins in tissues prepared for electron microscopy have advanced in recent years. The combination of these techniques with antibodies conjugated to electron opaque markers such as colloidal gold provide a vehicle for investigating the ultrastructural distribution of antigens (Polak and Varndel, 1984; Roth, 1982;

Griffiths, 1993). This technique was employed to define the ultrastructural localisation of endogenous IgG.

CHAPTER 2: Genesis and structure of the human placenta and fetal membranes.

2.1 INTRODUCTION.

The extraembryonic or fetal membranes are comprised of the chorion, amnion, yolk sac and allantois. These extraembryonic tissues develop from the conceptus but do not form a part of the embryo (with the exception of parts of the yolk sac and allantois). Differentiation of these tissues commences shortly after the oocyte is fertilised giving rise to a zygote.
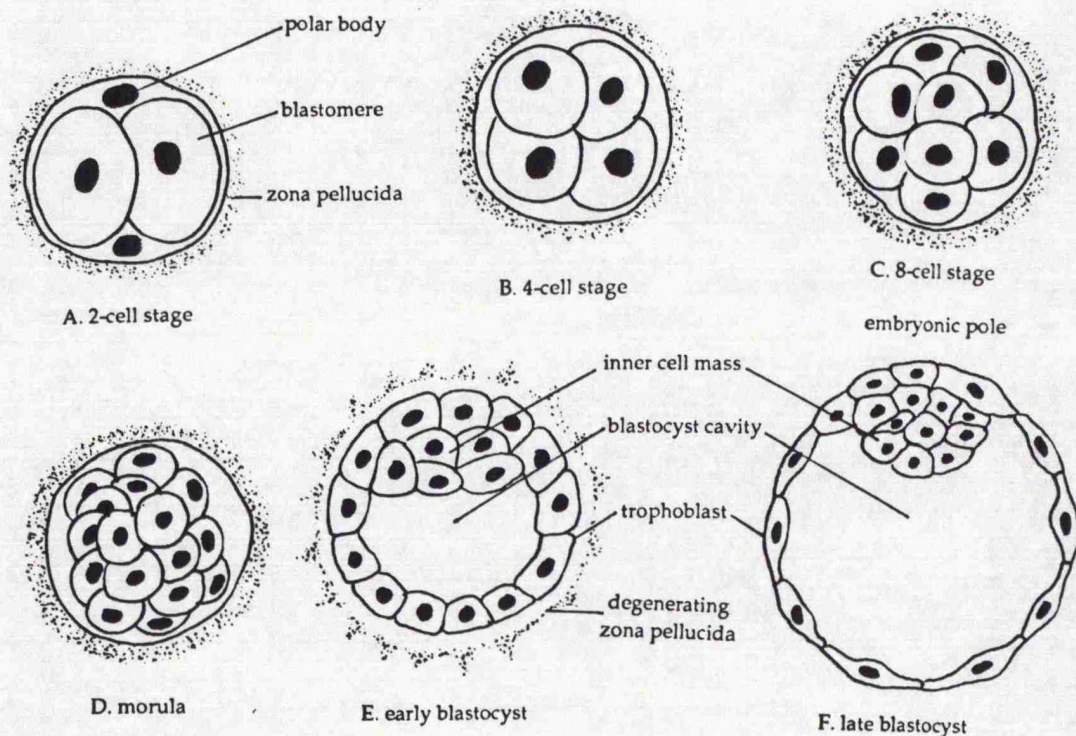
Figure 2.1. Diagram illustrating the cleavage of the zygote and formation of the blastocyst. A to D represent various stages of cleavage to form a compact ball of cells termed the morula. E and F demonstrate the blastocyst in which large fluid-filled spaces have coalesced to form the blastocyst cavity. Note that the inner cell mass, which develops into the embryo, projects into this cavity.

As the zygote passes down the lumen of the oviduct it undergoes a series of mitotic divisions resulting in progressively smaller cells called blastomeres. These subsequently form a ball of 12-16 blastomeres, termed the morula, about three days after fertilisation. At this time the cells of the morula undergo a process called compaction as demonstrated in the mouse (Johnson et. al., 1986; Fleming and Johnson, 1988) whereby they adhere more tightly together making cell boundaries less distinct. These cells then begin to pump fluid from the uterus into cavities between the cells and, as the fluid increases, it separates the cells into two parts: i) an outer layer, the trophoblast which gives rise to part of the placenta and ii) a group of centrally located cells, the inner cell mass, which give rise to the embryo. The fluid

filled spaces soon become continuous to form a single large space called the blastocyst cavity. At this stage of development the conceptus is termed the blastocyst (Boyd and Hamilton, 1970). The inner cell mass at this stage projects into the blastocyst cavity whilst the trophoblast forms the surrounding wall (Figure 2.1).

The blastocyst lies free in the uterine secretions for about two days before the zona pellucida, which surrounds it, degenerates allowing it to attach to the uterine endometrial epithelium. At this point the trophoblast begins to proliferate rapidly and differentiates into two layers: i) an inner cellular layer called the cytotrophoblast layer and ii) an outer layer consisting of a multinucleated syncytium, called the syncytiotrophoblast, in which cytotrophoblast cells have fused and the cell boundaries have disappeared (Figure 2.2). Projections of the syncytiotrophoblast at the embryonic pole penetrate the endometrial epithelium and invade the underlying stroma resulting in a superficially implanted blastocyst by the end of the 1st week of gestation. By the 10th day of gestation the conceptus has become completely embedded in the endometrium and the implantation site in the uterine epithelium has sealed with maternal coagulum. The epithelium overlying the conceptus regenerates resulting in the complete interstitial implantation of the conceptus. At this time cytotrophoblast cells are mitotically active and form new cells that migrate into the increasing mass of the syncytium where they fuse and lose their cell membranes.
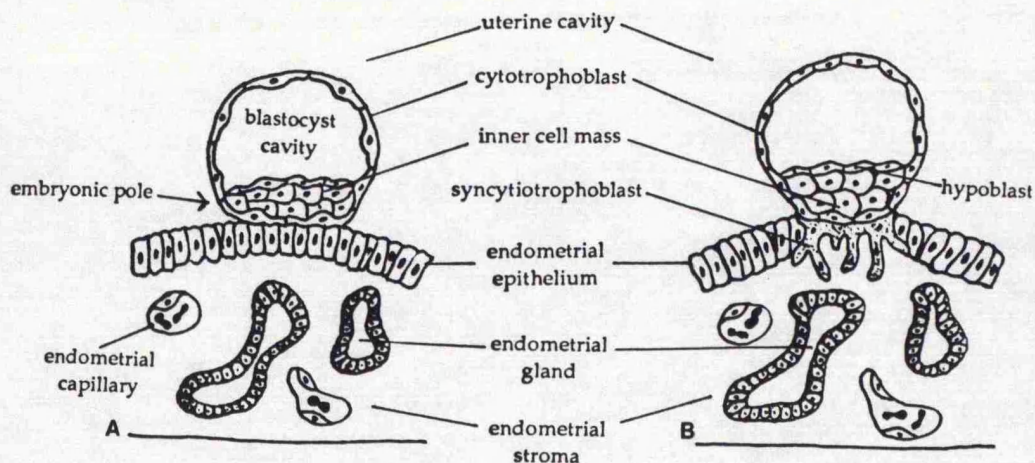
Figure 2.2. Illustration of the early stages of implantation. **A** The trophoblast attaches to the endometrial epithelium at the embryonic pole of the blastocyst. **B** The trophoblast differentiates to form an outer layer of syncytiotrophoblast and an inner cytotrophoblast cellular layer. The syncytiotrophoblast forms projections which invade the endometrial stroma.

Simultaneous with the trophoblastic development, small fluid-filled spaces form between the inner cell mass and the invading trophoblast and by the 8th day of gestation these spaces have coalesced to form a single amniotic cavity (Figure 2.3). As this cavity enlarges it acquires a thin epithelial roof, called the amnion, which

arises from the differentiation of a population of cytotrophoblast cells immediately adjacent to the dorsal aspect of the embryonic germ disc. Hertig (1945) and Hertig et. al. (1956) have described how trophoblast cells in this area differentiate to form amniogenic cells. The epiblast of the developing embryonic disc forms the base of the amniotic cavity. Simultaneously, other cells delaminate from the cytotrophoblast layer and form a thin exocoelomic membrane, often called Heuser's membrane (Figure 2.3, Heuser, 1938; 1932a; 1932b). This membrane is continuous with the hypoblast of the embryonic disc and surrounds a large fluid-filled cavity called the exocoelomic cavity (Hertig and Rock, 1943; 1945) or the primary yolk sac (Hamilton et. al., 1952; 1966). Heuser's membrane consists of a flattened layer of stellate cells of the fibroblast type (Hertig, 1945).
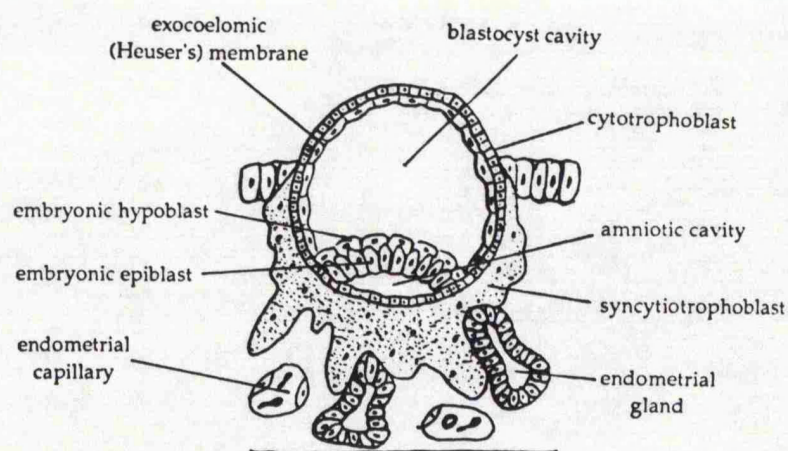
Figure 2.3. Illustration of the implantation of the blastocyst and genesis of the amniotic cavity and exocoelomic membrane. The amniotic cavity forms from a coalition of fluid-filled spaces and is bounded by the amnion and epiblast of the developing embryo. Simultaneously a thin exocoelomic (Heusers') membrane delaminates from the overlying cytotrophoblast layer.

Further delamination from the inner surface of the surrounding trophoblast cells gives rise to a layer of loosely arranged cells, the extraembryonic mesoderm, around the amnion and primary yolk sac (Figure 2.4). This extraembryonic mesoderm increases and, by day 11, fluid filled coelomic spaces are evident within it which rapidly fuse to form the extraembryonic coelom. This fluid-filled cavity surrounds the amnion and yolk sac except where the amnion is attached to the chorion by the connecting stalk. As this extraembryonic coelom forms, the primary yolk sac is reduced in size and a secondary yolk sac forms. The method of development of the secondary yolk sac is in doubt (Hamilton et. al., 1952) but evidence indicates that it is formed by an outgrowth from the portion of the exocoelomic membrane adjacent to the fetus. The coelom splits the extraembryonic mesoderm into two layers i) the extraembryonic somatic (somatopleuric) mesoderm,

underlying the trophoblast and surrounding the amnion and ii) the extraembryonic splanchnic (splanchnopleuric) mesoderm around the yolk sac (Figure 2.4). The extraembryonic somatic mesoderm and the trophoblast together constitute the chorion and form the chorionic sac in which the embryo, amnion and yolk sac are suspended by the connecting stalk. The extraembryonic coelom becomes the chorionic cavity.
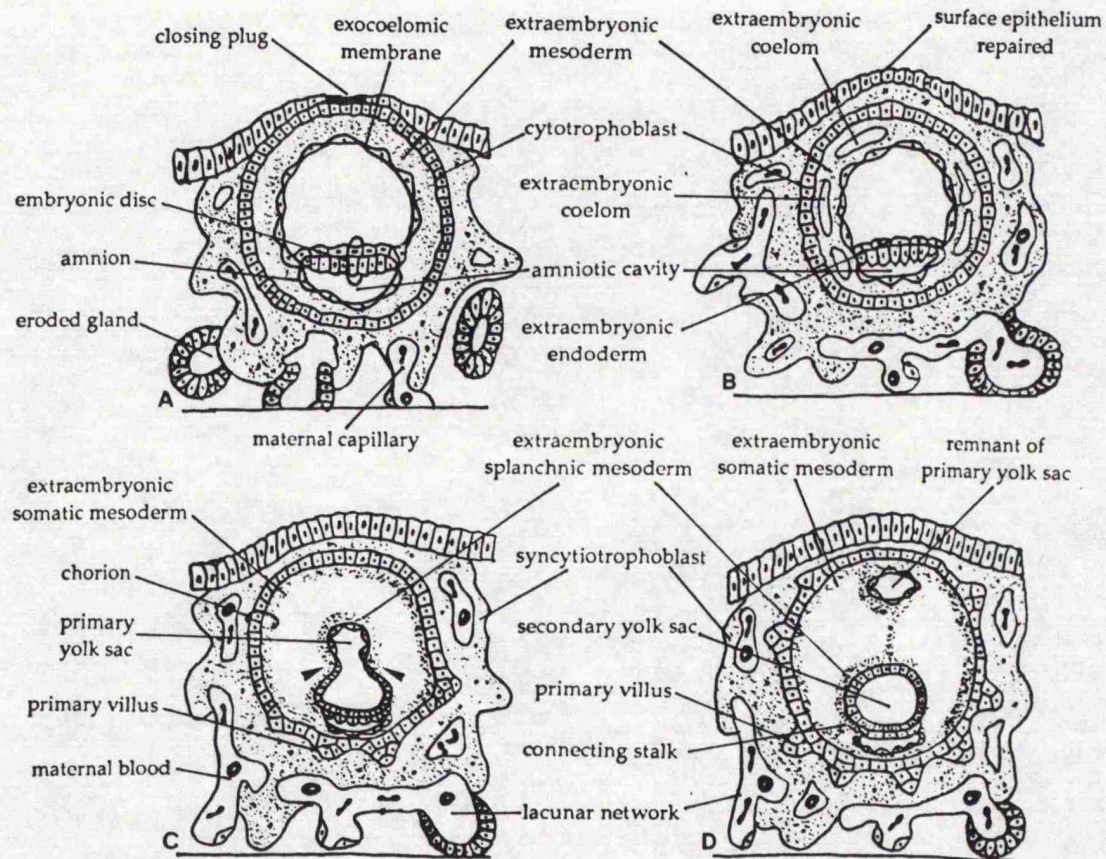
Figure 2.4. Illustration of a partially implanted blastocyst. Note the extensive syncytiotrophoblast which has now eroded maternal blood vessels and endometrial glands to form isolated lacunae and which develop to form the intervillous spaces. **A** Further delamination of the surrounding cytotrophoblast gives rise to the extraembryonic mesoderm surrounding the amnion and primary yolk sac (formerly the blastocyst cavity). **B** Large cavities appear in the extraembryonic mesoderm which soon become continuous to form the extraembryonic coelom. **C** As the extraembryonic coelom forms a small secondary yolk sac develops and the primary yolk sac becomes 'pinched off'. **D** The extraembryonic coelom splits the extraembryonic mesoderm into two layers; extraembryonic somatic mesoderm lining the trophoblast and covering the amnion, and extraembryonic splanchnic mesoderm around the yolk sac.

At around day 9, isolated cavities appear in the syncytiotrophoblast. These become filled with maternal blood from ruptured capillaries and secretions from eroded endometrial glands. Adjacent lacunae fuse to form networks which first

develop at the embryonic pole and progress to form the intervillous spaces of the placenta (Figure 2.4). By day 13 of development the proliferating cytotrophoblast cells form projections into the overlying syncytiotrophoblast and this represents the first stage in the development of chorionic villi (Boyd and Hamilton, 1970). These are termed primary chorionic villi. Shortly after the first occurrence of these primary chorionic villi they begin to branch. By around 15 days of gestation mesenchyme, arising from the proliferating extraembryonic somatopleuric mesoderm of the chorion, invests these villi to form a loose connective tissue core. The villi at this stage are termed secondary chorionic villi and cover the entire surface of the chorion (Figure 2.5). Mesenchymal cells within the villi soon begin to differentiate and condense to form blood capillaries, at which stage they are termed tertiary chorionic villi (Figure 2.5). At around day 21 of development the cytotrophoblast cells of the chorionic villi penetrate the syncytiotrophoblast and join to form a cytotrophoblastic shell which attaches the conceptus to the endometrial tissues (Siegenbeek van Heukelom, 1898; Peters, 1899). Villi that are attached to maternal tissues in this way are called anchoring villi, whilst villi that project into the maternal blood lakes are termed intermediate or terminal villi.
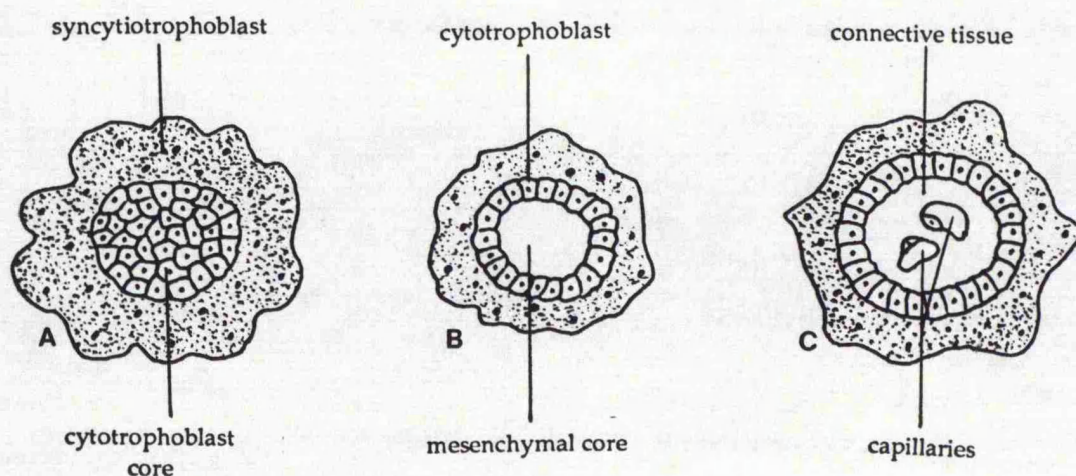
Figure 2.5. The development of chorionic villi. **A** Cytotrophoblast cells proliferate and form projections into the overlying syncytiotrophoblast to form primary chorionic villi (transverse section). **B** Extraembryonic mesenchyme invests the primary chorionic villi to form the loose connective tissue core associated with secondary chorionic villi (transverse section). **C** Mesenchymal cells within the villi differentiate and form fetal capillaries, at which stage they are termed tertiary chorionic villi (transverse section).

The term 'decidua' is applied to the functional layer of the maternal endometrium indicating that it is shed at parturition. Three regions of the decidua

are identified according to their location with respect to the implantation site. The part that underlies the conceptus subsequently forms the maternal component of the placenta and is termed the decidua basalis. The superficial portion overlying the conceptus after implantation is the decidua capsularis and all of the remaining uterine endometrium represents the decidua parietalis.
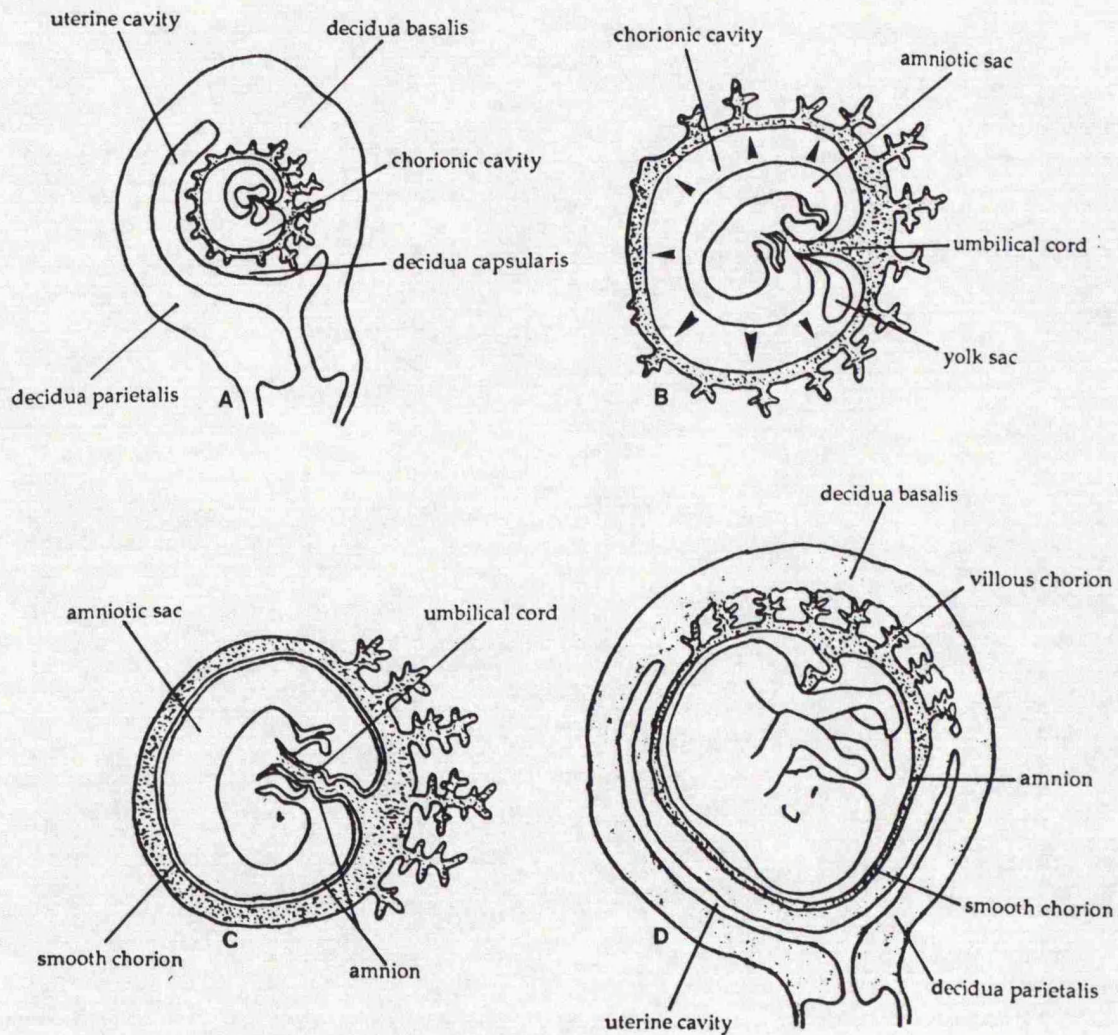
Figure 2.6. Illustration of the expanding chorionic sac and amniotic cavity. **A** Sagittal section showing the relation of the amniotic cavity, chorionic sac, decidua capsularis and decidua parietalis. **B** As development proceeds, the amnion enlarges (arrows) within the chorionic sac. **C** Eventually the amnion fuses with the chorion to form the amniochorion membrane and obliterates the chorionic cavity. **D** The amniochorion and associated decidua capsularis eventually fuse with the decidua parietalis and obliterates the uterine lumen.

Until around the 8th week of pregnancy, villi cover the entire surface of the conceptus. As it grows, however, the villi associated with the decidua capsularis regress over a large area resulting in an area known as the chorion laeve (smooth chorion) which contains only small atrophic villi. Concurrently, the villi associated with the decidua basalis increase in number, branch profusely and enlarge to form the villous chorion or chorion frondosum (leafy chorion). As the conceptus enlarges the decidua capsularis bulges into the uterine lumen. Eventually the decidua capsularis fuses with the decidua parietalis thus obliterating the uterine lumen (Figure 2.6). The amniotic sac enlarges somewhat faster than the chorionic sac with its associated decidua and soon fuses to form the amniochorionic membrane. It is this membrane that ruptures prior to parturition.

The chorionic villi of the placental disc undergo transitional changes as the period of gestation proceeds. As pregnancy advances, the trophoblast surrounding the mesenchymal villus core becomes progressively thinner and many capillaries come to lie in close apposition with the trophoblast to facilitate the increased metabolic demands of the fetus. Furthermore, after around 20 weeks of gestation villus cytotrophoblast cells (also known as Langhans cells) no longer form a continuous layer beneath the syncytiotrophoblast. Instead an attenuated population of cytotrophoblast stem cells remain (Figure 2.7). These have been termed residual cells by Panigel and Anh (1963).
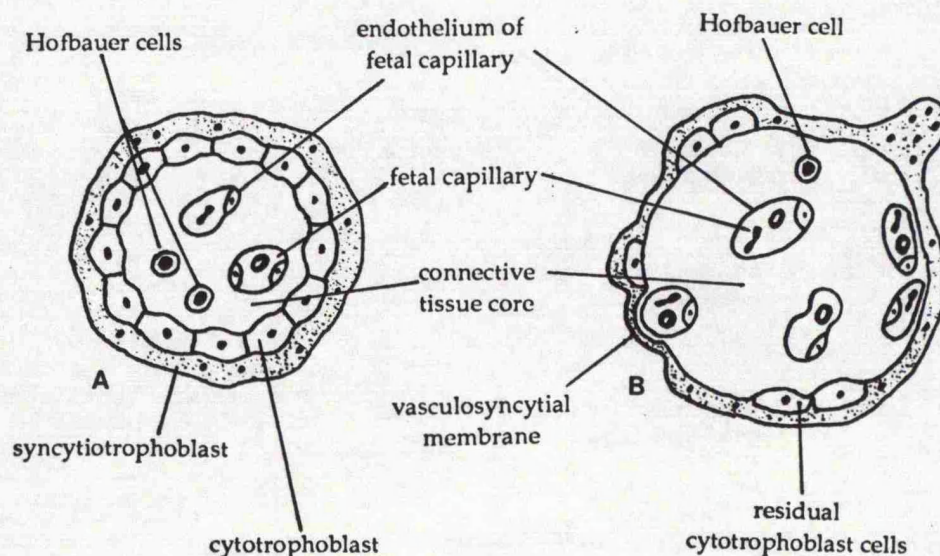
Figure 2.7. Illustration of a transverse section through a 1st trimester (A) and term (B) chorionic villus. Note the peripheral organisation of the blood vessels forming the so-called vasculosyncytial membrane and the attenuated layer of cytotrophoblast cells beneath the syncytium at term.

2.1.1 Hofbauer cells.

The presence of large, isolated macrophage cells in the chorionic villi has been established for more than a century. However, following a comprehensive study of Hofbauer in 1905 these cells have become known as 'Hofbauer cells' and may be identified in all areas of the chorionic and amniotic mesoderm (Boyd and Hamilton, 1970; Bourne, 1962). These cells are more common in immature than term placentae.

The most likely origin of the Hofbauer cell is from the chorionic mesoderm and they may be differentiated from the fibroblasts of both the amnion and chorion (Wynn, 1967). Nuclear sex staining shows that they are of fetal origin and, therefore, do not migrate from the uterine wall (Bourne, 1962; Wynn, 1967). It is now widely accepted that these cells are phagocytic and have macrophage function. However, Boyd and Hamilton (1970) are of the opinion that Hofbauer cells may also play a nutritional role.

2.1.2 The amniochorion.

The amnion of a human embryo of 5-6mm in size is seen to comprise 3 layers (Schwarzacher, 1960; Hoyes, 1970). The innermost layer towards the amniotic cavity is the amniotic epithelium. Outside this is a layer of connective tissue containing a few cells, some of which may be likened to tissue macrophages (Hofbauer cells). The outermost layer separating the amnion from the extraembryonic coelom consists of a single layer of flattened cells. These cells which stem from the extraembryonic mesenchyme, are known as mesothelium (Grosser, 1927; Schwarzacher, 1960). In later stages of development the connective tissue is more pronounced and possesses fibroblast cells of typical morphology and the mesothelium disappears when the amnion and chorion start to unite (Schwarzacher, 1960).

As development proceeds the amniotic cavity grows and its surrounding membrane, the amnion, eventually fuses with the chorion to obliterate the chorionic cavity. Thus, by term, the human fetal membranes are comprised of a fusion of the amnion, chorion laeve and maternal decidual tissues. Bourne (1960; 1962) identified 5 distinct histological layers associated with the amnion.

a) The epithelium.

The amniotic epithelium is composed of simple cuboidal non-ciliated cells with centrally located nuclei. These cells possess apical microvilli and basal processes. Contacts between amniotic epithelial cells become more numerous as

development proceeds, cell processes invaginate into adjacent cells (interdigitation) and desmosomes form connections with neighbouring cells. After the 16th week of development hemidesmosomes form at the base of the cells to form an intimate contact with the basal lamina (Hempel, 1972). This epithelium is generally considered to be involved in amniotic fluid homeostasis.

Many researchers have observed differences in the affinity for stain of the amniotic epithelial cells. Lanzavecchia and Morano (1959), Wynn and French (1968) and Schmidt (1965) have drawn attention to these differences. However, Thomas (1965) undertook a more detailed analysis of this phenomenon. This divided the amniotic epithelial cells into two types on the basis of the different structure and arrangement of the organelles and cytoskeleton. Golgi-type cells are characterised by a well developed rough endoplasmic reticulum (rER) and Golgi apparatus. Mitochondria are frequently observed and there are many vesicles. Furthermore, lysosomes and multivesicular bodies are also found in the cytoplasm (Hempel, 1972) and thus Thomas asserted that these cells have secretory function. Schmidt (1992) recently designated these as type I cells. Fibrillary type cells are electron dense and contain an abundance of cytoskeletal filaments. This type of cell, which occurs more frequently than the Golgi type, possesses a Golgi apparatus which is sparsely developed and is considered to be absorbent. Schmidt (1992) has designated these as type II cells.

b) The basement membrane.

The amniotic epithelial cells rest upon a narrow band or reticular tissue on which it is firmly adherent. Schmidt (1992) has recently designated this basement membrane as 'basement membrane 1'. It consists of an 80-100nm thick lamina densa protruding between the basal processes of the amniotic epithelial cells and a thin lamina lucida between the plasmalemma and the lamina densa. It is not known at what time this structure forms but the lamina densa probably develops at a very early stage as a product of amniotic epithelial cells.

c) The compact layer.

The compact layer is a dense acellular connective tissue layer which lies beneath the basement membrane and accounts for most of the strength of the amnion (Bourne, 1962; Malak et. al., 1993). The high tensile strength of this layer (Klima et. al., 1989) is apparently due to the parallel arrangement of the collagen fibres whose structure within the compact layer is not interrupted by embedded cells.

d) The fibroblast layer.

The fibroblast layer represents the main thickness of the amnion and is composed of fibroblast cells embedded in a meshwork of extracellular matrix fibres. Mesenchymal cells are responsible for the formation of the fibrillary meshwork of the amniotic connective tissue. These cells are elongated with a spindle-shaped nucleus, have abundant rough endoplasmic reticulum and free ribosomes, pronounced Golgi apparatus and large accumulations of glycogen (Hoyes, 1970). Bautzmann and Schröder (1955) have described the morphology of the amniotic connective tissue of an 11mm embryo. In this fusiform cells predominate and arrange themselves in unidirectional patterns, apparently in response to tensile stresses. The fibrous meshwork forms according to this cell pattern. Initially fibroblasts extend to just under the basal membrane but by term the fibroblast cells are distanced from the basement membrane by the acellular compact layer. Bautzmann and Schröder conclude that as development proceeds the fibroblasts continually distance themselves from the basal membrane by the steady formation of collagenous fibres.

In early developmental stages histiocytes have already differentiated (Bautzmann and Schröder, 1955; 1958) and settled in the spaces between the fibres. According to these observations, this is a special type of mesenchymal cell that is formed before the amnion and chorion unite or that migrated from the chorion through the extraembryonic coelom into the amniotic connective tissues. These cells, either rounded or with pseudopodia, and with a highly vacuolised cytoplasm, correspond to the placenta's Hofbauer cells. Schmidt (1992) refers to them as 'histiocytic connective tissue cells' and considers them to have differentiated from pluripotent fibroblasts. This is supported by his observations that fibroblast cells from the amnion become Hofbauer cells within 5 days of cell culture.

e) The spongy layer.

Judging by its position, texture and composition the spongy layer is derived from the mesoderm of the extraembryonic coelom which has become compressed between the chorion and the enlarging amnion. The connective tissue meshwork of this layer embeds fibroblasts and a small number of Hofbauer cells.

The second component of the fetal membranes, the chorion, is in contact with the amnion and is in immediate apposition with the maternal decidua capsularis until about the 12th week of gestation. At this time the uterine lumen becomes obliterated and the chorion becomes separated from the decidua parietalis by a

greatly attenuated decidua capsularis. Bourne (1960; 1962) identifies 4 layers associated with the chorion.

f) The cellular layer.

This layer, which is easily demonstrated in early embryos is frequently absent at term. This layer is derived from the extraembryonic somatopleure and is morphologically similar to the fibroblast layer of the amnion. It is related to the allantoic mesenchyme of the connecting stalk, from which the chorionic mesoderm is vascularised (Mossman, 1987).

g) The reticular layer.

The reticular layer forms the main thickness of the chorion and is responsible for most of its strength. It consists of a reticular network of fibres which embed fibroblasts and a diffuse scattering of Hofbauer cells.

h) The pseudo-basement membrane.

This is a narrow band of acellular reticular tissue forming the basement membrane of the trophoblast cells. Bourne ascribed the name 'pseudo-basement membrane' to this tissue to avoid confusion with the amniotic epithelial basement membrane. However, based upon the results of a recent study in which the molecular composition of the basement membranes of this tissue was studied we have renamed this the chorion laeve trophoblast basement membrane (Ockleford et. al., 1993b) since the term 'pseudo' implies that this basement membrane is atypical. Schmidt (1992) applied the term 'basement membrane 2' to this tissue and considers it to be an extension of the extracellular matrix enmeshing the trophoblast cells. However, if this were the case it would not have a different refractive index and it would not be possible to distinguish it as a visibly discrete structure in immunofluorescence studies of basement membrane components (Ockleford et. al., 1993b; Smith and Ockleford, 1994).

i) The trophoblast.

This is a layer of trophoblast cells, 2-10 deep, which rests upon the pseudo-basement membrane and is in intimate contact with the maternal decidua. The remains of chorionic villi from earlier in gestation are frequently observed in this layer. Only cytotrophoblast cells remain in this layer at term and the spaces between them are invested with extracellular matrix material. No syncytiotrophoblast

remains in the chorion laeve at term. It is generally considered that the chorion laeve is little more than a permeable layer (diffusion barrier) for the paraplacental transport of products from the decidual vessels (Schmidt, 1992).

The maternal component of the fetal membranes at term is the decidua. This contains decidual cells, maternal leucocytes and capillaries. A schematic representation of the amniochorion, as suggested by Bourne (1960), is shown in Figure 2.8.
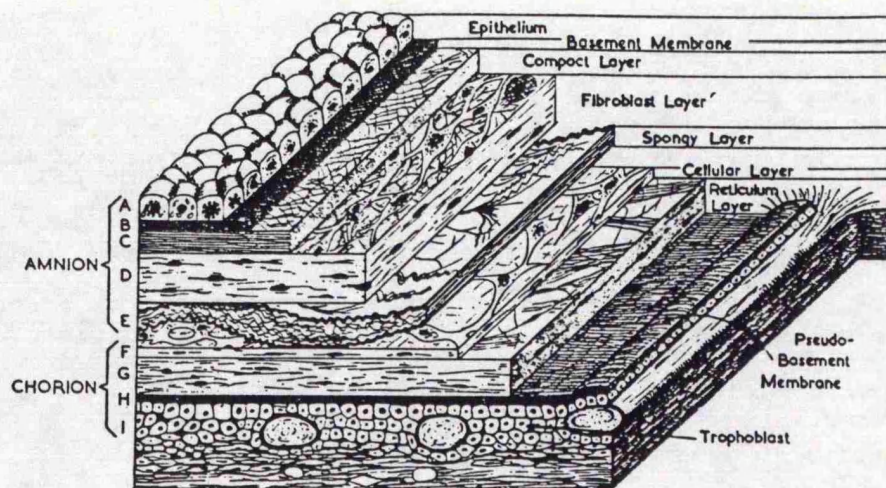
Figure 2.8. Schematic illustration demonstrating the histologically identifiable layers of the amniochorion membrane at term (from Bourne, 1960).

2.1.3 Hydatidiform mole.

Hydatidiform mole is a premalignant form of placenta occurring in about 1 in 1500 pregnancies in the U.K. The tumours are either the malignant choriocarcinoma or the benign invasive mole. Hydatidiform moles have been divided pathologically into two types (Szulman and Surti, 1978). Complete moles are androgenetic in origin (Kajii and Ohama, 1977; Jacobs et. al., 1980) and arise by ejection of the female pronucleus prior to fertilisation. Duplication of a haploid sperm results in a homozygous genome (Lawler et. al., 1979; 1982b) whereas dispermy results in a heterozygous genome (Ohama et. al., 1981). Partial moles are triploid (Szulman and Surti, 1978), have a maternal contribution to the genome and usually arise by dispermy (Jacobs et. al., 1982; Lawler et. al., 1982a).

Complete moles have no fetus and total hydatidiform change whereas partial moles have a range of villi from normal to hyperplastic and the presence of a fetal compartment (Vassilakos et. al., 1977). Hydatidiform moles generally require therapeutic intervention since there is only an aberrant conceptus and the possibility of a resultant choriocarcinoma. Attempts have been made to define neoplastic phases in villi from moles with a view to developing predictive tests for persistent trophoblastic disease. No unique feature was discerned but disruption of the microvillous surface and surface irregularities are more extensive in complete that partial moles. The degree of hydropic swelling is also greater (Ockleford et. al., 1989).

The aim of the work presented in this chapter is to examine the normal anatomical, histological and ultrastructural morphology of the human placenta and fetal membranes using light microscopy (LM), transmission electron microscopy (TEM) and scanning electron microscopy (SEM) techniques.

2.2 MATERIALS AND METHODS.

2.2.1 Tissue collection and examination.

Tissue from the placentae of uncomplicated pregnancies was obtained from the Leicester Royal Infirmary Maternity Hospital or from the Department of Obstetrics and Gynaecology. Throughout these investigations high priority was given to the rapid collection of specimens in an attempt to prevent post-delivery degenerative or autolytic changes to the tissue. Small pieces of the tissue were gently dissected from placentae, fixed and transported to the laboratory. This tissue was subsequently examined using light microscopy, transmission electron microscopy and scanning electron microscopy.

2.2.1.1 First trimester chorionic villi.

The chorionic villi from first trimester placentae were obtained from voluntary, legal terminations of pregnancy at 8-12 weeks of gestation (n=3). The tissue was rinsed briefly with 0.1M Phosphate Buffered Saline (PBS, Appendix I) to remove maternal blood and subsequently processed, within 3 minutes of delivery, for observation using one of the three techniques described hereafter.

2.2.1.2 Term chorionic villi.

Term placentae were obtained from either normal, uncomplicated, vaginal deliveries within 30 minutes of delivery (n=5) or from routine elective Cesarean section within 3 minutes of delivery (n=5). The chorionic villi were gently dissected from the blood lakes of healthy cotyledons, rinsed with 0.1M PBS to remove maternal blood, and processed for examination using one of the three techniques described.

2.2.1.3 Term amniochorion.

The amniochorion was obtained from placentae delivered via uncomplicated routine (n=5) or Cesarean section deliveries (n=5) as described in section 2.2.1.2. The membrane was examined to ensure that the amnion and chorion had not separated, rinsed with 0.1M PBS and processed for microscopy. In addition to the reflected amnion of the fetal membranes, the placental amnion from the chorionic plate of the disc of the placenta and the umbilical amnion from the umbilical cord was examined using these procedures.

2.2.1.4 Hydatidiform mole.

Hydatidiform mole specimens (n=3) were obtained from the Leicester Royal Infirmary Department of Obstetrics and Gynaecology. These moles were diagnosed clinically as partial or complete according to the presence or absence of evidence of a fetus, and histologically by the presence of blood vessels and scalloping of the epithelium. Chorionic villi from these samples were rinsed briefly with 0.1M PBS and processed for microscopy within 3 minutes of delivery.

2.2.2 Light microscopic examination.

Chorionic villi from freshly obtained 1st trimester termination of pregnancy, hydatidiform mole and term Cesarean section were gently dissected with a fine pair of forceps. This tissue was mounted on a Tessovar microscope and photographed using Ilford FP4 film.

For light microscopic examination of term amniochorion each specimen was cut into strips 10mm x 30mm and rolled with the amnion innermost. The tissue rolls were placed vertically in a disposable plastic mould and filled with Tissue-Tek O.C.T. tissue embedding compound (BDH). The tissue was then snap-frozen by immersion of the mould embedding the tissue roll into a Dilvac Dewar flask containing a liquid hexane / solid CO_2 (dry ice) slush at -70°C. It was then transported to the laboratory and transferred to a Lerose (-40°C) freezer where it was stored over dry ice.

Tissue sections were cut using a Leitz cryostat (Leitz Kryostat 1720 Digital). The working temperature of the cabinet was maintained at -23°C, the tissue block at –17°C and the knife at -20°C. Prior to mounting the frozen block above the blade, the disposable plastic mould was removed and the block was trimmed using a razor blade. Transverse cryosections (5-10μm) were cut and melted onto glass slides, mounted with D.P.X. mountant and the coverslip applied.

Tissue samples were examined using Nomarski differential interference contrast microscopy (Allen et. al., 1969) using a Zeiss Axiovert 10 (Zeiss, Oberköchen) inverted microscope with infinity corrected optics. Data was recorded using a Biorad MRC 600 lasersharp confocal attachment coupled to a microcomputer. Photographic images were recorded using a Sony U-P 3000 video printer.

Other small pieces (approximately 2mm^3) of tissue were fixed with 3% glutaraldehyde in 0.1M phosphate buffer (Appendix II) for 3 hours at 20°C, washed

with 0.1M phosphate buffer at 4°C (1 hour, then overnight) and embedded in resin according to the processing schedule described in Appendix III. Semi-thin (0.5-2.0μm) sections were cut using a Reichert OMU-3 or OMU-4 ultramicrotome and floated onto a droplet of distilled water on a glass slide. The sections were then dried down onto the slide using a hot plate at 65°C prior to staining with 1% toluidine blue in a solution of 1% borax (di-sodium tetraborate). The sections were washed with distilled water, dried, mounted with D.P.X. and covered using a Chance Propper Ltd. No. 0 thickness glass coverslip. The sections were examined using a Leitz Diaplan photo-microscope using bright field illumination. Black and white micrographs were taken using Ilford FP4 film.

2.2.3 Transmission electron microscopy (TEM).

Small pieces of tissue (approximately 2mm^3) were fixed for 3 hours at 20°C with 3% glutaraldehyde in 0.1M phosphate buffer, washed with 0.1M phosphate buffer at 4°C (1 hour, then overnight) and processed according to the embedding protocol described in Appendix III (Glauert, 1975). Thin sections (80-100nm; silver to gold in interference colour) of the resin embedded material were cut using a Dupont or Diatome diamond knife mounted on a Reichert OMU-3 or OMU-4 ultramicrotome according to standard procedures (Griffin, 1972). The sections were collected on 200 mesh copper electron microscope grids (Agar Aids) and stained with 10% methanolic uranyl acetate for 30 seconds and lead citrate (Reynolds, 1963) for 6 minutes in an atmosphere of sodium hydroxide. They were then examined using a Jeol 100CX electron microscope at an operating voltage of 80kV. Micrographs were taken according to conventional procedures.

2.2.4 Scanning electron microscopy (SEM).

Small pieces (approximately 5mm^3) of the tissue were fixed for 3 hours at 20°C with 3% glutaraldehyde in 0.1M phosphate buffer, washed (1 hour, then overnight) with 0.1M phosphate buffer at 4°C and processed according to the protocol described in Appendix IV. Specimens were critical point dried (Anderson, 1950), attached to aluminium mounting stubs with Scotch double-sided adhesive tape and coated with approximately 25nm of gold in a Polaron (E5150) sputter coating unit. The coated tissue was then examined using an ISI-60 or ISI DS-130 scanning electron microscope. Micrographs were taken according to conventional procedures.

In addition, studies were performed to examine the three-dimensional structure of the connective tissue cores of the villus specimens and the intercellular architecture of the amniochorion, rather than just examining the surface relief of

these specimens. To do this some specimens were dehydrated to 70% ethanol as described in Appendix IV and transferred to a polystyrene cylinder and frozen with liquid nitrogen according to Humphreys et. al. (1974), Castellucci et. al. (1980) and Castellucci and Kaufmann (1982). Longitudinal and transverse fractures of the tissue specimens were performed with a frozen razor blade and hammer. Care was taken to ensure that the specimen fractured rather than being sliced by the blade. The fractured specimens were returned to 90% ethanol and subsequently processed in the same manner as described in Appendix IV. The specimens were then attached to metal stubs, coated and examined as previously described.

2.3.1 Term placenta.

At term the placenta, together with the umbilical cord and the fetal membranes, constitute the 'afterbirth' which is discharged during the third stage of labour. The human placenta is a flat discoid organ with an approximate diameter of 20cm and a weight of about 500g.

The two sides of the placental disc differed markedly in their appearance. The umbilical cord was attached to the fetal side of the placenta known as the chorionic plate. The cord was normally attached to the centre of the chorionic plate although attachment nearer the edge was not uncommon (battledore placentae). Cotyledonary blood vessels radiated out from the umbilical vessels across the chorionic plate and were covered by a thin layer of chorion. The blood vessels subsequently ramified through the disc of the placenta where they branched to serve the chorionic villi of the placental disc. Overlying the chorionic plate at term was a thin membrane, the amnion. This was continuous with the amniochorion that surrounds the amniotic cavity.

The opposite side of the placental disc (the maternal side), known as the basal plate, attaches to the maternal uterine endometrium. It consisted of a number of lobes, which were divided into one or more cotyledons, and these were separated by grooves known as the placental septae. Each cotyledon possessed a blood supply derived from the blood vessels of the umbilical cord.

2.3.1.1 Light microscopy.

By dissecting the chorionic villi and examining with a Tessovar photomicroscope it was possible to reveal that the main branch or stem villus divides into numerous intermediate and terminal villi (Figure 2.10).

The human placenta comprised 3 layers: trophoblast, connective tissue and capillary endothelium. The histological organisation of the placental chorionic villi at term may be seen in figure 2.14. This is a low-power light micrograph of a semi-thin (0.5μm) section of resin embedded tissue prepared as described in section 2.2.2. There was an outer intensely stained layer of syncytiotrophoblast which surrounded the whole villus. This layer possessed a well-marked microvillus brush border at the cell surface which would project into the maternal blood lakes *in situ*. Many nuclei were observed in this layer and in places these nuclei clumped together to form

syncytial knots. No cell boundaries were observed in the syncytiotrophoblast since the trophoblast cells had fused together to form a true syncytium. This layer stained more densely than the other histological tissue layers due to the large number of nuclei and other dense cytoplasmic granules and inclusions. Examination of the tissue at higher power revealed that there were many large vacuoles and smaller vesicular inclusions present within the syncytiotrophoblast.

Immediately beneath the syncytiotrophoblast was the cytotrophoblast layer which consisted of cells resting upon a basement membrane. In contrast to first trimester placentae, where cytotrophoblast cells formed a complete layer beneath the syncytiotrophoblast, by term this cellular layer became greatly attenuated. As a consequence only a proportionally small number of residual cytotrophoblast stem cells remained and thus the syncytiotrophoblast was often in direct contact with the basement membrane. Cytotrophoblast cells were characteristically less darkly stained than the syncytium. Beneath the cytotrophoblast cells and basement membrane was the mesenchymal core of the villus. At term the core was comprised of extracellular matrix connective tissues, undifferentiated extraembryonic mesenchymal cells, fibroblasts and a small population of tissue macrophages (Hofbauer cells). A prominent feature of term chorionic villi was the rich network of sinusoidal blood capillaries which occupied a large cross-sectional area of the villus core, particularly in terminal villi. At term the blood capillaries were frequently in close apposition to the trophoblast tissue and in such areas the thickness of the overlying trophoblast was often greatly reduced. This arrangement constitutes the vasculosyncytial membrane and minimises the 'barrier' between maternal and fetal blood, thus facilitating the large metabolic demands of the fetus for oxygen.

At term the umbilicus consisted of a mesenchymal core containing blood vessels (two arteries and one vein), undifferentiated mesenchymal cells, fibroblasts and Hofbauer cells. The cord was surrounded by a layer of amnion cells (Figure 2.22) which rested upon a basement membrane and were continuous with the amniotic epithelial cells of the chorionic plate (Figure 2.23) and reflected amnion of the amniochorionic membranes (Figures 2.17-2.21).

2.3.1.2 Transmission electron microscopy (TEM).

Trophoblast.
By examining term human placental chorionic villi using TEM the considerable difference between the syncytiotrophoblast and cytotrophoblast was revealed (Figure 2.33). It was immediately apparent that the syncytiotrophoblast was more electron-dense than the underlying cytotrophoblast cells due to the high

concentrations of organelles and cytoplasmic inclusions in the syncytial cytoplasm. Furthermore the syncytial nuclei were often more electron dense than those of the cytotrophoblast cells, owing to the increased presence of heterochromatin around the margin of the nuclear envelope. Large numbers of nuclear pores were present in the syncytial nuclear envelope.

A further characteristic feature of the syncytiotrophoblast was the apical microvillus brush border and glycocalyx which, *in vivo*, was in intimate contact with maternal blood. At the base of the microvilli membrane invaginations were found. These were smooth membrane pits or they had a cytoplasmic coating of protein - the so-called coated pit. These membrane invaginations contributed to the general vacuolated appearance which was a prominent feature of term syncytiotrophoblast. Large vacuoles were often found close to the syncytial nuclei, the so-called juxtanuclear vacuoles. Some of the larger inclusions appeared to have electron-dense material within them and very dark staining droplets were often found in the syncytial cytoplasm which did not appear to be bounded by a limiting membrane. Mitochondria were also present in the syncytiotrophoblast and contributed further to the electron-density of this layer.

Beneath the syncytiotrophoblast was the cytotrophoblast layer which consisted of individual cells resting upon a basement membrane. In immature placentae (1st trimester) these cells formed an almost continuous layer beneath the syncytiotrophoblast (see Figures 2.13 and 2.30) but by term this had become an attenuated epithelial layer and only a comparatively sparse population of cytotrophoblast stem cells remained. Therefore, by term, large areas of syncytiotrophoblast were in direct apposition with the basement membrane.

The cytotrophoblast cells were more electron lucent than the syncytiotrophoblast and contained fewer organelles. These cells possessed surface microvilli which interdigitated with the syncytiotrophoblast and desmosomes were frequently found in association with these regions of cell contact and between adjacent cytotrophoblast cells. The nuclei of cytotrophoblast cells were often lobulated, pale staining and the chromatin was finely dispersed within the nucleoplasm with the remainder located at the periphery in association with the nuclear envelope. Nucleoli, mitochondria and small amounts of dilated endoplasmic reticulum were present in the cytotrophoblast cells although the ER was less pronounced than in the syncytiotrophoblast. The mitochondria were large, well developed and quite unlike the smaller ones of the syncytium. Cytoplasmic filaments, coated vesicles, coated pits, vacuoles and inclusions containing electron-dense material, glycogen, polyribosomes and a Golgi apparatus were also common

features of cytotrophoblast cells. These cells and the syncytiotrophoblast rested upon a basement membrane and were attached to it by hemi-desmosomes.

Villus core.

Underlying the trophoblastic tissue was the mesenchymal connective tissue core. This consisted of a loose connective tissue stroma of extracellular matrix materials which enmeshed numerous mesenchymal cells, fibroblasts, blood capillaries and some Hofbauer cells. Endothelial cells contained a large amount of glycogen, occasional lipid droplets, numerous pinocytic vesicles, and a marked development of microfilaments and intermediate filaments. These cells, which rested upon a basement membrane, were joined by tight junctions and were not fenestrated. Characteristic features of these cells were the intraluminal projections or flaps which overlap into the vessel lumen.

2.3.1.3 Scanning electron microscopy (SEM).

The branching 'tree-like' structure of the chorionic villi at term was apparent when the tissue was examined using scanning electron microscopy (Figure 2.26). The trophoblastic surface microvilli were clearly revealed. By rapidly freezing the tissue with liquid nitrogen and using a frozen razor blade and hammer to crack the tissue along natural lines of weakness it was possible to obtain three dimensional data regarding the structure of the connective tissue stroma.

2.3.2 First trimester placenta.

First trimester placentae were obtained from voluntary legal terminations of pregnancy by suction curettage and thus were delivered as fragments of tissue.

2.3.2.1 Light microscopy.

Trophoblast.

The branching nature of immature chorionic villi is demonstrated in the Tessovar photomicrograph (Figure 2.9). At this stage of gestation the chorionic villus fronds were considerably less differentiated than those at term.

Examination of semi-thin (0.5μm) sections of resin embedded 1st trimester tissue (Figure 2.13), prepared as described in section 2.2.2, revealed a similar but immature morphology to that of term placentae. In comparison to term placentae the trophoblast surrounding the chorionic villi could be distinguished as a syncytiotrophoblast and an underlying cytotrophoblast layer. However, in 1st

trimester villi there was a palisade of cytotrophoblast cells (Langhans cells) which formed an almost complete and continuous layer beneath the syncytium. Occasionally, however, it was possible to identify syncytiotrophoblast extending between cytotrophoblast cells and contacting the basement membrane. These regions increased in number and extent as gestation advanced.

The syncytiotrophoblast possessed a characteristic apical microvillous brush border and highly vesiculated cytoplasm containing many vacuoles. The syncytial nuclei had a characteristic electron-dense appearance due to the presence of darkly staining heterochromatin. Occasionally a cytotrophoblast cell was observed possessing a more darkly stained cytoplasm than normal whilst still maintaining a limiting membrane. Such intermediate morphology suggested that these cells may have been in the process of forming syncytiotrophoblast.

Villus core.
Beneath the cytotrophoblast cell layer was the mesenchymal connective tissue core which contained mesenchymal cells, fibroblasts and Hofbauer cells. In the villi of early gestational age the stromal fibroblasts possessed extensive processes which converted the stroma into a meshwork of fine filaments. At this stage of gestation the blood vascular system of the placenta was still immature and consisted of a few small evenly distributed vessels which only occasionally underlie the trophoblast and, in contrast to term chorionic villi, did not occupy a large cross-sectional area of the villus core. These vessels often contained nucleated red blood cells. Furthermore it was possible to observe areas of tissue where the mesenchymal cells had condensed locally and had presumably differentiated to form blood vessels.

2.3.2.2 Transmission electron microscopy (TEM).

Examination of first trimester chorionic villi by TEM revealed the presence of many organelles and features demonstrated in term placentae (Figures 2.30-2.32). In the syncytiotrophoblast many vesicles and vacuoles were apparent, including coated pits and vesicles at the apical microvillous membrane. Mitochondria, ER and electron dense inclusions, probably lipid droplets, were also abundant. Cytotrophoblast cells possessed a similar morphology to that described for term tissue including a less electron dense cytoplasm in which mitochondria, ER and other vesicular inclusions were present. The continuous nature of the cytotrophoblast cell layer is indicated in figure 2.30 but occasionally the syncytium may be observed penetrating between cytotrophoblast cells and contacting the basement membrane (Figure 2.31). These cells rested upon a basement membrane in which densely staining osmiphillic granular deposits were frequently observed.

The loose connective tissue stroma underlying the trophoblastic tissue consisted of banded collagenous fibres with 64nm periodicity enmeshing a network of cells. Hofbauer cells were frequently observed in the stroma and fetal capillaries. Blood vessels were often immature and newly forming capillaries could be distinguished by the condensed appearance of several mesenchymal cells. The elongated spindle-shaped mesenchymal cells possessed a small Golgi apparatus, numerous polyribosomes, a characteristic rough dilated ER and many small vesicles and vacuoles. Transmission electron microscopy suggested that the processes of many fibroblasts were continuous in the meshwork resulting in continuity between cells.

Hofbauer cells.

Hofbauer cells of the connective tissue core were between 10-40μm in diameter and were round, oval or polyhedral in shape. Nuclei were rounded and frequently eccentric. A striking characteristic of Hofbauer cells was the degree of vacuolation, the contents of which possessed varying electron-density. The surface of the cell had numerous filopodial processes, often of a bizarre shape. These processes came into intimate contact with projections of fibroblasts but never fused with them. In comparison with fibroblasts of the stroma the absence of a rough ER was striking. Characteristic mitochondria were frequently present and were usually elongated with well-developed cristae. The Golgi apparatus was difficult to identify and not elaborate in structure.

2.3.2.3 Scanning electron microscopy (SEM).

By SEM chorionic villi were seen to possess numerous microvilli (Figures 2.24-2.25). The trophoblast contained many vacuoles but the boundaries between trophoblast cells were not easy to define using the freeze-cracking technique. The connective tissue stroma, however, was well characterised by this technique and was mainly composed of a network of fibrous bundles in which numerous cells were enmeshed. The fibres surrounding the blood vessels were often more densely packed. Small cavities and channels were present within the mesenchymal core and were limited by fibrils and flattened cells. Hofbauer cells appeared round in shape, were characterised by numerous blebs at their surface and, when cross-fractured, by many cytoplasmic vacuoles (Figure 2.25). These cells were found enmeshed in the fibrils or lying in the stromal cavities. Occasionally Hofbauer cells were observed in the lumen of blood vessels.

Irregular shaped and sized compartments were often limited by cytoplasmic processes of stromal cells and collagenous fibrils. In villi fractured in the

longitudinal plane these compartments appeared to be organised into a system of differently sized intercommunicating channels with parallel organisation to the long axis of the villus. There were often openings between channels and the compartments frequently contained Hofbauer cells.

Fetal capillaries were located mostly at the periphery of the villi near to the overlying trophoblast. Larger fetal vessels were usually centrally located in the villus core (Figure 2.24).

2.3.3 Term amniochorion.

Term amniochorion was obtained from elective Cesarean section or routine uncomplicated vaginal delivery. Samples of the amnion overlying the chorionic plate of the placenta and the umbilical cord were also obtained from these deliveries.

2.3.3.1 Light microscopy.

By obtaining a roll of amniochorion and embedding with Tissue Tek OCT embedding compound it was possible to cut 5-10μm transverse sections, mount and observe the tissue with Nomarski differential interference contrast or conventional phase contrast microscopy as described in section 2.2.2. Differences in refractive indices of the component layers in the tissue contributed to either highlights or shadows at the intervening boundaries. Using this technique the distribution of several layers comprising the amniochorion and maternal decidua was discerned (Figure 2.12).

Bright field microscopy of chemically fixed, plastic embedded semi-thin (0.5μm) sectioned material, prepared as described in appendix III and contrasted with 1% toluidine blue, clearly revealed the morphology of the tissue (Figures 2.17-2.21). Several features were discernible at the light microscope level:

Amnion.
The amniotic epithelium was a simple cuboidal epithelium 15-17μm high in transverse section with a convex apical cell surface. The nuclei were round (spherical to lentiform), contained loosely structured chromatin and, normally, one or two nucleoli. The nuclear envelope was often deeply folded and it was evident that the nucleus was always centrally located (Figure 2.19).

The amniotic epithelial cells displayed varying affinities for the stain. A small population of cells from routine term deliveries stained less darkly (Figures 2.17 and

2.20). However, this phenomenon was rarely observed in tissue obtained within minutes of an elective Cesarean section. Furthermore, in tissue samples obtained from routine term vaginal deliveries, there were often 'roads and islands' of degenerated epithelial cells with evidence of nuclear pyknosis or the complete absence of nuclear affinity for stain. These cells had usually relinquished contact with neighbouring cells and exposed the underlying connective tissue. Therefore, it appeared that degenerative changes occurred in a number of epithelial cells between the time of membrane rupture and the time of tissue collection and fixation. These cells could be identified by their reduced affinity for stain.

In the placental amnion of the chorionic plate the amniotic epithelial cells were simple columnar with the nucleus preferentially apical (Figure 2.23). The cells were separated by markedly wider intercellular spaces. Like the amniotic epithelial cells of the reflected amnion these cells showed signs of degenerative changes when delivered routinely at term. The umbilical amniotic epithelium was noticeably different (Figure 2.22). These cells were transitional between the other amnion cells and the epidermis of the early embryo. They formed flattened cells (2-5µm thick) with broad intercellular spaces.

The amniotic epithelial cells rested upon, and interdigitated with, a narrow band of reticular material - the basal lamina. Underlying the basal lamina was the cell free compact layer which possessed little affinity for stain and omnidirectional orientated fibres. Careful examination revealed hour-glass shaped regions of less intense staining with toluidine blue in this layer (Figure 2.21). These structures were subjected to detailed ultrastructural examination. The fibroblast layer was characterised by wavy bundles of fibres with cells interspersed between the bundles. These cells contained an oval, chromatin-poor nucleus with a single nucleolus. The nucleus was often folded along the longitudinal axis. The fibroblast cells possessed numerous cytoplasmic processes and several cells were often in contact with one another.

Chorion.
Two forms of fibroblast cell were distinguished on the basis of structure in the chorionic connective tissue. Adjacent to the amnion these cells were elongated with rod-shaped compact nuclei and extended processes. Adjacent to the trophoblast, however, these cells resembled 'typical' fusiform fibroblasts with pale cytoplasm and an oval, chromatin-poor nucleus. These cells were often in contact with each other and extended processes to the chorion laeve (pseudo) basement membrane that spread out like feet (Figure 2.18).

The chorion laeve basement membrane was easily identified at the light microscope level and penetrated between the cytotrophoblast cells. The trophoblast layer consisted of a cluster of cells 2-8 thick. These were rounded polyhedral or elongated and their size was inconsistent. There were numerous surface protrusions and interconnections and they were enmeshed in extracellular matrix connective tissue. The basal cells near to the chorion laeve basement membrane (basal trophoblast) were closely packed with minimal extracellular matrix but near to the decidua (superficial trophoblast) the cells became separated by abundant extracellular matrix. The remnants of degenerated chorionic villi were often observed in the trophoblast layer. The cytotrophoblast cell nuclei occupied various volumes (for example the polyploid nuclei of giant cells) and possessed various densities of nuclear chromatin.

It was often difficult to establish where the trophoblast layer ended and the maternal decidual layer began. In many instances the trophoblast cells extended deeply into the decidua. The maternally derived decidual layer, that is shed with the placenta at parturition, possessed large elongated decidual cells, rounded maternal leucocytes and blood capillaries (Figure 2.18).

2.3.3.2 Transmission electron microscopy.

Amniotic epithelium.
Examination of amniotic epithelial cells by TEM (Figure 2.38) revealed that they possessed numerous surface microvilli. The lateral cell membranes also contained microvilli, cell contacts, desmosomes and intercellular bridges. Therefore, the intercellular space was extraordinarily complicated.

Intermediate filament bundles were well characterised and could be demonstrated in the apical cytoplasm of the amniotic epithelial cells. Terminal or subterminal association of some of these bundles was noted with classical desmosomes. Some intermediate filaments were also noted in close association with the external surface of the nuclear envelope. Others were noted in the basal region inserting into hemidesmosomal attachments with the basal lamina. The basal regions of the cells possessed numerous highly interdigitating foot-processes that interlocked with the basal lamina.

The cytoplasm of the amniotic epithelial cells demonstrated pronounced vacuolisation, occasionally containing amorphous to granular material of low electron-density. It was apparent that cells which possessed little affinity for stain in semi-thin sections stained with toluidine blue, also contained cytoplasm that was less

electron dense. In these cells it was possible to observe an extensive ER, Golgi, many vesicles and vacuoles, lysosomes and multivesicular bodies. Darker staining bundles of intermediate filaments were easily identified coursing through the cytoplasm and interacting with desmosomes and hemidesmosomes. These features were shared with cells that had relinquished their contacts with neighbouring cells or the basal lamina. The nuclei of these cells was often pyknotic or completely absent and thus they were damaged or dead (Figure 2.38).

The more numerous cells possessing an electron dense cytoplasm contained an abundance of microfilaments and intermediate filaments. The nuclei were rich in heterochromatin. The epithelial cells of the amnion overlying the chorionic plate possessed a similar ultrastructural appearance but these cells possessed an apical nucleus situated in a columnar cell (Figure 2.36). The flattened cells of the umbilical amnion (Figure 2.37) had broad intercellular spaces with protruding microvilli connected by desmosomes.

Connective tissue stroma.
TEM revealed that an 80-100nm thick lamina densa protruded between the basal foot processes of these cells. A thin lamina lucida was found between this and the basal plasmalemma, traversed only at hemi-desmosomes by fine filaments. There was a concomitant increase in the electron density of the lamina densa opposite to the hemi-desmosomes. These anchoring structures did not occur in the trophoblast layer despite the fact that this was a stratified epithelium based upon an apparently normal basal lamina.

Ultrastructural examination of the extracellular matrix material of the amniochorion revealed three main components. Large banded fibres, that showed a periodicity of approximately 64nm, were found in all layers of the fetal membranes. In the compact layer of the amnion (Figure 2.38) they formed an extensive network where they were organised mainly parallel to the amniotic epithelium. In the reticular layer of the chorion (Figure 2.39) they were orientated in various directions. No banded fibres were observed in the intercellular spaces of the trophoblast cells but they were present between the trophoblast cells and decidual cells where the latter extended into the trophoblast layer. These fibres formed the main fibrous skeleton in the extracellular matrix of the amnion and chorion. Unbanded fibres were observed in the immediate vicinity of the amniotic and chorionic basal laminae (Figure 2.39) but were quite distinct from the homogeneous electron dense material of the lamina densa. These unbanded fibres extended from the basal lamina deep into the neighbouring compact layer, thus connecting the basal lamina and the other fibrous elements of the stroma.

The tightly packed banded collagen fibres typical of the compact layer were sparse and disorganised in distinct but widely separated hour-glass shaped areas extending from the amniotic epithelial basal lamina. These components had long axes orthogonal to the plane of the compact layer (Figure 2.40). The dimensions of these structures measured from electron micrographs were as follows: Length 12.2µm (n=8, SD=2.2), maximum width at amnion basal lamina surface 8.3µm (n=7, SD=2.9), maximum width at fibroblast layer surface 9.4µm (n=5, SD=1.2), minimum width at the waist 3.1µm (n=8, SD=0.6).

Accumulations of medium electron density material, similar in appearance to the amniotic epithelial lamina densa, occurred within the hour-glass shaped regions (Figure 2.40). Some sections demonstrated direct contact between the amniotic epithelial basal lamina and these regions. This material traversed the compact layer. The course of these strands was usually curved and in sections appeared to form the periphery or margins of the 'rivet'. This pattern was reflected in images of semi-thin toluidine blue stained sections where the intense staining, characteristic of the basal lamina, formed the margin of the rivet thus giving rise to its waisted appearance. Highly synthetic fibroblast-like cells beneath these sites extended processes into the region and curved around the margins of the structure (Ockleford et. al., 1994).

Areas of homogeneous electron dense substance were found in the amnion and chorion. This electron dense substance formed the lamina densa of the amniotic (Figure 2.38) and the chorionic (Figure 2.39) basal laminae. Furthermore, in the amniotic and chorionic connective tissue, there were also areas of homogeneous electron dense material. This extracellular matrix material was of a similar structure to the lamina densa. This material could also be observed to extend from the chorion laeve basement membrane between cytotrophoblast cells of the trophoblast layer and forming the basement membrane on which the endothelial cells of the maternal decidual layer rested. It was interesting in these latter two cases that there was not an associated lamina lucida.

The fibroblast cells of the mesenchymal layers (fibroblast and reticular layers) stored considerable amounts of lipids. There were numerous glycogen granules in the vicinity of these lipid droplets. TEM revealed that the well developed ER of these cells often widened to form pronounced cisterns which had a fine-grained content of similar appearance to the fibrous material surrounding these cells (Figure 2.39). This may indicate that these cells were actively depositing extracellular matrix material. Mitochondria were sparsely populated. They possessed surface vesicles, a large proportion of which were coated. These numerous invaginations were presumably connected with endocytosis. Intermediate filament bundles were well characterised,

particularly in the foot processes of the cells present within the reticular layer adjacent to the trophoblast basement membrane. These intermediate filaments (10nm in diameter) were orientated in the long axis of these highly anisometric cells and their surface extensions. Thin filaments were also observed in the cytoplasm but the EM fixation techniques applied here did not preserve the ultrastructure of microtubules except in a few instances.

Trophoblast.
The trophoblast cells of the chorion laeve possessed cytoplasm of varying electron density containing rER, free ribosomes, small round mitochondria with few cristae, Golgi, lipid inclusions, lysosomes and multivesicular bodies. There were varying degrees of vacuolisation but these cells frequently possessed coated pits and vesicles at the cell surface and many microvilli. There was often an extensive dilated ER containing fine grained material with a similar texture to the surrounding extracellular matrix. This may indicate that these cells actively deposit extracellular matrix materials. These cells contained numerous intermediate (10nm) filaments coursing through the cytoplasm which terminated in desmosomal attachments between cells. There was no evidence of hemidesmosomes attaching the basal trophoblast cells to the chorion laeve basal lamina or to the surrounding extracellular matrix material.

2.3.3.3 Scanning electron microscopy.

Using the cryofracture techniques described, ultrastructural images of the amniochorion have been taken using SEM. The simple cuboidal amniotic epithelium is demonstrated with its characteristic appearance (Figure 2.38). In cross-cryofracture these cells exhibited a concave apical surface and a flattened basal surface as revealed by conventional light microscopy and TEM. The apical cell surface possessed a plethora of microvilli. Lateral intercellular channels could be observed between the cells which contained numerous cellular processes. At high magnification the large centrally located nucleus could be observed with a 'honeycomb' interior. Numerous intracellular cytoplasmic spherical inclusions could also be identified.

At low magnification the basal lamina, upon which the amniotic epithelium rested, appeared as a straight line separating the epithelium from the compact layer. More detail, however, was revealed at higher magnification which showed the incursions of the basal lamina between the basal foot processes of the epithelial cells. These were clearly anchoring structures. The basal lamina marked a clear

transformation between the epithelium and the acellular underlying compact layer (Figure 2.28).

The compact layer was composed of closely packed collagenous bundles. These bundles were largely orientated parallel to the amniotic epithelium as demonstrated using the other microscopy techniques. The fibroblast layer could be identified by the presence of fibroblast cells embedded in an extracellular matrix fibrous meshwork which was less tightly packed. This technique revealed very few other distinctive characteristics associated with this layer.

It was hard to resolve the spongy layer and the fibroblast layer as separate structures. Using light microscopy there was often a characteristic separation between these two layers. It was evident using SEM that the amnion and chorion separate despite residual fibrous connections which could be observed traversing the gap between the two layers. Because cryofracture occurred along natural planes of weakness in the tissue, this allowed the surface relief to be studied. The fracture periodically occurred along the plane of separation between the amnion and chorion revealing the exposed surface of the reticular layer. This demonstrated the presence of folds or ridges of extracellular matrix bundles. Where the reticular layer and spongy layer were both exposed the surface relief suggested that these ridges may interdigitate and provide structural stability.

The interface between the reticular and trophoblast layers revealed the distinct change between cellular and acellular fibrous tissues. The trophoblast cells possessed a characteristic ultrastructural appearance and appeared as a relatively thick band of cells that contained an abundance of spherical inclusions. The maternal decidua was difficult to distinguish using this technique but clearly possessed blood vessels which contained erythrocytes.

The loose Whartons Jelly connective tissue of the umbilical cord was easily identified using this technique surrounded by a flattened layer of amniotic epithelial cells (Figure 2.29).

2.3.4 Hydatidiform mole.

Hydatidiform mole samples were obtained by suction curettage and thus were delivered as fragments of tissue.

2.3.4.1 Light microscopy.

Trophoblast.

The Tessovar photomicrograph of an excised hydatidiform mole chorionic villus reveals the swollen nature which typically resembles a 'bunch of grapes' (Figure 2.11).

Examination of semi-thin (0.5µm) sections of resin embedded hydatidiform mole specimens (Figures 2.15 and 2.16), prepared as described in section 2.2.2, yielded a similar morphology to that of 1st trimester placentae. The trophoblast surrounding the chorionic villi could be distinguished as a syncytiotrophoblast and an underlying cytotrophoblast layer.

Villus core.

Beneath the cytotrophoblast cell layer was the greatly swollen mesenchymal connective tissue core which contained mesenchymal cells. There was no evidence of a blood vascular system or Hofbauer cells in hydatidiform mole placentae. However, local condensations of connective tissue mesenchyme (Figure 2.16) possibly identified sites of attempted angiogenesis.

2.3.4.2 Transmission electron microscopy (TEM).

Examination of hydatidiform mole chorionic villi by TEM revealed the presence of many organelles and features demonstrated in first trimester placentae (Figures 2.34 and 2.35). In the syncytiotrophoblast many vesicles and vacuoles were apparent, including coated pits and vesicles at the apical microvillous membrane. Mitochondria, ER and electron dense inclusions, probably lipid droplets, were also apparent. Cytotrophoblast cells possessed a similar morphology to that described for 1st trimester tissue but bore a comparable electron density to the overlying syncytiotrophoblast (Figure 2.34).

The loose swollen connective tissue stroma underlying the trophoblastic tissue consisted of collagenous fibres enmeshing a network of cells. Hofbauer cells were not identified in the stroma. The elongated spindle-shaped mesenchymal cells possessed a small Golgi apparatus, numerous polyribosomes, a characteristic rough dilated ER and many small vesicles and vacuoles.

2.3.4.3 Scanning electron microscopy (SEM).

By SEM hydatidiform mole villi were seen to possess numerous microvilli, ridges and processes (Figure 2.27). The trophoblast contained many vacuoles but the boundaries between cells were not easy to define using the freeze-cracking technique. The greatly distended connective tissue stroma was well characterised by this technique and comprised of a network of fibrous bundles in which cells were enmeshed. Mesenchymal cells did not possess pronounced vacuoles and Hofbauer cells or blood capillaries were not identifiable using this technique.

FIGURES 2.9 - 2.40.

Figures 2.9 - 2.12: Morphology of the placental tissues.

Figure 2.9: Tessovar photo-micrograph of an excised healthy first trimester chorionic villus frond. Scale bar represents 1mm.

Figure 2.10: Tessovar photo-micrograph of an excised mature (term) chorionic villus frond. Note the highly branched villus tree. Scale bar represents 1mm.

Figure 2.11: Tessovar photo-micrograph of an excised hydatidiform mole chorionic villus frond. Note the greatly swollen villi which typically resemble a 'bunch of grapes'. Scale bar represents 1mm.

Figure 2.12: Nomarski differential interference contrast micrograph of a $5\mu m$ section through an amniochorion roll. Several features are apparent using this technique. The plane of separation of the amnion (A) and the chorion (C) is typically in the region of the spongy layer (arrow). The maternal decidua (D) is also evident. Scale bar represents $100\mu m$.
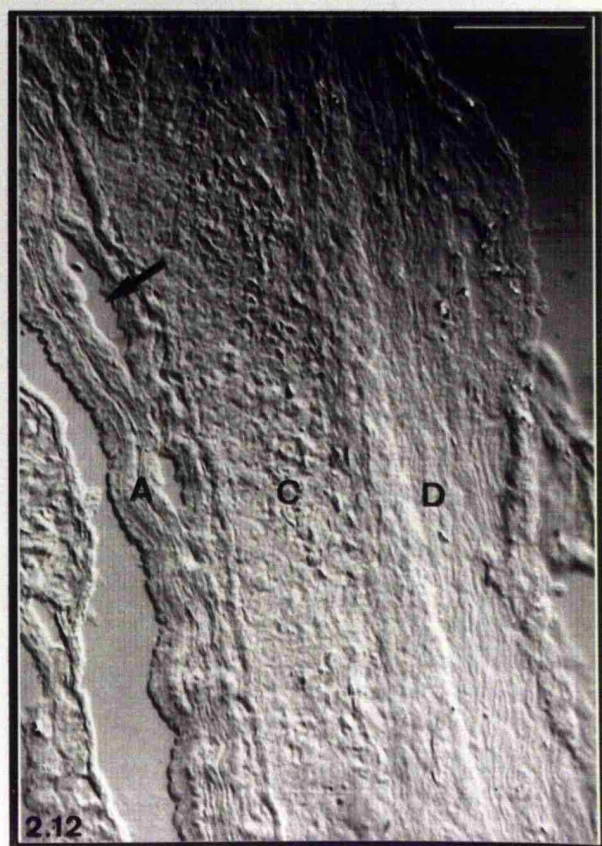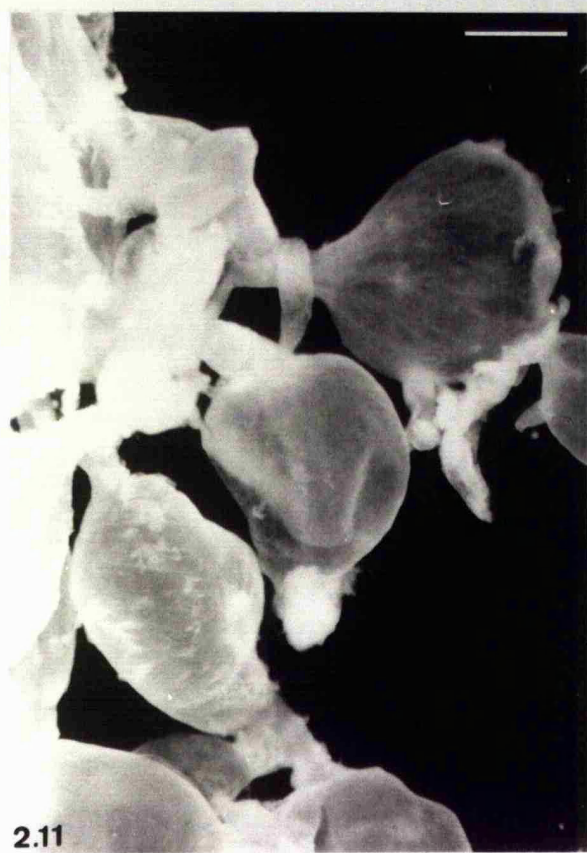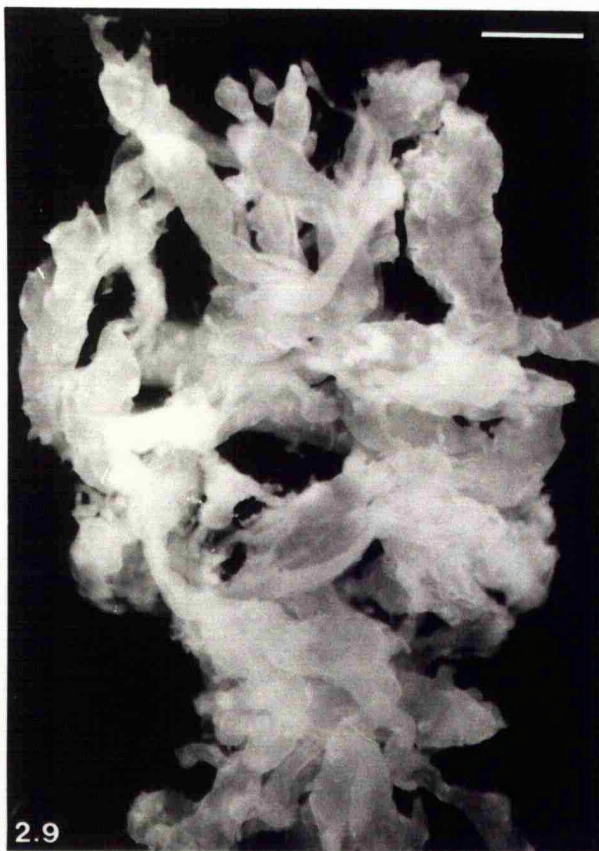
2.9

2.10

2.11

2.12

Figure 2.13: 1st trimester chorionic villus. The villus is surrounded by a darkly stained syncytium (Sy) which possesses a characteristic microvillus brush border, nuclei, cytoplasmic inclusions and vacuoles. Underlying the syncytium is a pale-stained layer of cytotrophoblast cells (C) which is almost continuous in the 1st trimester. One of the cytotrophoblast cells (arrowhead) is in late anaphase of mitosis. The loose mesenchymal connective tissue stroma (St) of the villus contains immature blood vessels (V), mesenchymal cells and vacuolated Hofbauer cells (H). Erythrocytes which would occupy the maternal blood lakes (M) in situ have been washed away in this preparation. Scale bar represents 20μm.

Figure 2.14: Term chorionic villi. The darkly stained syncytiotrophoblast surrounding the villus has become thinner by term but still possesses cytoplasmic inclusions, a brush border and numerous nuclei which occasionally clump together into syncytial knots. The underlying pale-stained cytotrophoblast cells (arrowheads) have become widely separated by term with the result that large areas of the syncytiotrophoblast are in direct contact with the basal lamina. The connective tissue stroma (St) contains numerous mature blood vessels and sinusoids which often directly underlie the syncytiotrophoblast to form the vasculosyncytial membrane (V). Some residual maternal erythrocytes have remained in the maternal blood space (M). Scale bar represents 30μm.

Figure 2.15: Hydatidiform mole chorionic villi. Note that the darkly stained syncytiotrophoblast layer (Sy) possesses a brush border, numerous cytoplasmic vacuoles and darkly stained nuclei. The underlying cytotrophoblast cells (arrowheads) possess similar staining characteristics unlike the pale-staining cytotrophoblast cells of healthy villi and the nuclei are darkly stained with an abundance of heterochromatin. The stroma (St) is greatly swollen in these villi and consists of a loose mesenchymal connective tissue in which blood vessels and vacuolated Hofbauer cells are absent. Maternal blood space (M). Scale bar represents 50μm.

Figure 2.16: Hydatidiform mole chorionic villus. Occasionally a condensation of cells (arrows) may be observed in the stroma (St) of hydatidiform mole villi. This may be indicative of an attempt by these cells to differentiate into capillary endothelial cells. Scale bar represents 20μm.
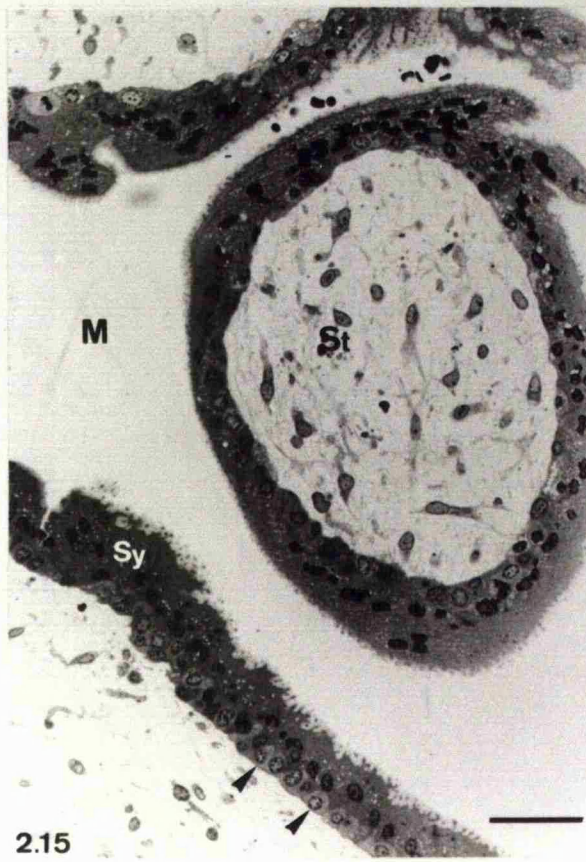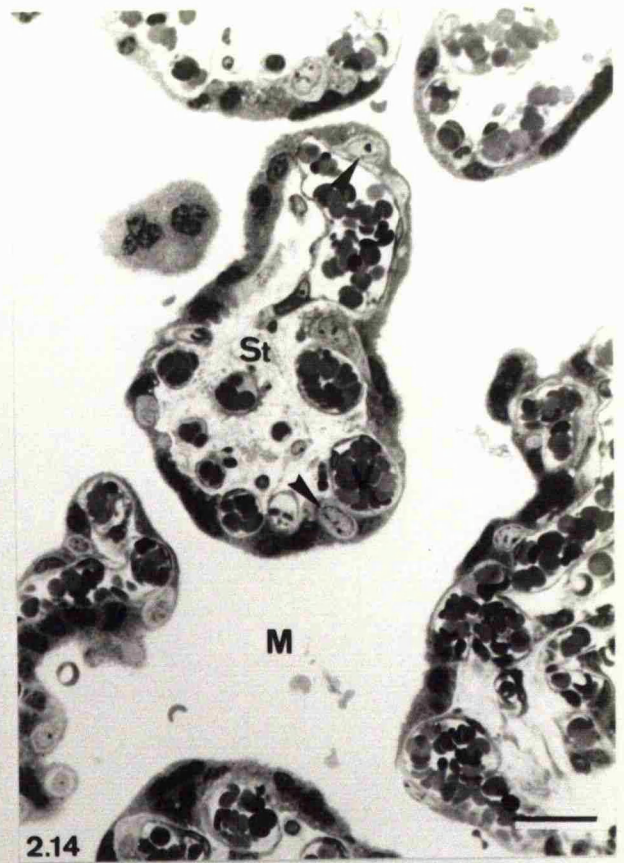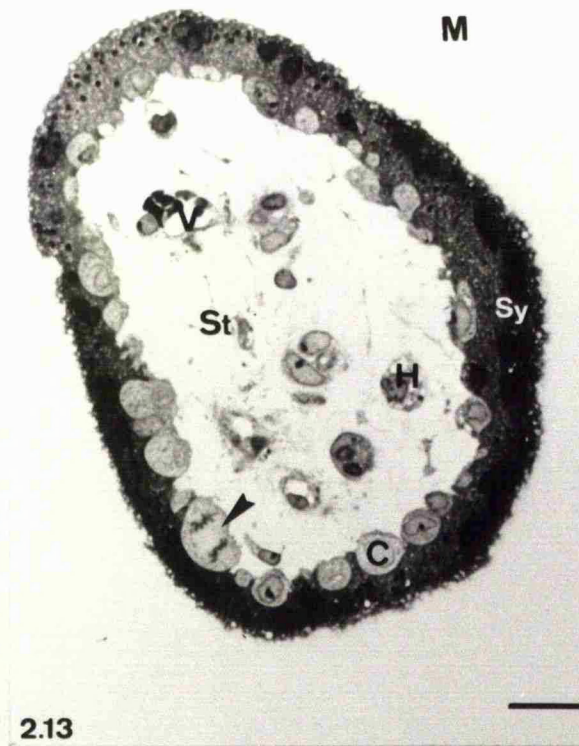
2.13

2.14

2.15

2.16

Figure 2.17: Term amnion. This consists of a simple cuboidal amniotic epithelium (A) resting upon a basal lamina. Underlying the epithelium is the acellular compact layer (C) and fibroblast layer (F) containing numerous fibroblast cells. Occasionally amniotic epithelial cells may be observed which possess a reduced affinity for stain (arrow). This cell has become detached from its neighbours and contains a highly pyknotic nucleus. Scale bar represents 40μm.

Figure 2.18: Term chorion. This consists of the reticular layer (R), which enmeshes numerous fibroblast cells, the trophoblast layer (T) which possesses a 2-8 cell layer of cytotrophoblast cells and the maternal decidua (D) which contains decidual cells and maternal blood vessels (V). Cytotrophoblast cells are separated by extracellular matrix material. Scale bar represents 40μm.

Figure 2.19: Healthy amnion. Note the simple cuboidal amniotic epithelial cells (A) possess a centrally located nucleus, lipidic inclusions and vacuoles. These cells rest upon the basal lamina which is in contact with the acellular compact layer (C). Fibroblast layer (F). Scale bar represents 20μm.

Figure 2.20: Damaged amnion. Note the damaged epithelial cells with reduced affinity for stain which have become detached from the basal lamina and neighbouring cells (arrowhead). Compact layer (C); Fibroblast layer (F). Scale bar represents 20μm.

Figure 2.21: Human amnion. Broadly spaced hour glass-shaped regions (arrowheads), which stain less intensely with toluidine blue, traverse the acellular compact layer from the basal lamina of the amniotic epithelium (A) to adjacent fibroblast cells (F). We have called this structure an 'anchoring rivet'. Scale bar represents 10μm.

Figure 2.22: Umbilical cord. A transitional layer of flattened amniotic epithelial cells (A) overlie the loose Whartons jelly connective tissue (W) which enmeshes numerous undifferentiated mesenchymal cells and fibroblasts. Scale bar represents 30μm.

Figure 2.23: Chorionic plate. A simple columnar amniotic epithelium (A) overlays the chorionic plate. Note the hour-glass shaped anchoring rivet (arrowheads) which traverses the adjacent mesenchyme. Scale bar represents 20μm.

2.17

2.19

2.18

2.20

2.21

2.22

2.23
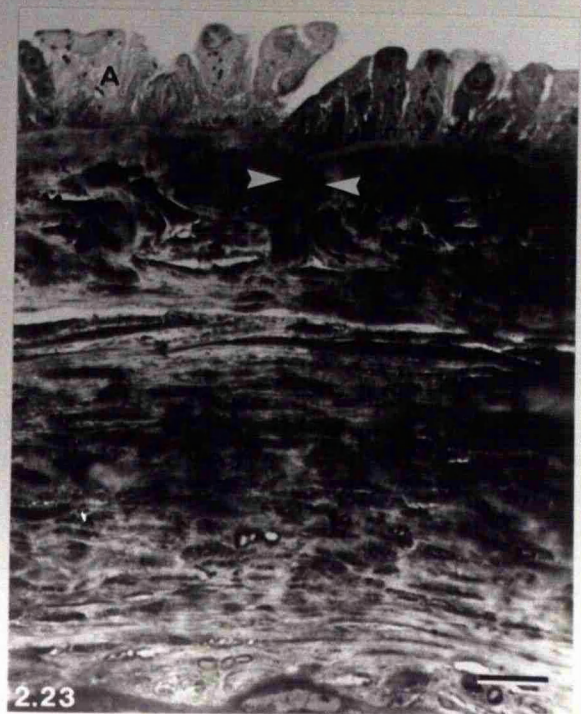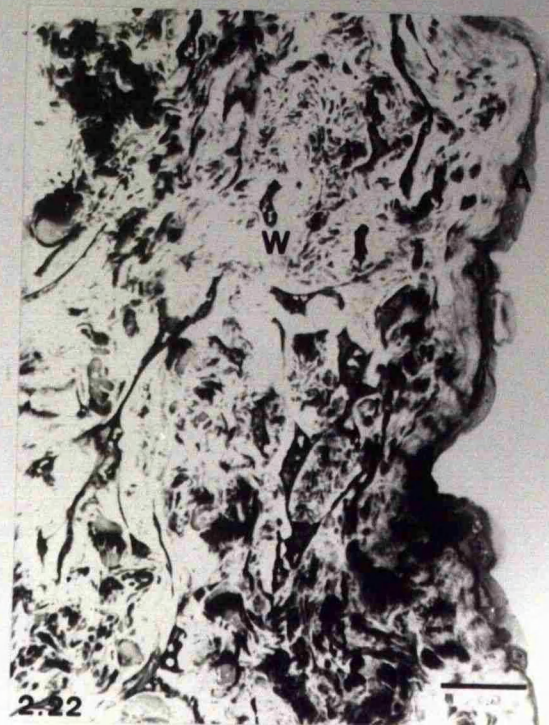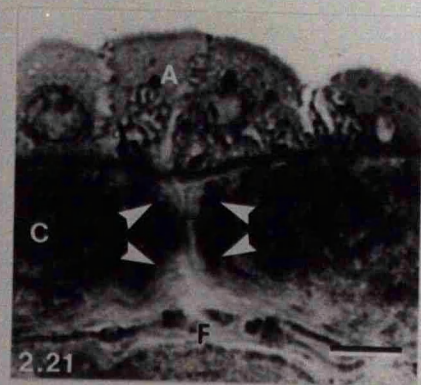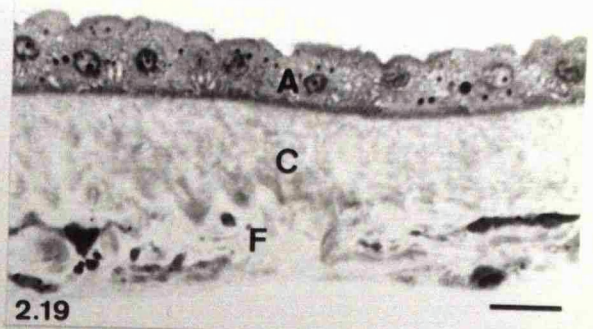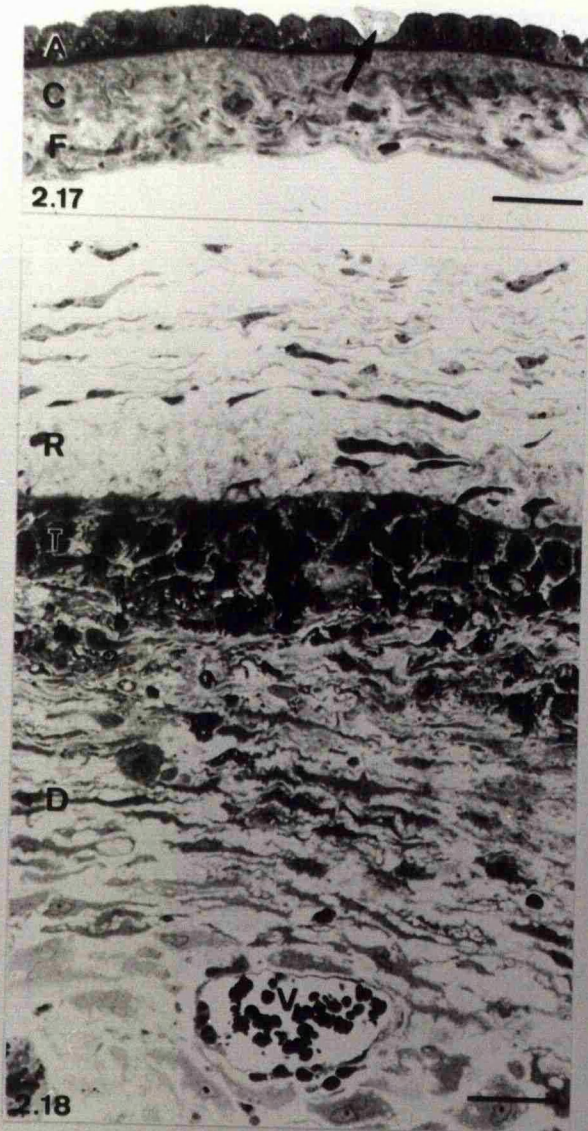
Figures 2.24-2.26: Scanning electron micrographs of cryofractured 1st trimester and term chorionic villi.

Figure 2.24: 1st trimester villus. The trophoblast surrounding the villus is just distinguishable as a syncytiotrophoblast (Sy) and a continuous underlying cytotrophoblast layer (arrowheads) using the cryofracture techniques. The loose connective tissue stroma (St) enmeshes cells and fetal blood vessels (V) which contain immature erythrocytes. Scale bar as indicated.

Figure 2.25: 1st trimester villus. This scanning electron micrograph clearly illustrates the microvillus brush border of the syncytiotrophoblast (*). Furthermore the connective tissue stroma (St) possesses numerous interconnecting channels and spaces which often contain cryofractured vacuolated Hofbauer cells (arrow). Scale bar as indicated.

Figure 2.26: Term chorionic villus. The highly branched nature of mature chorionic villi is evident in this micrograph. The microvillus brush border of the syncytiotrophoblast (Sy) is evident overlying the connective tissue stroma (St). The stroma enmeshes numerous mesenchymal cells and blood vessels (V). Scale bar as indicated.

2.24 15KV 0.78KX 12.8M 0618

2.25 15KV 0.77KX 13.0M 0621

2.26 15KV 466X 21.5M 0642
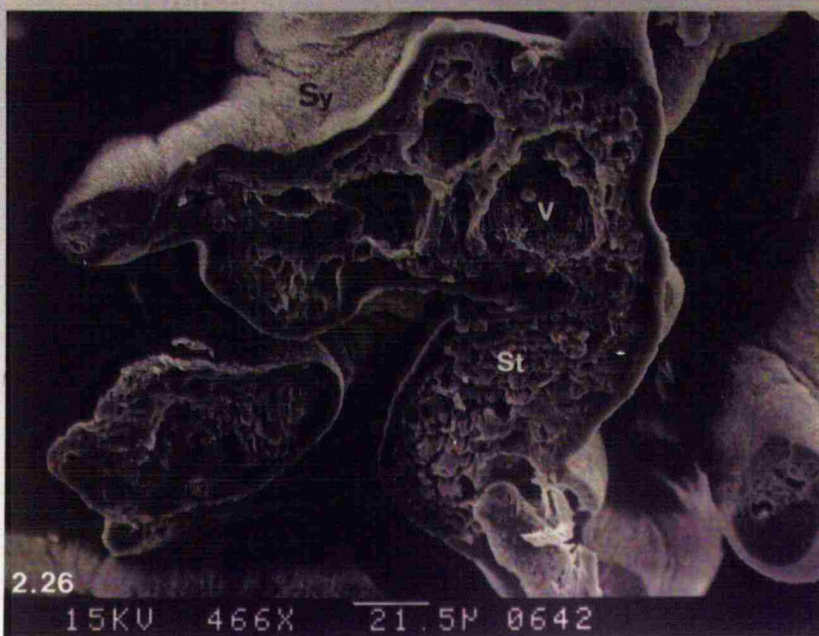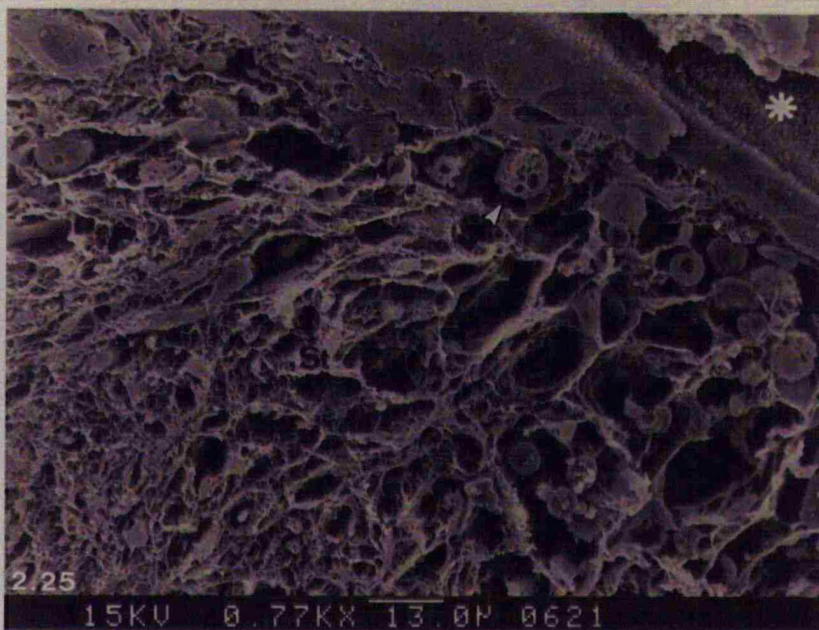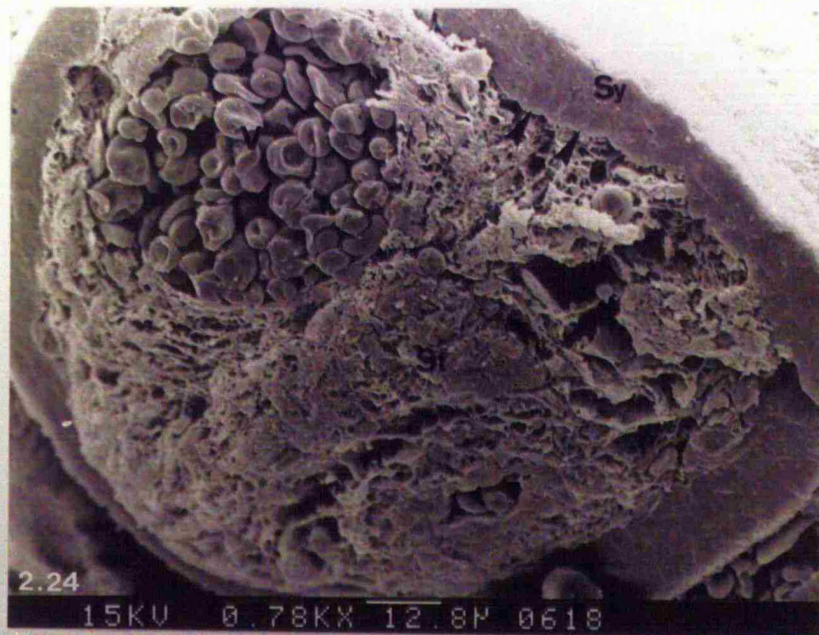
Figures 2.27-2.29: Scanning electron micrographs of cryofractured hydatidiform mole villi, amnion and umbilical cord.

Figure 2.27: Hydatidiform mole. The highly vacuolated syncytiotrophoblast (Sy) is clearly evident overlying cytotrophoblast cells (C) which do not possess an abundance of cytoplasmic vacuoles. The connective tissue stroma (St) enmeshes undifferentiated mesenchymal cells which do not contain large cytoplasmic vacuoles. Fetal blood vessels and Hofbauer cells are not apparent in this tissue. Scale bar as indicated.

Figure 2.28: Human amnion. Amniotic epithelial cells (A), which possess an apical microvillus brush border and cytoplasmic vacuoles, overlie the compact layer (C) and fibroblast layer (F). The fibres of the extracellular matrix are orientated in a largely omnidirectional nature. Scale bar as indicated.

Figure 2.29: Umbilical cord. The transitional cells of the amniotic epithelium (A) overlie the loose Whartons jelly connective tissue (W) which enmeshes numerous cells. Scale bar as indicated.

2.27 15KV 1.49KX 6.71M 0623

2.28 15KV 1.55KX 6.45M 0629

2.29 15KV 169X 59.2M 0645
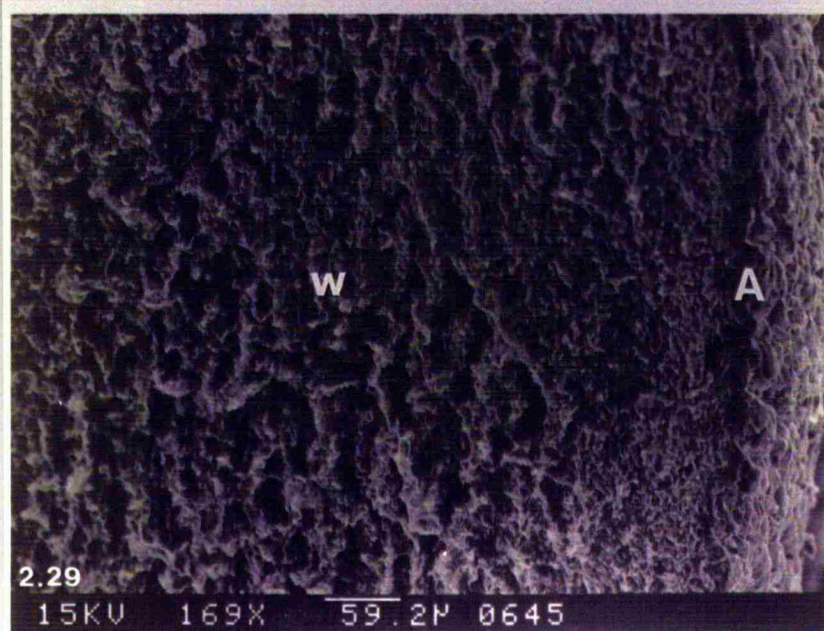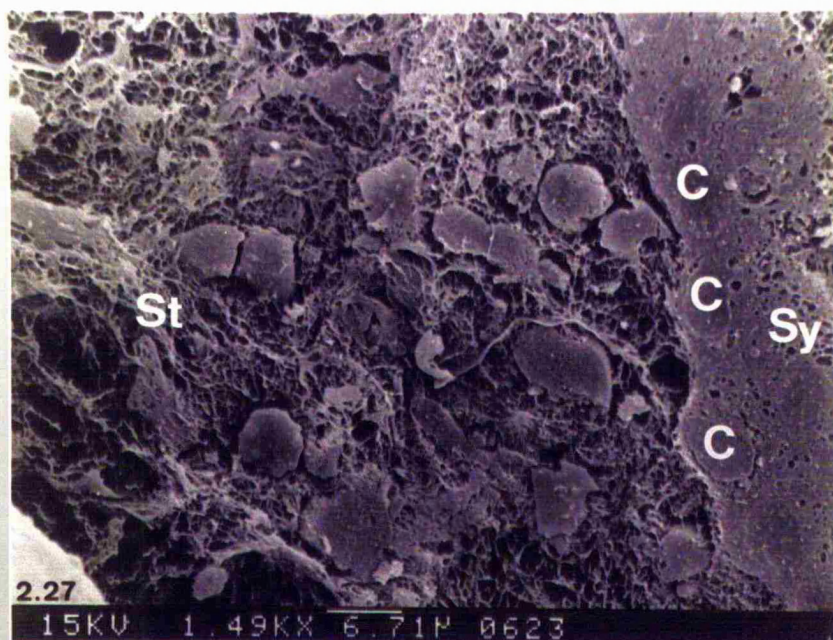
Figures 2.30-2.33: Transmission electron micrographs of 1st trimester and term chorionic villi.

Figure 2.30: 1st trimester chorionic villus. The syncytiotrophoblast (Sy) of 1st trimester villi possesses a brush border and plethora of cytoplasmic vacuoles and inclusions. Nuclei (N) contain characteristic highly electron-dense heterochromatin. The continuous layer of cytotrophoblast cells (C) are less electron dense than the overlying syncytiotrophoblast and are ultrastructurally simple. The stroma (St) of the villus core consists of undifferentiated mesenchymal cells and fibroblasts. Scale bar represents 4μm.

Figure 2.31: 1st trimester chorionic villus. At a higher magnification occasional projections of the syncytiotrophoblast (Sy) may be observed to penetrate between the usually continuous cytotrophoblast cells (C) and contact the basal lamina (arrow). Scale bar represents 2μm.

Figure 2.32: 1st trimester chorionic villus. This transmission electron micrograph of a 1st trimester villus core reveals that endothelial cells (E) have differentiated from mesenchymal cells to form a fetal capillary with a clearly defined lumen (L). Scale bar represents 3μm.

Figure 2.33: Term chorionic villus. At term residual cytotrophoblast cells (C) have become widely separated and form a greatly attenuated epithelial layer underlying the syncytiotrophoblast (Sy). Large areas of contact between the syncytiotrophoblast and the basal lamina are, therefore, evident. Mature fetal erythrocytes (E) are present in the capillary lumen (L) of fetal vessels at this stage of gestation. The capillary is separated from the trophoblast by only a thin layer of connective tissue. Scale bar represents 3μm.

2.30

2.31

2.32

2.33
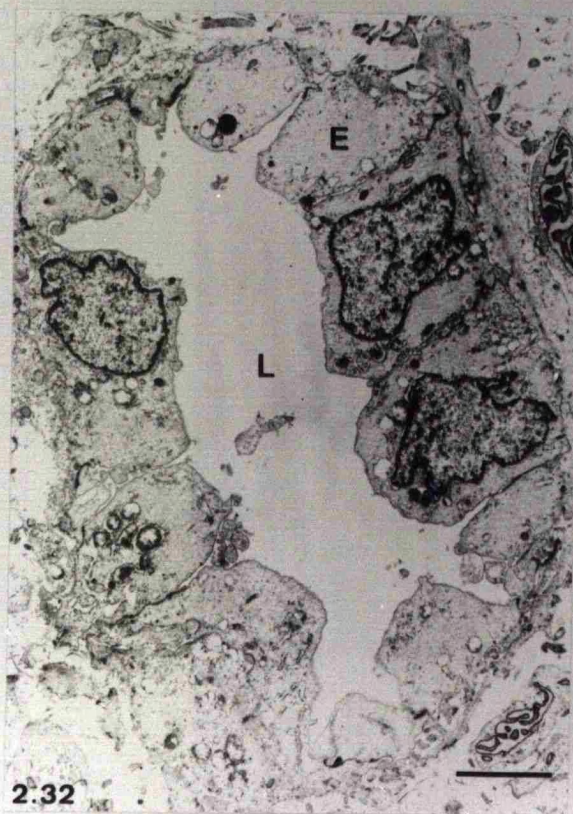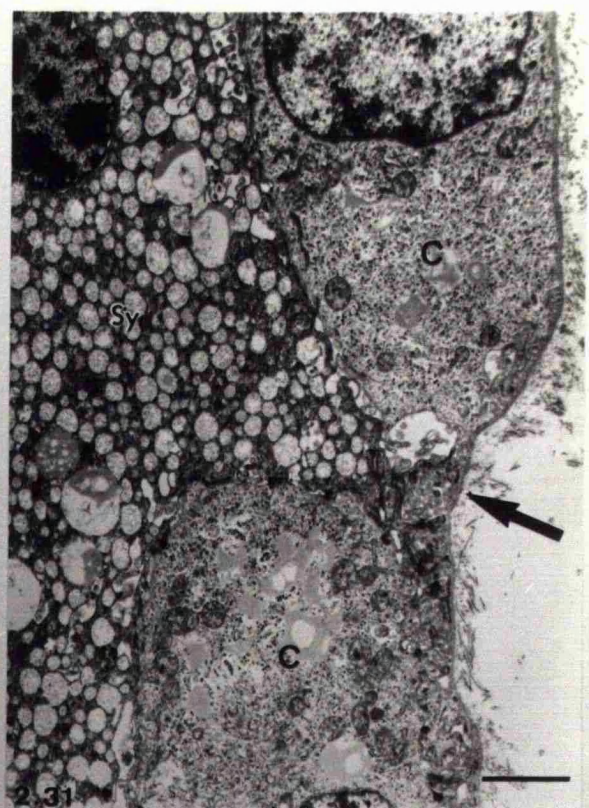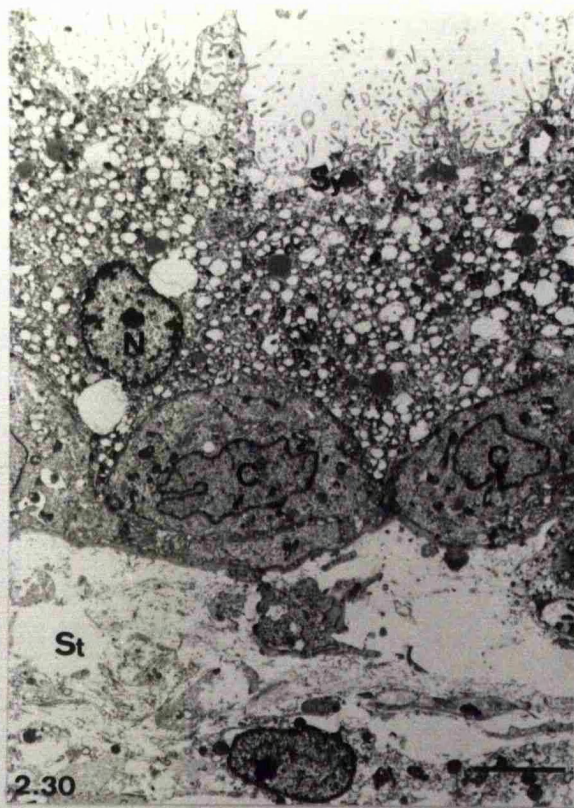
Figures 2.34-2.37: Transmission electron micrographs of hydatidiform mole chorionic villi, chorionic plate amnion and umbilical cord amnion.

Figure 2.34: Hydatidiform mole. This transmission electron micrograph of the trophoblast of a hydatidiform mole specimen indicates the syncytiotrophoblast (Sy) is of a very similar electron-density to the underlying continuous layer of cytotrophoblast cells (C). The nuclei of the cytotrophoblast cells possess highly electron-dense heterochromatin quite unlike the situation in healthy 1st trimester cells. The stroma (St) reveals a paucity of cells. Scale bar represents 4μm.

Figure 2.35: Hydatidiform mole. The connective tissue stroma (St) of hydatidiform mole specimens reveals sparsely differentiated mesenchymal cells with a characteristic dilated rough endoplasmic reticulum. Scale bar represents 4μm.

Figure 2.36: Chorionic plate amnion. This transmission electron micrograph of the amniotic epithelial cells overlying the chorionic plate demonstrates that these cells are simple columnar in nature with a highly interdigitating intercellular space, vacuolated and possess an apically associated nucleus (N). The base of these cells consists of foot-processes which interlock with the basal lamina. Scale bar represents 3μm.

Figure 2.37: Umbilical cord amnion. The transitional amniotic epithelium (A) of the umbilical cord consists of flattened overlying cells attached by desmosomes. These cells are associated with a loose collagenous Whartons Jelly (W) connective tissue which contains numerous mesenchymal cells. Scale bar represents 4μm.
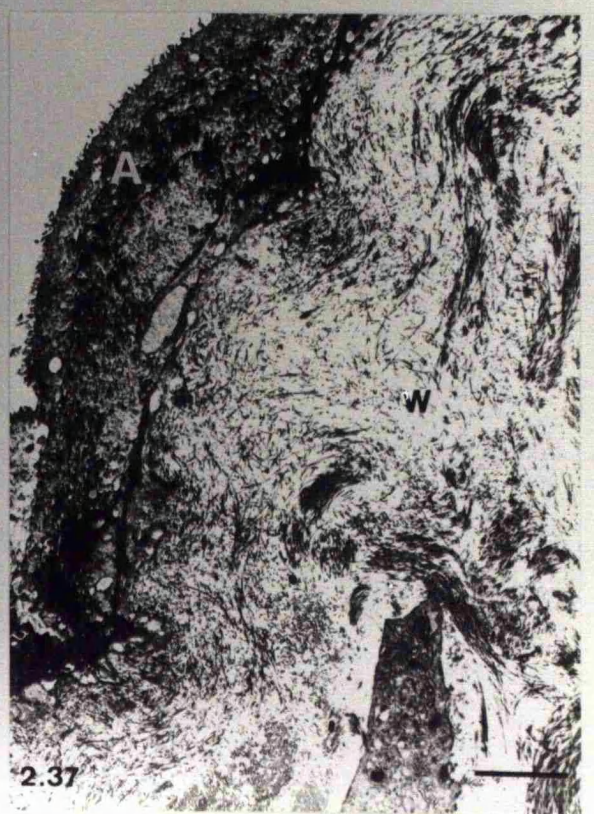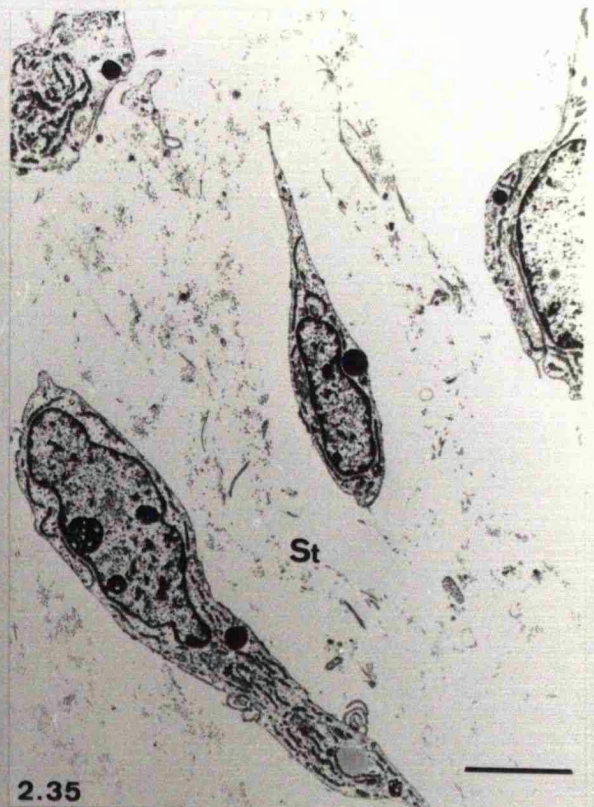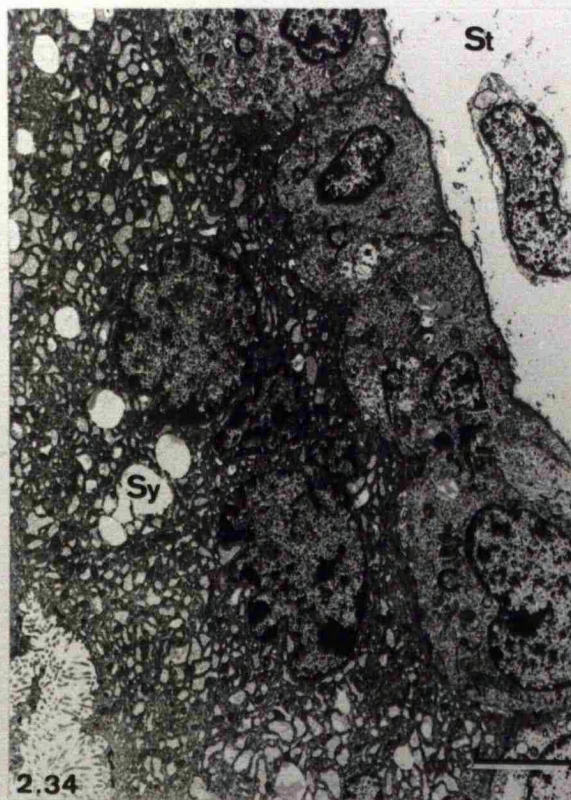
2.34

2.35

2.36

2.37

Figure 2.38: Term amnion. Amniotic epithelial cells (A) interlock via basal foot-processes with the basement membrane (BM). The basement membrane is attached to the underlying compact layer (C), consisting of omnidirectional orientated banded collagenous fibres, by unbanded fibres. This field also demonstrates a damaged amniotic epithelial cell (D) adjacent to the healthy cell (A). Note that the damaged cell is considerably less electron dense and consists of large vacuoles and sparse intermediate filament bundles. This cell has clearly relinquished contact with the healthy cell in the apical regions. The healthy cell, however, consists of an electron dense cytoplasm in which the vacuoles are less evident against the residual cytoplasmic proteins. Scale bar represents 1μm.

Figure 2.39: Term chorion laeve. This field illustrates the trophoblast layer consisting of cytotrophoblast cells (C) which rest upon the chorion laeve basement membrane (arrows). Cytotrophoblast cells contact one another via desmosomal attachments and are surrounded by extracellular matrix material. Fibroblast cells with a vastly dilated endoplasmic reticulum are present in the reticular layer (R). In addition short segments or trabeculae of extracellular material, which resemble the basal lamina, are evident at sites in the reticular layer distant from the basal lamina (arrowheads). Scale bar represents 3μm.

Figure 2.40: Transmission electron micrograph illustrating the overall appearance of a section through the amniotic epithelium (A) and anchoring rivet. The ultrastructural appearance is similar to that observed in semi-thin toluidine blue-stained sections. The organisation of the banded collagen fibres in the compact layer (C) is interrupted as these approach the margins of the rivet (arrowheads). The margin of the rivet consists of moderate electron dense material with similar ultrastructural appearance to that found in the basal lamina. Irregular clumps of basement membrane-like material are evident in the upper margins of the rivet (*). The fibroblast-like cell immediately beneath the rivet appears to have extended a process into the rivet. At intervals there is very close approximation between the fibroblast cell surface and the basement membrane-like margins of the rivet. Scale bar represents 1μm.

2.4 DISCUSSION.

2.4.1 Chorionic villi.

There is an enormous body of literature which comprehensively deals with the histology and ultrastructure of the human placenta at all developmental stages (Wislocki and Dempsey, 1955; Boyd and Hamilton, 1970; Wynn, 1975; Jones and Fox, 1991; Dearden and Ockleford, 1983; Kaufmann and Burton, 1994).

Histology.
The human placenta comprises three layers: trophoblast, connective tissue stroma and capillary endothelium. The placental trophoblast, which is in intimate contact with maternal blood, is relatively thick in early development but becomes progressively thinner throughout gestation. Towards the end of the first trimester the Langhans cells (villus cytotrophoblast) decrease in relative prominence, although they persist throughout gestation. These cytotrophoblast cells remain the source of the syncytium.

As the placenta matures, the terminal villi form increasingly numerous subdivisions. The more obvious histological changes that are consistent with increased efficiency of transfer include an increase in the ratio of villus surface to volume, a decrease in the thickness of the syncytium, discontinuity of the cytotrophoblast cell layer and a reduction in the proportion of villus connective tissue relative to the trophoblast (Kaufmann and King, 1981; Mayhew and Burton, 1988; Kaufmann and Burton, 1994). In the villi of placentae of early gestational age, fibrocytes with branching processes are separated by an abundant, loose extracellular matrix. The core of the mature villus comprises a denser stroma with closely packed spindle-shaped mesenchymal cells. The villus capillaries, moreover, increase in number and progressively approach the surface. Occasionally the fetal capillaries lie directly adjacent to the syncytiotrophoblast which is extremely thin. These areas are termed vasculosyncytial membranes. It has been proposed that they are specialised regions adapted to facilitate gas exchange (Baker et. al., 1944). During placental maturation the so-called Hofbauer cells are also markedly reduced in number. The origin and significance of these cells has been contemplated by Wynn (1967) and Enders and King (1970).

Ultrastructure.
The syncytiotrophoblast may be demonstrated to be a true syncytium using transmission electron microscopy and microinjection (Gaunt et. al., 1986; Gaunt and Ockleford, 1986). The numerous organelles present in the syncytium are the cause of

the basophilia observed with light microscopy. These organelles have been extensively investigated by the above authors and have been observed using the methods employed in this study. The free surface of the syncytiotrophoblast is characterised by a microvillus border associated with coated or uncoated vesicles and vacuoles. Mitochondria, Golgi apparatus, endoplasmic reticulum, ribosomes, lipid droplets, glycogen, vacuoles and cytoskeletal elements are all common elements of this highly complex syncytium (Boyd and Hamilton, 1970). Polymeric cytoskeletal proteins including microtubules, microfilaments and intermediate filaments have been found in the syncytiotrophoblast. A definitive layer of cytoskeletal elements composed of microtubules and actin filaments (Ockleford and Whyte, 1977) has been demonstrated in this region using electron microscopy. These authors have proposed the name syncytioskeletal layer for this region. Furthermore, cytokeratins are the only intermediate filament proteins associated with the syncytium (Ockleford et. al., 1983) and this finding supports the notion that the trophoblast is ectodermally derived.

Typical cytotrophoblast cells are ultrastructurally simple, with large nuclei, prominent nucleoli, large mitochondria and a sparse Golgi apparatus. The cytoplasm is studded with numerous free ribosomes (Boyd and Hamilton, 1970) but is relatively devoid of a well developed endoplasmic reticulum. The cytotrophoblast cell layer is usually continuous in early gestation but occasionally the syncytium is observed to penetrate between cells and contact the basement membrane. This cellular layer becomes increasingly attenuated as gestation advances with the size and number of contacts between the syncytium and the basal lamina increasing. However, residual cytotrophoblast cells may be observed throughout gestation.

The cytotrophoblast layer is the germinative layer of the trophoblast and DNA synthesis and mitotic figures are confined to cytotrophoblast cell nuclei (Richart, 1961; Galton, 1962). Evidence for the production of syncytiotrophoblast from the cytotrophoblast stem cells comes from the occurrence of cells with intermediate morphology between the two cell types (Yoshida, 1964). The cytotrophoblast cell nuclei are more uniform in shape than the syncytial nuclei and are more electron-lucent with finely dispersed chromatin. There are usually one or two nucleoli present. For a comprehensive account of the histology and ultrastructure of the normal human placenta the reader is referred to Boyd and Hamilton (1970).

Cryofracture and scanning electron microscopy of chorionic villi provides an excellent three-dimensional account of the ultrastructural morphology of these structures. The 'freeze-cracking' data presented in this chapter serves to introduce the reader to the structure of chorionic villi of various gestational ages but has been

comprehensively performed in excellent studies by Castellucci et. al. (1980) and Castellucci and Kaufmann (1982).

2.4.2 Amniochorion.

An account of the histology and ultrastructure of this complicated tissue is provided in a monograph by Bourne (1962). Schmidt (1992) also provides a description of the structure of the amniochorion. There is currently renewed interest in the structural organisation of the human fetal membranes (amnion and chorion) and its relation to their functional and physical properties (Malak et. al., 1993; Ockleford et. al., 1993a; 1993b; 1993c). It is generally considered that the most important property of the amniochorion is its mechanical integrity which maintains the fluid environment upon which the fetus depends for survival *in utero*. Failure of this property leads to early rupture of the membranes before the onset of labour, a condition which is associated with high risk of maternal morbidity and neonatal morbidity and mortality (Alger and Pupkin, 1986; Gazaway and Mullins, 1986).

Considerable effort is being expended on studying the extracellular and intracellular polymeric protein strength-giving components of this tissue, particularly the extracellular matrix collagens. During the routine morphological investigations used in this study several ultrastructural features have been observed in this tissue for the first time (Malak et. al., 1993; Ockleford et. al., 1993b; 1993c; 1994). The presence of a 'homogeneous electron-dense substance' was first described in the extracellular matrix of the fibroblast, spongy and reticular layers and we suggested that this bore ultrastructural resemblance to the morphology of the lamina densa of a typical basement membrane (Malak et. al., 1993). This observation was supported by immunofluorescence investigations which demonstrated type IV collagen immunoreactivity in the fibroblast, spongy and reticular layers. We were further able to characterise the presence of these short segments, or trabeculae, in the extracellular matrix using ultrastructural immunocytochemistry (Ockleford et. al., 1993b; see also chapter 6). These structures contain type IV collagen and share some of the ultrastructural features of the lamina densa and anchoring plaques of the skin (Keene et. al., 1987). These structures, which we name microtrabeculae, are clearly dissimilar from both of these features on grounds of composition, location and size. They may however, be related to them in some as yet undefined way.

Presently the origin and function of these structures are obscure. However, it may be relevant that the spongy layer, close to which the microtrabeculae are found, originates from the extraembryonic coelom and thus is not embryologically part of the amnion or the chorion. At term the cellular layer, which forms the boundary

between the spongy layer and the reticular layer, is usually absent. Earlier in development it is a consistent but simple unicellular layer. Therefore it is conceivable that microtrabeculae are the remnants of a basal lamina of this layer. If the trabeculae were originally part of a continuous lamina densa then controlled disassembly during the regression of a previously functional sheet may result in the observed 'remnants'. In addition, it is possible that these structures originate from Heuser's membrane, which delaminates from trophoblast cells, or from the cells of the extraembryonic coelom which group together to form the fluid-filled lakes that eventually coalesce to form the extraembryonic coelom. Furthermore, it is now appreciated that type IV collagen-containing structures are not restricted to basal laminae and therefore the immediate environment of an epithelium (Pratt and Madri, 1985; Nanaev et. al., 1991). Extracellular matrix plaques containing type IV collagen may act as cross-linkers which help to integrate the mechanical network of the collagens since we have described type VII collagen-containing structures extending from the amniotic epithelial basement membrane to interact with these microtrabeculae (Ockleford et. al., 1993a; 1994).

The 'hour-glass' strands of material crossing the compact layer may integrate the basal lamina to the fibrous network of the underlying mesenchyme. These structures are over ten times larger than the previously described plaques containing type IV collagen with which the carboxyl terminal regions of type VII collagen interact (Sakai et. al., 1986; Keene et. al., 1987). We have recently named these structures 'anchoring rivets' (Ockleford et. al., 1993a; 1994).

It is conceivable that unusual local circumstances exist beneath the amniotic epithelial basement membrane where a massive lamina reticularis, or compact layer, of the order of 10μm thick exists. Usually basement membranes including the lamina reticularis are only 20-50nm across (Duance & Bailey, 1983). Since the compact layer is generally devoid of type IV collagen it thus forms an unusually large scale potential barrier to integration of layers (Malak et. al., 1993). Structures normally anchoring basal laminae to underlying type IV collagen in the mesenchyme must bridge this layer; the largest recorded length for an anchoring fibril is 800nm (Bruns, 1969).

The relationship between underlying fibroblast cells and rivets is interesting. Processes from these cells extend around the margin and may thus be important in defining the shape of the rivet. The medium electron dense strands appear to make localised contacts with the fibroblast cell processes. There are small electron dense regions of cell surface at the contact points. Dual immunofluorescence studies are consistent with this linkage, involving α6β4 integrin binding at the cell surface

(Ockleford et. al. 1994; Byrd et. al., 1994). The morphogenesis of the rivet and/or synthesis of rivet components may thus be controlled by these cells.

At term the amnion may become detached from the chorion laeve, and it is possible to separate the amnion from the chorion. The plane of separation is invariably along the spongy layer between the fibroblast and reticular layer. Therefore, the interaction of the amniotic epithelium with the compact layer and the compact layer with the fibroblast layer must be strongly mechanically integrated. It is logical to propose that at least some of the cohesion between the three amniotic layers is provided by the rivets containing type VII collagen.

The structure called the pseudo basement membrane (to avoid confusion with the amniotic epithelial basement membrane) by Bourne (1962) appears to be a structurally and compositionally normal embryonic basement membrane associated with the chorion laeve trophoblastic epithelium. We have recommended that the use of the term 'pseudo basement' membrane be replaced with 'chorion laeve basement membrane' (Ockleford et. al., 1993b). Ultrastructurally visible extensions project from this basement membrane into the overlying trophoblast layer and the underlying mesenchymal extracellular matrix of the reticular layer (Malak et. al., 1993) and we have confirmed this by using ultrastructural immunocytochemistry for the presence of type IV collagen at these sites (Ockleford et. al., 1993b). It is clear from light and electron micrographs that the trophoblast cells of the chorion laeve are separated from one another by an abundant extracellular matrix and only contact via sparse desmosomal attachments. Therefore it is conceivable that large macromolecules may be freely able to penetrate between these cells.

The ultrastructural characteristics of the cellular components of the amniochorion are well documented elsewhere (Bourne, 1962; Schmidt, 1992; Thomas, 1965). Relatively few new features have been observed in the current study (Ockleford et. al., 1993c) and these are restricted to studies of the cellular cytoskeleton. In this study, ultrastructural observations are correlated with the results of immunocytochemical experiments designed to assess the cytoskeletal composition of cells. Amniotic epithelial cells and cytotrophoblast cells possess anti-keratin immunoreactivity and possess 10nm intermediate filament bundles, consistent with their ectodermal origin. These bundles terminate in hemi-desmosomal or desmosomal attachments. No hemi-desmosomes are observed in cytotrophoblast cells. However, ultrastructural investigations demonstrate that keratin intermediate filaments may also form associations with the nuclear pore complex and thus it is conceivable that there is an integration resulting in mechanical continuity between nuclear lamins, intermediate filament proteins and extracellular

matrix fibrous elements. Other cellular ultrastructural features of the amniochorion are as previously published.

Several authors have observed differences in the affinity for stain of the amniotic epithelial cells (Lanzavecchia and Morano, 1959; Wynn and French, 1968; Schmidt, 1965). Thomas (1965) undertook a detailed ultrastructural study to account for these differences and divided the cells into two types on the basis of the different structure and arrangement of the organelles and cytoskeleton. She characterised 'Golgi-type' cells by a well developed rER and Golgi apparatus, many vesicles and mitochondria and asserted that they may have secretory (possibly gamma-globulin) function. Schmidt (1992) recently designated these as type I cells. Thomas characterised the second type of cell as 'fibrillary' type which are electron dense and contain an abundance of cytoskeletal filaments. This type of cell occurs much more frequently than the 'Golgi-type' and is considered by Thomas to be 'sparsely developed and absorbent'. Schmidt (1992) has designated these as type II cells.

However, I do not subscribe to the views of these two authors that the amniotic epithelium possesses two types of cell. Throughout these investigations light microscopical and ultrastructural observations have been made on the amniochorion obtained from either full term deliveries or elective Cesarean section deliveries. The 'reduced affinity for stain' observed by other authors in some cells of the amniotic epithelium was only evident in tissue which had been collected from routine vaginal deliveries. This phenomenon was very rarely associated with the amniotic epithelial cells from placentae delivered via elective Cesarean section. I attribute the occurrence of these cells to the stresses associated with parturition or the delay between delivery of the placenta and tissue fixation. Thus 'light cells' in my opinion are indicative of cell degeneration.

This hypothesis is supported on two accounts. Firstly Schmidt (1992) concedes that there are 'rivers and islands' of degenerative [amniotic epithelial] cells at term because we are dealing with a tissue which is at the end of its functional life. Furthermore these cells are unable to exclude dye in trypan blue exclusion tests performed on the fetal membranes at term (Hans J. Wolf; personal communication). This suggests that these cells have lost their mechanical integrity and have thus become permeable to the dye. Histological and ultrastructural observations of the 'Golgi-type' cells indicates that they have frequently relinquished contact with neighbouring cells and/or the basement membrane indicating that they are degenerative. Re-evaluation of the data obtained by Thomas (1965) shows that these 'Golgi-type' cells, on which her hypothesis is based, have also relinquished contact with neighbouring cells and are not part of a continuous epithelium.

Therefore these cells, it would appear, have degenerated or died. The reduced affinity for stain is reflected in the loss of cytoplasm from these cells which has presumably become extracted. This phenomenon would further explain Thomas's assertion that these cells are 'Golgi-type' cells since these organelles would be more clearly visualised in an 80-90nm thin section in which the cytoplasm has been extracted. In healthy cells the Golgi apparatus and cytoplasmic vacuoles would be more difficult to identify against the background electron density of the residual cytoplasmic proteins within the section thickness. Therefore, Thomas's hypothesis that these cells may secrete gamma-globulin is entirely speculative.

Cryofracture and scanning electron microscopy of the amniochorion has recently been described by Fawthrop and Ockleford (1994). The observations presented in this chapter using the 'freeze-cracking' technique are consistent with the observations of these two authors. Correlation with transmission electron microscopy data permits greater understanding of how these cellular and acellular layers interconnect and maintain their integrity as a multilaminous tissue. High resolution micrographs of the amniotic epithelium and acellular layers provides a more complete description of their structure than previously available.

2.4.3 Hydatidiform mole.

Hydatidiform mole specimens are obtained at a similar gestational age to 1st trimester specimens but exhibit a morphology quite unlike the healthy tissue. Macroscopic examination of this tissue reveals the characteristic swollen appearance of the villi which very much resemble a 'bunch of grapes'. Histologically this tissue is of similar but distended proportions to its healthy equivalent. However, one striking difference with hydatidiform mole tissue is that there is an absence of vascularisation in the connective tissue core although occasionally there is evidence that the mesenchyme has condensed in an effort to form capillaries. These observations are easily verified using transmission electron microscopy.

Scanning electron microscopy has been used to study the surface organisation of hydatidiform mole specimens and revealed characteristic paddle-shaped sprouts, ridging of the syncytial trophoblast cell surface and structures called microgibbosities (Ockleford et. al., 1989). However the cryofracture technique of Castellucci et. al. (1980) and Castellucci and Kaufmann (1982) has been newly applied to this tissue in the present study. Micrographs of the fractured surface of hydatidiform mole chorionic villi demonstrate the swollen nature of the loose connective tissue stroma and clearly demonstrate the absence of fetal blood vessels.

Hofbauer cells were not identified using this technique. The absence of Hofbauer cells in the stroma of this tissue is a novel finding and raises intriguing questions concerning their source since they are of 'fetal origin' (Bourne, 1962; Wynn, 1967). It is likely that the origin of these cells is from undifferentiated mesenchymal cells of the villus core and that this is in some way restricted in the pathological condition. In the latter stages of gestation Hofbauer cells may be supplemented by fetal bone marrow-derived cells once the circulation is established (Castellucci and Kaufmann, 1990).

CHAPTER 3: Clathrin.

3.1 INTRODUCTION.

As explained in section 1.1.6 the protein clathrin is a ubiquitous component of the coated pits and vesicles that are responsible for receptor-mediated uptake of ligands. In the human placenta, the various models that have thus far been proposed for the mechanism by which IgG traverses the syncytiotrophoblast nearly all concur with the view that coated vesicles mediate at least some role in this process. Whether clathrin coated pits are responsible for IgG transport across capillary endothelial cells of the placenta has not yet been established. The aim of the work presented in this chapter is to investigate the distribution of this important molecule in the cells of the human placenta and fetal membranes using the technique of immunocytochemistry.

3.1.1 Immunocytochemistry.

The aim of immunocytochemistry is to identify the location of a tissue component *in situ* by using a specific antigen-antibody 'reaction' and its visualisation with a specific label. Early attempts to label antibodies were not successful because the ordinary dyes used in these studies could not be detected with the microscope. The technique of immunocytochemistry became established when Coons and his colleagues conceived the idea of identifying antigens using specific antibodies labelled with the fluorescent dye, fluorescein isocyanate. Coons et. al. (1941) initially labelled a specific antibody itself with this fluorescent marker (direct method) but later introduced a more versatile and sensitive indirect technique (Coons et. al., 1955). Riggs et. al. (1958) subsequently labelled antibodies with fluorescein isothiocyanate (FITC), a molecule that is easier to conjugate to the antibodies and, to the present date, this molecule is the preferred label. Fluorescein compounds, even when the labelling is with low concentrations to prevent steric hindrance of the antibody molecule, yield a bright apple-green fluorescence on irradiation with ultraviolet light (maximum absorbance at 490nm, emission at 520nm). An additional fluorescent label for use with simultaneous labelling of two antigens is tetramethylrhodamine isothiocyanate (TRITC) which fluoresces red.

The disadvantages of these immunofluorescence techniques are that they require a fluorescence microscope, background details are difficult to appreciate and the preparations are not permanent because the fluorescent labels do not tolerate dehydration. However, the speed and simplicity of the immunofluorescence techniques ensure that this remains a popular procedure, particularly with the recent innovation of confocal laser scanning microscopy (CLSM) which provides increased resolution of the immunofluorescence preparations.

Other immunocytochemical techniques require the use of different light microscopical labels including enzymes, particularly peroxidase, introduced by Nakane and Pierce (1966) and alkaline phosphatase, used for enzyme-linked immunoabsorbant assay (ELISA; Engvall and Perlmann, 1971). Tissues used in conjunction with these techniques may be fixed and embedded in paraffin wax and the enzyme labels are developed histochemically at the end of the antibody-antigen reaction to reveal intensely coloured end products that are viewed with conventional light microscopy techniques. Further adaptations as we shall see in chapter 6, involve the use of tissues prepared for electron microscopy and the application of electron-opaque markers to localise the antigen of interest.

To obtain meaningful results from immunocytochemical studies requires the use and production of well characterised antibodies of defined specificities. Antibodies are immunoglobulins produced by vertebrates as a natural defence mechanism against foreign or abnormal agents (antigens) such as toxins, viruses, bacteria or tumour cells. The immune system can recognise antigens as foreign particles and this stimulates the production of antibodies which combine with the antigen and, as a consequence of secondary functions effected by this binding, neutralise it. Under appropriate conditions the antigen-antibody combination is specific. The cells responsible for generating this immune specificity are a class of white blood cells called B lymphocytes.

This natural antibody-antigen response may be exploited experimentally. Almost any macromolecule including virtually all proteins and most polysaccharides can elicit an immune response as long as it is foreign to the recipient. The production of polyclonal antibodies involves immunization (by injection) of a suitable animal (eg. rabbit, mouse, guinea pig or goat) with the chosen antigen, administration of further doses of the antigen to induce a secondary response, and finally collection of immune serum. Because of the polyclonal nature of the immune response, immunization of an animal with a single protein antigen will give rise to an antiserum containing a heterogeneous mixture of antibodies of various affinities and directed against a variety of sites or 'epitopes' on the antigen molecule. Polyclonal antibodies are derived from different cells. The antibodies produced by each individual cell are homogeneous and the descendants of the cell are a clone. This information has allowed a method of producing monoclonal antibodies which are specific for a single epitope on the antigen molecule.

Milstein and his colleagues have devised an ingenious method for producing pure and reproducible antibodies (Kohler and Milstein, 1975; Milstein et. al., 1979). Mice of a certain strain, eg. BALB/C, are immunised and when antibodies are being

produced the mice are sacrificed and the antibody-producing plasma cells from the spleen are mixed with cultured myeloma (plasmacytoma) cells from the same strain of mice. These authors showed that B lymphocytes, if induced to fuse with an immortal myeloma cell, acquired the myeloma's ability to grow indefinitely in culture while continuing to secrete antibody. This new cell line, with the properties of both the parent myeloma cell and the B cell, is known as a hybridoma. Naturally, the hybrid cell population will produce as many assorted antibodies as the original immunised mouse. To obtain pure antibodies, the culture must be divided and the culture medium from each subculture must be screened for antibody production. Only cultures producing the desired antibody are kept, and these are further divided and tested until clones derived from a single cell and producing specific antibody are achieved. The culture medium from these clones may then be used as a monospecific antibody to the original antigen. The cloned cells may be frozen and stored until supplies of antibody are needed. The universal and continual availability of one particular antibody, free from unwanted contamination, is an enormous advantage and justifies the effort required for its production.

A possible disadvantage of monoclonal antibodies results directly from their high specificity. A monoclonal antibody will only react with a single epitope on the antigen molecule whereas a polyclonal antiserum contains heterogeneous antibodies which recognise different epitopes of the molecule thereby increasing the sensitivity of the polyclonal labelling method. Similarly, it is possible that the particular epitope to which a monoclonal antibody is directed may be altered by the tissue preparation procedures such as fixation, dehydration or embedding. This antigen would, therefore, not be detected by a monoclonal antibody.

Since the binding of an antibody to its antigen is, in principal, always reversible it may be expressed in terms of an affinity constant (K_A). Affinity is thus a measure of the precision of fit between the antigen binding site of the antibody and its complementary epitope. Values for K_A are most frequently found in the range of 10^7-10^9M^{-1} although they may be as high as 10^{12}M^{-1}. Since antibodies have a minimum of two antigen binding sites it is evident that when an antibody binds to a polyvalent antigen (eg. one containing identical, repeating epitopes), binding of the first site may increase the likelihood of the second site being able to bind. This will be reflected by much tighter binding of the antibody as a whole and is referred to as the avidity. Another term which is frequently referred to as a characteristic of an antibody preparation is 'titre'. This is literally a value for how much an antibody can be diluted before its association with antigen can no longer be detected. Clearly, the titre of any given antiserum will depend on both the affinities and the avidities of the

various antibodies in the preparation, on their initial concentrations and on the sensitivity of the detection system employed.

The direct method of immunocytochemical staining is a one-step process. In this procedure the specific antibody to the antigen of interest is covalently labelled with a fluorochrome (usually FITC or TRITC) to form a conjugate. This conjugate is subsequently applied directly to the tissue and the immunoreactivity examined using a fluorescence microscope. The indirect method is a more widely used technique and is a two-step process. The conjugate in this system is a second antibody which is raised against antigens presented on the immunoglobulins of another species (eg. a fluorochrome conjugated goat anti-rabbit IgG would recognise and bind to antibodies raised in rabbit). Therefore, only a few types of sera need to be labelled for the indirect method, which is an advantage over the direct method which requires labelling of all antibodies used. A further advantage of the indirect method is increased sensitivity. Several antibodies may bind to a single antigen and these antibodies may subsequently each be bound by several conjugated antibodies of the second layer. This results in a considerable amplification of the signal.

Occasionally non-specific fluorescence makes it difficult to interpret the results of immunofluorescence staining. This fluorescence may originate from non-specific cross-reactivity of the immunological reagents and conjugates used or by autofluorescence in which natural fluorescence is produced on excitation of certain cell or tissue constituents. The possibility of non-specific fluorescence emphasises the importance of including control tissue samples in which antibodies and conjugates of non-specific nature are used. A negative control section should be performed using non-immune serum (preferably pre-immune serum from the animal used to raise the specific antiserum) or, to check for non-specific immunoglobulin cross reactivity, an inappropriate antiserum of the same dilution. A further control is to pre-absorb the primary antibody with an excess of its specific antigen so that no antibody combining sites are available to react with the tissue. If staining occurs then it must be attributed to some cause other than the specific antibody-antigen reaction under investigation.

The antigen to be located must be insoluble or rendered insoluble by being fixed in the tissue, but it must also be available to the antibody in its antigenic form. The best morphological preservation is usually seen after fixation with conventional fixatives such as formaldehyde or glutaraldehyde which produce inter- and intramolecular cross-linkages among proteins in the tissue. The fixation process must not destroy the antigenicity of the molecule to be localised and this has to be determined empirically. However, some molecules are rendered partially or

completely non-immunoreactive by fixation or by the paraffin-embedding process, and in such cases unfixed cryostat sections of fresh frozen tissue are necessary.

3.1.2 Microscopy.

The most frequently used fluorochrome conjugate for localising antigens with the fluorescence microscope is FITC which emits a bright apple-green fluorescence upon irradiation with U.V. light (490nm). The principle of fluorescence microscopy is straightforward. Briefly, a fluorophore is irradiated with light of a wavelength spanning its absorption maximum from a source such as a mercury vapour (HBO-50) lamp. The incident light is filtered so that it is not viewed by the eyepiece and thus the object is viewed against a dark (back)ground. Irradiation of the fluorochrome excites its orbital electrons which obtain higher energy levels. Subsequently these electrons decay to their original orbitals and in so doing emit light irradiation in the visible part of the spectrum. However, during excitation there is a gradual reduction of the intensity of fluorescence. This fading may be the result of photobleaching caused by decomposition of the fluorescing molecules. Glycerol-mounted immunfluorescence preparations containing a photobleaching retardant mountant are preserved undiminished for many months when sealed and stored at 4°C in the dark.

The design of fluorescence microscopes was originally similar to conventional transmitted illumination 'bright-field' microscopes. The instrument of choice recently has an epi-illumination system. Light from a mercury vapour emission source is directed at a dichromatic beam-splitter placed at an angle of 45° to reflect light of a certain wavelength down onto the specimen. This light is brought to a focus on the specimen using the objective lens. When the fluorochrome is excited in this way, its emission radiation is collected by the objective lens and passes back up to the dichroic mirror which allows light of this wavelength to be transmitted. The fluorescence may then be viewed with the eyepieces or used to expose photographic film.

3.1.3 Confocal laser scanning microscopy.

The scanning confocal microscope was invented by Minsky in 1961, but practical and effective devices have only recently been developed (eg. White and Amos, 1987). The main disadvantage of conventional fluorescence microscopy is out-of-focus blur resulting from illumination of the whole field of view. This blur reduces contrast and may seriously compromise the final image. The confocal laser scanning microscope possesses a pinhole aperture which strongly selects for in-focus

light. Therefore, the specimen may also be optically sectioned in the z-plane. This is a particularly useful technique which can be used to produce an extended focus image or even high resolution three-dimensional data sets showing the relative positions of fluorescent labels within cells or tissues. The image is displayed on a black and white or colour monitor and may be digitally enhanced and photographically recorded. From the digitised image it is possible to make various quantitative measurements such as the levels of intensity of fluorescence at different points of the image. It is also possible to compare several images on the screen simultaneously and thus the enormous flexibility of the system allows each specimen to be studied in the most appropriate manner.

3.2 MATERIALS AND METHODS.

3.2.1 Tissue collection.

Fresh specimens of 1st trimester chorionic villi (n=6), term chorionic villi (n=14) and amniochorion from normal delivery (n=10) or elective Cesarean section (n=5) were obtained from the Leicester Royal Infirmary as described in section 2.2.1. Chorionic villi were covered with Tissue-Tek O.C.T. embedding medium (BDH) in disposable plastic moulds or aluminium foil cups. Amniochorionic membranes were cut into strips (10mm x 30mm) and rolled with the amnion innermost prior to being placed vertically into the plastic mould or foil cup and embedded with O.C.T. embedding compound. Snap-freezing of the tissue blocks was effected by immersion of the moulds into a Dilvac Dewar flask containing liquid hexane / dry ice slush (–70°C). The tissue blocks were subsequently transported to the laboratory and stored over dry ice in a Lerose (-40°C) freezer until required.

3.2.2 Indirect immunofluorescence.

Cryosections (5-10μm) were cut from the tissue blocks using a Leitz cryostat (Leitz Kryostat 1720 Digital) and melted onto Flow Laboratories 10-well multitest slides or Dispo Diagnostic 10-well teflon-coated immunofluorescence slides. The working temperature of the cabinet was maintained at -23°C, the tissue block at –17°C and the knife (Raymond Lamb Laboratory Supplies) at -20°C. The slides on which the tissue sections were adhered were then placed into a humid Petri-dish containing filter paper soaked with PBS. The tissue was then washed with 0.1M PBS (2 x 2 minutes). Care was taken during the entire procedure to ensure that the sections did not dehydrate and, when pouring solutions onto the slides, to prevent tissue sections from being dislodged. The solutions were removed using a BDH tap driven vacuum filter pump with a clean glass pipette.

Two optional steps were included in half of the immunofluorescence experiments performed. The tissue was fixed using 3% formaldehyde diluted in 0.1M PBS for 10 minutes at room temperature, washed with PBS (3 x 5 minutes) and, to ensure that the antibodies gained access to intracellular antigens, permeabilised for 10 minutes with 0.05% Triton X-100 diluted in PBS. The slides were then washed thoroughly until their hydrophobic properties returned using PBS.

The primary antibody was diluted to the required concentration in PBS and the non-immune serum from the species in which the second stage antibody was raised. It was necessary to include a concentration of 5% non-immune serum to

block any non-specific interactions of the second stage fluorochrome-conjugated antibody with the tissue sections. This procedure minimises the possibility of obtaining false-positive results. The solutions were made in Eppendorf tubes using a Gilson pipette and centrifuged at 13000 RPM for 10 minutes in an Eppendorf MSE Micro Centaur microcentrifuge to remove any antibody aggregates.

Excess PBS was removed from the teflon-coated slides leaving only the PBS covering the tissue sections in the wells to ensure that it remained hydrated. A 20μl aliquot of the first stage antibody dilution was then applied to each of the wells containing tissue. Two wells on the same slide had control solutions applied as described in section 3.2.2.4. Care was taken to avoid intermixing the solutions. The sections were then incubated at 37°C for 1 hour in a humid chamber placed in a LEEC incubator with 5% CO_2. Optionally the tissue sections were immunoreacted with the primary antibody solution for 24 hours at 4°C. Following the incubation the slides were rinsed briefly in PBS (3 changes) and washed for 1 hour at 4°C to remove any unbound primary antibodies.

The second stage fluorochrome-conjugated antibody was diluted and applied following exactly the same procedure except that this solution was also applied to control tissue. A 5% non-immune serum block raised in the same species as the secondary fluorochrome-conjugated antibody was included in these solutions. The slides were incubated at 37°C for 1 hour, rinsed with PBS (3 changes) and washed in PBS for 30 minutes at 4°C. An example of a typical immunofluorescence protocol is given in appendix XIII.

3.2.2.1 Primary antibodies.

The primary antibodies used in this study were directed against clathrin purified from bovine brain as immunogen. These antibodies, raised in goat, specifically label the heavy chain band of clathrin by immunoblotting (Sigma, Code No.: 65-781; Lot No.: H077) and was used at an optimal dilution of 1/50. The dilutions tested ranged from 1/20 - 1/400. This antibody was stored at -18°C in 10μl aliquots until required. Once thawed the antibodies were stored at 4°C to prevent the deleterious effects caused by repeated freeze-thawing.

3.2.2.2 Secondary antibodies.

The secondary antibody used in this investigation was FITC-conjugated rabbit anti-goat IgG (heavy and light chain; ICN Biomedicals, Code No.: 65-176; Lot No.: 0012). This antibody was used at a dilution of 1/500. The dilution range tested was 1/100 - 1/2000. This antibody was stored at -18°C in 10μl aliquots and subsequently at 4°C when required.

3.2.2.3 Non-immune serum.

Throughout these experiments a 5% blocking serum, from the species in which the second stage antibody was raised (rabbit), was maintained in the solutions to prevent non-specific labelling (Sigma, Code No.: R9133).

3.2.2.4 Control experiments.

On each slide twoáwells were left without tissue during sectioning to separate the wells with control tissue from the rest of the wells of the slide. This prevented intermixing of the solutions containing specific antisera with control solutions. Control experiments were performed by omitting the specific primary antibody from the solution and incubating the sections in 0.1M PBS containing 5% non-immune rabbit serum (NRS) or by replacing the primary goat antibody with an equivalent dilution (1/50) of non-immune goat serum (NGS; Sigma, Code No.: G9023) in PBS containing 5% NRS. This was to investigate the non-specific interactions engaged by goat immunoglobulins with the tissue sections. The controls were treated in an identical manner to the other wells at all subsequent stages.

3.2.3 Mounting.

PBS was removed from the slides and a small amount of photobleaching retardant mountant (Citifluor) was applied. A clean glass coverslip (Chance Propper Ltd. No. 0 thickness) was then lowered carefully onto the slide and sealed with nail-varnish. Alternatively the slides were mounted with permanent mountant (Gurrs Fluoromount) and left to dry. The immunofluorescence preparations were viewed immediately or stored in the dark at 4°C until required.

3.2.4 Microscopy and photography.

The mounted slides were first viewed using a Zeiss epifluorescence / phase microscope equipped with Neofluar (pH 2x16 and pH 2x40) and Planapo (x63 and

pH 3x100; Zeiss) objectives. BDH inert immersion oil was used with the x63 and x100 oil immersion lenses. The specimens were photographed using a Zeiss M35 SLR camera and a Zeiss MC63 electronic exposure control unit to expose Fujichrome 400D colour slide film. It is often found that deliberate underexposure, obtained by setting the electronic exposure meter to too high a film-speed setting, achieves a more satisfactory result when colour transparency films such as Fujichrome are used due to the high fluorescence intensity set against the dark (back)ground. Therefore, the camera unit was deliberately set at 600 ASA to underexpose the film. Exposure times were set automatically with the unit and timed. Immunofluorescence preparations and control sections were exposed for identical times. Therefore, the measure of fluorescence intensity between experimental and control tissue may be directly compared.

The films yielded direct colour positive transparencies after standard reversal processing from which it was possible to obtain colour prints. All films were processed by the Central Photographic Unit (C.P.U.) of the University of Leicester.

3.2.5 Confocal laser scanning microscopy.

An MRC 600 Lasersharp confocal attachment (Biorad) coupled to a Zeiss Axiovert 10 (Zeiss, Oberköchen) inverted epifluorescence microscope equipped with infinity corrected optics was used to examine immunofluorescence preparations of exceptional quality. The confocal principle exhibits a number of advantages over conventional epifluorescence microscopy.

The major disadvantage of conventional epifluorescence microscopy is the out-of-focus blur resulting from illumination of the entire field of view. This reduces contrast and may seriously degrade the quality of the final image of the specimen. The Biorad MRC 600 confocal attachment has an adjustable pinhole aperture which strongly selects for emitted light from the point of focus of the objective lens. Thus the specimen may be optically sectioned through the z-axis and light from out-of-focus elements may be virtually eliminated.

There are several additional advantages over conventional optical microscopy including the significant improvement in resolution in the plane of focus. The microscope is also capable of direct non-invasive serial optical sectioning of intact specimens. This is a particularly useful technique which can be used to produce an extended focus image or high resolution three-dimensional data sets of fluorescent labels within cells or tissues. In addition, by coupling a sensitive photomultiplier detector output via an analogue to digital converter digital images can be saved via a

microcomputer equipped with a digital frame store. In this way it is possible to manipulate images and obtain direct quantitative measurements such as the relative fluorescence intensity of particular areas of the specimen, or direct comparison of several images simultaneously. The image is displayed on a video monitor and may be digitally enhanced and photographically recorded.

Techniques used throughout this investigation for photographically recording images captured with the confocal microscope were 1) for colour transparencies a Polaroid Quick Print loaded with E6 colour process slide film, 2) for direct colour micrographs a Sony UP-3000 video printer and 3) for black and white transparencies a Shackman flat screen monitor and camera attachment loaded with Ilford FP4 film.

3.2.6 Transmission electron microscopy.

Specimens for transmission electron microscopy were prepared as described in section 2.2.3 and Appendix III.

3.3 RESULTS.

The structural component of coated pits, the protein clathrin, was localised in the cells of the human placenta and fetal membranes using immunocytochemistry. This was found to be a ubiquitous cellular protein.

3.3.1 First trimester chorionic villi.

In 1st trimester chorionic villi clathrin immunoreactivity was associated with the syncytiotrophoblast, cytotrophoblast cells, cells of the villus stroma and endothelial cells of the fetal capillaries (Figure 3.2a). Particularly intense immunoreactivity was seen at the apical syncytiotrophoblast cell surface. These data correlated with transmission electron microscopy findings (Figure 3.6) which clearly demonstrated the presence of coated pits and coated vesicles at the apical cell surface. Clathrin was also present in the underlying cytotrophoblast cells and transmission electron microscopy confirmed the presence of coated pits (Figure 3.7) and coated vesicles in these cells. This suggests that these cells are capable of receptor-mediated endocytosis.

The mesenchymal cells and endothelial cells of the connective tissue core were also immunoreactive with the anti-clathrin antibodies. This observation could be verified using electron microscopy (Figures 3.8 and 3.9). Furthermore Hofbauer cells, which were abundant in the cores of 1st trimester villi, possessed this important protein.

3.3.2 Term chorionic villi.

The cells of the chorionic villi of term placentae also possessed anti-clathrin immunoreactivity (Figure 3.1). The most significant observation was that in syncytiotrophoblast this immunofluorescence was very intense at the apical cell surface. Little or no clathrin was associated with the basal syncytiotrophoblast. This correlated with observations made in the electron microscope (Figure 3.10) which demonstrated the predominance of coated pits and coated vesicles at the apical cell surface. Cytotrophoblast cells also possessed this protein and, in contrast to the syncytiotrophoblast, these cells demonstrated frequent coated pits at the basal plasmalemma (Figure 3.12).

Fibroblast cells, mesenchymal cells and Hofbauer cells of the villus core also expressed this protein and in endothelial cells surrounding the fetal capillaries clathrin immunoreactivity could be observed (Figure 3.1). Immunolocalisation of

this molecule revealed its consistent presence throughout the cytoplasm of these cells and at the basal (basement membrane) and apical cell surfaces. These observations correlated with the observations made in the transmission electron microscope which demonstrated coated pits at the apical cell surface, opening into the blood vessel lumen (Figure 3.11), and at the basal cell surface opening onto the basal lamina. Coated vesicles were observed intracellularly at all depths within these cells.

3.3.3 Term amniochorion.

Clathrin was expressed by all cell types present in term amniochorion (Figure 3.3). A diffuse cytoplasmic immunolocalisation pattern was observed throughout amniotic epithelial cells. Using TEM coated pits were observed at the basal (Figure 3.15), lateral and apical aspects of these cells suggesting a role in receptor-mediated uptake. The mesenchymal cells of the amnion and chorion also contained this protein indicative of an involvement in receptor-mediated uptake. This could be clearly verified using TEM (Figure 3.17).

The cytotrophoblast cells of the chorion laeve, similar to those of the placental villi, possessed intense anti-clathrin immunofluorescence (Figure 3.3). By examining these cells with conventional TEM it was possible to identify numerous coated pits and coated vesicles associated with the cell surface (Figure 3.16). This suggests that coated vesicle mediated uptake is an important function in these cells. Maternal leucocytes, decidual cells (Figure 3.18) and maternal endothelial cells of the decidua also possessed clathrin.

Placental and umbilical amnion.
Anti-clathrin immunofluorescence was associated with the columnar amniotic epithelial cells which overlie the chorionic plate of the placental disc (Figure 3.4; correlated transmission electron microscopy: Figure 3.19) and with the amnion of the umbilical cord (Figure 3.5). In these tissues an association was also found with mesenchymal cells or fibroblasts of the connective tissue stroma (or Whartons jelly). Umbilical cord endothelial cells were also immunoreactive confirming the ubiquitous cellular expression of this important molecule.

3.3.4 Hydatidiform mole.

Due to the limited availability of this tissue, it was not possible to perform immunocytochemical investigations into the distribution of clathrin. However, using routine transmission electron microscopy it was possible to identify coated pits and coated vesicles in the syncytiotrophoblast (Figure 3.13), cytotrophoblast cells and in

connective tissue mesenchymal cells (Figure 3.14). An association with endothelial cells was not possible to establish due to the absence of blood vessels in this tissue.

3.3.5 Control experiments.

Control experiments were performed by omitting the primary specific goat anti- clathrin antiserum and reacting the tissue sections with PBS or an equivalent dilution of non-immune goat serum. These control experiments did not yield specific immunofluorescence (Figure 3.2b) indicating that the immunolocalisations obtained were a consequence of the antigen specificity of the antibodies used to conduct these investigations.

FIGURES 3.1 - 3.19.

Figures 3.1-3.5: Anti-clathrin immunoreactivity in human placental tissues.

Figure 3.1: Dual channel confocal micrograph illustrating a) Nomarski differential interference contrast and b) indirect immunofluorescence of anti-clathrin immunoreactivity in a term chorionic villus. Clathrin immunoreactivity is predominant at the apical syncytiotrophoblast surface (arrowheads), in cells of the connective tissue stroma (St), and in the capillary endothelium surrounding fetal vessels (V). Scale bar represents 50μm.

Figure 3.2: Confocal indirect immunofluorescence micrograph illustrating a) anti-clathrin immunoreactivity and b) a control preparation in 1st trimester chorionic villi. a) Fluorescence is localised in the surrounding trophoblast and developing endothelial cells of the core. b) In this control preparation, taken from a similar area to that shown in a), an application of an equivalent concentration of non-immune goat serum was used to replace the specific anti-clathrin antiserum. The tissue was subsequently immunoreacted with an identical concentration of the fluorochrome conjugated anti-goat antibody. Note that there are background levels of immunofluorescence only. Scale bar represents 50μm.

Figure 3.3: Confocal indirect immunofluorescence micrograph of anti-clathrin immunoreactivity in term amniochorion. Amniotic epithelial cells (arrowhead), fibroblast cells of the mesenchymal layers (*) and cytotrophoblast cells of the trophoblast layer (T) are immunoreactive in this preparation. Scale bar represents 100μm.

Figure 3.4: Epifluorescence micrograph of anti-clathrin immunoreactivity in amniotic epithelial cells (A) overlying the chorionic plate of the placenta. Fluorescence is concentrated at the apical and basal cell surfaces and is present throughout the cytoplasm of the cells. Fibroblast cells (arrowhead) in the underlying mesenchyme are also immunoreactive. Scale bar represents 20μm.

Figure 3.5: Epifluorescence micrograph of anti-clathrin immunoreactivity in the amniotic epithelium (A) overlying the umbilical cord. Undifferentiated mesenchymal cells and fibroblasts of the Whartons jelly connective tissue are also immunoreactive (arrowheads). Scale bar represents 20μm.

a) b)

3.1

a) b)

3.2

AMNIOCHORION: CLATHRIN IMMUNOREACTIVITY.   100 μM

3.3

3.4   3.5
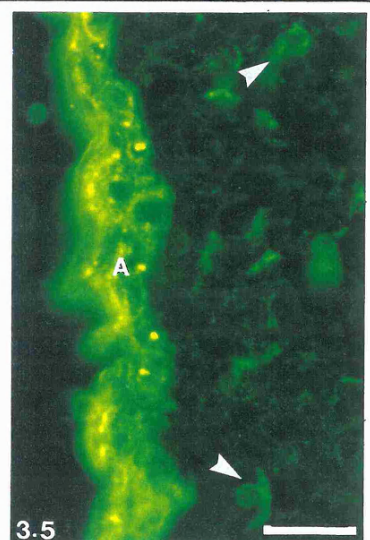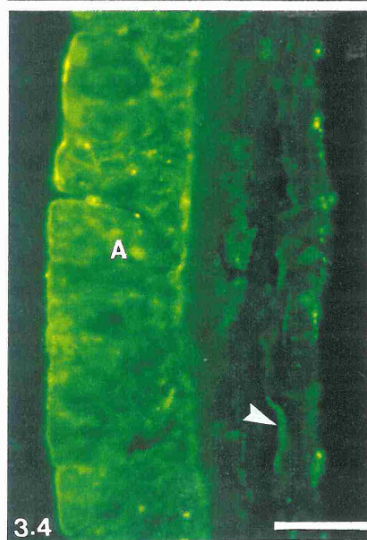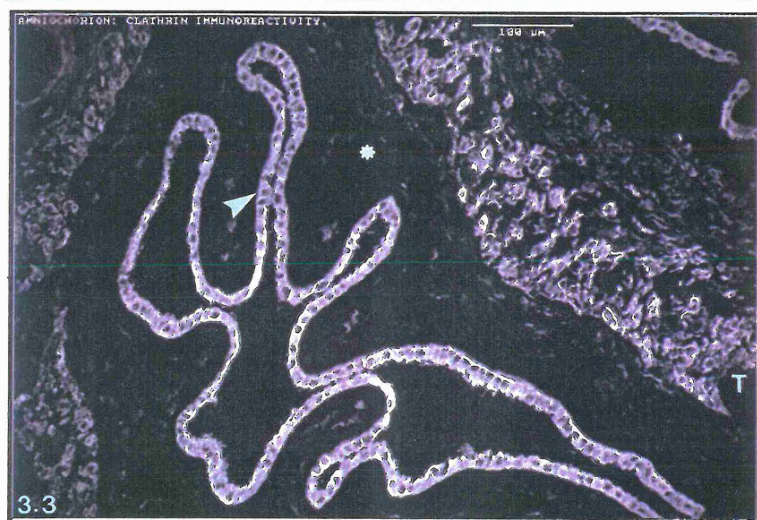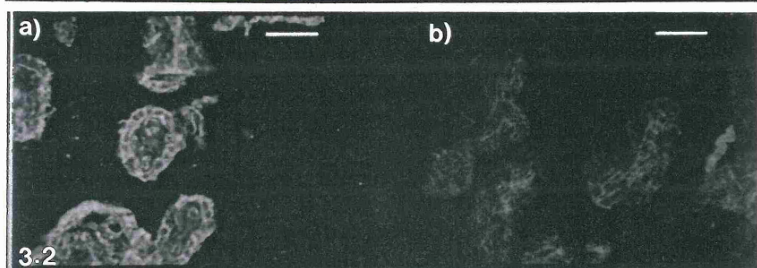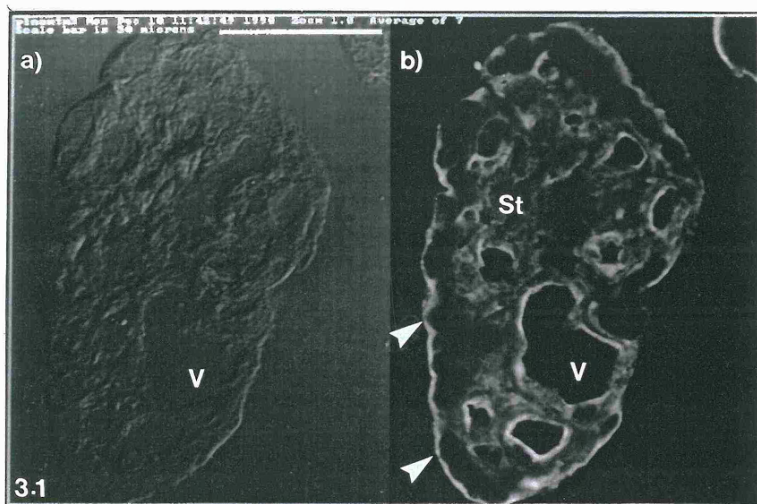
Figures 3.6-3.9: Transmission electron microscopy of coated pits and coated vesicles in a 1st trimester chorionic villus.

Figure 3.6: Coated vesicles (arrowheads) are common features of the apical syncytiotrophoblast (S) cell surface. However, coated pits and vesicles are sufficiently rare at the basal surface to escape detection. Scale bar represents 300nm.

Figure 3.7: TEM of a coated vesicle (arrowhead) pinching off from the apical surface of a 1st trimester cytotrophoblast cell (C). Syncytiotrophoblast (S). Scale bar represents 300nm.

Figure 3.8: TEM of a coated pit (arrowhead) forming at the intercellular cleft between two adjacent 1st trimester endothelial cells (E). Scale bar represents 300nm.

Figure 3.9: TEM of coated pits (arrowheads) and a coated vesicle forming at the cell surfaces of 1st trimester mesenchymal cells (M) in the connective tissue core. Scale bar represents 300nm.

Figures 3.10-3.12: Transmission electron microscopy of coated pits and coated vesicles in a term chorionic villus.

Figure 3.10: A coated pit (arrowhead) and vesicle (arrow) are present at the apical surface of the syncytiotrophoblast (S) in this micrograph of a term chorionic villus. This pattern correlates with the incidence of coated pits and vesicles in 1st trimester syncytiotrophoblast. Scale bar represents 400nm.

Figure 3.11: A coated vesicle (arrowhead) is caught in the act of fusing or pinching off from the luminal (L) plasma membrane of a term endothelial cell (E). Coated pits may also be seen at the abluminal plasma membrane and coated vesicles are often observed intracellularly (not shown). Scale bar represents 400nm.

Figure 3.12: TEM illustrating the presence of a coated vesicle (closed arrow) and coated pits (arrowheads) in a term cytotrophoblast cell (C). A desmosome (open arrow) is also evident attaching the cytotrophoblast cell to the syncytiotrophoblast (S). Basement membrane (BM). Scale bar represents 400nm.
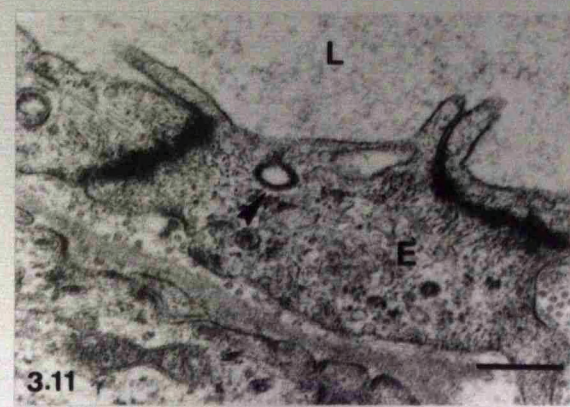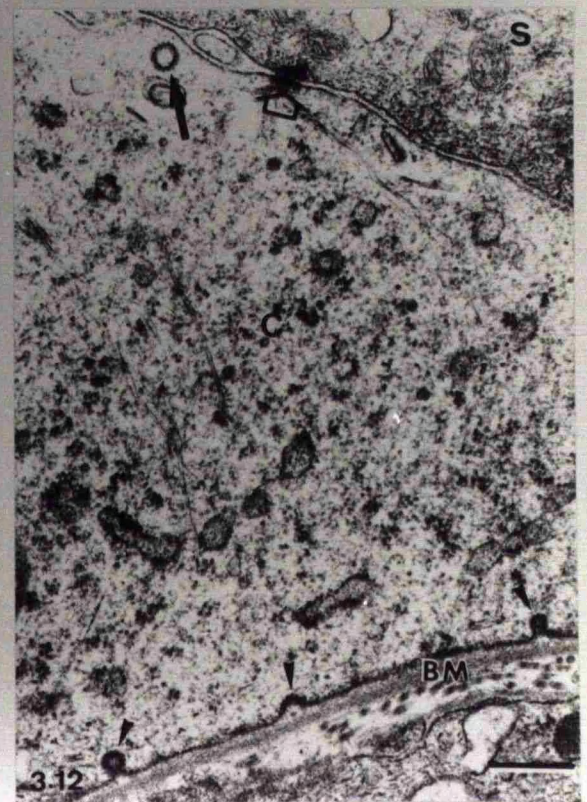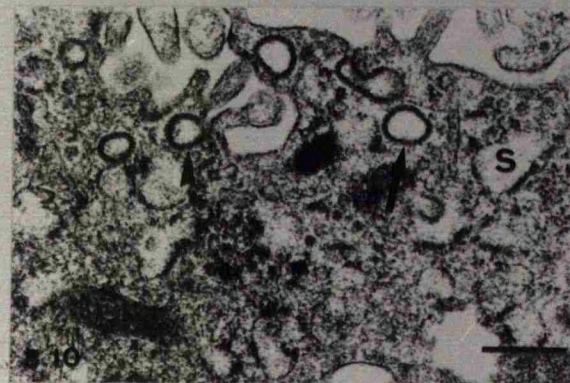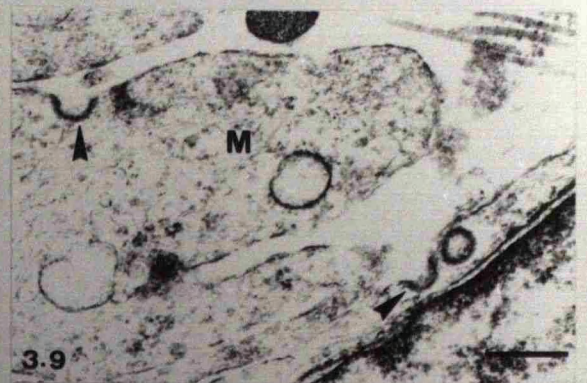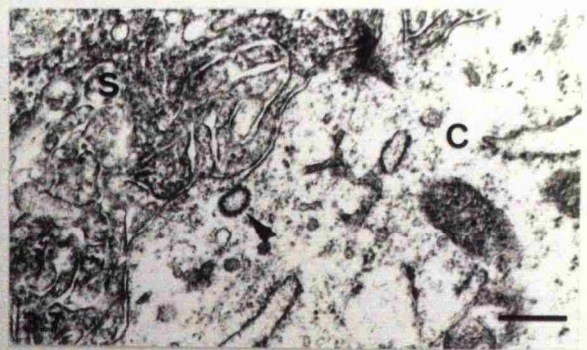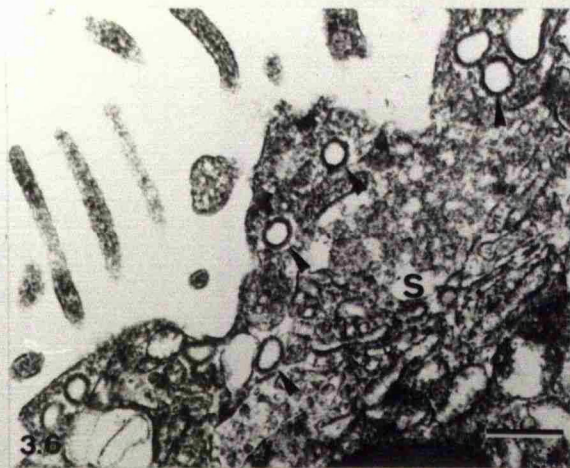
Figures 3.13-3.14: Transmission electron microscopy of coated pits and coated vesicles in a hydatidiform mole chorionic villus.

Figure 3.13: TEM illustrating coated pit formation (arrowhead) and a coated vesicle (arrow) at the apical syncytiotrophoblast surface of a complete homozygous hydatidiform mole specimen. Scale bar represents 400nm.

Figure 3.14: TEM illustrating a coated vesicle (arrow) in a mesenchymal cell of the connective tissue core of a hydatidiform mole specimen. Scale bar represents 400nm.

Figures 3.15-3.19: Transmission electron microscopy of coated pits and coated vesicles in term amniochorion and chorionic plate.

Figure 3.15: Coated pits (arrowheads) forming at the basal foot processes of an amniotic epithelial cell in the amniochorion. Coated pits and coated vesicles are difficult to detect owing to the residual electron-density of the cytoplasmic proteins and numerous electron-dense hemi-desmosomes attaching the epithelial cells to the basement membrane (BM). Scale bar represents 300nm.

Figure 3.16: Coated pits (arrowheads) forming at the surface of cytotrophoblast cells (C) in human term amniochorion. Scale bar represents 300nm.

Figure 3.17: High magnification micrograph of a coated pit forming at the surface of a fibroblast cell (F) in the fibroblast layer of term amniochorion. Scale bar represents 300nm.

Figure 3.18: TEM illustrating a coated pit at the surface of a maternal decidual cell (D) in the decidua parietalis associated with the amniochorion. Scale bar represents 300nm.

Figure 3.19: TEM illustrating the presence of a coated vesicle (arrow) in the basal cytoplasm of an amniotic epithelial cell associated with the placental chorionic plate. Similar to the case with amniotic epithelial cells of the amniochorion these features are difficult to observe due to the presence of hemi-desmosomes and an electron-dense cytoplasm. Basement membrane (BM). Scale bar represents 300nm.

3.13

3.14

3.15   BM

3.16   C

3.17   F

3.18   D

3.19   BM
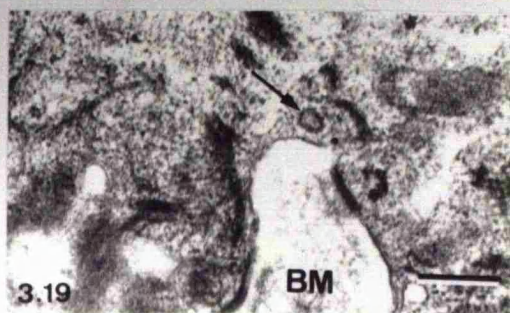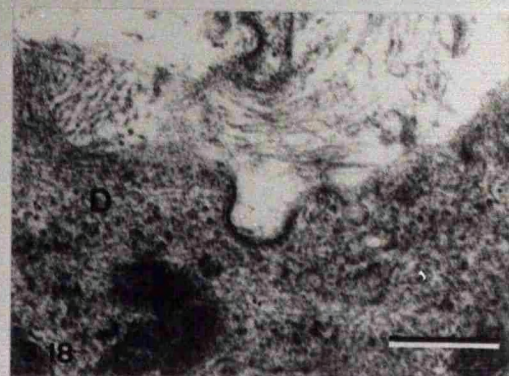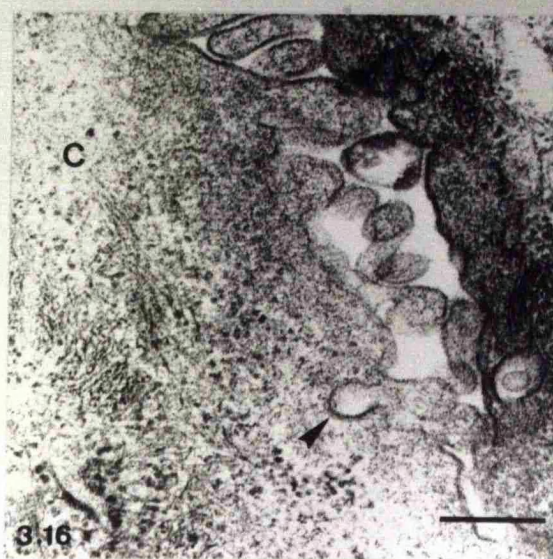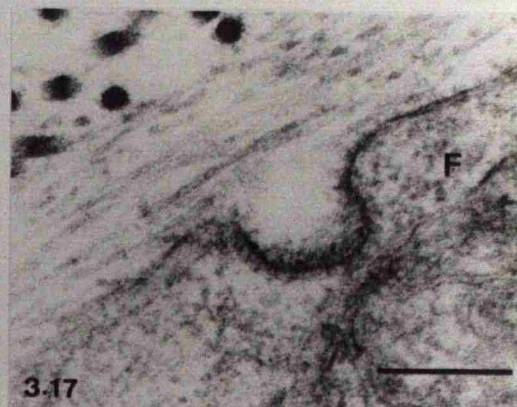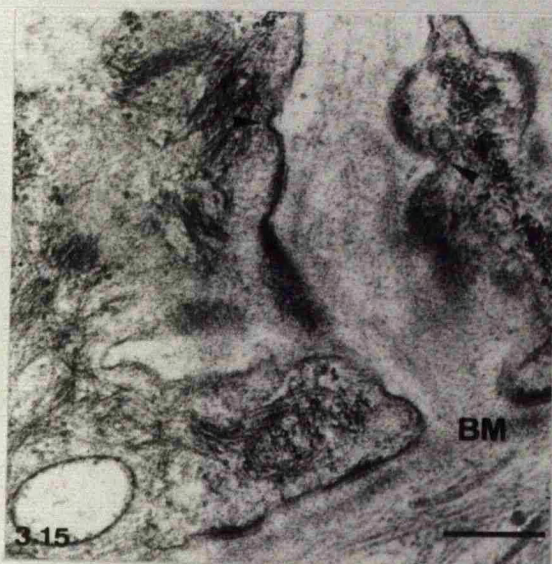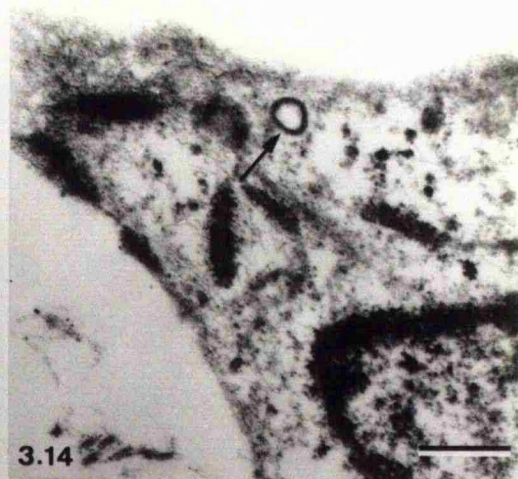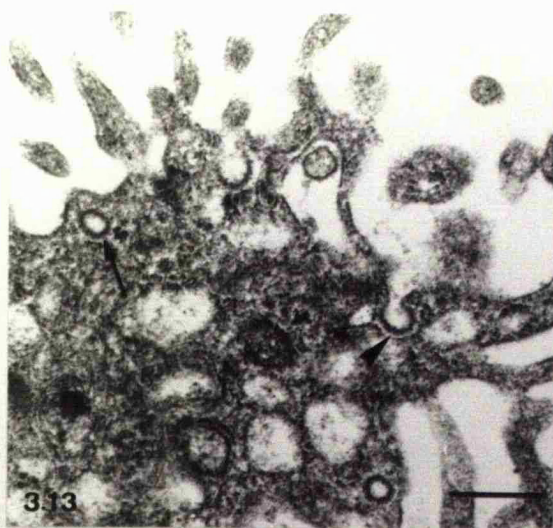
3.4 DISCUSSION.

By correlating the results of the anti-clathrin immunocytochemical experiments with conventional ultrastructural observations of coated pits and vesicles, it has been possible to confirm and extend the known distribution of this molecule in the human placenta and fetal membranes. Clathrin, it would appear, is a ubiquitous cellular protein in the placenta.

Ockleford (1976) and Ockleford and Whyte (1977) were the first to identify clathrin coated pits and vesicles in human placental syncytiotrophoblast. The observations by these authors indicate that coated pits and vesicles are observed only very rarely deep to the maternally orientated apical syncytiotrophoblast surface. This observation has been confirmed using the immunocytochemical experiments performed in the present study since anti-clathrin immunoreactivity is concentrated at the apical syncytiotrophoblast cell surface in first trimester and term chorionic villi. However, this does not exclude the possibility that there may be soluble pools of clathrin within the cell cytoplasm. These cytoplasmic pools could conceivably be washed out into the solutions used to perform the immunocytochemical labelling and thus it is likely that the immunofluorescence localisations achieved are a consequence of insoluble clathrin lattices. Coated vesicles are sufficiently rare to escape frequent detection at the basal plasmalemma in electron micrographs (Ockleford, 1976; Ockleford and Whyte, 1977) and the results of the present study are consistent with this observation since anti-clathrin immunoreactivity was not detected at the basal aspect of the syncytiotrophoblast. It is clear from ultrastructural observations and immunofluorescence that cytotrophoblast cells also possess clathrin coated pits and vesicles.

The distribution of coated vesicles and coated pits in other cell types of the human placenta has not, however, been directly investigated. Anti-clathrin immunoreactivity is associated with cells of the mesenchymal core, including Hofbauer cells. Transmission electron microscopy also reveals the morphologically distinct coated pits and vesicles in these cell types. Endothelial cells surrounding fetal capillaries also possess anti-clathrin immunoreactivity throughout the cell. Ultrastructurally this is reflected in the presence of coated pits at both the luminal (apical) cell surface and the basal (stromal) cell surface. Coated vesicles are evident throughout the cytoplasm of these cells. It is not clear, therefore, if coated vesicles are responsible for transcytosis across the whole cell or if coated pits are responsible for uptake of receptor-bound ligands from both the villus mesenchyme and the capillary lumen.

The distribution of clathrin in cells of the amniochorion has not previously been recorded. This study has demonstrated that anti-clathrin immunoreactivity is associated with the amniotic epithelial cells, fibroblast cells of the mesenchyme, trophoblast cells of the chorion and maternal cells of the uterine decidua including decidual cells, leucocytes and endothelial cells. These localisations may be verified with the observation of coated pits and coated vesicles in these cells in the transmission electron microscope. The amniotic epithelium overlying the placenta and umbilical cord is also immunoreactive with anti-clathrin antibodies. These observations strongly suggest that all of the cells of the human placenta, with the exception of erythrocytes, are adapted for receptor-mediated uptake of ligands. In placental endothelial cells and amniotic epithelial cells the diffuse immunoreactivity pattern may be indicative of transcytosis in these cells.

In the human placenta there is evidence that IgG is associated with vesicular structures. Johnson et. al. (1982) demonstrated an association between IgG and the syncytiotrophoblast using immunofluorescence labelling on cryostat sections. They also found a punctate pattern of labelling indicating that IgG may be taken up into discrete vesicular structures. Furthermore, Lin (1980) discovered IgG in micropinocytotic vesicles, using immunoperoxidase, which correlated in size with coated vesicles. King (1977) reported the localisation of IgG-horseradish peroxidase (HRP) probe in syncytiotrophoblast coated vesicles. Pearse (1982) identified IgG 'heavy chains' in a highly purified sample of coated vesicles from human placenta. Booth and Wilson (1981) were not able to identify IgG in their isolates but these were mainly coated vesicle lattices. Ockleford and Clint (1980) identified tritiated IgG in an isolated fraction enriched in coated vesicles using their wide aperture counting studies.

Whether coated vesicles transport internalised proteins to their destination in the placental syncytiotrophoblast is unknown. This seems unlikely since there is an apical association of clathrin coated pits and vesicles, of which 89% lie within the vesicles largest measured diameter of 540nm (Ockleford, 1976; Ockleford and Whyte, 1977), which suggests that ligands taken up by this route must first pass through an intermediary organelle before being transported to their ultimate destination. It is generally thought that soon after coated vesicle formation that the clathrin dissociates and is recycled back to the surface to participate in further internalisation events (Anderson et. al., 1977; Goldstein et. al., 1979; Pearse, 1980; Heuser, 1980).

Various models have been proposed by which the internalisation of protein within coated vesicles occurs. It is generally accepted that the coated pits pinch off from the plasma membrane to form coated vesicles. However, the mechanism of

invagination and detachment from the surface is not clear. Kaneseki and Kadota (1969) proposed a model of membrane motility for coated vesicle formation. They suggested that extensive hexagonal lattices of clathrin existed beneath the plasma membrane and that binding of ligand to a surface receptor resulted in some of the hexagons in the lattice being converted to pentagons. Such an alteration would thus result in the curvature of the membrane. However, there is no evidence for the existence of such extensive sheets of clathrin lattice and an alternative model of coated pit formation was proposed by Ockleford (1976) and Ockleford and Whyte (1977). This model suggested that vesicle formation is similar to membrane patching. Coated pit formation in this model is induced by binding of the ligand to a receptor molecule which either spans the plasma membrane or is connected to a linker molecule. Binding of ligand acts as a trigger and permits association with clathrin. The addition of further units of receptor-linker permits polymerisation of the clathrin molecules resulting in curvature of the membrane and formation of a coated vesicle.

It is possible that the cytoskeletal elements of the tissue may be involved in coated pit formation since it has been shown that during mitosis coated pits formed at the cell surface do not invaginate (Fawcett, 1965). During mitosis the cytoskeleton of the cell undergoes reorganisation and it is conceivable that the temporary suppression of coated vesicle formation is a consequence of this re-organisation. Thus cytoskeletal components are implicated in coated pit and vesicle function. Calmodulin is also implicated in coated pit formation. Salisbury (1981) demonstrated that inhibition of uptake into coated pits occurred when a calmodulin inhibitor was used. He suggested that calmodulin is involved in conversion of submembranous clathrin to form the coat, or in recruitment of cytoplasmic pools of clathrin into the membrane.

Wehland et. al. (1981) questioned the existence of coated vesicles as separate entities from the plasma membrane. Several sections through apparent coated vesicle profiles showed them to be connected to the plasma membrane by a slender stalk. In addition they suggest that if clathrin molecules were recycling back to the plasma membrane one would expect to find free 'pools' of clathrin within the cytoplasm. These authors were unable to demonstrate the existence of such 'pools'. The model for internalisation proposed by Wehland et. al. (1981) is that the clustered ligand is transferred to a large uncoated intracellular vesicle which is formed either as an invagination from the adjacent plasma membrane or through an opening in the lattice, and that coated vesicles are, in fact, coated pits which do not leave the plasma membrane. They suggest that the vesicular structures seen by other workers (Anderson et. al., 1977; Roth and Porter, 1964) could possibly be joined to the surface

beyond the plane of section. Coated vesicles may be isolated from various tissues by homogenisation (Kaneseki and Kadota, 1969; Pearse, 1976) but Wehland et. al. (1981) suggest that this may be an artefact of the preparation method. However, Fan et. al. (1982) have presented direct evidence supporting the existence of coated vesicles. By serial sectioning 3T3 L1 cells which had been incubated with cationic ferritin these authors were able to demonstrate that 47% of apparent coated vesicles were true vesicles and were not connected to the surface since they contained no ferritin, whereas the other 53% were coated pits containing ferritin. Another study using human fibroblasts demonstrated the existence of coated vesicles as intermediates in absorptive endocytosis (Peterson and Van Deurs, 1983) and therefore this evidence suggests that coated vesicles do play an important role in receptor-mediated endocytosis.

Since coated pits have been shown to have such desirable properties in selecting, and rejecting, proteins for intramembrane transfer, it seemed likely that all selective membrane transport would be initiated by coated pits (Pearse and Bretscher, 1981). Rothman and Fine (1980) examined the role of coated vesicles in the transport of newly synthesised proteins. Their results on the newly synthesised G protein of vesicular stomatitis virus in infected cells indicated that this protein is found in coated vesicles *en route* from the endoplasmic reticulum to the Golgi apparatus, and later in a second transport step from there to the plasma membrane. Furthermore clathrin coated vesicles have been demonstrated in association with clusters of caveolae (Dr. Robert Parton; personal communication). However, the precise roles of intracellular coated vesicles remains to be determined. The structure, function and composition of coated vesicles has been the subject of much debate and is beyond the scope of this thesis. The reader is referred to reviews by Pearse (1987) and Ockleford (1982).

CHAPTER 4: Immunoglobulin G.

4.1 INTRODUCTION.

The human immunoglobulins are a group of structurally and functionally similar macromolecular glycoproteins that confer humoral immunity (Spiegelberg, 1974). The 'backbone' of the immunoglobulin protein consists of 'heavy' and 'light' chains based upon their relative size. Five classes of immunoglobulins have been distinguished on the basis of non cross-reacting determinants in regions with highly conserved amino acid sequences in the constant domains of the heavy chains (Goodman, 1987). As we have seen previously (section 1.1.2) only IgG class antibodies are capable of traversing the placenta in significant amounts.
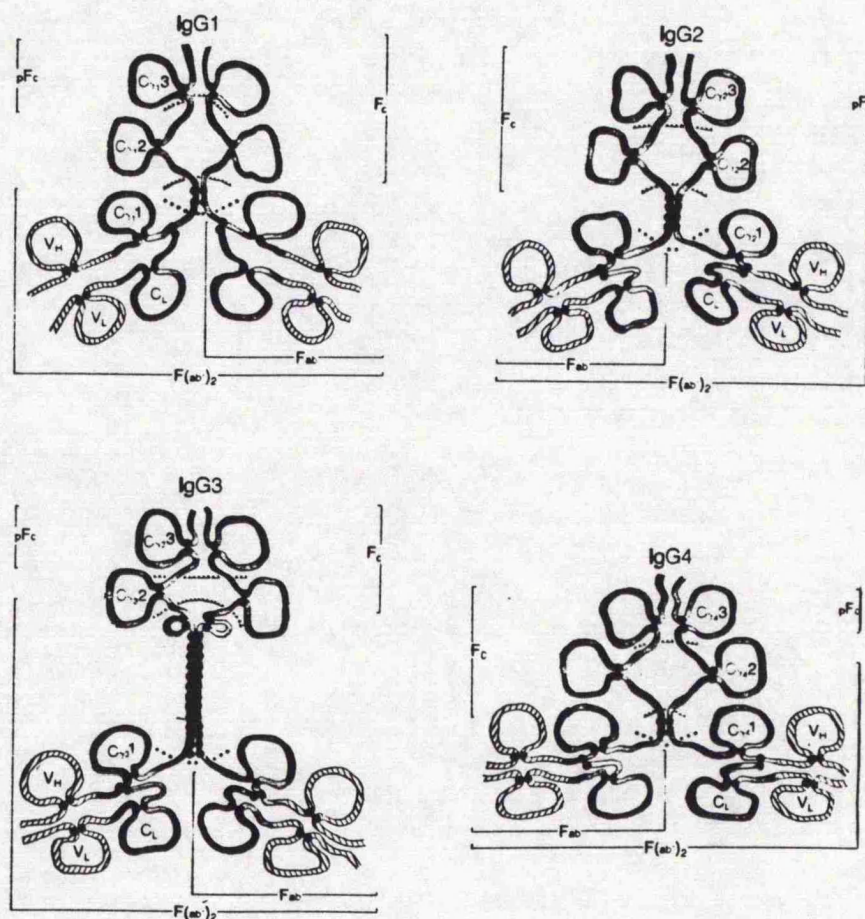
Figure 4.1. Schematic diagram illustrating the four human IgG subclasses. The figure demonstrates the major pepsin cleavage points (•••), papain cleavage points (▲▲) and disulphide (●●) bonds (from Hamilton, 1987).

Four distinct heavy chain subgroups of human IgG were first demonstrated in the 1960s by using polyclonal antisera prepared from animals immunised with human myeloma proteins (Ballieux et. al., 1964; Dray, 1960; Grey and Kunkel, 1964;

Lichter and Dray, 1964; Terry and Fahey, 1964a; 1964b). They were defined as IgG_1, IgG_2, IgG_3 and IgG_4 based upon their relative concentration in normal serum and the frequency of their occurrence as myeloma proteins. The structure and function of each human IgG subclass protein has been extensively investigated using polyclonal antisera and, more recently, monoclonal antibodies. They are glycoproteins composed of two heavy and two light chains linked by interchain disulphide bonds (Burton et. al., 1986; Frangione, 1969; Schur, 1972). Schematic diagrams of the human IgG subclasses are presented in Figure 4.1.

The first approaches to structural analysis were adopted by Porter (1959) who applied proteolytic enzymes, most notably papain, to achieve a limited cleavage of the gammaglobulin fraction of serum into fragments. He obtained antigen binding (Fab) and crystallisable (Fc) fragments. Subsequently other enzymes such as pepsin were used in a similar fashion by Nisonoff et. al. (1960). Edelman (1959) took a different approach. He attempted to cleave molecules of IgG into polypeptide chains by reduction of their disulphide bonds using exposure to denaturing solvents such as 6M urea. This resulted in a significant drop in molecular weight, demonstrating that the IgG molecule is a multichain structure. These polypeptide chains were of two kinds, now called heavy and light chains, and were obviously different from the fragments obtained by proteolytic cleavage.

Some patients with multiple myeloma excrete urinary proteins, antigenically related to immunoglobulins. The nature of these had remained obscure after their first discovery by Henry Bence Jones in 1847. These Bence Jones proteins could be readily obtained from urine in large quantities, were homogeneous, and had low molecular weights. Edelman and Poulik (1961) suggested that these proteins represented one of the chains of the immunoglobulin molecule that was synthesised by the myeloma tumour but not incorporated into the homogeneous myeloma protein. Edelman and Gally (1962) compared light chains of myeloma immunoglobulins with Bence Jones proteins in urea using starch-gel electrophoresis and, by peptide mapping, Schwartz and Edelman (1963) confirmed this hypothesis. The results of experiments with Bence Jones proteins and purified intact myeloma immunoglobulins have a number of significant implications. Because different Bence Jones proteins had different amino acid compositions it became clear that immunoglobulins must vary in their primary structures (Koshland and Engelberger, 1963). The first report by Hilschman and Craig (1965) on partial sequences of several different Bence Jones proteins indicated that the structural heterogeneity of the light chains was confined to the amino terminal (variable) region, whereas the carboxyl terminal half of the chain was the same in all chains of the same type (the constant region).

Amino acid sequence analysis of the Fc region of normal rabbit γ-chains by Hill et. al. (1966) demonstrated that the carboxyl terminal portion of heavy chains were homogeneous. Comparisons of the complete amino acid sequence and arrangement of the disulphide bonds of entire human immunoglobulin G myeloma proteins showed that heavy chains had variable (V_H) regions in the amino terminus (Edelman, 1973). The studies of Edelman and his co-workers further demonstrated that the variable regions of the light and heavy chains are homologous to one another but not to the constant regions of these chains. It also became clear that the constant region of the heavy chains consist of three homologous regions, C_H1, C_H2 and C_H3 which show homology with each other and the constant regions of the light chains. Thus Edelman and his colleagues, having elucidated that these regions contained intrachain disulphide bonds postulated that these regions folded into globular domains. A schematic representation of the IgG molecule is shown in Figure 4.2. The precise structural details and the genetics underlying the generation of antibody diversity are beyond the scope of this introduction but the reader is referred to comprehensive accounts of these studies elsewhere (Silverton et. al., 1977; Edelman, 1973; Leder, 1982; Gough, 1981).
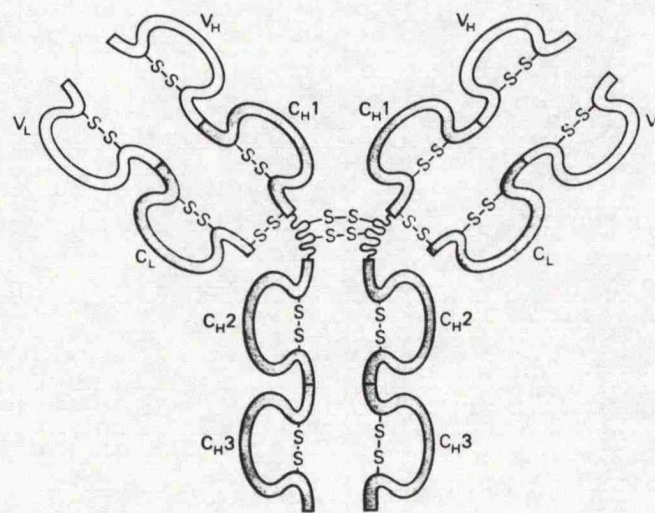
Figure 4.2. Schematic illustration of human IgG demonstrating that the light and heavy chains are folded into globular domains. The variable domains of the light and heavy chains (V_L and V_H) make up the antigen binding sites. The constant domains of the heavy chains (mainly C_H2 and C_H3) determine the other biological properties of the molecule (from Alberts et. al., 1983).

Two types of light chain may be identified based upon their significantly different amino acid sequences. These are called Kappa (κ) and lambda (λ) light chains. Differences in the amino acid content of the heavy chains and the ratio of κ to λ light chains are characteristic of the different subclasses of IgG. While the primary amino acid sequences of the constant regions of the IgG subclass heavy chains are greater than 95% homologous, major structural differences are found in the hinge

region in terms of the number of residues and the number of interchain disulphide bonds. The IgG_1 hinge is 15 amino acid residues long and freely flexible such that the Fab fragments may rotate about their axes (Colman et. al., 1976). IgG_2 has a shorter 12 amino acid hinge with 4 disulphide bridges at the Fab base. The hinge region also lacks a glycine residue which almost completely prevents rotation and restricts lateral movement of the Fabs (Pumphrey, 1986). IgG_3 has a unique elongated hinge region containing 62 amino acids (including 21 prolines and 11 cysteines) that has been described as an inflexible polyproline double helix (Burton et. al., 1986; Michaelsen et. al., 1977; Pumphrey, 1986; Saluk and Clem, 1975). This makes it more readily available for the binding of complement component 1q (C1q). The hinge region of IgG_4 is shorter than that of IgG_1 and some rotation may occur around a glycine residue. However access of C1q to the IgG_4 Fc is hindered by the shortness of the hinge region (Pumphrey, 1986).

The point of light chain attachment to the heavy chain also differs among the subclasses. IgG_1 light chains are bound near the midpoint of the heavy chain, while IgG_2, IgG_3 and IgG_4 are joined one quarter the distance from the heavy chain amino termini (Pumphrey, 1986). Both the heavy and light chains contain intrachain disulphide bonds that form parts of the molecule into compact globular regions called domains. These domains participate in the biological functions of the immunoglobulin. Unique antigenic determinants are generally found in the Fc region of IgG_1, IgG_2 and IgG_4 and the hinge region of IgG_3. Genetic markers (Gm allotypes) are regular minor differences in primary amino acid sequences between molecules of an IgG subclass that occur throughout a species as a result of gene mutation (Van Loghem, 1978; 1986). In man, some allotypic markers are restricted to constant region domains of single IgG subclasses, while others are shared by several subclasses. Discussions of the human IgG allotypes and their importance in man are presented elsewhere (Litwin and Balaban, 1972; Morell et. al., 1972b; Schanfield, 1976; Shakib and Stanworth, 1980).

The concentration of each immunoglobulin in the serum of healthy individuals depends in part on the number of plasma cells that produce that particular immunoglobulin, the rate of synthesis, catabolism and the exchange between intra- and extravascular spaces. In adults, IgG_1 is highest in concentration (5-12 mg/ml) followed by IgG_2 (2-6 mg/ml), IgA_1 (0.5-2 mg/ml), IgM (0.5-1.5 mg/ml), IgG_3 (0.5-1 mg/ml), IgG_4 (0.2-1 mg/ml), IgD (0-0.4 mg/ml), IgA_2 (0-0.2 mg/ml) and IgE (0-0.002 mg/ml) (French, 1986; Shakib and Stanworth, 1980). IgG has the highest synthetic rate and longest biological half-life of any immunoglobulin in serum. Studies of clearance rates of radiolabelled IgG myeloma proteins *in vivo*

have demonstrated a higher catabolic rate for human IgG_3 than IgG_1, IgG_2 and IgG_4 (Morell et. al., 1970; Speigelberg and Fishkin, 1972).

The biological properties of the human IgG subclasses may be categorised as specific reactions of the Fab region with antigen (primary function) and effector (secondary functions) that occur as a result of antigen binding and that are properties of the constant regions of the heavy chains, particularly the Fc. Complement activation is probably the most important biological function of IgG. Activation of the complement cascade by the classical pathway is initiated by the binding of C1q to sites on the Fc portion of human IgG. The globular heads of C1q interact with amino acids in the second heavy chain constant region (C_H2). Reactivity of complement with IgGs of the four human subclasses varies as a function of steric interference by the Fab arms in the approach of C1q to the C_H2 sites ($IgG_3 > IgG_1 > IgG_2 > IgG_4$; Brunhouse and Cebra, 1979; Feinstein et. al., 1986; Ishizaka et. al., 1967).

Another vitally important function of human IgG is its ability to bind to cell surface Fc receptors as we shall see in chapter 5. Once IgG is bound to the surface of certain cell types it may complex antigen and facilitate the clearance of immune complexes by phagocytosis. Binding of IgG to these receptors also triggers other effector functions. In addition the human IgG subclasses are known to bind with other proteins. The Fc region of human IgG_1, IgG_2 and IgG_4 bind to protein A from *Staphylococcus aureus* (Kronvall and Frommel, 1970; Kronvall and Williams, 1969). A single amino acid substitution of arginine for histidine at amino acid position 435 in the Fc region prevents binding of protein A to IgG_3 (Recht et. al., 1981). In recent years it has also been demonstrated that protein G from various strains of Streptococci binds to the Fc of various immunoglobulins (Björk and Kronvall, 1984; Åkerström et. al., 1985). Although there are similarities between protein A and G, the latter appears to bind to a wider species range of antibodies and, in most cases, its affinity for those antibodies is higher (Åkerström and Björck, 1986).

This overview has summarised some of the major differences in the structure and effector functions of the human IgG subclasses. The aim of the work presented in this chapter is to examine the normal anatomical and histological distribution of IgG in the human placenta and fetal membranes using immunofluorescence microscopy. This may facilitate a better understanding of how the fetal circulation acquires maternal immunoglobulins.

4.2 MATERIALS AND METHODS.

4.2.1 Tissue collection.

Freshly dissected samples of 1st trimester (n=6), term (n=10), term Cesarean section (n=14) and hydatidiform mole (n=3) chorionic villi were obtained from the Leicester Royal Infirmary. The amniochorion from Cesarean section (n=14) and term (n=10) placentae was also collected from these deliveries and the tissue was stored as described in section 3.2.1.

A variation performed was to pre-fix the tissue for 3 hours at room temperature with 4% paraformaldehyde in 0.1M PBS. This tissue was subsequently embedded with O.C.T. and processed as previously described. First trimester chorionic villi (n=3), term Cesarean section chorionic villi plus chorionic plate (n=3), term Cesarean section amniochorion and umbilical cord (n=3) were processed in this way.

4.2.2 Indirect immunofluorescence.

Cryosections of the frozen tissue blocks were adhered to immunofluorescence slides as described in section 3.2.2. Optional steps included the application of 3% formaldehyde diluted in 0.1M PBS for 10 minutes at room temperature and permeabilisation with 0.05% Triton X-100 in 0.1M PBS for 10 minutes. Immunofluorescence preparations of anti-human IgG immunoreactivity were made according to the procedures described in section 3.2.2.

4.2.2.1 Primary antibodies.

The various primary antibodies used in this study were directed against human immunoglobulin G. Polyclonal goat anti-human IgG (whole molecule) was developed in goat using IgG from pooled normal human serum as the immunogen (Sigma, Code No.: I-1886; Lot No.: 29F-4897). Whole antiserum is fractionated and further purified by ion exchange chromatography to provide the IgG fraction of antiserum in this product. This antibody was stored at -18°C in 10µl aliquots until required and then at 4°C for up to 1 month. It was applied to tissue sections at a dilution of 1/100 (dilution range tested: 1/20 - 1/400). A concentration of 5% NRS was included in this dilution to act as a block for non-specific immunoglobulin interactions.

To avoid the possibility of cross-reactivity of the exogenous immunological reagents used with endogenous Fcγ receptors of the tissue (see chapter 5), thus giving false positive localisations, immunofluorescence experiments to localise endogenous IgG were performed with reagents likely to possess minimum cross-reactivity. To conduct these experiments biotinylated F(ab')$_2$ fragments of goat anti-human IgG (γ-chain specific; Sigma, Code No.: B1518; Lot No.: 88F8985) were applied as the primary antibody. The F(ab')$_2$ fragment of the goat anti-human IgG in this product was isolated from a pepsin digest of fractionated antiserum and affinity-isolated to remove essentially all goat serum proteins and immunoglobulins which do not bind specifically to the γ-chain of human IgG. These fragments are conjugated with Sigma N-Hydroxysuccinimidobiotin (Code No.: H-1759). This product was applied to the tissue at a dilution of 1/50 (dilution range tested: 1/20 - 1/500) and included a 5% concentration of NGS to block non-specific interactions of the goat antibodies. This product was stored in 10µl aliquots at -18ºC until required and subsequently for up to 1 month at 4ºC.

4.2.2.2 Secondary antibodies.

The secondary reagents used in this investigation were as follows: i) Primary goat anti-human IgG antibodies were localised with FITC-conjugated rabbit anti-goat IgG (heavy and light chain; ICN Biomedicals, Code No.: 65-176; Lot No.: 0012). This antibody was applied at a dilution of 1/500 (range tested: 1/100 - 1/2000) containing 5% NRS. This antibody was stored as previously described (section 3.2.2.2).

The primary biotinylated antibodies were detected with FITC- or TRITC-conjugated ExtrAvidin (Sigma, Code No.: E2761, Lot No.: 090H4881 and Sigma, Code No.: E3011, Lot No.: 59F-4807 respectively). ExtrAvidin is a uniquely modified avidin reagent prepared from chick egg white avidin. It is a tetrameric protein containing 4 high affinity binding sites for biotin (vitamin H) and combines the high specific activity of avidin with the low background staining of streptavidin, a biotin binding protein produced by the bacteria *Streptomyces avidinii*. ExtrAvidin binds biotin with the high affinity of egg white avidin (Kd = 10^{-15} M^{-1}) but it does not, however, exhibit the unwanted non-specific binding reported for egg white avidin at physiological pH such as the staining of mast cells. Thus the binding of avidin to biotin by the essentially irreversible non-covalent interaction is utilised in immunoassays by coupling antibodies to biotin and conjugating avidin to marker molecules such as fluorochromes (Bayer et. al., 1979; Wilchek and Bayer, 1984). These products were used at a dilution of 1/500 (range tested: 1/100 - 1/2000) containing 5% NGS. Storage was at -18ºC for long periods and at 4ºC for up to 1 month when required.

4.2.2.3 Direct immunofluorescence.

Direct immunofluorescence investigations were performed to verify the data obtained from the indirect immunofluorescence experiments. Tissue was processed as described in section 3.2.2 and affinity-purified $F(ab')_2$ fragments of rabbit anti-human IgG conjugated to FITC (Serotec, Code No.: ST-AR 9A, Batch No.: 001) were applied to the tissue sections for 1 hour at 37°C or 24 hours at 4°C. These antibodies were diluted 1/100 in 0.1M PBS (range tested: 1/50 - 1/500) containing 5% NRS as a block for non-specific interactions. Storage was at -18°C for long periods and at 4°C for up to 1 month when required.

4.2.2.4 Non-immune sera.

Throughout these investigations a concentration of 5% non-immune rabbit serum (NRS; Sigma, Code No.: R9133) or 5% non-immune goat serum (NGS; Sigma, Code No.: G9023) was included with the primary and secondary antibody dilutions as appropriate, to prevent non-specific labelling.

4.2.2.5 Control experiments.

Four independent control experiments were conducted during these investigations in the manner described in section 3.2.2.4. The first control was performed by omitting the primary specific antibody and incubating the sections with blocking reagents only. The control tissue was treated identical to experimental tissue at all subsequent stages. The second control experiment was performed by replacing the primary specific anti-human IgG antibody with an equivalent dilution (1/100) of non-immune (goat) serum to investigate the non-specific interactions engaged by goat antibodies.

The third control was conducted by challenging the primary specific anti-human IgG antibodies with an addition of exogenous polyclonal human IgG (ICN Biomedicals, Code No.: 64-145-1, Lot No.: A0680). Exogenous human IgG was added to the primary antibody solution at a concentration of 1×10^{-6}g ml^{-1} to 1×10^{-4}g ml^{-1} and the reduction in fluorescence intensity, compared to sections immunoreacted without the presence of IgG challenge, was observed. An additional control, performed in conjunction with the direct immunofluorescence experiments, was to incubate the tissue sections with an equivalent dilution (1/100) of FITC-conjugated $F(ab')_2$ fragments of rabbit antibodies directed against an inappropriate antigen. This was performed by incubating the control sections with a 1/100 dilution of FITC-

conjugated F(ab')$_2$ rabbit anti-mouse IgG (Serotec, Code No.: ST-AR 9, Batch No.: 016).

4.2.2.6 Fluorescence nuclear counterstaining.

In some of the immunofluorescence investigations described, the nuclei of cells in the tissue sections were counterstained with a solution of propidium iodide (appendix V) as described by Ockleford et. al. (1981). This was performed during the penultimate wash for 5 minutes at 4°C. The sections were rinsed for a further 2 x 5 minutes with 0.1M PBS prior to mounting.

4.2.2.7 Slide subbing.

Tissue sections of samples which had been pre-fixed with 4% paraformaldehyde in 0.1M PBS were adhered to immunofluorescence slides which had been coated with a slide subbing solution of 2% 3-Aminopropyltriethoxysilane (appendix VI) to prevent the sections from dislodging from the slides during the subsequent changes of solutions.

4.2.3 Mounting.

The tissue sections were mounted with Citifluor photobleach retardant mountant or Gurrs fluoromount under No. 0 thickness coverslips (Chance Propper Ltd.) and sealed with nail-varnish as described in section 3.2.3.

4.2.4 Microscopy and photography.

The immunofluorescence preparations were examined and recorded as previously described in sections 3.2.4 and 3.2.5.

4.3 RESULTS.

The results of these investigations confirmed the presence of endogenous IgG in the cells and tissues of the placenta and fetal membranes.

4.3.1 First trimester chorionic villi.

Endogenous IgG was clearly demonstrated in the syncytiotrophoblast surrounding 1st trimester villi (Figures 4.3-4.12). The connective tissue core of 1st trimester villi possessed little or no immunoreactivity for IgG in unfixed frozen tissue sections or sections post-fixed with 3% formaldehyde (Figures 4.3 and 4.12). However, the connective tissue core of specimens pre-fixed with 4% paraformaldehyde did, on occasion, display detectable immunoreactivity with the antibodies used in this investigation (Figures 4.7-4.8 and 4.10-4.11). These observations suggest that soluble endogenous antibodies present in the tissue sections may be washed out into the incubating solutions, even when the tissue is immediately immersed into fixative solutions after sectioning. By pre-fixing the tissue with 4% paraformaldehyde it was possible to establish firstly that IgG immunoreactivity is conserved and secondly that a limited presence of endogenous antibody is associated with the stroma of the villus core.

The most striking observation to emerge from this investigation was that cytotrophoblast cells underlying the syncytiotrophoblast were not immunoreactive with the panel of anti-human IgG antibodies used to conduct these experiments (Figures 4.7-4.11). By counterstaining nuclei with propidium iodide (Figure 4.12) or examining specimens with Nomarski optics (Figures 4.7-4.8) these experiments revealed that cytotrophoblast cells did not contain endogenous IgG but that the overlying syncytiotrophoblast was immunoreactive. Furthermore, at intermittent places where the cytotrophoblast cell layer had become discontinuous, immunoreactive syncytiotrophoblast was seen to extend to the basal lamina (Figures 4.8 and 4.10-4.11). This was more clearly seen in preparations which were optically sectioned using the confocal laser scanning microscope and demonstrated that these fine projections of immunoreactive syncytiotrophoblast only extended to the basal lamina where the cytotrophoblast cells had relinquished contact with one another. These observations were made in preparations of 4% paraformaldehyde pre-fixed material since the tissue morphology was vastly superior to unfixed material.

The enhanced tissue morphology of these preparations and sensitivity of the dark-field confocal microscopy techniques also permitted visualisation of subcellular vesicular inclusions in the apical syncytiotrophoblast (Figure 4.5). IgG

immunoreactivity was concentrated at the periphery of these vesicular inclusions and 3-dimensional reconstruction of serial optically sectioned vesicles, using the confocal laser scanning microscope, demonstrated that they were roughly spherical in structure.   Apical punctate immunoreactivity was also observed in the syncytiotrophoblast (Figure 4.6) indicating the presence of endosomal or lysosomal-like inclusions.

4.3.2 Term chorionic villi.

In the villi of term placentae IgG was associated with endothelial cells and cells of the villus core. It was often concentrated in regions of the extracellular matrix (Figures 4.14-4.16). In immunofluorescence preparations of unfixed frozen tissue sections the contents of the fetal blood capillaries were frequently washed out into the solutions used to wash, incubate or fix the material. However, improved tissue morphology was achieved by pre-fixing the tissue sections with 4% paraformaldehyde.   In experiments performed with this tissue, IgG immunoreactivity was clearly associated with the serum proteins in the lumen of fetal capillaries but erythrocytes were negative (Figure 4.15). The villus stroma was intensely immunoreactive for endogenous IgG when compared to immunoreactivity in first trimester chorionic villi.

The trophoblast of term villi was also immunoreactive. This localisation was predominantly apically associated and, upon examination using the confocal laser scanning microscope, the increased resolution afforded visualisation of a punctate apical pattern of fluorescence.   This was more clearly demonstrated in grazing sections of the syncytial trophoblast (Figure 4.14). The labelled vesicular inclusions observed in 1st trimester chorionic villi were not apparent. By counterstaining nuclei with propidium iodide or examining specimens with Nomarski optics this study revealed that cytotrophoblast cells did not contain endogenous IgG.

In transverse sections through the chorionic plate of the placenta it was possible to demonstrate IgG immunoreactivity associated with the serum proteins of the placental blood vessels and with the extracellular matrix (Figure 4.16).   The immunofluorescence intensity was greatly reduced in the adventitia.

4.3.3 Amniochorion.

Endogenous IgG immunofluorescence was demonstrated in the extracellular matrix of the amnion, chorion and maternal decidua (Figures 4.17-4.20). In addition, IgG immunoreactivity was associated with a population of cells of the fibroblast and

reticular layers and with cells of the maternal uterine decidua. This study failed to reveal endogenous IgG immunofluorescence associated with either cells of the amniotic epithelium or cytotrophoblast cells of the chorion laeve (Figure 4.17).

Using material which had been pre-fixed with 4% paraformaldehyde it was possible to demonstrate that finger-like projections of the amniotic epithelial basement membrane possessed IgG immunoreactivity that extended between the basal foot-processes of the amniotic epithelium (Figure 4.18). However, no immunoreactive molecules were associated with the epithelial cells or their intercellular spaces. A notable exception to this observation was that damaged, dying or dead amniotic epithelial cells did contain endogenous IgG (Figure 4.19). These cells had frequently relinquished contact with neighbouring cells and/or the basement membrane thus exposing the underlying mesenchyme. They were noticeably more anisotropic than surrounding healthy epithelial cells in phase contrast suggesting that they had lost soluble cytoplasmic contents. The nuclear envelope, surrounding the nuclei of these cells often maintained its integrity and thus excluded IgG (Figure 4.19). These small populations of immunoreactive cells could frequently be observed in the amniotic epithelium of tissue delivered by routine term vaginal delivery. However, in tissue delivered by elective Cesarean section, immunoreactive cells were observed infrequently and occurred in only two out of fourteen cases.

Cytotrophoblast cells of the trophoblast layer of the amniochorion did not display immunoreactivity with the panel of anti-human IgG antibodies used in these investigations. These data are consistent with observations that IgG was not associated with cytotrophoblast cells of term (section 4.3.2) or 1st trimester chorionic villi (section 4.3.1). However, these experiments indicated that IgG was associated with the extracellular matrix surrounding the trophoblast cells.

Placental amnion.
Transverse sections through the chorionic plate of the placenta demonstrated that it possessed a surface covering of amniotic epithelial cells (placental amnion). Immunofluorescence investigations of anti-human IgG immunoreactivity showed that these epithelial cells, like those of the amniochorion, did not contain endogenous antibody (Figure 4.22). Tissue obtained from routine vaginal delivery possessed damaged cells that had relinquished cell-cell and basement membrane contacts. These cells possessed endogenous antibody (Figure 4.23).

Umbilical cord.

These observations could also be extended to the amniotic epithelium overlying the umbilical cord which was not immunoreactive for endogenous IgG (Figure 4.24). However, antibody was clearly present in the Whartons jelly of the umbilical cord and was associated with cellular components of the cord. Strands of IgG immunoreactivity penetrated between the cells of the adventitia surrounding the umbilical vessels but the endothelium was not immunoreactive. The plasma proteins of the vessels did possess IgG as did leucocytes present in the lumen of the vessels.

4.3.4 Hydatidiform mole.

Anti-human IgG immunofluorescence preparations of human hydatidiform mole specimens yielded consistent results to those obtained with 1st trimester villi of similar gestational age. Specimens in which the cell nuclei had been counterstained with propidium iodide (Figure 4.13) or when observed using phase contrast or Nomarski optics revealed that cytotrophoblast cells underlying the syncytium did not contain endogenous antibody. However, the syncytiotrophoblast was strongly immunoreactive. Low levels of immunofluorescence were associated with the connective tissue core but, since complete hydatidiform moles did not possess a vascular system, an association with endothelium was not noticed.

4.3.5 Control experiments.

Control experiments, performed by incubating the primary anti-human IgG antibodies in the presence of exogenous IgG (Figure 4.21), replacing the primary specific antiserum with an equivalent concentration of non-immune serum from the same species or by omitting the primary specific antiserum, yielded negligible levels of background. Chorionic villi, from 1st trimester placentae, term placentae and hydatidiform mole placentae demonstrated low levels of background using these control experiments as did control preparations of the umbilical cord, chorionic plate and amniochorion.

The fluorescence intensity of serial sections of term amniochorion, incubated with $F(ab')_2$ fragments of rabbit anti-human IgG conjugated to FITC, decreased when progressively higher concentrations of exogenous human IgG were added to the solutions (Figure 4.21). This demonstrated that endogenous human IgG in the tissue sections was the antigen to which the · antibodies bound and that the immunofluorescence observed was not a consequence of non-specific interactions. Furthermore, direct application of similar concentrations of fluorochrome-conjugated

F(ab')$_2$ fragments of rabbit anti-mouse IgG (instead of rabbit anti-human IgG) did not reveal specific immunofluorescence (Figure 4.4d).

FIGURES 4.3 - 4.24.

Figures 4.3-4.6: Anti-human IgG immunoreactivity in 1st trimester chorionic villi.

Figure 4.3: Confocal direct immunofluorescence micrograph of F(ab')$_2$ rabbit anti-human IgG:FITC immunoreactivity in an unfixed frozen section of a 1st trimester chorionic villus. Utilisation of F(ab')$_2$ fragments of immunological reagents excludes the possibility of cross-reactivity with endogenous Fcγ receptors. Immunoreactivity is confined to the syncytiotrophoblast but the underlying cytotrophoblast cells (arrowheads) and connective tissue stroma (St) are devoid of endogenous antibodies. Scale bar represents 50μm.

Figure 4.4: Multi-channel montage of confocal Nomarski (a and c), direct immunofluorescence (b) and control (d) preparations in 4% paraformaldehyde pre-fixed frozen tissue sections. a) Nomarski DIC of panel b). b) Direct F(ab')$_2$ rabbit anti-human IgG:FITC immunoreactivity demonstrating fluorescence in the surrounding trophoblast and a low level of detectable fluorescence in the stroma. c) Nomarski DIC of panel d). d) Control preparation utilising an equivalent concentration of F(ab')$_2$ rabbit anti-mouse IgG. No immunofluorescence is detectable. Scale bar represents 100μm.

Figure 4.5: High resolution confocal indirect immunofluorescence micrograph of endogenous IgG immunoreactivity in the trophoblast of a 4% paraformaldehyde pre-fixed frozen 1st trimester chorionic villus section. The primary antibody was F(ab')$_2$ goat anti-human IgG (γ-chain specific) detected with ExtrAvidin:FITC. The increased resolution in the z-plane achieved by this instrument facilitates detection of IgG at the periphery of vesicular inclusions in the syncytiotrophoblast (Sy) since out-of-focus blur is essentially abolished. Underlying cytotrophoblast cells (C) are not immunoreactive. Scale bar represents 10μm.

Figure 4.6: High resolution confocal indirect immunofluorescence micrograph of endogenous IgG immunoreactivity prepared as described above. The increased resolution afforded by this instrument facilitates detection of immunoreactive apical endosomal inclusions in the syncytiotrophoblast (Sy). Underlying cytotrophoblast cells (C) are not immunoreactive. Scale bar represents 10μm.

4.3

St

1st TRIMESTER CHORIONIC VILLI.
NOMARSKI DIC.
a

IgG.
b

NOMARSKI DIC.
c

CONTROL.
d

4.4   100 µm

C

Sy

4.5

C

Sy

4.6
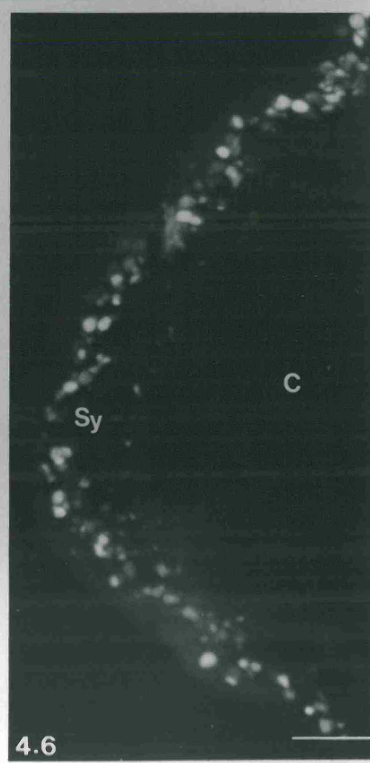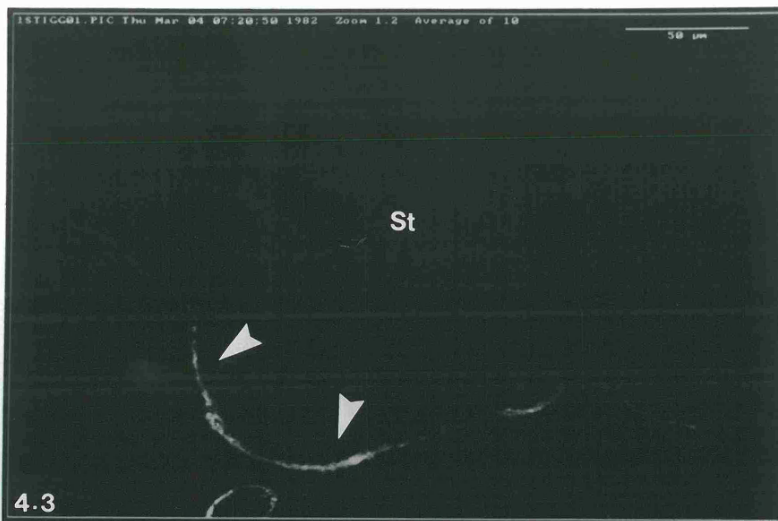
Figures 4.7-4.13: Anti-human IgG immunoreactivity in 1st trimester chorionic villi.

Figure 4.7: Dual-channel colour confocal micrograph illustrating Nomarski DIC (grey channel) and endogenous IgG immunoreactivity (green channel) in a 4% paraformaldehyde pre-fixed frozen 1st trimester chorionic villus section. The surrounding syncytiotrophoblast is intensely immunoreactive but cytotrophoblast cells, sectioned in an appropriate plane (black arrowheads), are not immunoreactive. There is low, but detectable, immunofluorescence in the stroma (St) of villi prepared in this way. Association of immunofluorescence with immature capillary endothelial cells (white arrowhead), which are known to express Fcγ receptors, is often evident. Scale bar represents 100μm.

Figure 4.8: High resolution, dual-channel, colour confocal indirect immunofluorescence micrograph of endogenous IgG immunoreactivity (green channel) prepared as described above. The syncytiotrophoblast is strongly immunoreactive but underlying cytotrophoblast cells (arrowheads) are devoid of endogenous antibody. Note that the syncytium is immunoreactive where it penetrates between cytotrophoblast cells (open arrow) and there is evidence of detectable IgG in the stroma (St) beneath this region. Scale bar represents 10μm.

Figure 4.9: Confocal indirect immunofluorescence micrograph of IgG immunoreactivity in the syncytiotrophoblast of a 4% paraformaldehyde pre-fixed chorionic villus. Note that the complete layer of cytotrophoblast cells (open arrows) underlying the syncytium is devoid of endogenous antibodies as is the villus stroma (St). Scale bar represents 50μm.

Figures 4.10 and 4.11: In these micrographs, prepared as described above, endogenous IgG immunoreactive syncytiotrophoblast may be seen to penetrate between cytotrophoblast cells (open arrows) to contact the basement membrane (closed arrows). There is evidence of endogenous IgG in the stroma (St) underlying these regions. Scale bars represent 50μm and 20μm.

Figure 4.12: Confocal F(ab')$_2$ direct immunofluorescence localisation of endogenous IgG (green channel). Nuclei (red channel) have been counterstained with propidium iodide. Cytotrophoblast cells (arrowheads) and the connective tissue stroma (St) are not immunoreactive. Scale bar represents 50μm.

Figure 4.13: Confocal direct immunofluorescence localisation of endogenous IgG in a hydatidiform mole specimen prepared as described above. Cytotrophoblast cells (arrowheads) and the stroma are not immunoreactive. Scale bar represents 50μm.

4.7 1st TRIMESTER CHORIONIC VILLUS.
GREY: NOMARSKI DIC; GREEN: IgG.

4.8 1st TRIMESTER TROPHOBLAST.
GREY: NOMARSKI DIC.
GREEN: IgG.

4.9 1st TRIMESTER TROPHOBLAST : IgG

4.10 1st TRIMESTER TROPHOBLAST : IgG

4.11 1st TRIMESTER TROPHOBLAST : IgG

4.12 1st TRIMESTER TROPHOBLAST.
RED: PROPIDIUM IODIDE; GREEN: IgG.

4.13 HYDATIDIFORM MOLE.
RED: PROPIDIUM IODIDE; GREEN: IgG.
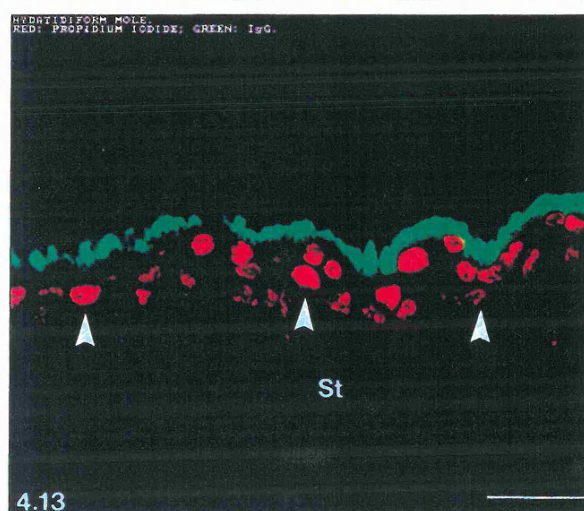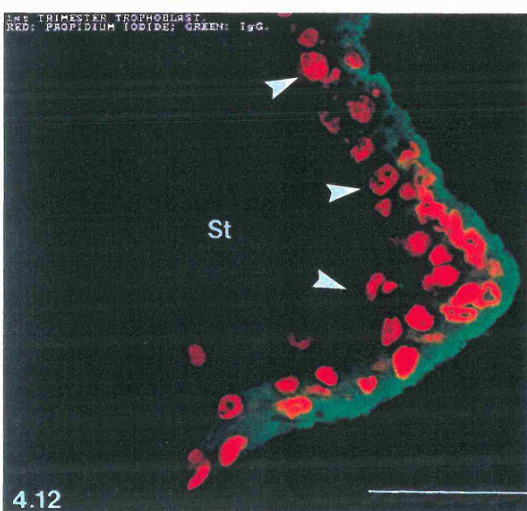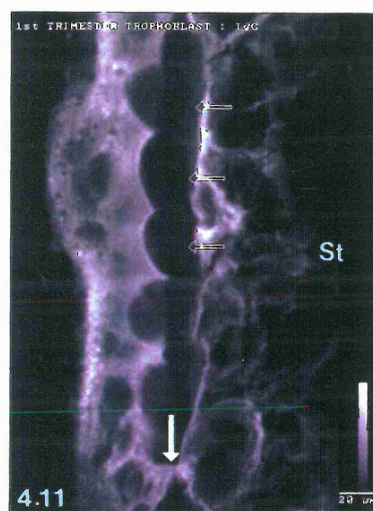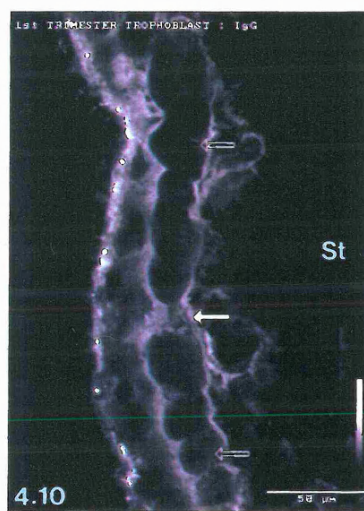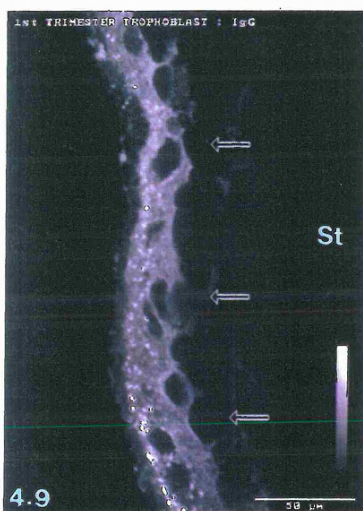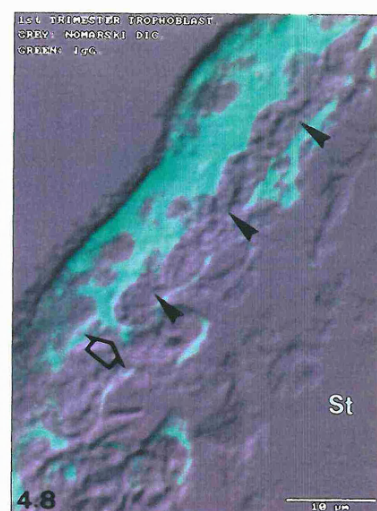
Figures 4.14-4.16: Anti-human IgG immunoreactivity in term chorionic villi.

Figure 4.14: F(ab')$_2$ direct anti-human IgG immunoreactivity in an unfixed frozen tissue section subsequently post-fixed with 3% formaldehyde. IgG is concentrated in the villus stroma (St) and is evident in punctate apical syncytiotrophoblast endosomal inclusions where the syncytium is sectioned in an oblique plane (arrowheads). Scale bar represents 25μm.

Figure 4.15: F(ab')$_2$ direct anti-human IgG immunoreactivity in a 4% paraformaldehyde pre-fixed frozen tissue section. IgG is concentrated in the villus stroma (St) and is clearly evident in fetal capillaries. Erythrocytes, present within the lumen of fetal vessels in this preparation, are not immunoreactive (arrowheads). Scale bar represents 250μm.

Figure 4.16: F(ab')$_2$ direct anti-human IgG immunoreactivity in a 4% paraformaldehyde pre-fixed frozen tissue section of term chorionic plate. IgG is concentrated in the stroma (St) and is evident in fetal blood vessels (V). The tunica intima, tunica media and tunica adventitia surrounding fetal vessels in the chorionic plate and stem villi are not immunoreactive (arrowheads). Scale bar represents 100μm.

4.14

TERM CHORIONIC VILLI: IgG.
4% PARAFORMALDEHYDE PRE-FIXATION.

250 µm

St

4.15

TERM CHORIONIC PLATE: IgG.

St

100 µm

4.16
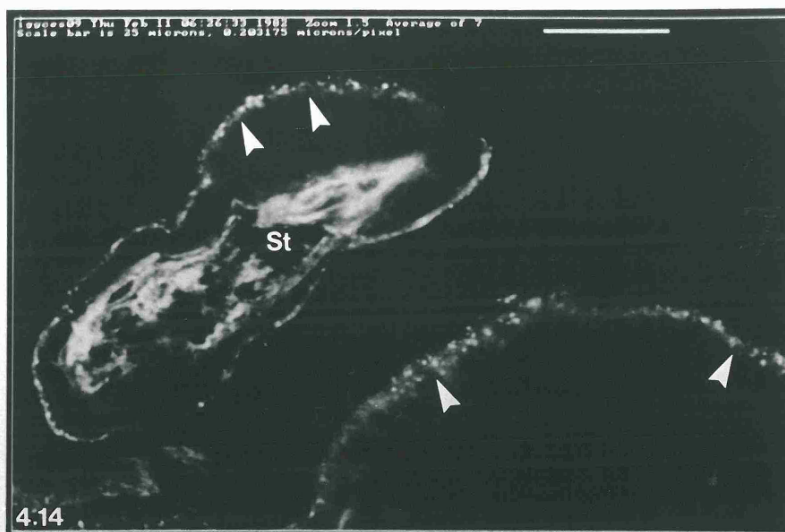
Figures 4.17-4.19: Anti-human IgG immunoreactivity in term amniochorion.

Figure 4.17: Colour confocal indirect immunofluorescence localisation of endogenous IgG (green channel) in term amniochorion. Nuclei (red channel) have been counterstained with propidium iodide. IgG is concentrated throughout the extracellular matrix and is evident between cytotrophoblast cells of the chorion laeve. Amniotic epithelial cells (A) and cytotrophoblast cells of the trophoblast layer (T) do not contain endogenous antibodies. Maternal decidua (D). Scale bar represents 100μm.

Figure 4.18: High resolution confocal indirect immunofluorescence micrograph of endogenous IgG immunoreactivity in a frozen section of 4% paraformaldehyde pre-fixed term amniochorion. The amniotic epithelium (A) is not immunoreactive. However, the compact layer (C) is intensely immunoreactive and IgG is evident between the basal foot-processes of the amniotic epithelial cells (arrowheads). Scale bar represents 5μm.

Figure 4.19: Dual-channel confocal micrograph illustrating a) F(ab')$_2$ direct anti-human IgG immunoreactivity and b) Nomarski DIC of term amnion. Amniotic epithelial cells (A) are not immunoreactive with anti-human IgG antibodies. The exception to this observation is the single damaged epithelial cell in this field (arrowhead) which contains endogenous antibodies. Scale bar represents 25μm.

GREEN, IgG : RED, PROPIDIUM IODIDE.

100 µM

A

T

D

4.17

TERM AMNION: IgG.

5 µm

A

C

4.18

a)

A

b)

A

4.19
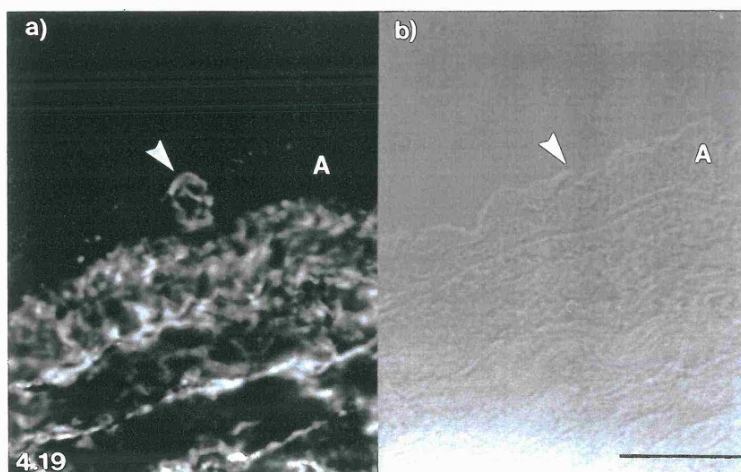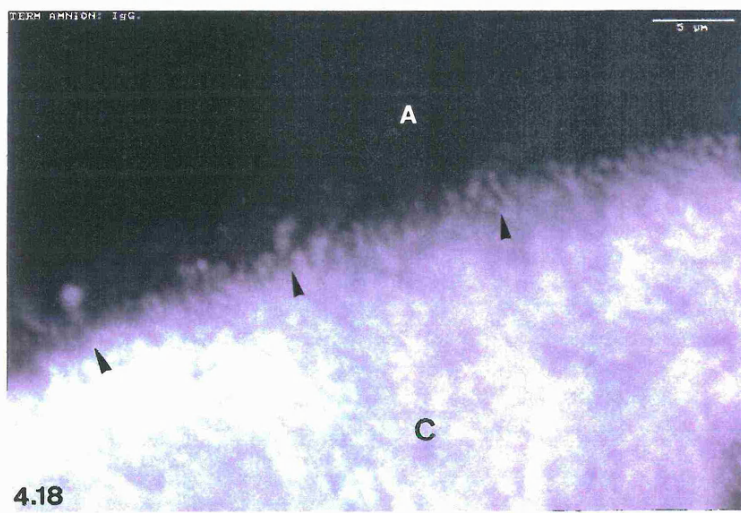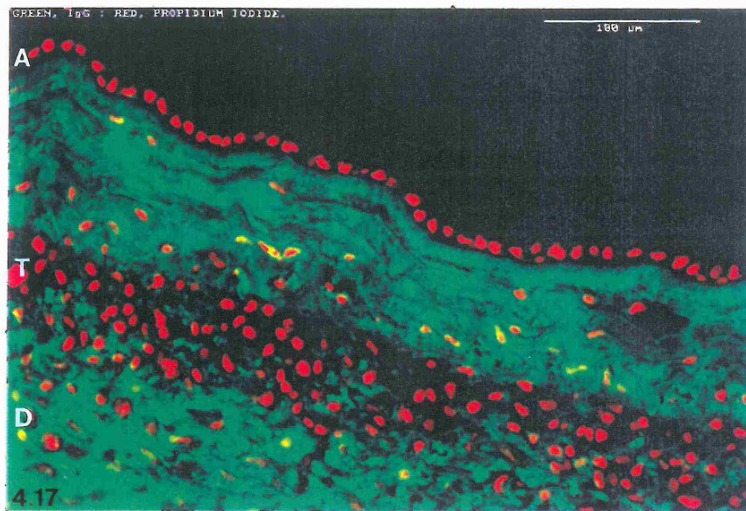
Figures 4.20-4.24: Anti-human IgG immunoreactivity in term amniochorion, chorionic plate and umbilical cord.

Figure 4.20: Epifluorescence micrograph of F(ab')$_2$ direct anti-human IgG:FITC immunoreactivity in a frozen section of unfixed human term amniochorion. Note that the amniotic epithelium (A) and cytotrophoblast cells of the trophoblast layer (T) are not immunoreactive but that the mesenchymal connective tissue (M) is. Scale bar represents 20μm.

Figure 4.21: Control epifluorescence micrograph of F(ab')$_2$ direct anti-human IgG:FITC immunoreactivity in a serial section to figure 4.20. In this preparation an equivalent concentration of F(ab')$_2$ rabbit anti-human IgG:FITC to that used in figure 4.20 was applied but challenged with 1×10^{-4}g ml^{-1} of exogenous human polyclonal IgG. Immunofluorescence has been almost completely abolished thus validating the affinity of the antibody. Note the yellow patches of autofluorescence. Scale bar represents 20μm.

Figure 4.22: Epifluorescence micrograph of F(ab')$_2$ direct anti-human IgG:FITC immunoreactivity in a 4% paraformaldehyde pre-fixed frozen section of chorionic plate from a Cesarean section delivery. Phase-contrast illumination has been used to visualise the tissue morphology. Note that the amniotic epithelium (A) is devoid of endogenous IgG but the underlying mesenchyme (M) is strongly immunoreactive. Scale bar represents 20μm.

Figure 4.23: Epifluorescence micrograph of F(ab')$_2$ direct anti-human IgG:FITC immunoreactivity in a 4% paraformaldehyde pre-fixed frozen section of chorionic plate from a routine term delivery. Phase-contrast illumination has been used to visualise the tissue morphology. Note that the amniotic epithelium (A) possesses many damaged immunoreactive cells but some healthy cells (arrowheads) do not contain IgG. The mesenchyme (M) is immunoreactive. Scale bar represents 20μm.

Figure 4.24: Epifluorescence micrograph of F(ab')$_2$ direct anti-human IgG:FITC immunoreactivity in a 4% paraformaldehyde pre-fixed frozen section of umbilical cord. Note that the amniotic epithelium (A) is not immunoreactive but the Whartons jelly connective tissue does contain endogenous antibodies. Scale bar represents 20μm.

4.20

4.21

4.22

4.23

4.24
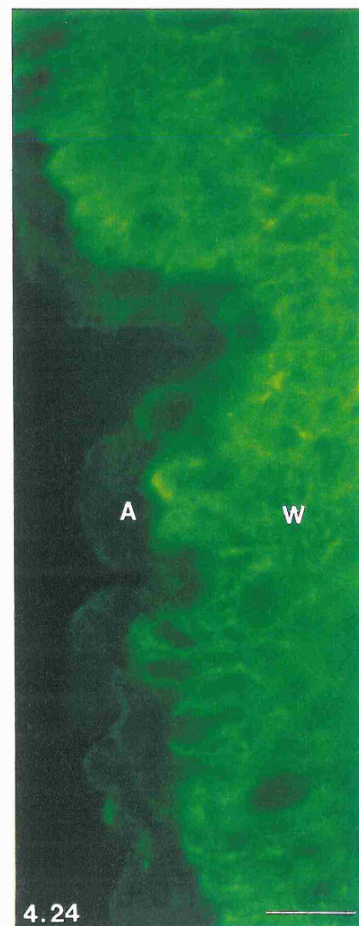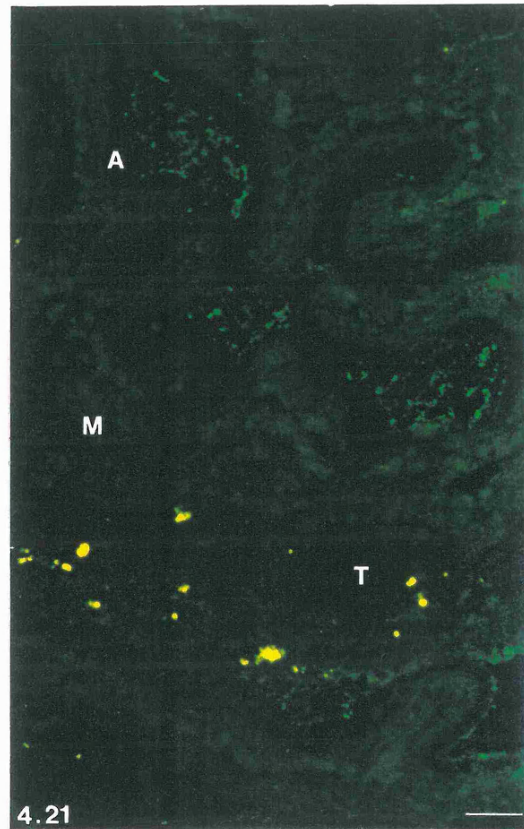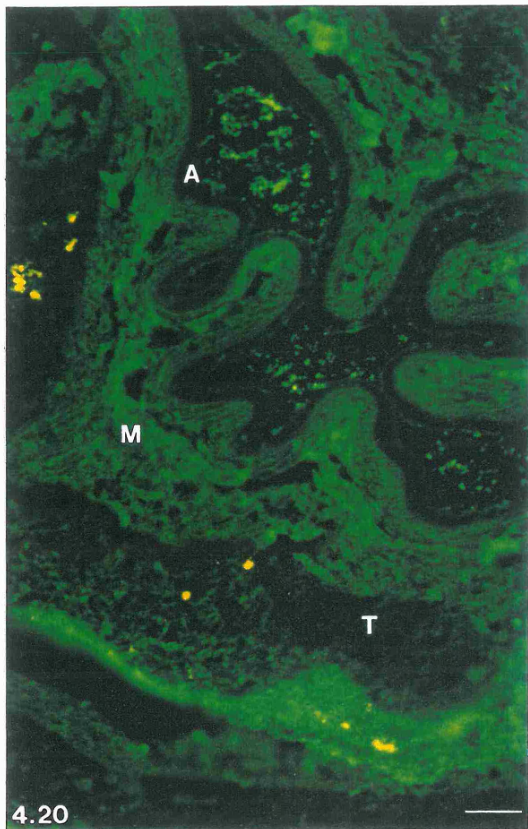
4.4 DISCUSSION.

These investigations confirm the existence of endogenous immunoglobulin G in the cells and tissues of the human placenta and fetal membranes.

First trimester placentae.
Endogenous IgG in 1st trimester villi is mainly confined to the syncytiotrophoblast. This may represent a barrier to the transepithelial transport pathway since IgG accumulates in the syncytium, thus accounting for the low level of transport observed by Gitlin and Biasucci (1969) before 22 weeks of gestation. Cytotrophoblast cells form an almost complete layer beneath the syncytiotrophoblast in immature placentae and at this time transmission of IgG is very inefficient compared with the effective transport against a concentration gradient at term when these cells form an attenuated epithelial layer. Thus it is possible that the degenerating cytotrophoblast layer is responsible for the "increased permeability of the human placenta for IgG" described by these authors at 22 weeks of gestation. This observation may, therefore, account for the paradox that early transport does not appear to be rate-limited by a lack of specific IgG receptors (Gitlin and Gitlin, 1976).

These observations suggest that cytotrophoblast cells inhibit the transmission of IgG to the human conceptus (Bright et. al., 1994; Bright and Ockleford, 1994b). The low levels of antibody acquired in the first trimester may be a consequence of localised areas of syncytiotrophoblast which are in intimate contact with the basement membrane. By utilising paraformaldehyde pre-fixed tissue it has been possible to conserve IgG antigenicity and also to significantly improve the morphology of the tissue specimens. In these preparations it was possible to clearly demonstrate that IgG immunoreactivity is not associated with the cytotrophoblast cells. This cytotrophoblast (Langhans) layer is normally complete in immature placentae but the syncytiotrophoblast occasionally penetrates between these cells to contact the basement membrane. This phenomenon may be observed at all stages of gestation (Boyd and Hamilton, 1970; Wynn, 1975). This study has demonstrated that the syncytiotrophoblast which penetrates between cytotrophoblast cells, and contacts the basal lamina, possesses endogenous IgG. Therefore, this is conceivably a route which may be utilised to transport antibody across the trophoblast (Bright and Ockleford, 1994b). It is particularly intriguing in this respect that, in exceptional instances where these inter-cytotrophoblast incursions occur, there is evidence of IgG immunofluorescence in the stroma immediately beneath the area of contact between the syncytium and the basement membrane.

Early investigations using unfixed cryostat sections, or sections post-fixed for 10 minutes with 3% formaldehyde, demonstrated that the mesenchymal villus cores of first trimester placentae contain no endogenous immunoglobulin G (Bright et. al., 1994). However, in subsequent investigations using 4% paraformaldehyde pre-fixed cryostat sections it was occasionally possible to demonstrate low levels of IgG in the villus core (Bright and Ockleford, 1994b). This may be a consequence of low levels of soluble antibody being washed away into the solutions used to wash, fix or permeabilise cryostat tissue sections. Furthermore, the chances of observing endogenous IgG immunoreactivity in the villus core increased with advanced gestational age of the tissue, suggesting that the trophoblast becomes increasingly 'permeable' to IgG transmission as the placenta matures. This is likely to be a function of the increased areas of contact between the syncytiotrophoblast and the underlying trophoblast basal lamina as gestation advances. The concentration of IgG in the basal lamina, and its presence in the stroma underlying these regions of contact, is striking when compared with regions in which the cytotrophoblast layer is continuous.

Furthermore, it has been possible to demonstrate the existence of subcellular inclusions in the syncytiotrophoblast which possess IgG. Transport of IgG is believed to be mediated via receptors which first cluster into coated pits and are subsequently internalised into coated vesicles. However, the route which is utilised to transmit IgG from this point is not established. The resolving power of the conventional light microscope is not sufficient to demonstrate what subcellular inclusions are associated with IgG. However, using the confocal laser scanning microscope it has been possible to demonstrate an association of IgG with large inclusions in the syncytiotrophoblast. The IgG is localised at the periphery of these inclusions which indicates that the ligand is probably still bound to its receptor instead of having been released into the lumen of the inclusion. It is not clear if these are apical endosomal or CURL compartments but it is conceivable that coated vesicles discharge their contents into these inclusions. Three-dimensional re-construction of these inclusions from a stack of images, taken from various depths within the trophoblast, demonstrate a roughly spherical nature. Recently a new endosome-like organelle has been characterised which accumulates MHC class II molecules in human lymphocytes (Amigorena et. al., 1994; Tulp et. al., 1994; West et. al., 1994). The roles of the inclusions observed in the present study remain to be characterised.

Term chorionic villi.
The localisation of IgG in term villi is clearly different; it is associated with syncytiotrophoblast, capillaries, endothelium, extracellular matrix and with cells of

-112-

the stroma (Bright et. al., 1994). This suggests that IgG is readily transported across the trophoblast from the maternal circulation to the villus core.

IgG immunoreactivity in the syncytiotrophoblast was predominant at the apical cell surface. This pattern might reflect rate-limiting dynamics of transport across the apical aspect of the cell. It is unclear whether the punctate pattern observed was a consequence of lysosome or endosome-like compartments. Cytotrophoblast cells do not possess IgG immunoreactivity, consistent with the observation in first trimester chorionic villi.

Similar to observations in first trimester placentae, there are often areas in the trophoblastic basal lamina which concentrate IgG. In addition there are local concentrations within the mesenchyme of the villus core which are frequently associated with capillaries. These may reflect connective tissue channels which concentrate the antibodies in the region of fetal capillaries. An alternative explanation for this observation may be that these are immune complexes. The transport machinery of the human placenta is unable to distinguish helpful from deleterious antibody since it recognises the Fc region of the molecule. Therefore antibodies directed against fetal antigens may also be transported across the trophoblast. It is possible that these antibodies encounter and bind to fetal antigens in the placenta, thus preventing potentially harmful antibodies from being transmitted to the fetal circulation.

In studies performed with unfixed cryostat sections it was only possible to detect IgG immunoreactivity with residual serum proteins of the villus capillary lumen. However, in experiments performed with 4% paraformaldehyde pre-fixed tissue the vessel contents were cross-linked by the aldehyde and thus were prevented from diffusing into the washing solutions. These studies clearly showed that intense IgG immunoreactivity was associated with the plasma proteins of the placental blood vessels. However, erythrocytes present within these capillaries were not immunoreactive which provides a good internal negative control. The endothelium surrounding these vessels was also immunoreactive which implies that they are responsible for uptake of IgG. This was characterised by a diffuse cytoplasmic staining. Therefore, this evidence suggests that IgG is internalised into these cells and does not traverse the vessel wall via a paracellular route.

A novel finding was that IgG was not associated with endothelial cells of vessels in the chorionic plate and umbilical cord. Furthermore the adventitia surrounding these vessels possess little immunoreactivity. This suggests that the larger fetal vessels are not involved in antibody transport. However, the

extracellular matrix tissues do possess IgG as do the fetal serum proteins in the blood vessels. A further observation, consistent with the localisation obtained in the amniochorion, is that cells of the umbilical cord and underlying the amnion of the chorionic plate, do contain IgG immunoreactivity (Chapter 5).

Hydatidiform mole specimens possess identical IgG immunoreactivity to first trimester specimens. IgG is concentrated in the surrounding syncytiotrophoblast but the cytotrophoblast cells are devoid of endogenous antibody. Using 4% paraformaldehyde pre-fixed specimens it has been possible to demonstrate the existence of IgG in the villus mesenchyme. However, since this tissue does not possess capillaries an association with these structures was not noted. This pre-malignant tissue is otherwise not significantly different from healthy first trimester tissue.

Amniochorion.
These investigations have confirmed the presence of IgG in human term amniochorion (Bright and Ockleford, 1994a). Endogenous antibody was demonstrated throughout the extracellular matrix of the amnion, chorion and decidua. The only cellular association of IgG was demonstrated in cells of extraembryonic mesenchymal origin, in the fibroblast and reticular layers of the tissue, and with leucocytes present within the maternal decidual layer (Chapter 5).

Cytotrophoblast cells of the chorion laeve and amniotic epithelial cells do not contain endogenous IgG. It is particularly intriguing that IgG is not observed in the intercellular spaces between amniotic epithelial cells since King (1982b) has demonstrated that these cells do not possess tight junctions. Schmidt (1992) is of the opinion that other regulatory processes may restrict the passage of molecules between amniocytes on the basis of size. By using 4% paraformaldehyde pre-fixed cryostat sections of amniochorion it was possible to demonstrate intense immunoreactivity in the connective tissues. By combining this technique with the increased resolution afforded by the confocal laser scanning microscope it was possible to detect IgG between the basal foot processes of the amniotic epithelial cells that extend into the amniotic epithelial basal lamina. This observation implies that the connective tissues do not constitute a barrier to the diffusion of immunoglobulin molecules. However, amniotic epithelial cells are evidently capable of excluding IgG at the basal plasmalemma.

Two complete layers of epithelial cells in the amniochorion (the amniotic and trophoblastic epithelia) do not contain endogenous IgG. This data supports the consensus view that maternally derived passive immunity is not acquired by the

fetus using the paraplacental transamniochorion route. However, the amniotic fluid does contain IgG class antibodies (Monif and Mendenhall, 1970; Gadow et. al., 1974; Usategui-Gomez et. al., 1967) of maternal origin (Cederqvist et. al., 1972). The route by which IgG gains access to amniotic fluid is not established. This study indicates that IgG is not actively transported across the amniotic epithelium.

However, the existence of damaged or dead amniotic epithelial cells which do contain endogenous antibody (Bright and Ockleford, 1993) does not appear to be consistent with the hypothesis that these cells prevent access of IgG to the amniotic fluid. It is certainly possible that IgG may diffuse through damaged cells and thus enter the amniotic compartment. However, it is not known if this occurs *in vivo* since damaged cells are observed infrequently in tissue specimens delivered via Cesarean section. Tissue specimens delivered by routine vaginal delivery have become subject to the trauma associated with parturition and are thus more susceptible to damage. Therefore, it may be concluded that IgG is not actively transported from the amniotic mesenchyme to the amniotic fluid (or vice versa) across a healthy, intact, amniotic epithelium. However, the concession must be made that if cells of this simple epithelium lose their integrity *in vivo*, it is possible that IgG may freely diffuse through them. Small quantities of IgG may thus gain access to the amniotic fluid via this route. It is unlikely that the human placenta employs an active IgG transport mechanism which relies upon cells being damaged.

The observation that the amniotic epithelium is devoid of endogenous antibody may be extended to the cells of the placental amnion and those overlying the umbilicus. This suggests that there is a continuous layer of cells lining the amniotic cavity that lack the potential to transport IgG. Amniotic cells overlying the chorionic plate of the placenta reveal a similar likelihood to become damaged by a routine term delivery as those of the amniochorion. Thus individual cells sometimes contain IgG. However, the amnion overlying the umbilicus never contains endogenous IgG which suggests that these cells may be more robust.

The demonstration that cytotrophoblast cells of the chorion laeve do not contain endogenous antibody is consistent with the lack of antibody observed in this cell type in the placenta. The cytotrophoblast cells of the amniochorion are in lateral continuity with those of the chorionic villi. Thus, prior to 20 weeks of gestation, there is a shell of cytotrophoblast cells which surround the human extraembryonic membranes and do not contain endogenous antibody.

The origin of IgG in the mesenchymal layers of the amniochorion is not clear. It is possible that lateral movement from the mesenchyme of the disc of the placenta

occurs. A further possibility indicated by low levels of fluorescence in the trophoblast layer extracellular matrix suggests a possible pathway between these cells. This is intriguing because if IgG gains access from the maternal decidua, through the chorion laeve extracellular matrix and into the mesenchymal extracellular matrix, it has potential access to the placenta by lateral diffusion through the mesenchymal layers (Bright and Ockleford, 1994a). Antibodies acquired in this way could contribute to maternally derived passive immunity since Fcγ receptors on fetal endothelial cells in the placenta would be unable to discriminate IgG derived in this way from that transported across the syncytiotrophoblast. This notion is supported by the results of a clinical study performed by Kulangara et. al. (1965). These authors demonstrated that purified BSA could not be detected in fetal cord blood after injection into the amniotic cavity near term. However, they were able to demonstrate that BSA deposited over the extraplacental chorion in the uterine lumen was detected in cord serum and they concluded that transport of proteins between mother and fetus is not restricted to direct exchange between maternal and fetal blood in the chorioallantoic placenta.

CHAPTER 5: Fcγ Receptors.

5.1 INTRODUCTION.

Macrophages, granulocytes and many lymphocytes express surface receptors for the Fc domain of IgG. These IgG Fc receptors (FcγR) comprise a group of molecules with structural and functional heterogeneity. Not only do these receptors possess different affinities for the immunoglobulin G subclasses, they also mediate activities ranging from triggering the secretion of cytotoxic and inflammatory agents by macrophages to endocytosis of the bound ligand. Recently a considerable amount has been learned concerning the structure and function of the Fcγ receptors expressed by murine and human leucocytes due to the availability of specific anti-receptor antibodies and the isolation of Fc receptor complementary DNA clones.

Unkeless et. al. (1981) demonstrated that murine macrophages, granulocytes and lymphocytes express at least 3 distinct classes of FcγR. These classes, referred to by the nomenclature as murine FcR (mFcR)I, mFcRII and mFcRIII, were defined by their various affinities for different IgG subclasses and reactivities with monoclonal anti-receptor antibodies. Murine FcRI exhibits a relatively high affinity for monomeric mouse IgG_{2a} and is expressed on macrophages and macrophage cell lines. Murine FcRII, the most abundant and widely distributed of the three receptors, is usually found on all FcR positive cells. This receptor has poor affinity for monomeric IgG but selectively binds polyvalent immune complexes of mouse IgG_1, IgG_{2b} and possibly IgG_{2a} (Unkeless, 1977; Unkeless, 1979; Mellman and Unkeless, 1980). Murine FcRIII, expressed by macrophages and macrophage cell lines, is distinct from mFcRI and mFcRII by its affinity for aggregated IgG_3.

While mFcRI and mFcRIII have, to date, been poorly characterised, the structure and expression of mFcRII has been extensively investigated. The receptor has been purified using immunoaffinity chromatography with specific anti-mFcRII monoclonal antibody 2.4G2 bound to sepharose (Unkeless, 1979; Mellman and Unkeless, 1980). It is a 50-60kD transmembrane glycoprotein, as determined by microsome digestion experiments, containing 4 complex N-linked oligosaccharide chains (Green et. al., 1985) and no detectable O-linked sugars (Howe et. al., 1988). Much of the variability of the molecular weights of this receptor has been attributed by Green et. al. (1985) and Lewis et. al. (1986) to the heterogeneity in terminal glycosylation.

One of the best characterised activities of mFcRII is receptor-mediated endocytosis. When expressed on macrophages, mFcRII is capable of mediating both the phagocytosis of large IgG-coated particles (Mellman et. al., 1983) and receptor-mediated endocytosis of soluble antibody-antigen complexes via coated pits and

vesicles (Mellman and Plutner, 1984; Ukkonen et. al., 1986). After internalisation the receptor and bound ligand are transferred to lysosomes and catabolised leading to 'down-regulation' of surface mFcRII. Interestingly, if this receptor is bound to a monovalent ligand such as the Fab fragment of the anti-receptor antibody 2.4G2, internalised receptors escape lysosomal degradation and are rapidly recycled to the cell surface from pre-lysosomal endosomes (Mellman et. al., 1984; Ukkonen et. al., 1986). It is likely that mFcRII is responsible for clearing extracellular immune complexes, although binding of ligand also generates a transmembrane signal which triggers a variety of other events important for macrophage function (see review, Aderam et. al., 1988)

Prospects for understanding the molecular basis of the structural and functional heterogeneity of FcγRs have increased dramatically in recent years as a result of the application of cDNA cloning techniques. Using polyclonal anti-FcγR antibodies and sequence information obtained from purified receptor protein, cDNAs encoding mFcRII have now been isolated from both macrophage and lymphocyte cDNA libraries (Hibbs et. al., 1986; Lewis et. al., 1986; Ravetch et. al., 1986). The amino acid sequence deduced from these cDNA clones suggests a molecule whose amino-terminal extracellular domain contains 4 potential sites for N-glycosylation, a single hydrophobic membrane spanning segment and a hydrophilic cytoplasmic domain. However, it is interesting to note that the hydrophilic cytoplasmic domain was found not to exhibit sequences suggestive of a kinase-like activity found in receptors that are capable of mediating transmembrane signals (eg. insulin receptor, EGF receptor). It is likely that the mFcRII cDNA clones encode a complete functional receptor since Meittinen et. al. (1989) obtained expression of mFcRII cDNA in FcγR-negative cell lines including COS cells, CHO cells and MDCK cells. In each case, after transfection FcR expressed by these cells were fully reactive with all available antibodies to mFcRII, exhibited identical ligand binding and were still capable of mediating receptor mediated endocytosis.

Analysis of the amino acid sequence found in the receptors extracellular domain clearly indicates that mFcRII is a member of the immunoglobulin gene family. Four regularly spaced cysteine residues were found, the sequences around which were significantly related to sequences associated with the variable and/or constant domains of immunoglobulin molecules (Lewis et. al., 1986). These cysteines have also been shown to engage in intrachain disulphide bonds (Hibbs et. al., 1988). It is interesting that the number of residues within each cysteine loop (42-44) is considerably shorter than the number usually found in the corresponding immunoglobulins (typically 70-80 amino acids).

Perhaps the most interesting feature resulting from the cDNA cloning work is the finding that mFcRII exists as multiple isoforms. At least 3 predicted and closely related structures may be distinguished which seem to be the products of two distinct genes (Figure 5.1; Ravetch et. al., 1986; Lewis et. al., 1986; Hibbs et. al., 1986). The first two receptor isoforms, mFcRII-B1 and mFcRII-B2, are identical except for a 47 amino acid insertion occurring at position 6 in the cytoplasmic domain of mFcRII-B1. It is believed that this insertion reflects alternative mRNA splicing. Thus mFcRII-B1 has a cytoplasmic domain of 94 amino acids while mFcRII-B2 has only 47 amino acids. The third isoform, mFcRII-A, is 95% identical to -B1 and -B2 in the extracellular domain but differs entirely in its transmembrane and cytoplasmic domains. Thus it seems likely that the A and B transcripts are the products of different genes (Ravetch et. al., 1986; Lewis et. al., 1986). Each of the receptor isoforms reacts with the same panel of mFcRII monoclonal and polyclonal antibodies. Recent results suggest that there may be some significant functional differences between mFcRII-B1 and -B2. In COS or CHO cells transfected with mFcRII-B2 this receptor is capable of mediating the rapid internalisation and delivery to the lysosomes of bound IgG. Mouse FcRII-B1 is far less efficient at performing this function (Meittinen et. al., 1989).
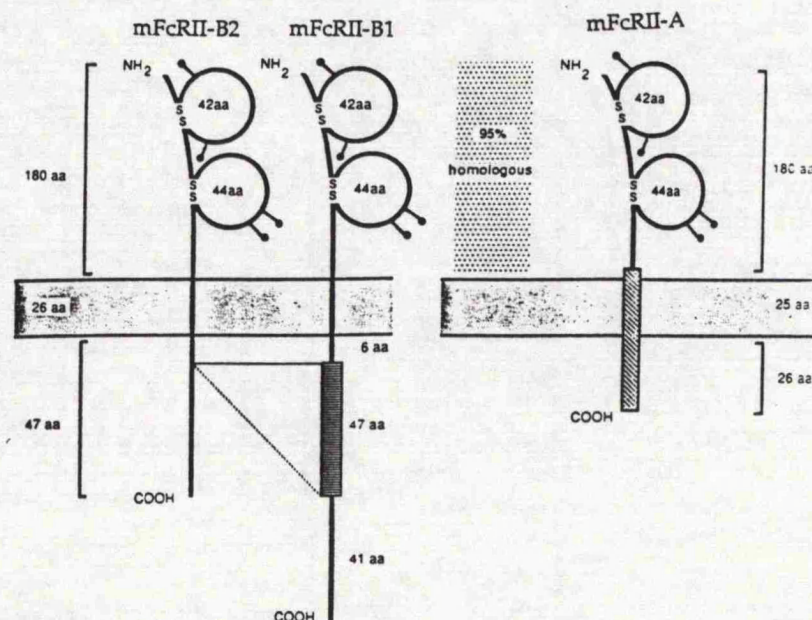
Figure 5.1. The structure of the three distinct murine FcγRII receptors deduced from complementary DNA sequences. Note the 47 amino acid insertion in the cytoplasmic domain of mFcRII-B1 and the extracellular glycosylated immunoglobulin-like domains (adapted from Mellman et. al., 1988).

The difference between the mFcRII-B1 and mFcRII-B2 isoforms appears to correlate with the inability of -B1-bound ligand to localise in clathrin coated pits on the cell surface. It is not inconceivable that the insertion of an additional amino acid

sequence into the cytoplasmic domain of mFcRII-B1 inhibits clathrin coated pit localisation and subsequent endocytosis. The difference in trafficking of these two isoforms of the receptor has been further emphasised by results from polarised MDCK cells transfected with FcγR DNA (Hunziker and Mellman, 1989). Mouse FcRII-B2 was capable of mediating efficient apical to basolateral transcytosis of IgG and, in addition, it was apparent from this study that it is capable of transcytosis of both polyvalent IgG and monovalent fragments.

Like their murine counterparts FcγRs expressed by human leucocytes can be divided into three general classes on the basis of ligand affinity and reactivity with class specific monoclonal antibodies (Anderson and Looney, 1986). To help understand the structure and function of leucocyte surface molecules, an internationally accepted classification of antibodies and molecules has been developed. The classification system divides the antibodies into groups or 'Clusters of Differentiation' (CD) that share specific cellular recognition patterns. Thus the cell surface molecules recognised by these antibodies are known as CD antigens. Four Leucocyte Typing Workshops held in Paris (1982), Boston (1984), Oxford (1986) and Vienna (1989) have resulted in 78 'clusters' being identified to date.

Human FcγRI (CD64) appears to be functionally homologous to mFcRI in that it has high affinity for monomeric IgG (Anderson, 1982; Cohen et. al., 1983). It is also found only on cells of monocyte origin. Human FcγRII (CDw32), on the other hand, is more widely distributed on monocytes, lymphocytes and granulocytes and, like mFcRII, is reported to bind aggregated or polyvalent IgG (Looney et. al., 1986; Vaughn et. al., 1986). A third human FcγR (FcγRIII; CD16) exhibits a low affinity for aggregated IgG and is present largely on granulocytes, natural killer (NK) cells and to some extent on monocytes and macrophages (Fleit et. al., 1982; Perussia et. al., 1984). The functions of human FcγRs have not been extensively studied. They are capable of mediating endocytosis and phagocytosis of IgG (Anderson and Looney, 1986) and of triggering a variety of events associated with effector cell function.

Recent cDNA cloning work has indicated that like its murine homologue, human FcγRII comprises a family of at least 3 highly related receptors. Stuart et. al. (1989) isolated and characterised 3 distinct human FcγRII cDNAs all of which are immunoglobulin-like membrane proteins with identical domain organisation to the murine receptors. The sequence of the first of the human receptors (hFcRII-A) is 70% identical to both mFcRII isoforms in the extracellular domain although two of the four N-glycosylation sites found in the murine sequence are lost. The membrane spanning segment is 50% identical to mFcRII-B1 and mFcRII-B2 but the cytoplasmic domain bears no homology to any mFcRII sequence. The second cDNA (hFcRII-B) is

90-95% identical to hFcRII-A. Two distinct transcripts are derived from the hFcRII-B gene by alternative mRNA splicing. These differ in their predicted amino acid sequence by only 6 amino acids (Ravetch and Kinet, 1991) deleted from various sites in the hFcRII-B sequence, although they retain 3 of the 4 glycosylation sites found on the murine receptors (Stuart et. al., 1989). Finally, hFcRII-C has signal sequence and extracellular domains which are almost identical to hFcRII-B, containing only a single amino acid change. However, hFcRII-C differs completely from hFcRII-A and -B in the cytoplasmic domain.

By selecting for FcγRIII (CD16) and FcγRI (CD64) cells after cDNA transfection into COS cells, Stengelin et. al. (1988) and Simmons and Seed (1988) have isolated cDNA clones encoding human FcγRI and FcγRIII. Although related to human and mouse FcγRII, both sequences possess a number of important differences. Human FcγRIII has an extracellular domain consisting of two immunoglobulin-like loops which are highly homologous to murine FcRII and human FcγRII although they contain 6 potential sites for N-linked glycosylation (Simmons and Seed, 1988).

Two FcγRIII isoforms, encoded by 2 distinct but highly homologous genes, have been described in the human: FcγRIIIA and FcγRIIIB (Ravetch and Perussia, 1989). The products of both genes encode proteins with an extracellular region of 191 amino acids containing two immunoglobulin-like constant domains. The striking difference between the products of these two genes is that FcγRIIIA encodes a transmembrane receptor (FcγRIIIa) with a 25 amino acid cytoplasmic region and FcγRIIIB encodes a receptor (FcγRIIIb) which is coupled to the plasma membrane via a glycosylphospatidylinositol (GPI) moiety (Huizinga et. al., 1988; Selvaraj et. al., 1988; Selvaraj et. al., 1989). A single amino acid substitution at position 203 (phe^{203} for FcγRIIIa and ser^{203} for the FcγRIIIb GPI-linked moiety) differentiates the transmembrane and GPI-linked isoforms (Hibbs et. al., 1989; Kurosaki and Ravetch, 1989; Lanier et. al., 1989; Scallon et. al., 1989).

The transmembrane form of human FcγRIII (hFcγRIIIA) has been shown to be present on macrophages and NK cells in association with other molecules referred to as receptor subunits. In macrophages, this receptor is associated with the γ-chain homodimer of the high affinity receptor for IgE and is thus designated hFcγRIIIA(γ) (Hibbs et. al., 1989; Kurosaki and Ravetch, 1989; Lanier et. al., 1989). In NK cells, both homo- and heterodimers of this γ-chain and a ζ-chain (typically associated with the T-cell receptor-CD3 complex) are linked with this receptor (Anderson et. al., 1990; Lanier et. al., 1989; Vivier et. al., 1992). Thus in NK cells the receptor is associated with γ-γ homodimers (hFcγRIIIA(γ)), ζ-ζ homodimers (hFcγRIIIA(ζ)) or γ-ζ heterodimers (hFcγRIIIA:ζ:γ) as shown in Figure 5.2. The ζ and γ family of molecules

are low molecular weight integral membrane proteins involved in the coupling of cell surface receptors to the signal transduction machinery (Ashwell and Klausner, 1990). These molecules are transmembrane proteins possessing short (5 to 9 amino acids) extracellular domains and long intracellular domains (36 to 155 amino acids). The functional significance of these receptor subunits is not yet established.
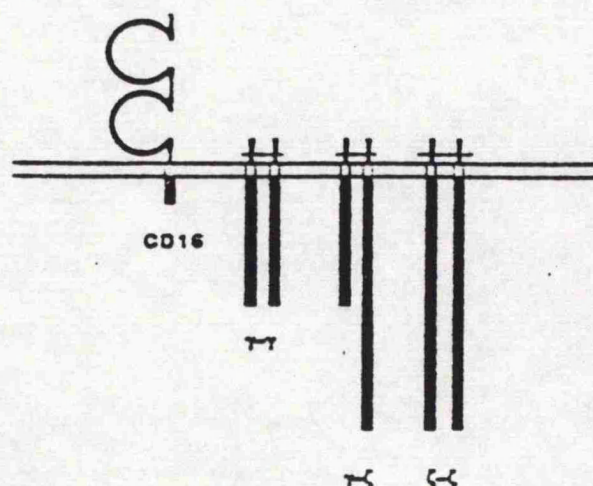
Figure 5.2. Schematic representation of the association of the human FcγRIIIa (CD16) transmembrane isoform with the γ-chain homodimer of the high affinity FcεRI receptor and the ζ-chain of the T-cell receptor CD3 complex. These molecules are thought to be responsible for signal transduction (from Vivier et. al., 1992).

Human FcγRI (CD64), a 72kD glycoprotein receptor expressed by mononuclear phagocytes, possesses high affinity for monomeric human IgG (Anderson and Looney, 1986). The receptor is heavily glycosylated and has a core protein of 55kD after removal of the N-linked carbohydrates (Peltz et. al., 1988). Three distinct cDNAs have been described (Allen and Seed, 1989), encoding a predicted extracellular region of 273-292 amino acids containing three immunoglobulin-like domains (Williams and Barclay, 1988), a transmembrane region of 21 amino acids and a charged cytoplasmic domain of either 63 (encoded by two cDNAs) or 31 amino acids (Ravetch and Kinet, 1991) as shown in Figure 5.3. Two of these transcripts represent polymorphisms and the third, as indicated, demonstrates diversity in the predicted cytoplasmic domain. However, southern blot and genomic cloning studies are consistent with a single human FcγRI gene since DNA sequences have not been detected for the third DNA with its novel cytoplasmic domain.

Transcripts of 1.7kB and 1.6kB are evident after being induced by the presence of IFNγ in culture (Allen and Seed, 1989; Pan et. al., 1990).
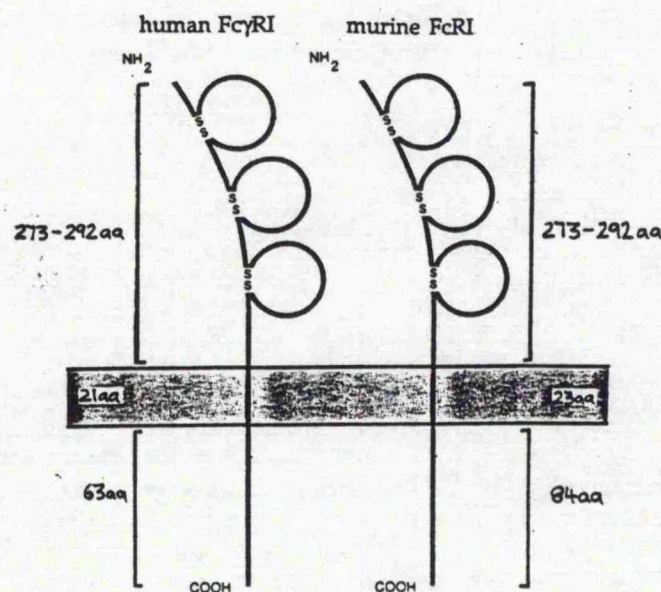
Figure 5.3. Diagram illustrating the transmembrane organisation of the human FcγRI molecule. Note the third immunoglobulin-like extracellular domain and similarity with the homologous murine receptor.

Transfection of these clones into COS cells resulted in 70kD surface molecules which bound IgG with an affinity and specificity similar to that determined for the native molecule in *in vivo* studies. Furthermore, these molecules reacted with FcγRI-specific monoclonal antibodies. The first two extracellular immunoglobulin-like domains are homologous to the extracellular domains of FcγRII and FcγRIII, while the third reveals little similarity. Ravetch and Kinet (1991) suggest that this third domain may account for the high affinity binding of this receptor. Sears et. al. (1990) have identified cDNA clones for murine FcRI. The predicted amino acid sequence reveals 65-75% identity with human FcγRI in the three extracellular domains and the transmembrane domain. However, the cytoplasmic domain is 21 amino acids longer and is only 25% identical to human FcγRI.

The aim of the work presented in this chapter is to define the anatomical and histological distribution of the human FcγR subtypes in the placenta and fetal membranes using immunocytochemical techniques. A knowledge of the distribution of these receptors may provide valuable insights into their role in the immunological protection of the fetus.

5.2 MATERIALS AND METHODS.

5.2.1 Tissue collection.

Freshly dissected samples of 1st trimester (n=6), term (n=10), Cesarean section (n=14) and hydatidiform mole (n=3) chorionic villi were obtained from the Leicester Royal Infirmary. The amniochorion from Cesarean section (n=14) and term (n=10) placentae was also collected from these deliveries and the tissue was stored as described in section 3.2.1.

A variation performed was to pre-fix the tissue for 3 hours at room temperature with 4% paraformaldehyde in 0.1M PBS. This tissue was subsequently embedded with O.C.T. and processed as previously described. First trimester chorionic villi (n=3), term Cesarean section chorionic villi (n=3), chorionic plate and term Cesarean section amniochorion (n=3), placental amnion and umbilical cord (n=3) was processed in this way.

5.2.2 Indirect immunofluorescence.

Indirect immunofluorescence preparations of Fcγ receptor immunoreactivity were made according to the general techniques described in section 3.2.2. Optional steps, performed in approximately half of the experiments described, were to post-fix tissue sections with 3% formaldehyde diluted in 0.1M PBS for 10 minutes at room temperature, 100% acetone for 20 minutes at -18°C, or 100% methanol for 20 minutes at -18°C. Formaldehyde fixed tissue was additionally permeabilised with 0.05% Triton X-100 in 0.1M PBS for 10 minutes.

5.2.2.1 Primary antibodies.

Mouse monoclonal antibodies to three subtypes of Fcγ receptor were employed for this study. Mouse monoclonal anti-human FcγRI (CD64) was purchased from Serotec (Code No.: MCA 756; Batch No.: 001; Clone 10.1; Mouse isotype, IgG_1) and was provided as a tissue culture supernatant. This antibody was stored at -18°C in 10μl aliquots until required and then at 4°C for up to 1 month. Mouse monoclonal anti-human FcγRII (CDw32) was supplied by Serotec (Code No.: MCA 581; Batch No.: 09; Clone 2E1; mouse isotype, IgG_{2a}) as 0.2mg of purified lyophilised ascites. This was reconstituted with 1ml of double distilled water and stored at -18°C in 10μl aliquots until required and then at 4°C for up to 1 month. Mouse monoclonal anti-human FcγRIII (CD16) was supplied by Serotec (Code No. MCA 741; Batch No.: 153282C; Clone GRM-1; mouse isotype, IgG_1) as a tissue culture

supernatant and was aliquoted and stored at -18°C prior to use and subsequently at 4°C for up to 1 month. These antibodies were diluted 1/50 (anti-FcγRI and FcγRII at a concentration of 4μg/ml; anti-FcγRIII at a concentration of 1μg/ml) in 0.1M PBS (dilution range tested: 1/20 - 1/400) containing 5% non-immune serum from the second stage species. 20μl aliquots were applied to the tissue sections and immunoreacted for 24 hours at 4°C.

In addition, experiments were performed to investigate the normal distribution of connective tissue macrophages (Hofbauer cells). This was performed by immunoreacting sections of the human placenta and fetal membranes with a monoclonal antibody directed against monocytes/macrophages (Flavell et. al., 1987). This antibody was purchased from Serotec (Code No.: MCA 874; Batch No.: CH-B:VI; Clone MAC387; mouse isotype, IgG$_1$) and was supplied as a tissue culture supernatant. This product was stored at 4°C and 20μl aliquots were applied to the tissue sections undiluted as directed by the manufacturers.

5.2.2.2 Secondary antibodies.

The monoclonal antibodies used in this investigation were detected using i) F(ab')$_2$ fragments of rabbit anti-mouse IgG conjugated to FITC (Serotec, Code No.: ST-AR 9; Batch No.: 016) and ii) F(ab')$_2$ fragments of rabbit anti-mouse IgG conjugated to TRITC (Serotec, Code No.: ST-AR 10; Batch No. 012). These reagents (10μl aliquots) were stored at -18°C prior to use and subsequently at 4°C for up to 1 month. They were applied at a dilution of 1/500 (range tested: 1/200 - 1/2000) in 0.1M PBS containing 5% NRS.

In addition, increased sensitivity of detection of primary mouse antibodies was achieved by utilising a three-step immunocytochemical procedure. Primary monoclonal antibodies were localised with affinity-purified biotinylated goat anti-mouse IgG (Amersham, Code No.: RPN 1177) diluted 1/100 in 0.1M PBS (range tested: 1/50 - 1/500) containing 5% NGS. These were subsequently localised with a 1/500 dilution of ExtrAvidin conjugated to FITC (Sigma, Code No.: E-2761; Lot No.: 090H4881) as described in section 4.2.2.2.

5.2.2.3 Simultaneous antibody labelling.

In further experiments, simultaneous labelling of the three FcγR subtypes was accomplished using a cocktail of the three primary mouse monoclonal antibodies diluted 1/50 in 0.1M PBS containing 5% NGS and immunoreacted with the tissue

sections for 24 hours at 4°C. These antibodies were detected using the three-step bridge technique described in section 5.2.2.2.

These preparations were counterstained with propidium iodide as described in appendix V and compared with serial sections labelled with single anti-receptor monoclonal antibodies. In this way it is possible to estimate the degree of co-expression of these FcγR subtypes and the number of receptor-negative cells.

5.2.2.4 Dual-labelling.

Dual-labelling of Fcγ receptors and endogenous human immunoglobulin G was performed to ascertain whether there is an association of IgG with receptor-bearing cells. This was accomplished by incubating the tissue sections with a 1/100 dilution of FITC-labelled F(ab')$_2$ fragments of polyclonal rabbit anti-human IgG in 0.1M PBS containing 5% NRS for 1 hour at 37°C. The tissue was washed and a 1/50 dilution of the monoclonal anti-Fcγ receptor antibody (as described in section 5.2.2.1) in 0.1M PBS containing 5% NRS was applied for 24 hours at 4°C. After thorough washing, the mouse antibody was detected with a 1/500 dilution of TRITC-labelled F(ab')$_2$ fragments of rabbit anti-mouse IgG (1 hour, 37°C) as described in section 5.2.2.2.

5.2.2.5 Non-immune sera.

Throughout these investigations a concentration of 5% non-immune rabbit serum (NRS; Sigma, Code No.: R9133) or 5% non-immune goat serum (NGS; Sigma, Code No.: G9023) was included with the primary and secondary antibody dilutions to prevent non-specific labelling (as described in section 4.2.2.4).

5.2.2.6 Control experiments.

Negative control experiments were performed to assess the non-specific interactions engaged by the immunological reagents used in this investigation. The primary antibody was omitted in the first series of control experiments to yield the background fluorescence obtained by the application of the fluorochrome conjugated secondary (or third stage) antibody. Further control experiments were performed by replacing the specific mouse monoclonal anti-receptor antibodies with equivalent dilutions of the following reagents: i) Control mouse ascites fluid (Sigma, Code No.: M-8273; batch No.: 020H-4875; Clone, NS-1). This control mouse ascites fluid is a specially processed mouse ascites fluid obtained from BALB/c mice bearing the NS-1 myeloma and which does not produce immunoglobulins. This reagent acts as a

control for the anti-FcγRII antibody which is provided as purified ascites. ii) Non-immune mouse serum (Sigma, Code No.: M5905). iii) The definitive controls to test for mouse IgG isotype cross-reactivity were performed by replacing the primary antibodies with an equivalent dilution of purified mouse IgG_1 (Serotec, Code No.: MCA 928) or purified mouse IgG_{2a} (Serotec, Code No.: MCA 929). In all other respects the control tissue was treated identically to experimental sections.

5.2.2.7 Fluorescence nuclear counterstaining.

In some of the immunofluorescence investigations described, the nuclei of cells in the tissue sections were counterstained with a solution of propidium iodide (appendix V) as described by Ockleford et. al. (1981). This was performed during the penultimate wash for 5 minutes at 4°C according to the procedure detailed in section 4.2.2.6.

5.2.3 Mounting.

The tissue sections were mounted with Citifluor photobleach retardant mountant or Gurrs fluoromount under No. 0 thickness coverslips (Chance Propper Ltd.) as described in section 3.2.3.

5.2.4 Microscopy and photography.

The immunofluorescence preparations were examined and recorded as previously described in sections 3.2.4 and 3.2.5. Dual-labelled immunofluorescence preparations were examined using the rhodamine and fluorescein filter sets on the Zeiss epifluorescence microscope, and the A1 and A2 filters on the Biorad MRC 600 confocal laser scanning microscope attachment for simultaneous dual-channel localisation of the different fluorochromes. Measurements of structures were made using SOM and COMOS (Biorad) software.

5.3 RESULTS.

The results of the immunofluorescence investigations revealed that all 3 subtypes of Fcγ receptor were expressed by heterogeneous populations of cells in 1st trimester and term chorionic villi, and by cells of the amniochorion, chorionic plate and umbilical cord.

5.3.1 First trimester chorionic villi.

FcγRI.

FcγRI (CD64) immunoreactivity was associated with cells of the stroma in 1st trimester villi (Figure 5.4). These cells were rounded and probably represented Hofbauer cells and / or undifferentiated mesenchymal cells. However, these cells did not exhibit immunoreactivity with the anti-human monocyte / macrophage antibody (Flavell et. al., 1987; not shown) used in this study. The trophoblast surrounding the chorionic villi and the endothelial cells surrounding fetal capillaries were not immunoreactive.

FcγRII.

FcγRII (CDw32) immunoreactivity was associated with endothelial cells of 1st trimester chorionic villi (Figure 5.5). This receptor appeared to be expressed as soon as precursor mesenchymal cells had differentiated and condensed to form capillaries. In more mature capillaries, which had developed to form a capillary lumen, immunoreactivity was pronounced and examination of specimens with the confocal laser scanning microscope revealed a punctate association of this receptor with the endothelial cells. This receptor was also expressed by Hofbauer cells present in the connective tissue core.

FcγRIII.

FcγRIII (CD16) was expressed by the syncytiotrophoblast of immature villi (Figures 5.6-5.9). By counterstaining cell nuclei or examining immunofluorescence preparations with phase contrast or Nomarski optics (Figures 5.7-5.8) it was possible to show that cytotrophoblast cells underlying the syncytium did not possess this receptor. This was most clearly demonstrated in tissue specimens in which the morphology had been conserved by pre-fixation with 4% paraformaldehyde. Furthermore, this observation demonstrated that the epitope recognised by the monoclonal antibody used in this study was not destroyed by paraformaldehyde fixation. A fascinating observation was that where the cells of the cytotrophoblast layer had become discontinuous in the first trimester, it was possible to identify

regions of FcγRIII-immunoreactive syncytiotrophoblast penetrating between these cells and extending to the basal lamina.

The increased resolution and sensitivity of the dark-field confocal microscopy techniques used in this study permitted the visualisation of inclusions within the syncytium of 1st trimester villi that were immunoreactive with the anti-FcγRIII antibody (Figure 5.6). The average diameter of these inclusions was 1.4μm (n=57, SD=0.4). This immunoreactivity was maintained in unfixed tissue sections, specimens pre-fixed with 4% paraformaldehyde or specimens post-fixed with 3% formaldehyde or acetone. The receptor was localised at the periphery of these inclusions and was frequently concentrated at a pole. Nuclei present within the syncytium were not immunoreactive with this antibody. However, macrophages (Hofbauer cells) present within the connective tissue core also expressed this receptor.

Co-localisation of Fcγ receptors and endogenous IgG.
By dual-labelling the FcγR's and endogenous IgG simultaneously it was possible to discern if there was an association of the receptor with its ligand. FcγRI localised in cells of the connective tissue core of the villi. Immunofluorescence association of endogenous IgG with these receptor-bearing cells of the core was detected in low levels since endogenous IgG was only present in low concentrations in the first trimester. A similar immunolocalisation was observed with FcγRII-bearing cells of the core (Hofbauer cells and endothelial cells) although, similarly, this was difficult to detect since the endogenous antibody was not present in significant concentrations. However, a perfect correlation was observed between the expression of FcγRIII in the syncytiotrophoblast and the presence of endogenous IgG (Figure 5.9). Cytotrophoblast cells, which did not possess FcγRIII, did not contain endogenous antibody. Where the syncytiotrophoblast extended between the cytotrophoblast cells to contact the basement membrane, FcγRIII immunoreactivity and IgG were found to co-localise. However, the resolution of the light microscope was insufficient to resolve whether the receptor and its ligand were associated with the same subcellular organelles or with one another.

Monocyte / macrophages.
Experiments were performed using the monoclonal antibody to human monocytes / macrophages (MAC 387; Flavell et. al., 1987) in an attempt to assess the normal distribution of connective tissue macrophages (Hofbauer cells) in first trimester chorionic villi. This antibody did not display immunoreactivity with any cell type present in frozen sections of first trimester villi. However, maternal monocytes

present within the blood lakes were immunoreactive with this antibody, thus providing an internal positive control to validate the performance of the antibody.

5.3.2 Term chorionic villi.

FcγRI.

In term chorionic villi FcγRI (CD64) immunoreactivity was clearly associated with mesenchymal / fibroblast cells as well as Hofbauer cells. These cells were numerous in the core of the villi and possessed stellate or fusiform morphology (Figure 5.10). These observations suggested that immunoreactive cells in the core were not Hofbauer cells since these were rare in the villi of term placentae and, furthermore, possessed a rounded vacuolated morphology. Cells possessing the morphological characteristics of Hofbauer cells and leucocytes present in the lumen of fetal blood vessels (Figure 5.15) and maternal blood external to the tissue also expressed this antigen. Fluorescence counterstaining of cell nuclei demonstrated that not all nucleated cells present within the lumen of the fetal capillaries expressed this receptor which suggested that these were heterogeneous populations of cells. This was more clearly demonstrated in specimens pre-fixed with 4% paraformaldehyde and also illustrated that the epitope recognised by the monoclonal antibody used in this investigation survived fixation.

FcγRII.

FcγRII (CDw32) immunoreactivity was expressed by endothelial cells surrounding fetal capillaries of term chorionic villi. This receptor could be demonstrated in transverse (Figure 5.11) or longitudinal (Figure 5.13) sections through the endothelial cells. Furthermore, by employing the increased sensitivity of the confocal laser scanning microscope it was possible to detect the fact that association of this receptor with the endothelium was punctate. This suggested that the receptor localised in vesicles or inclusions (Figure 5.12). In addition it was possible to demonstrate an association of this receptor molecule with the apical (luminal) surface of the endothelium and with the basal (stromal) aspect of the cell, as well as intracellularly throughout the cell cytoplasm.

Immunoreactivity for this receptor was not demonstrated in the endothelium of the umbilical cord or vessels of the chorionic plate (Figure 5.16). However, FcγRII immunoreactivity was detectable in the endothelium surrounding vessels of the stem villi which extended from the chorionic plate. This immunoreactivity was only demonstrable using the more sensitive amplification obtained by using the 3-stage immunofluorescence protocol. FcγRII was easily identified in the endothelium of vessels in intermediate or terminal chorionic villi. This suggested that there was

heterogeneous expression of this receptor by endothelial cells dependant upon their position in the villus tree.

FcγRII immunoreactivity was also associated with Hofbauer cells of the villus stroma and with leucocytes present within fetal vessels (Figure 5.16). However, fluorescence nuclear counterstaining with propidium iodide indicated that not all nucleated cells present in the fetal circulation expressed this receptor. This demonstrated that there were heterogeneous populations of leucocytes present or cells of different maturational stages.

FcγRIII.

FcγRIII (CD16) was expressed by the syncytiotrophoblast of term villi. Using Nomarski optics on villi sectioned in an appropriate plane and specimens counterstained with propidium iodide it became apparent that cytotrophoblast cells did not exhibit immunoreactivity to this receptor. This was consistent with the localisation obtained with 1st trimester chorionic villi where this receptor was not associated with cytotrophoblast cells. Furthermore, FcγRIII was predominantly associated with the apical aspect of the syncytium in term trophoblast (Figure 5.14). However, it was not possible to demonstrate an association of this receptor with the vesicular inclusions reported for 1st trimester syncytiotrophoblast. Immunoreactivity in term syncytiotrophoblast appeared more homogeneous suggesting that the receptor was associated with cellular inclusions beyond the resolution of the optical microscope. This antigen also survived pre-fixation with 4% paraformaldehyde.

FcγRIII immunoreactivity could be demonstrated in association with the small population of Hofbauer cells present within the villus core in term villi. Leucocytes present within the fetal vessels and the maternal blood lakes also expressed this receptor (Figure 5.17). However, using fluorescence nuclear counterstaining with propidium iodide it was possible to demonstrate that not all nucleated cells present within the capillaries expressed this receptor. This was consistent with the data obtained with the other receptor subtypes and suggested that these were heterogeneous cells or in different maturational stages.

Co-localisation of Fcγ receptors and endogenous IgG.

Immunocytochemical experiments were performed to dual label each Fcγ receptor subtype used in this investigation and endogenous IgG. FcγRIII co-localised with endogenous IgG at the apical surface of the syncytiotrophoblast, in contrast to first trimester where this receptor was demonstrated throughout the cytoplasm. An association with the marginated vesicular inclusions was not apparent and FcγR

immunoreactivity was not demonstrably punctate. Similarly there was an association of endogenous IgG with the FcγRI receptor expressed by mesenchymal cells and FcγRII expressed by the capillary endothelium. However, these data revealed little more than the experiments in which single labelling was performed since the resolution of the light microscope was not sufficient to resolve whether the receptor and its ligand co-localised in the same subcellular inclusions. However, it was clear from these studies that the cell types which possessed a receptor also contained IgG but that cell types devoid of receptors (cytotrophoblast cells, endothelial cells of the umbilical cord and chorionic plate, cells of the adventitia surrounding fetal vessels and amniotic epithelial cells) did not contain endogenous IgG. Thus an association of the receptor with its ligand was strongly implicated.

Monocytes / Macrophages.

The distribution of monocytes and macrophages in the tissue was investigated using a monoclonal antibody marker (Flavell et. al., 1987). Immunoreactivity to this molecule was expressed by a population of cells in the maternal blood lakes and by cells present within the lumen of fetal blood vessels (Figure 5.18; inset). Occasionally immunoreactivity was associated with cells present within the core of term villi (Figure 5.18). These cells possessed the rounded morphology and a single rounded nucleus typical of monocyte cells or macrophages. These cells were not numerous in the villus stroma.

5.3.3 Term amniochorion.

FcγRI.

FcγRI (CD64) was expressed by cells present within the maternal decidual layer associated with the amniochorion. These were presumably immunocompetant maternal leucocytes. However, the novel finding that this receptor was expressed by cells of extraembryonic mesodermal origin in the amniochorion (fibroblast and reticular layers) was observed. Fluorescence nuclear counterstaining with propidium iodide revealed that immunoreactivity to this receptor was not associated with all cells of these layers (Figure 5.19). This suggested that these were heterogeneous populations of cells. Cells of epithelial type in the amniochorion (amniotic epithelial cells and cytotrophoblast cells of the chorion laeve) did not express this receptor.

FcγRII.

FcγRII (CDw32) was expressed by maternal leucocytes present within the decidual layer associated with the amniochorion. We have seen in sections 5.3.1 and 5.3.2 that this receptor was expressed by endothelial cells of immature and term chorionic villi.

However, this receptor was not expressed by endothelial cells forming the walls of blood vessels in the maternal decidua.

The novel finding that FcγRII was also expressed by cells of the mesenchymal layers of the amniochorion (fibroblast and reticular layers) was observed (Figure 5.20). However, the technique of counterstaining cell nuclei with propidium iodide revealed that not all the cells of these layers possessed this receptor. This suggested that these layers possessed heterogeneous populations of cells or cells in different developmental stages. Cytotrophoblast cells of the trophoblast layer and amniotic epithelial cells did not express this receptor.

FcγRIII.

FcγRIII (CD16) was expressed by leucocytes in the maternal decidual layer associated with the amniochorion. This receptor was also associated with a small proportion of cells of extraembryonic lineage in the amniochorion (fibroblast and reticular layers). This sparse population of cells was more clearly demonstrated in sections in which the cell nuclei had been counterstained with propidium iodide (Figure 5.21). A particularly interesting observation was that cytotrophoblast cells of the chorion laeve did not express this receptor. This was consistent with the observation that cytotrophoblast cells of immature and term chorionic villi did not express FcγRIII (sections 5.3.1 and 5.3.2).

Simultaneous anti-FcγR labelling.

The previous studies have demonstrated that the three subtypes of FcγR were expressed by heterogeneous populations of cells of the extraembryonic mesenchymal tissue layers of the amniochorion (fibroblast and reticular layers). However, it is conceivable that cells in these layers which did not express a receptor in experiments designed to localise a single subtype, may have expressed one of the other subtypes of immunoglobulin receptor. To investigate this possibility the tissue sections were simultaneously immunoreacted with a cocktail of the three anti-FcγR monoclonal antibodies. When combined with fluorescence nuclear counterstaining it was possible to obtain quantitative data about the number of cells of these layers that expressed immunoglobulin receptors. The incidence of immunoreactive cells when incubated with single anti-receptor antibodies or simultaneously with all 3 anti-receptor antibodies is shown in Table 5.1.

% of amniochorion cells immunoreactive.

antibody reactivity to:-	amniotic epithelium	fibroblast and reticular layers	trophoblastic layer
$\Sigma Fc\gamma R$	0	75.9(n=577)	0
$Fc\gamma RI$	0	48.1(n=241)	0
$Fc\gamma RII$	0	68.2(n=1253)	0
$Fc\gamma RIII$	0	7.5(n=478)	0

Table 5.1: The percentage of cells in the tissue immunoreactive with the three monoclonal antibodies or a combination of them all.

These data indicate that 24.1% of the cells present in the fibroblast and reticular layers of the tissue did not express a characterised immunoglobulin $Fc\gamma R$. Furthermore, the data indicates that there may have been considerable co-expression of receptor subtypes in those cells that did possess receptors. It is clear that $Fc\gamma RII$ was expressed by the majority of receptor-bearing cells. These experiments confirm that cytotrophoblast cells of the chorion laeve and amniotic epithelial cells did not express characterised $Fc\gamma$ receptors.

Co-localisation of $Fc\gamma$ receptors and endogenous IgG.

Dual-labelling studies demonstrated that intense immunoreactivity for IgG co-localised with $Fc\gamma$ receptor-bearing cells of the fibroblast and reticular layers (Figure 5.23) and with cells of the maternal uterine decidua. IgG was also clearly revealed in the connective tissue stroma surrounding these cells. This study failed to identify endogenous IgG immunofluorescence with either cells of the amniotic epithelium or the cytotrophoblast cells of the chorion laeve. Furthermore, these cells did not possess immunoreactivity to any of the three subtypes of characterised human leucocyte $Fc\gamma$ receptors employed in this investigation. Therefore, cells which did possess an $Fc\gamma R$ also contained endogenous antibodies but those that were devoid of a receptor were also devoid of IgG. The results of this study and morphology of the fetal membranes are summarised in figure 5.29.

Monocytes / Macrophages.

The anti-human macrophage / monocyte monoclonal antibody was immunoreactive with a population of cells of the maternal decidual layer possessing the morphological characteristics of macrophages (Figure 5.24). The cells of the

mesenchymal layers and the amniotic epithelial cells and trophoblast cells did not express this antigen.

5.3.3.1 Chorionic plate.

FcγRI.

FcγRI immunoreactivity in the chorionic plate was confined to leucocytes present within the lumen of fetal vessels (Figure 5.15). Mesenchymal cells of the connective tissue stroma and amniotic epithelial cells overlying the chorionic plate did not express this receptor. The single exception to this distribution was mesenchymal cells located immediately beneath the amniotic epithelium where it was possible to identify immunoreactivity to this receptor.

FcγRII.

FcγRII immunoreactivity in the chorionic plate was confined to leucocytes present within the lumen of fetal vessels. The endothelium surrounding these vessels was not immunoreactive (Figure 5.16). However, it was possible to detect FcγRII immunoreactivity in the endothelium surrounding the vessels of the stem villi branching from the chorionic plate, although no clear dividing line between receptor-positive and receptor-negative endothelial cells was apparent in these villi. Mesenchymal cells of the chorionic plate did not possess this receptor except those cells of the amnion that underlie the placental amniotic epithelium.

FcγRIII.

FcγRIII immunoreactivity in the chorionic plate was restricted to the leucocytes present within the lumen of fetal vessels (Figure 5.17). The syncytiotrophoblast of the chorionic plate, in contact with the maternal blood lakes, was also immunoreactive. The sensitivity of the techniques employed were sufficient to identify immunoreactive cells underlying the amniotic epithelium of the chorionic plate.

Monocytes / macrophages.

The anti-human monocyte / macrophage antibody used in this investigation recognised monocytes present within the lumen of fetal vessels only.

5.3.3.2 Umbilical cord.

FcγRI.

FcγRI was expressed by a population of leucocytes present within the umbilical vessels and by cells of the Whartons jelly connective tissue (Figure 5.25a). It was

-136-

clearly evident that not all cells of the stroma were immunoreactive. Furthermore, the endothelial cells of the vessels, the cells of the vessel adventitia and amniotic epithelial cells were negative.

FcγRII.
FcγRII immunoreactivity was associated with leucocytes present within the umbilical vessels and with cells of the Whartons jelly connective tissue (Figure 5.25b). These cells possessed stellate morphology but it was evident that not all cells were immunoreactive. The endothelial cells of the vessels, like those of the chorionic plate, were not immunoreactive with this monoclonal antibody. The amniotic epithelium, likewise, did not express this receptor.

FcγRIII.
FcγRIII immunoreactivity was associated with a population of leucocytes present within the vessels and with mesenchymal cells in the Whartons jelly (Figure 5.25c). Endothelium, cells of the vessel adventitia and amniotic epithelial cells were not immunoreactive.

Monocytes / macrophages.
Immunoreactivity to the monocyte / macrophage marker was identified in leucocytes present within the lumen of fetal vessels only.

5.3.4 Hydatidiform mole.

FcγRI.
FcγRI immunoreactivity was identified in cells of the mesenchymal connective tissue core (Figure 5.26). The trophoblast was not immunoreactive

FcγRII.
FcγRII expression was confined to cells of the mesenchymal connective tissue core (Figure 5.27). Since, the villi of hydatidiform mole specimens did not possess blood vessels an association of this receptor with endothelium was not observed. The trophoblast surrounding the villi was not immunoreactive.

FcγRIII.
FcγRIII immunoreactivity was associated with the syncytiotrophoblast, similar to the observation in healthy 1st trimester chorionic villi (Figure 5.28). This receptor was also associated with a sparse population of cells of the mesenchymal connective tissue core. However, cytotrophoblast cells did not express this receptor.

Monocytes / macrophages.

Monocyte / macrophage immunoreactivity was not associated with the chorionic villi of hydatidiform mole specimens. This observation correlated with the data obtained for normal healthy 1st trimester specimens.

5.3.5 Control experiments.

Control experiments performed by replacing primary monoclonal antibodies with non-specific mouse IgG isotype antibodies revealed negligible levels of background fluorescence (Figure 5.22b). Control experiments performed by omitting the primary specific antibodies and incubating with buffer alone or by replacing them with non-immune mouse IgG yielded similar (negative) outcomes (Figure 5.25d). These data indicated that the immunofluorescence localisation patterns obtained throughout these investigations were a consequence of the specificity of the antibodies for their antigen and were not a consequence of non-specific interactions engaged by these immunoglobulins or the reagents used to detect them.

FIGURES 5.4 - 5.29.

Figures 5.4-5.6: FcγR immunoreactivity in 1st trimester chorionic villi.

Figure 5.4: Confocal micrograph of FcγRI (CD64) immunoreactivity in a frozen section of an unfixed 1st trimester chorionic villus. Note that fluorescence is associated with cells of the stroma (St) but not with the surrounding trophoblast (T). This receptor is present within the cytoplasm which may indicate that the receptor and its ligand are internalised. Scale bar represents 50μm.

Figure 5.5: Confocal micrograph of FcγRII (CDw32) immunoreactivity in a frozen section of an unfixed 1st trimester chorionic villus. Fluorescence is associated with cells forming the blood vessel walls in the stroma (St) which have differentiated from the fetal mesenchyme. The surrounding trophoblast (T) is not immunoreactive. Scale bar represents 50μm.

Figure 5.6: Confocal micrograph of FcγRIII (CD16) immunoreactivity in a frozen section of an unfixed 1st trimester chorionic villus. FcγRIII is expressed by the syncytiotrophoblast and is associated with the periphery of marginated vesicular inclusions. Fluorescence is often more intense at a pole (arrowheads) which may reflect receptor-sorting in these organelles. Connective tissue stroma (St). Scale bar represents 10μm.

5.4

5.5

5.6
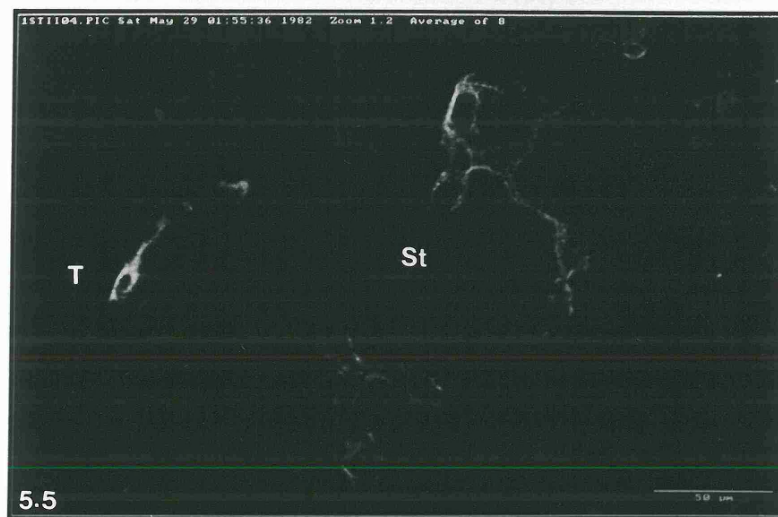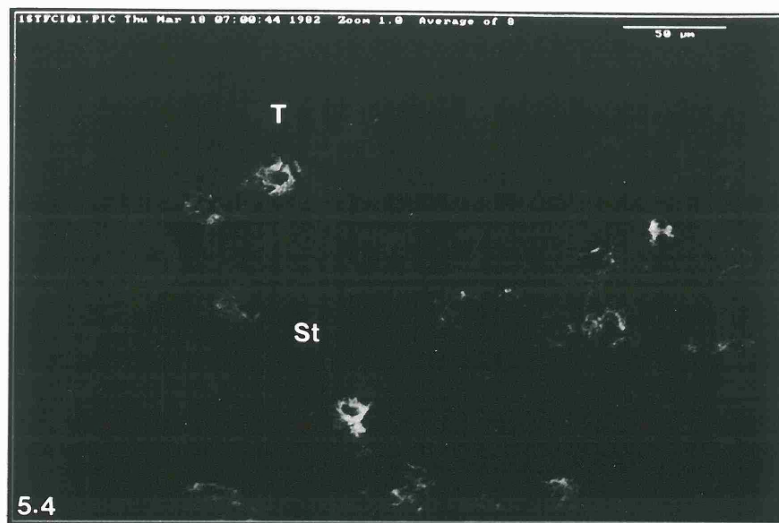
Figures 5.7-5.9: FcγRIII (CD16) immunoreactivity in 1st trimester chorionic villi.

Figure 5.7: Dual-channel colour confocal micrograph of FcγRIII (CD16) immunoreactivity (green channel) and Nomarski DIC (grey channel) of a frozen section of 4% paraformaldehyde pre-fixed 1st trimester chorionic villus. FcγRIII is expressed by the syncytiotrophoblast but underlying cytotrophoblast cells (open arrows) are not immunoreactive. Connective tissue stroma (St). Scale bar represents 250μm.

Figure 5.8: High resolution, dual-channel, colour confocal micrograph of FcγRIII (CD16) immunoreactivity (green channel) and Nomarski DIC (grey channel) of a frozen section of 4% paraformaldehyde pre-fixed 1st trimester chorionic villus. FcγRIII is expressed by the syncytiotrophoblast (Sy) but underlying cytotrophoblast cells (open arrows) and nuclei (N) are not immunoreactive. Connective tissue stroma (St). Scale bar represents 10μm.

Figure 5.9: Dual-channel, colour confocal micrograph of FcγRIII (CD16) immunoreactivity (red channel) and endogenous IgG immunoreactivity (green channel) in a frozen section of 4% paraformaldehyde pre-fixed 1st trimester chorionic villus. Co-localisation of FcγRIII and endogenous IgG is observed in the syncytiotrophoblast (yellow) but underlying cytotrophoblast cells (arrowheads) do not possess either antigen. Low levels of IgG immunoreactivity are evident in the connective tissue stroma (St). Scale bar represents 50μm.

GREY, NOMARSKI DIC ; GREEN, FCRIII

St

5.7

300 UM

GREY, NOMARSKI DIC ; GREEN, FCRIII

Sy

N

St

5.8

10 UM

1st TRIMESTER CORIONIC VILLUS.
RED: FcRIII; GREEN: IgG.

St

5.9

50 UM
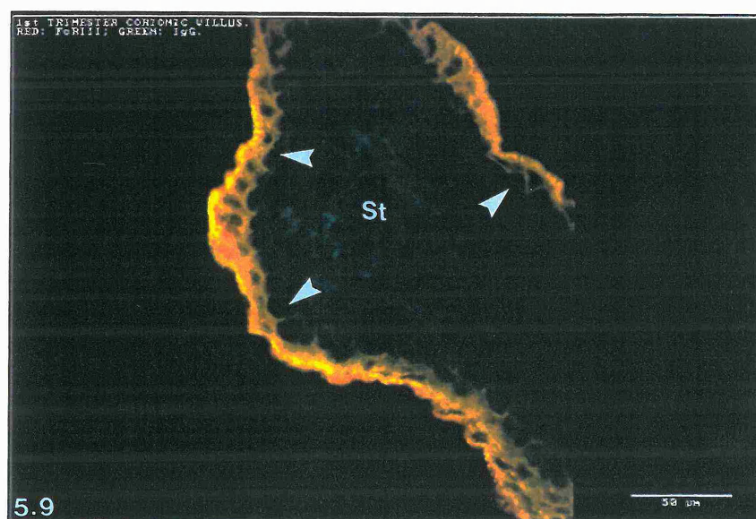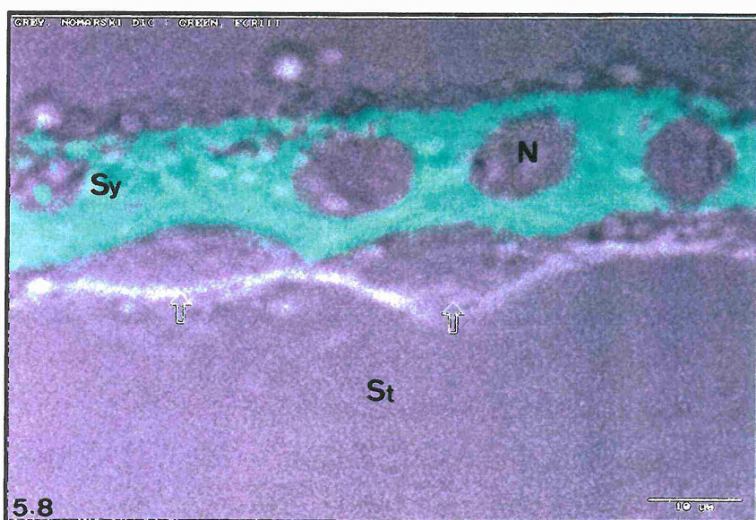
Figures 5.10-5.14: FcγR immunoreactivity in term chorionic villi.

Figure 5.10: Confocal micrograph of FcγRI (CD64) immunoreactivity in a frozen section of an unfixed term chorionic villus. Note that fluorescence is associated with stellate cells of the core. This receptor is present within the cytoplasm which may indicate that the receptor and ligand are internalised. The trophoblast (T) and endothelial cells surrounding a capillary (C) do not express this receptor. Scale bar represents 25μm.

Figure 5.11: Confocal micrograph of FcγRII (CDw32) immunoreactivity in a transverse frozen section of an unfixed term chorionic villus. FcγRII is expressed by the endothelium surrounding fetal vessels (V) where the diffuse cytoplasmic pattern may reflect a transendothelial shuttle of the receptor and its ligand. Villus stroma (St). Scale bar represents 100μm.

Figure 5.12: High resolution confocal micrograph of FcγRII (CDw32) immunoreactivity in a transverse frozen section of an unfixed term chorionic villus. This extended focus projection of a series of images from various depths within the section reveals a punctate pattern of immunoreactivity which may indicate that the receptor internalises its ligand into vesicles. Scale bar represents 25μm.

Figure 5.13: Confocal micrograph of FcγRII (CDw32) immunoreactivity in a longitudinal frozen section of an unfixed term chorionic villus. FcγRII is expressed by the entire length of the endothelium surrounding fetal vessels. Scale bar represents 50μm.

Figure 5.14: Confocal micrograph of FcγRIII (CD16) immunoreactivity in a frozen section of an unfixed term chorionic villus. FcγRIII is expressed by the syncytiotrophoblast and fluorescence is concentrated at the apical cell surface (arrowheads). Stroma (S). Scale bar represents 25μm.

5.10

5.11

5.12

5.13

5.14
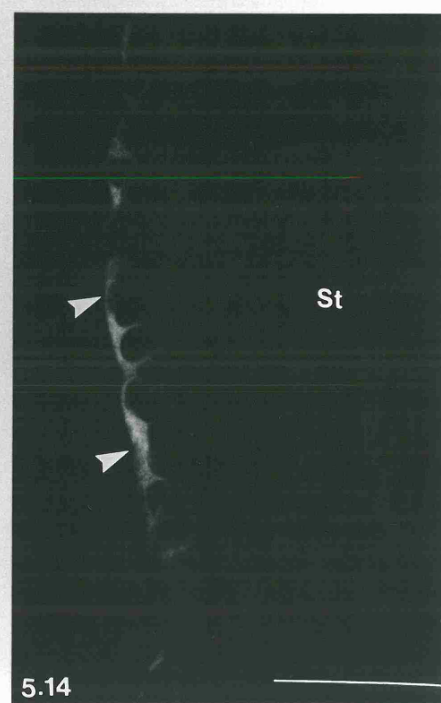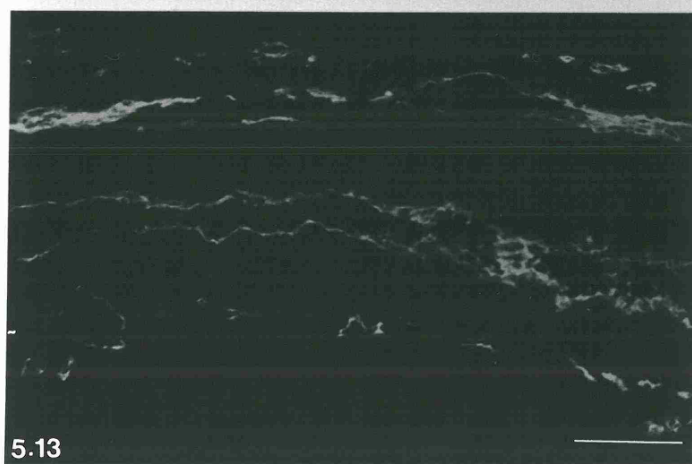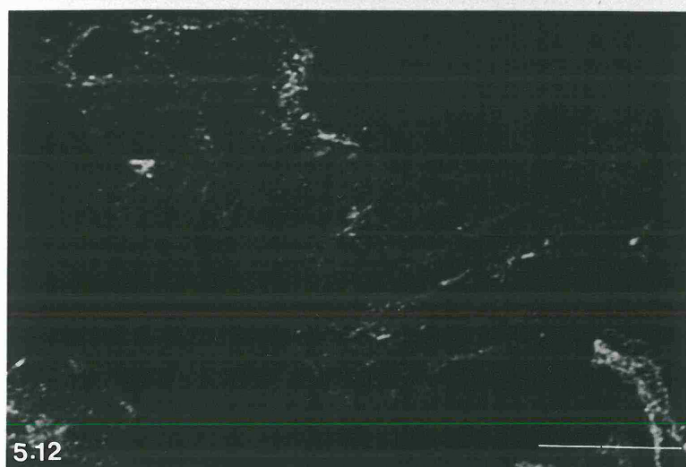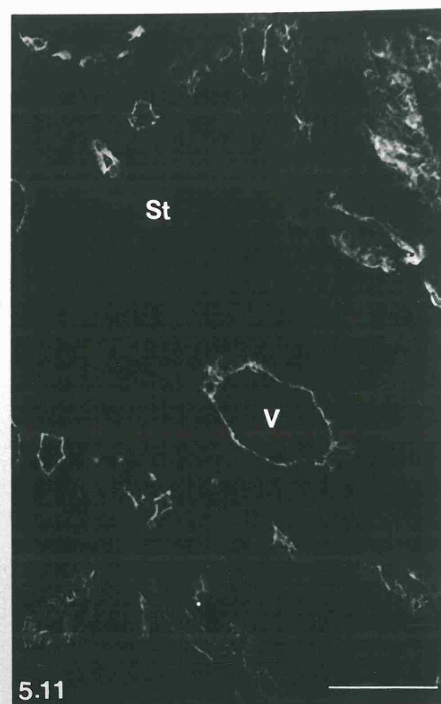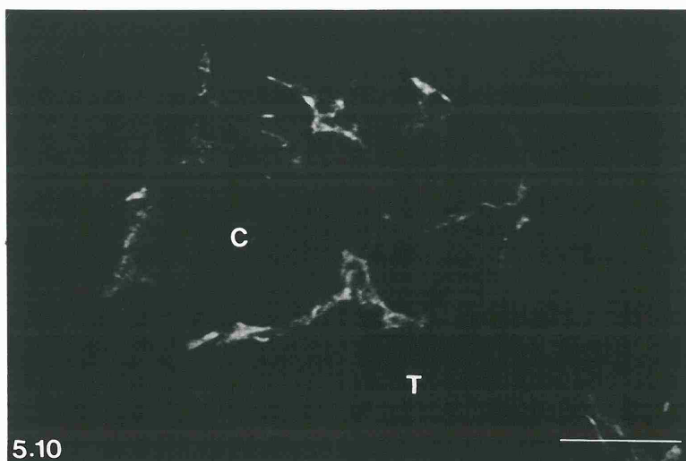
<u>**Figures 5.15-5.18: FcγR immunoreactivity in term chorionic plate.**</u>

Figure 5.15: Epifluorescence micrograph of FcγRI (CD64) immunoreactivity in a frozen section of 4% paraformaldehyde pre-fixed term chorionic plate. Note that fetal leucocytes present within the lumen (L) of a chorionic plate vessel express this receptor. Scale bar represents 20μm.

Figure 5.16: Epifluorescence micrograph of FcγRII (CDw32) immunoreactivity in a frozen section of 4% paraformaldehyde pre-fixed term chorionic plate. Fetal leucocytes present within the lumen (L) of a chorionic plate vessel express this receptor. Note, however, that the endothelium (E) surrounding the vessel lumen is not immunoreactive in the chorionic plate. Scale bar represents 20μm.

Figure 5.17: Epifluorescence micrograph of FcγRIII (CD16) immunoreactivity in a frozen section of 4% paraformaldehyde pre-fixed term chorionic plate. Fetal leucocytes present within the lumen (L) of a chorionic plate vessel express this receptor. Scale bar represents 20μm.

Figure 5.18: Epifluorescence micrograph of immunoreactivity to the monocyte / macrophage marker in a frozen section of 4% paraformaldehyde pre-fixed term chorionic plate (CP). Immunoreactive cells are evident in the chorionic villi (CV) associated with this section. Inset: Fetal leucocytes present within the lumen (L) of a chorionic plate vessel express this marker. Scale bars represent 20μm.

5.15

5.16

5.17

5.18
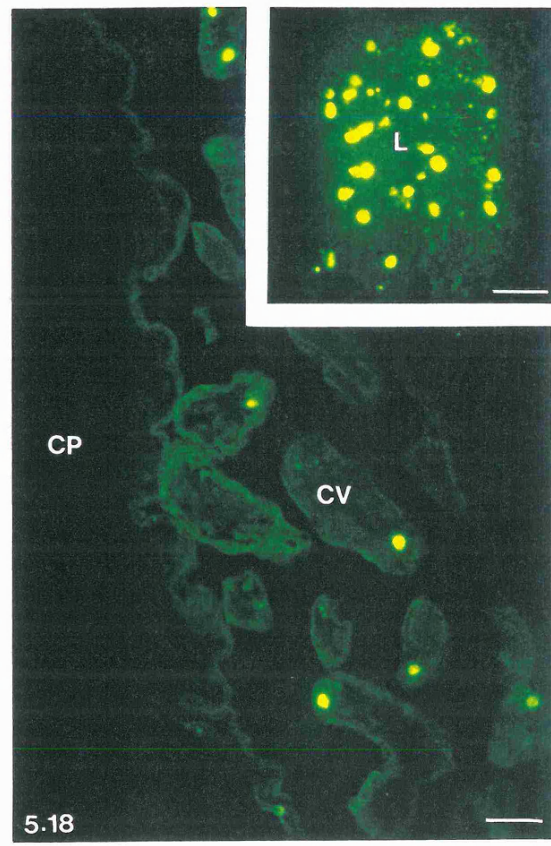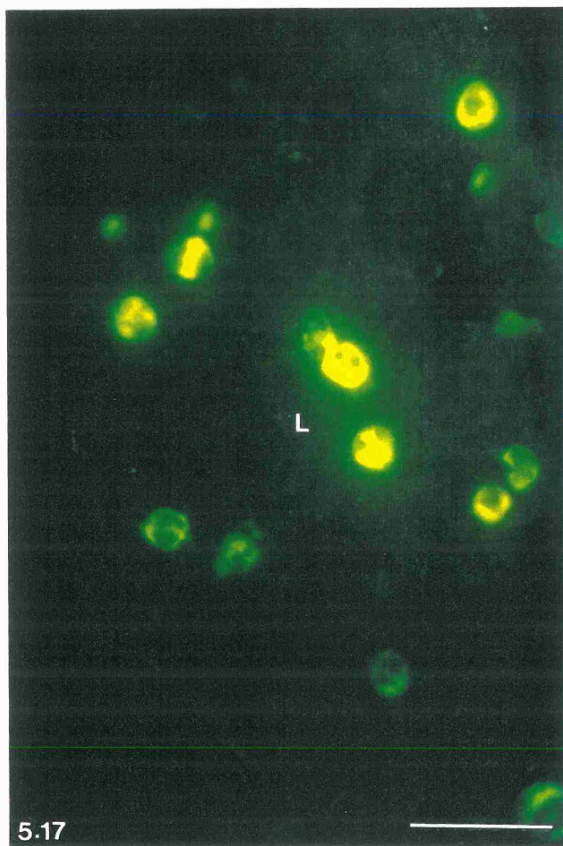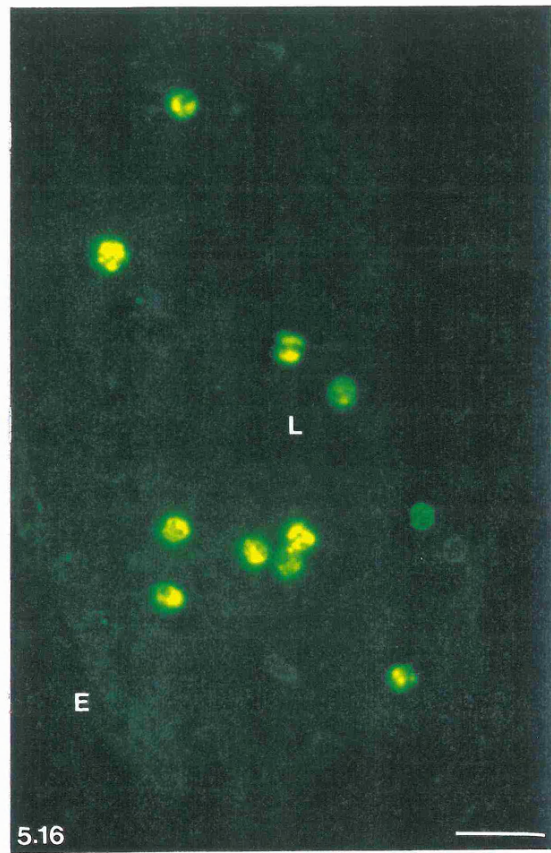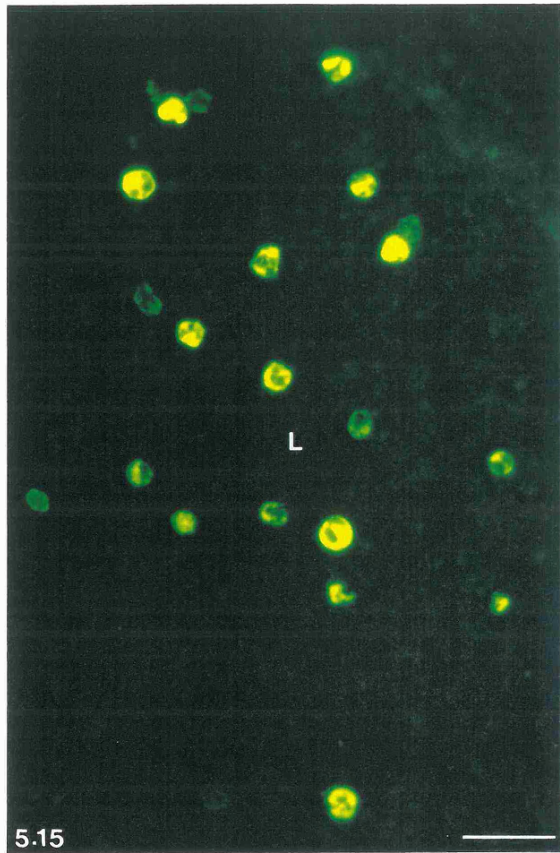
<u>**Figures 5.19-5.21: FcγR immunoreactivity in term amniochorion.**</u>

Figure 5.19: Colour confocal indirect immunofluorescence micrograph of FcγRI (CD64) immunoreactivity (green channel) in human term amniochorion. Nuclei have been counterstained with propidium iodide (red channel). Note that a population of cells of the maternal decidual layer (D) express this receptor. In addition a population of cells in the fibroblast and reticular layers of the extraembryonic mesenchyme express this receptor. However, not all cells of these layers display immunoreactivity (arrowheads). Cells of the amniotic epithelium (A) and trophoblast layer (T) do not exhibit immunoreactivity to this receptor. Scale bar represents 100μm.

Figure 5.20: Colour confocal indirect immunofluorescence micrograph of FcγRII (CDw32) immunoreactivity (green channel) in human term amniochorion. Nuclei (red channel) have been counterstained with propidium iodide. Very few cells in the fibroblast and reticular layers of the mesenchyme do not express this receptor (arrowheads). A population of cells of the maternal decidual layer (D) express this receptor but cells of the amniotic epithelium (A), cytotrophoblast layer (T) and endothelial cells in the maternal decidua do not exhibit immunoreactivity. Scale bar represents 100μm.

Figure 5.21: Colour confocal indirect immunofluorescence micrograph of FcγRIII (CD16) immunoreactivity (green channel) in human term amniochorion. Nuclei (red channel) have been counterstained with propidium iodide. This receptor is associated with only a few cells in the fibroblast and reticular layers (arrow) of the mesenchyme and with a population of cells of the maternal decidual layer (D). Cells of the amniotic epithelium (A) are unreactive. It is of particular interest that cytotrophoblast cells of the trophoblast layer (T) in this tissue do not express this receptor. Scale bar represents 100μm.

GREEN, FCRI : RED, PROPIDIUM IODIDE.

5.19

GREEN, FCRII: RED, PROPIDIUM IODIDE.

5.20

GREEN, FCRIII : RED, PROPIDIUM IODIDE.

5.21
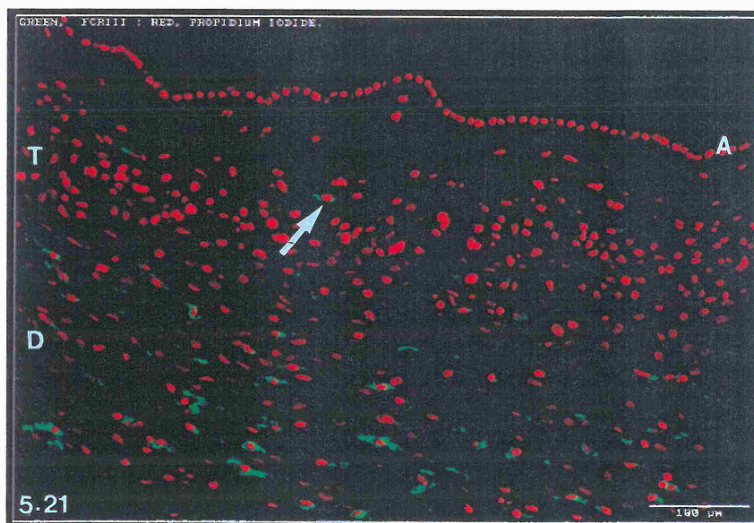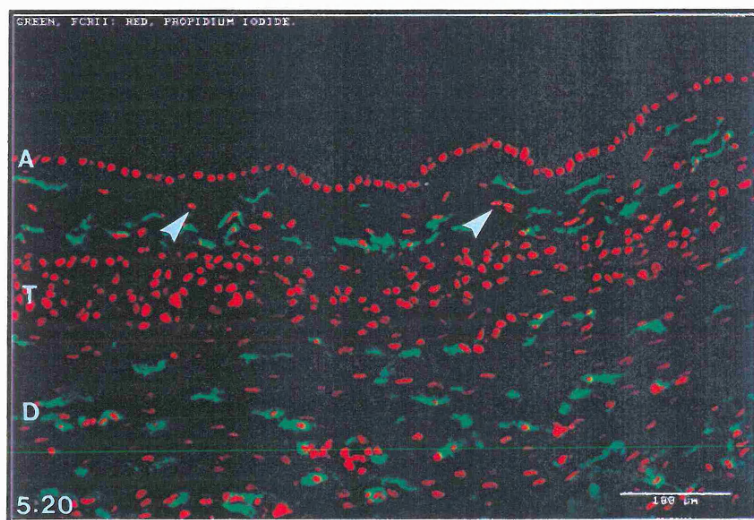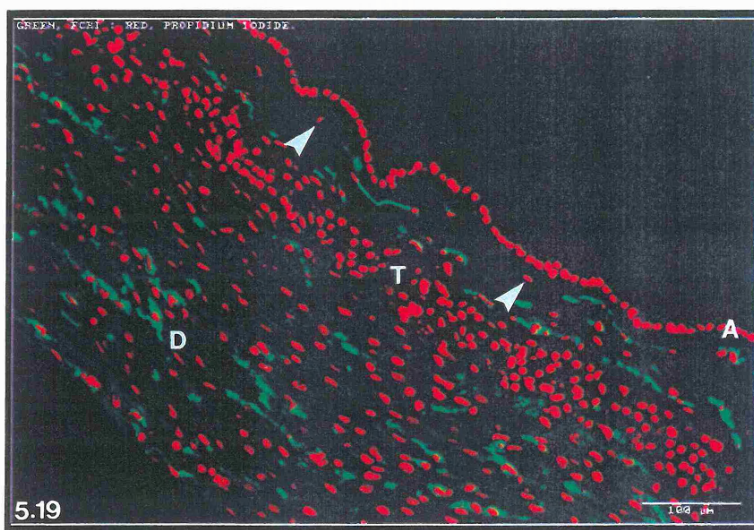
Figures 5.22-5.25: FcγR immunoreactivity in term amniochorion and umbilical cord.

Figure 5.22: a) Confocal indirect immunofluorescence micrograph of FcγRII (CDw32) immunoreactivity in an unfixed frozen section of human term amniochorion. b) Control preparation of a serial section to that shown in panel a). In this control experiment primary monoclonal anti-FcγRII antibodies were replaced with an equivalent concentration (4μg/ml) of purified mouse IgG$_{2a}$. All subsequent procedures were identical. Scale bar represents 100μm.

Figure 5.23: Dual-channel colour confocal micrograph illustrating localisation of IgG (green channel) and FcγRII (red channel) in the fibroblast layer (F) of term amniochorion. Co-localisation of the receptor and its ligand in the fibroblast cells is shown as yellow. Scale bar represents 10μm.

Figure 5.24: Epifluorescence micrograph illustrating immunoreactivity to the monocyte / macrophage marker in term amniochorion. Phase-contrast illumination has been used to reveal the underlying morphology. Note that macrophages present in the maternal decidual layer (D) are immunoreactive. Amniotic epithelium (A); Trophoblast layer (T). Scale bar represents 20μm.

Figure 5.25:: Montage illustrating confocal indirect immunofluorescence micrographs of a) FcγRI (CD64), b) FcγRII (CDw32), c) FcγRIII (CD16) and d) a control preparation, in which the primary specific monoclonal anti-FcγR antibodies have been omitted, in umbilical cord. Populations of mesenchymal cells present in the Whartons jelly are immunoreactive but the amniotic epithelium and blood vessel endothelial cells are not immunoreactive. Scale bar represents 100μm.

5.22 a) FcRII. b) CONTROL.

5.23 GREEN, IgG : RED, FCRII. F 10 μm

5.24 A T D

5.25 UMBILICAL CORD. a) FcRI. b) FcRII. c) FcRII. d) CONTROL. 100 μm
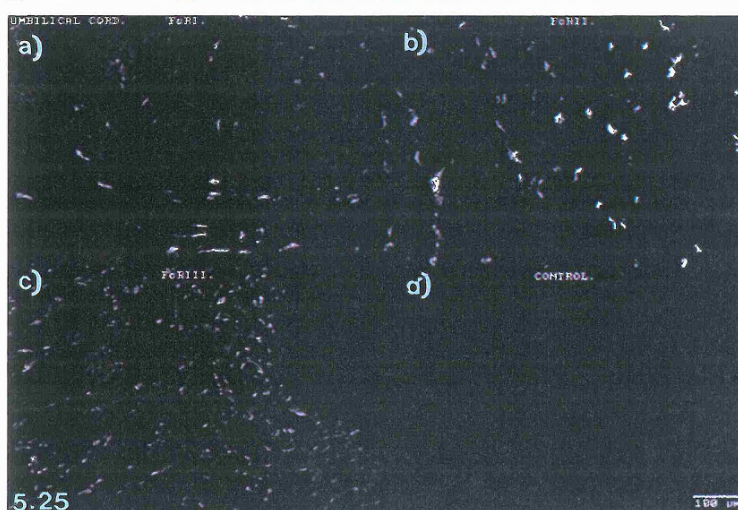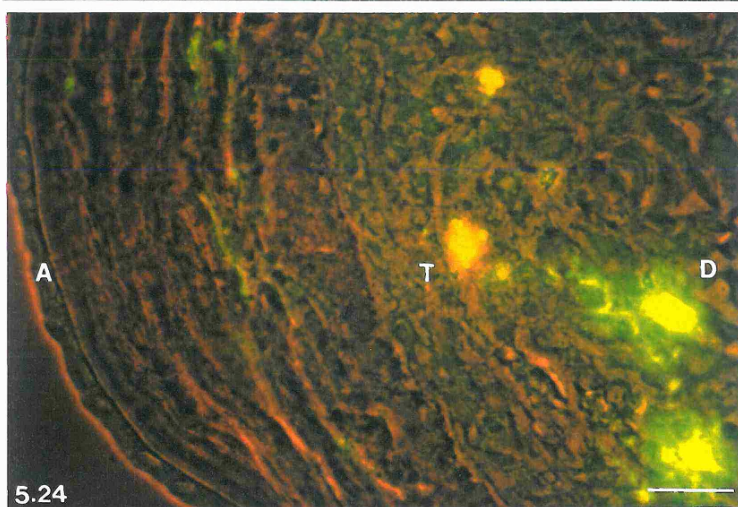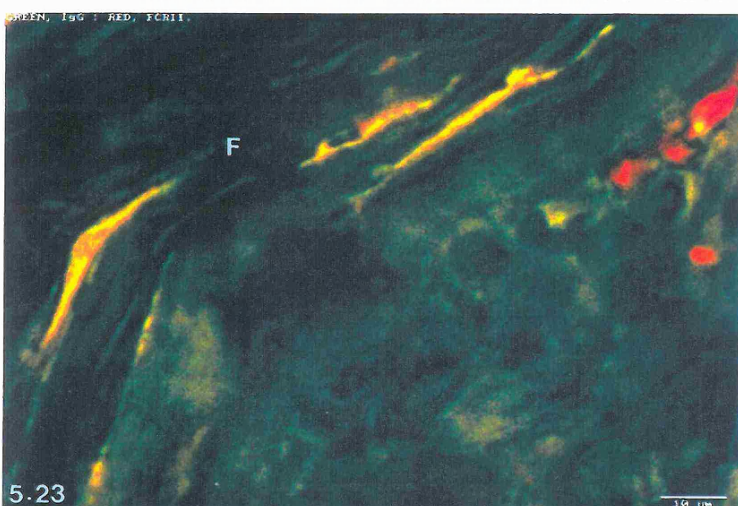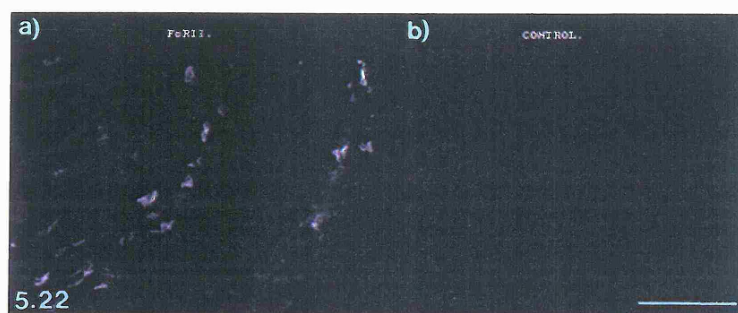
<u>**Figures 5.26-5.28: FcγR immunoreactivity in hydatidiform mole chorionic villi.**</u>

Figure 5.26: Epifluorescence micrograph illustrating FcγRI (CD64) immunoreactivity in an unfixed frozen tissue section of a complete homozygous hydatidiform mole chorionic villus. Note that a population of undifferentiated mesenchymal cells in the connective tissue stroma (St) are immunoreactive but the surrounding trophoblast (T) is not. Scale bar represents 20μm.

Figure 5.27: Epifluorescence micrograph illustrating FcγRII (CDw32) immunoreactivity in an unfixed frozen tissue section of a complete homozygous hydatidiform mole chorionic villus. Note that undifferentiated mesenchymal cells in the connective tissue stroma (St) are immunoreactive but the surrounding trophoblast (T) is not. It is not possible to identify blood vessels in this tissue. Scale bar represents 20μm.

Figure 5.28: Epifluorescence micrograph illustrating FcγRIII (CD16) immunoreactivity in an unfixed frozen tissue section of a complete homozygous hydatidiform mole chorionic villus. Note that mesenchymal cells in the connective tissue stroma (St) are not immunoreactive but the overlying syncytiotrophoblast (Sy) is. Close examination reveals a punctate pattern of immunoreactivity suggesting that the receptor is associated with vesicular inclusions. Scale bar represents 20μm.

5.26

5.27

5.28
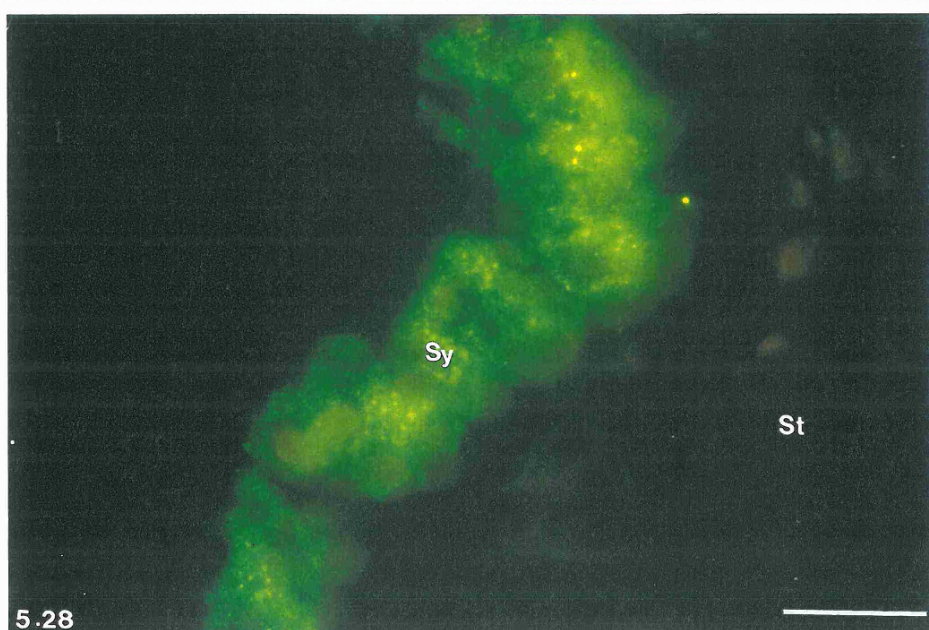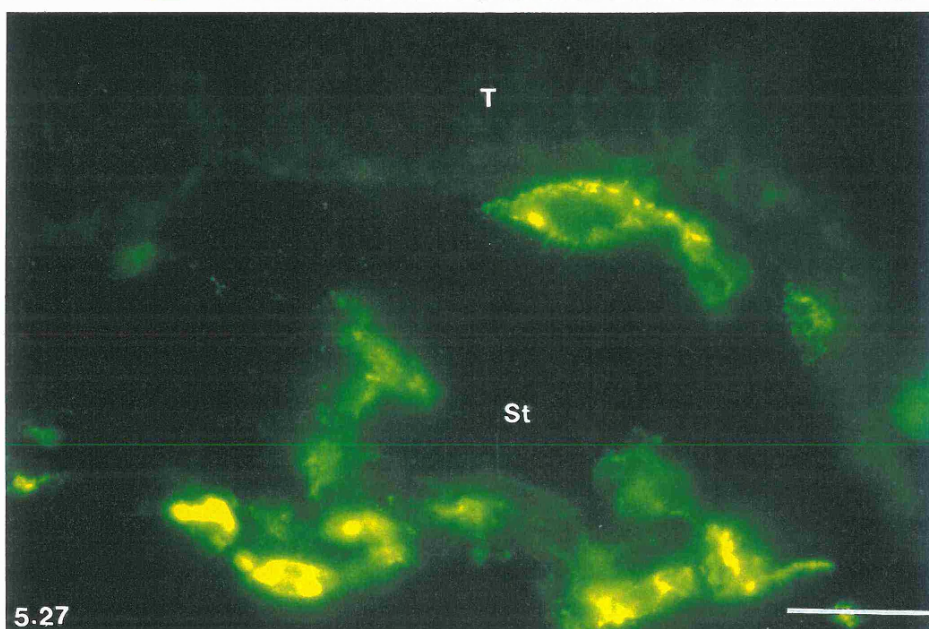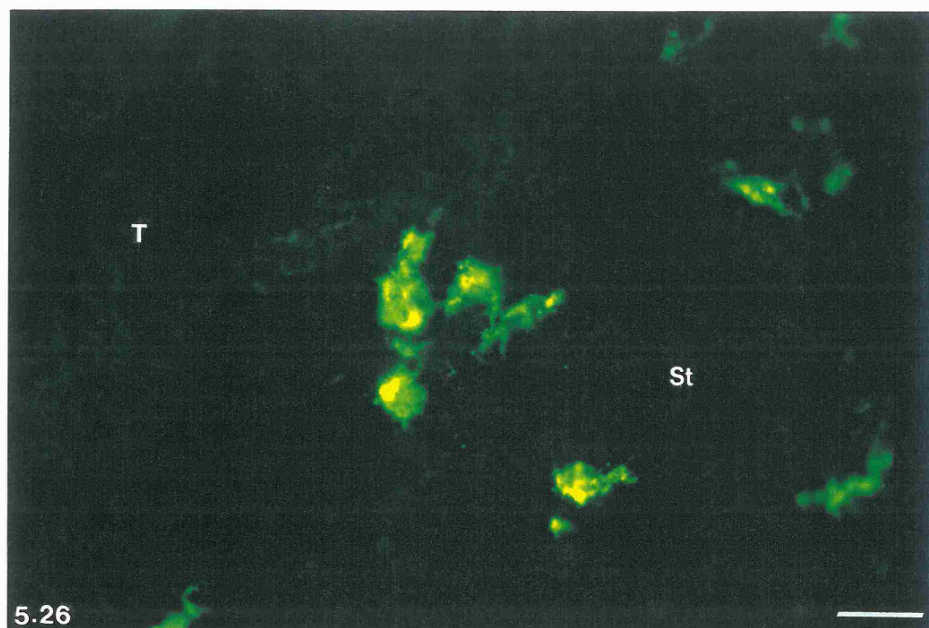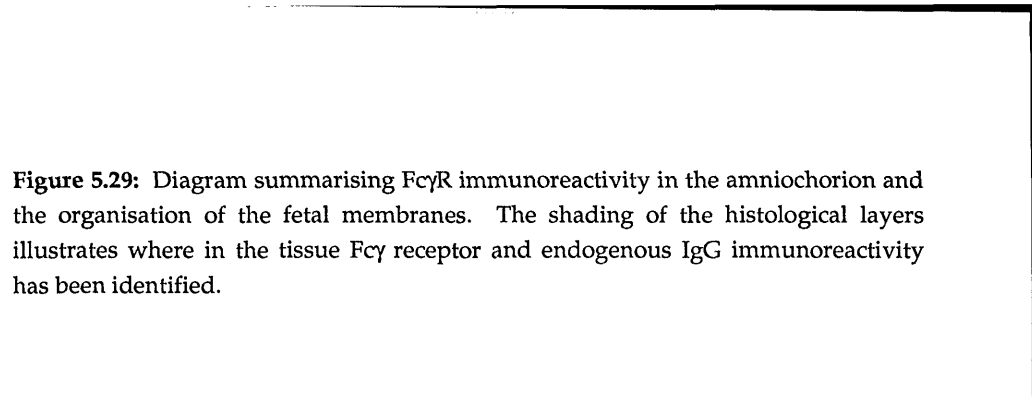
Figure 5.29: Diagram summarising FcγR immunoreactivity in the amniochorion and the organisation of the fetal membranes. The shading of the histological layers illustrates where in the tissue Fcγ receptor and endogenous IgG immunoreactivity has been identified.

5.29

AMNION

CHORION

DECIDUA

FcγRI (CD64)

FcγRII (CD32)

FcγRIII (CD16)

Endogenous IgG

Key: Immunofluorescence intensities

+++

++

← Amniotic Fluid
← Amniotic Epithelium
← Basal Lamina
← Compact Layer
← Fibroblast Layer
← Spongy Layer
← Reticular Layer
← Pseudo Basement
   Membrane
← Trophoblast Layer
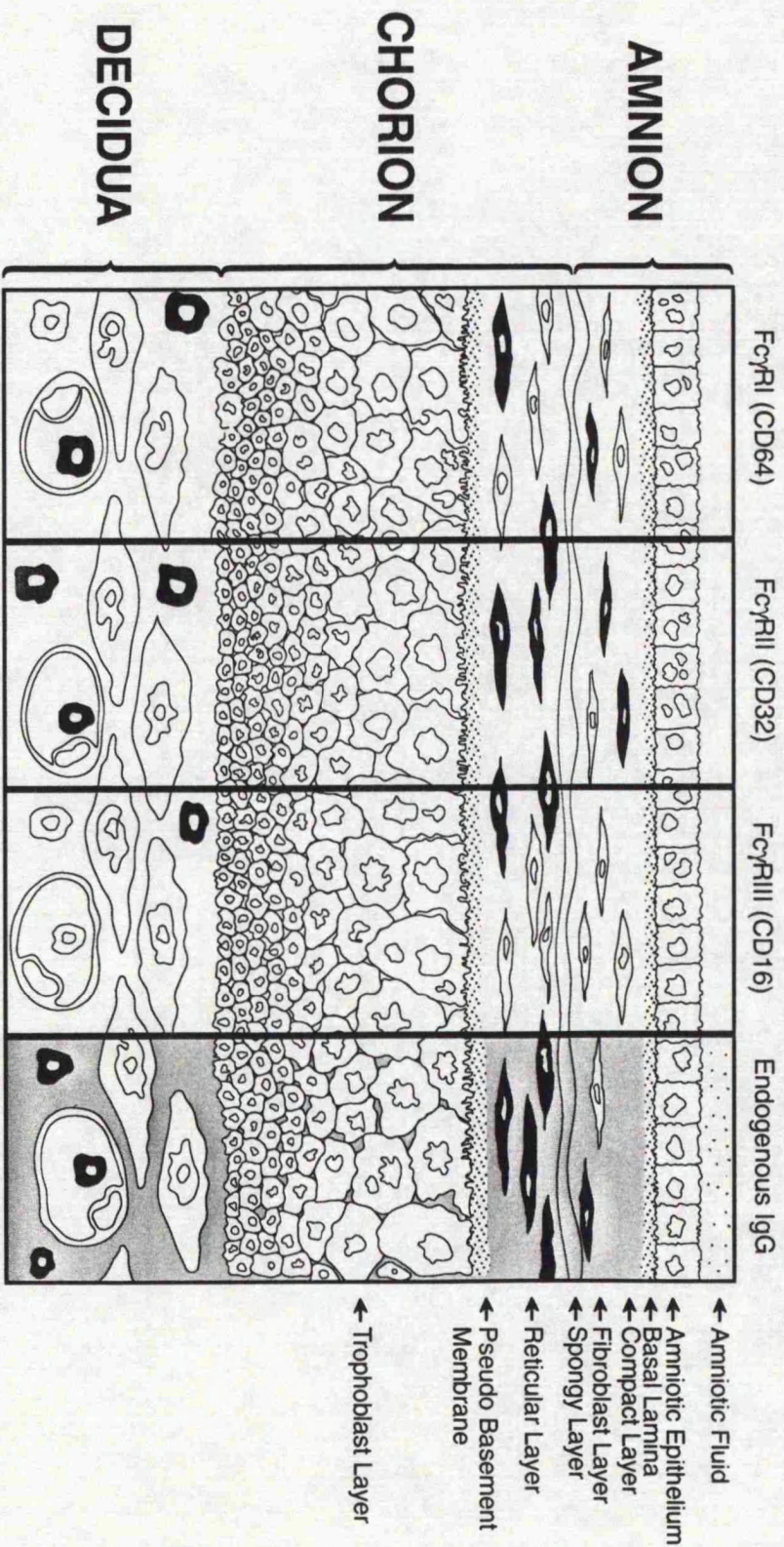
5.4 DISCUSSION.

Chorionic villi.

FcγRI.

The immunofluorescence investigations revealed heterogeneous expression of the 3 subtypes of Fcγ receptor in chorionic villi. FcγRI (CD64) is a 72kDa receptor expressed by mononuclear phagocytes and possesses high affinity for monomeric IgG (Anderson and Looney, 1986). This receptor was expressed by mesenchymal or fibroblast cells and Hofbauer cells. The cells of mesenchymal origin which expressed this receptor did not bear any morphological resemblance to Hofbauer cells which typically possessed rounded, vacuolated morphology. These mesenchymal cells were often greatly distended and possessed stellate or spindle-shaped morphology. Furthermore they were very abundant in the connective tissue stroma of term villi, in contrast to the low abundance reported for Hofbauer cells at this stage of gestation (Boyd and Hamilton, 1970; Enders and King, 1970; Fox, 1967). An association of this receptor with cells other than Hofbauer cells has not previously been recorded (Bright et. al., 1994). In first trimester villi the cells of the connective tissue core are not greatly differentiated and it is not possible to differentiate between them using dark-field microscopical techniques. Cells possessing immunoreactivity with the anti-CD64 monoclonal antibody used in this investigation were numerous and possessed rounded morphology. These may be undifferentiated extraembryonic mesenchymal cells and / or Hofbauer cells. An association of this receptor with mesenchymal cells of the core of hydatidiform mole chorionic villi was observed for the first time in this study.

FcγRII.

FcγRII (CDw32), a 40kDa receptor of which several isoforms have been identified, has been reported on granulocytes, B cells, monocytes / macrophages and platelets (Anderson and Looney, 1986). This receptor was expressed by endothelial cells of both 1st trimester and term chorionic villi (Bright et. al., 1994), extending the findings of Kristoffersen et. al. (1990) and Kameda et. al. (1991) who demonstrated this receptor in term endothelium only. In the present study FcγRII appeared to be expressed as soon as mesenchymal cells had differentiated to form endothelial cells, despite the immaturity of the blood vascular system of the placenta at this stage of development. It is possible that the ability to demonstrate this immunoreactivity may be attributed to the different monoclonal antibody used, the different immunocytochemical techniques employed in the present study or the greater sensitivity of the dark-field microscopical techniques. In addition, it was possible to demonstrate a punctate pattern of immunoreactivity which may indicate that this receptor and its ligand are internalised into vesicles. The presence of this receptor

throughout the cytoplasm of the cell may indicate that it transports IgG from one surface to the other. However, this receptor was not expressed by endothelial cells associated with the blood vessels of the chorionic plate or the umbilical cord. Vessels of the stem villi projecting from the chorionic plate demonstrated a low level of expression since the presence of this receptor could be detected using the increased amplification afforded by the three-step immunocytochemical procedures. Intense immunoreactivity was associated with intermediate and terminal chorionic villi. This suggests that there is heterogeneous expression of FcγRII by endothelial cells dependant upon their location in the villus tree. Endothelial cells surrounding blood vessels in the distal regions of the villus tree may, therefore, possess a key immunoglobulin-binding function. FcγRII was also associated with mesenchymal cells of the hydatidiform mole chorionic villus core. This localisation is previously unrecorded and may indicate that mesenchymal cells express this receptor prior to differentiation into endothelial cells or Hofbauer cells in healthy tissue.

FcγRIII.

FcγRIII (CD16), a 50-70kDa low-affinity receptor expressed on granulocytes, some macrophages and NK cells, was expressed by the trophoblast of 1st trimester and term chorionic villi consistent with the localisations obtained by Kristoffersen et. al. (1990) and Kameda et. al. (1991). In 1st trimester villi the increased sensitivity and resolution afforded by the dark-field confocal microscopical techniques employed permitted visualisation of sub-cellular vesicular structures not previously reported (Bright et. al., 1994). The receptor was localised at the periphery of these inclusions and was often concentrated at a pole. These compartments may correspond to receptor-sorting organelles such as endosomes or CURL (Geuze et al., 1983). In term villi FcγRIII was expressed by syncytiotrophoblast and since it is predominantly associated with the apical aspect, an observation which correlates with IgG localisation, this may indicate receptor/ligand interaction at the apex of the cell. It was not possible to demonstrate immunoreactivity with this receptor in cytotrophoblast cells (Bright et. al., 1994; Bright and Ockleford, 1994b). In hydatidiform mole chorionic villi this receptor was associated with the syncytiotrophoblast, consistent with the labelling in healthy tissue. However, this is in contrast to the distribution reported by Stuart et. al. (1989) who showed FcγRII expression and suggested a role in transcytosis. This may be a consequence of antibody cross-reactivity with shared epitopes on the different receptor subtypes.

Possible roles of FcγR-bearing cells in chorionic villi.

It is not possible to define the precise functional role(s) of the three Fcγ receptor subtypes when expressed by cells of the placenta. Members of the Fcγ receptor family are expressed by almost all cells of the immune system and exhibit a variety of

functions. FcγRI (CD64) is the only receptor that binds monomeric IgG with high affinity; FcγRIII (CD16) is expressed by a variety of leucocytes but binds monomeric and aggregated IgG with low affinity and, similarly, FcγRII (CDw32) binds multivalent or aggregated IgG (Anderson and Looney, 1986). The presence of FcγRI on cells of extraembryonic mesodermal lineage in the stroma of chorionic villi is a novel finding. It is possible that these cells may assist monomeric IgG across the stroma of chorionic villi or that they possess a hitherto unrecognised immunoregulatory role.

Multiple isoforms of human FcγRII exist (Stuart et. al., 1989) as has been found for the homologous class of murine Fc receptors. Studies performed with receptor negative cells transfected with mouse FcγRII cDNAs indicate that distinct functional differences exist. For example, mFcRII-B1 and mFcRII-B2 differ in their ability to undergo receptor-mediated endocytosis since only mFcRII-B2 is capable of accumulating over clathrin coated pits (Meittinen et. al., 1989). Expression of mFcRII-B2 in polarised Madin-Darby Canine Kidney cells shows that this receptor is capable of mediating efficient apical to basolateral transcytosis of IgG (Hunziker and Mellman, 1989). Furthermore, it is apparent from this study that mFcRII-B2 is capable of transcytosis of monovalent fragments and polyvalent IgG-complexes. The expression of an isoform of FcγRII by endothelial cells of the human placenta may be of particular immunological importance. Since this receptor is reported to possess significant affinity for multivalent or aggregated IgG only, it is not yet clear whether endothelial cells are responsible for clearing immune complexes from the fetal circulation or if FcγRII, when expressed by endothelial cells, is capable of mediating transport from the connective tissue to the fetal circulation. FcγRII has an affinity of 10^6-10^5M^{-1} for monomeric IgG (Leslie, 1980; Stengelin et. al., 1988). Hunziker and Mellman (1989) have asserted that monovalent fragments may be transcytosed, particularly where local concentrations of ligand around the receptor are high. Therefore, it may be possible for this receptor to transcytose IgG, particularly if it is present as dimeric or multimeric aggregates.

Receptors expressed by human trophoblast have been reported to bind both monomeric and aggregated IgG (Niezgodka et. al., 1981). FcγRIII, expressed by human trophoblast, is reported to possess measurable affinity for aggregated or multivalent IgG only (Anderson and Looney, 1986). It is conceivable that the monoclonal antibody used in this study reacts with an epitope of a placental FcγRIII-isoform that has not yet been characterised. Alternatively it may coexist with a fourth, structurally distinct receptor which is perhaps similar to the MHC class I-like molecule of neonatal rat jejunum (Simister and Mostov, 1989), that may account for the transmission of IgG. However, it is interesting that throughout these

investigations, cells which did not express a characterised receptor also contained no endogenous IgG (Bright et. al., 1994; Bright and Ockleford, 1994a; Bright and Ockleford 1994b). Endogenous IgG co-localised with FcγRIII in the syncytiotrophoblast but it is not yet clear if this was a circumstantial observation or if the placental FcγRIII isoform is capable of effecting a transepithelial transport role.

It is evident from the heterogeneous expression of these three characterised receptor subtypes in the human placenta that we must not fail to consider the management of antibody once it has been transported across the placental syncytiotrophoblast. It is conceivable that the different affinities exhibited by these receptors for the IgG subclasses may account for the inequality of subclasses present in fetal serum. FcγRII, for example, may be responsible for the inefficient transmission of IgG_2 from maternal to fetal blood. Comparative immunofluorescence investigations of endogenous human IgG_1, which is efficiently transported to the fetal circulation and IgG_2, which is inefficiently transported, demonstrate that the point of discrimination may be the endothelial cells since both subclasses are present in the villus stroma at term. However, IgG_1 is the only subclass which becomes concentrated in the endothelial cells (Mongan and Ockleford, 1994).

FcγRII is encoded by three genes located on chromosome 1 in the human being (Grundy et. al., 1989) called A, B and C (Qiu et. al., 1990). The molecule is known to exist as multiple isoforms designated hFcγRIIa1, hFcγRIIa2, hFcγRIIb1, hFcγRIIb2, hFcγRIIb3 and hFcγRIIc. That hFcγRIIa exists in allelic forms is demonstrated by its polymorphic reactivity with $mIgG_1$. Monocytes from different individuals interact strongly or weakly with $mIgG_1$ and are thus designated high responder (HR) or low responder (LR) respectively. These allelic forms may be distinguished on the basis of their immunoreactivity with monoclonal antibody 41H16 which recognises a unique epitope on the HR form of hFcγRIIa. Individuals may be homozygous or heterozygous with respect to the allelic forms of this molecule. Warmerdam et. al. (1990) have demonstrated that these molecules differ by only 2 amino acids. In the HR form a glutamine is substituted for tryptophan at position 27 in the first immunoglobulin-like extracellular domain, and an arginine is substituted for a histidine at position 131 in the second immunoglobulin-like domain.

It is intriguing that Warmerdam et. al. (1991) subsequently demonstrated that hFcγRIIa is also polymorphic for its ability to bind human IgG_2. In this instance only the LR form of the hFcγRIIa isoform is capable of binding IgG_2 which is attributed to the presence of the strongly basic histidine residue at position 131. It is possible that if the hFcγRIIa isoform is expressed by the endothelium of the human placenta the

presence of IgG_2 in fetal serum may depend upon the expression of the LR form of the molecule. This may account for the conflicting data in the literature where IgG_2 is reported to be present (Morrell et. al., 1972a; Virella et. al., 1972; Pitcher-Wilmott et. al., 1980) or absent (Wang et. al., 1970; Hay et. al., 1971; Schur et. al., 1973; Chudwin et. al., 1985; Einhorn et. al., 1987) from fetal serum. Preliminary data indicates that two isoforms of human FcγRII may be detected using immunoblotting experiments performed with purified placental coated vesicles (Laura Mongan, personal communication).

Term amniochorion.

The results of these investigations confirm the presence of cells bearing Fcγ receptors in human term amniochorion. This is the first localisation of the 3 characterised specific receptor molecules for IgG in this tissue (Bright and Ockleford, 1994a). FcγRI, FcγRII and FcγRIII were expressed by populations of cells present within the maternal decidual layer, which presumably represent maternal immunocompetent leucocytes, and by cells in the fetal mesenchyme.

FcγRI (CD64), a high affinity receptor for monomeric IgG that is expressed by monocytes (Anderson and Looney, 1986), was also expressed by a population of cells of the fibroblast and reticular layers. Immunoreactivity to FcγRI has been demonstrated in cells of the chorionic villi of term and immature human placentae (Bright et. al., 1994) where the receptor was associated with Hofbauer cells (placental tissue macrophages) and with mesenchymal cells of the connective tissue core. This observation offers further evidence that cells of extraembryonic mesodermal lineage express this receptor and may reflect a specialised function of FcγRI-bearing cells in the placenta and amniochorion.

FcγRII (CDw32), expressed by granulocytes, B cells, monocytes, macrophages, platelets and endothelium (Anderson and Looney, 1986), was also expressed by cells of mesenchymal origin in the fibroblast and reticular layers of the amniochorion. Since FcγRII is reported to possess greater affinity for aggregated or complexed IgG (Anderson and Looney, 1986) these cells may be responsible for arresting immune complexes that form in the connective tissue layers. Consistent with this view is the observation that these cells bind immune complexes of human IgG (Wood et. al., 1983). FcγRII is also associated with Langerhans cells of the skin (Caux et. al., 1992), which are highly efficient antigen-presenting cells, and thus it is possible that the expression of this receptor by cells of the mesenchymal layers in the amniochorion is indicative of a hitherto unrecognised immunoregulatory role.

This receptor has previously been reported in the endothelium of fetal vessels (Kristoffersen et. al., 1990; Kameda et. al., 1991; Bright et. al., 1994) where it may serve as a vehicle for transcytosis of passive immune IgG or it may be responsible for clearing immune complexes of IgG from the fetal circulation. FcγRII is also expressed by Hofbauer cells. However, when applied to the fetal membranes, the antibody against this receptor failed to label endothelial cells of the maternal decidua which demonstrates that not all endothelial cells express this receptor. The expression of FcγRII by endothelial cells of chorionic villi may, therefore, be of particular immunological importance.

FcγRIII (CD16), a low affinity IgG receptor typically expressed by granulocytes, some macrophages and NK cells, was expressed by a sparse population of cells of the fibroblast and reticular layers. Immunoreactivity with anti-FcγRIII monoclonal antibodies has previously been demonstrated in the syncytiotrophoblast surrounding chorionic villi (Kristoffersen et. al., 1990; Kameda et. al., 1991). The observations made in the present study (Bright et. al., 1994; Bright and Ockleford, 1994b) indicate that cytotrophoblast cells do not express this receptor. If FcγRIII is responsible for IgG transmission this may account for the inhibition of early transport to the conceptus since cytotrophoblast cells form an almost complete layer beneath the syncytiotrophoblast in immature placentae and thus potentially constitute a barrier. The results obtained with the amniochorion are consistent with this view since the cytotrophoblast cells of the chorion laeve, which are in lateral continuity with the villus trophoblast, do not express this receptor.

There appear to be heterogeneous populations of cells of extraembryonic mesodermal lineage present in the mesenchymal layers of the amniochorion that express receptors for IgG. However, it is conceivable that receptor-negative cells in immunofluorescence preparations performed with single anti-receptor antibodies expressed a different receptor subtype. To investigate this possibility sections were simultaneously immunoreacted with a cocktail of all 3 monoclonal anti-receptor antibodies. A similar pattern of immunolabelling was observed, indicating the presence of some receptor-negative cells. In these experiments, 75.9% (n=577) of the cells of the fibroblast and reticular layers expressed an FcγR of some type. Immunolabelling of individual receptor subtypes revealed that 48.1% (n=241) of these cells expressed FcγRI, 68.2% (n=1253) expressed FcγRII and 7.5% (n=478) expressed FcγRIII. This data suggests that there may be considerable co-expression of the FcγR subtypes by the cells of these layers. It is generally considered that only a very small percentage of these cells are Hofbauer cells (Bourne, 1962). FcγRIII has been demonstrated on Hofbauer cells of the placenta (Bright et. al., 1994) and thus it

is conceivable that the FcγRIII-bearing cells (7.5%) represent Hofbauer cells present within the amniochorion.

Endogenous IgG was localised throughout the extracellular matrix of the amnion, chorion and decidua. In addition, IgG was concentrated in cells of the fibroblast and reticular layers possessing Fcγ receptors and with receptor-bearing cells of the decidua, as demonstrated by dual-labelling immunofluorescence studies. However, cytotrophoblast cells of the trophoblast layer and amniotic epithelial cells, which lack Fcγ receptors, did not contain endogenous IgG. Therefore, two complete layers of epithelial cells in the amniochorion (the amniotic and trophoblastic epithelia) lack receptors which are potentially necessary for transepithelial IgG transport. These data support the consensus view that maternally derived passive immunity is not acquired by the fetus using the paraplacental transamniochorion route but does indeed utilise a transplacental route.

However, these data are inconsistent with the observations of Wood et. al. (1983) which suggest that amniotic epithelial cells and cytotrophoblast cells possess binding sites for monomeric human IgG. There are strong consistencies in the present data that demonstrate the presence of endogenous IgG only in cells that are also shown to express specific IgG receptors. Epithelial cells and cytotrophoblast cells, which do not express a characterised receptor, contain no demonstrable endogenous antibody. It is difficult to account for this apparent difference of experimental data but it is conceivable that it may be a consequence of cross-reactivity of reagents used in the exogenous methodology or the speed with which tissue was obtained in the present investigation, thus preventing degenerative changes.

In summary, endogenous IgG and IgG Fc receptor-bearing cells are present in the amniochorion which may potentially contribute to the immunological protection of the fetus. It is becoming apparent that cells of mesenchymal origin may have an important role in this context. Epithelial cells which do not possess Fcγ receptors do not contain endogenous antibody and are thus unlikely to be implicated in the role of transcytosis of maternal IgG.

Hofbauer cells.

Throughout these investigations immunofluorescence experiments have been performed with a monoclonal anti-human monocyte / macrophage antibody (MAC 387; Flavell et. al., 1987) in an attempt to identify the distribution of placental tissue macrophages (Hofbauer cells). This antibody demonstrates a broad reactivity with a

variety of tissue histiocytes, including infiltrating and reactive histiocytes, alveolar macrophages, Kupffer cells, follicle-center macrophages, splenic red pulp macrophages, tumour-infiltrating macrophages, sinus histiocytes and epitheloid giant cells. When applied to sections of the human placenta this monoclonal antibody immunolabelled mononuclear leucocytes present within the lumen of placental blood vessels and maternal blood lakes external to the chorionic villi. This antibody also recognised a sparse population of cells present within the stroma of term chorionic villi. However, in the stroma of first trimester villi cells possessing immunoreactivity with this antibody were not apparent, despite the presence of immunoreactive maternal cells adhering to the glass slide, thus providing an internal positive control. In the amniochorion this antibody was reactive with a population of cells present within the maternal decidual layer only. Based on these observations and the characterised distribution of Hofbauer cells (Boyd and Hamilton, 1970; Enders and King, 1970; Fox, 1967; Bourne, 1962) the conclusion must be made that this antibody does not recognise the so-called Hofbauer cells. This data reflects the unique nature and origin of Hofbauer cells which are considered to be derived from the extraembryonic mesenchyme. They are not maternally derived (Wynn, 1967; Bourne, 1962). What, then, are the cells present in chorionic villi which possess immunoreactivity with MAC 387 ?

Various studies have demonstrated that maternal leucocytes may traverse the human placenta. Desai and Creyer (1963) labelled maternal lymphocytes and reinjected these into the mother within 15 hours of delivery. Labelled lymphocytes were seen in cord blood after delivery. However, most studies involve the culture of cord blood lymphocytes and karyotypic study of male cases in an attempt to detect 46XX cells as evidence of transfer of maternal cells. The results from such studies are conflicting, with Turner et. al. (1966) and Schröder (1974) demonstrating limited numbers of such lymphocytes and Anderson and Smith (1971) and Olding (1972) finding none. However, it is generally accepted that small numbers of maternal lymphocytes do cross the placenta. Furthermore, there is a considerable body of evidence that suggests that the fetus is capable of a degree of active cellular immunity (see review: Nevard et. al. 1990). Therefore, it seems likely that monoclonal antibody MAC 387 recognises monocytes present in placental blood vessels produced by a fetal cellular immune response or by transplacentally transmitted maternal leucocytes.

Schmidt (1992) has demonstrated that in amnion culture most fibroblasts become Hofbauer cells within 5 days of culture. Wolf and Schmidt have demonstrated the presence of CD68 in the cytoplasm of these cells and observed HLA-DR on the cell surface (Hans Wolf, personal communication). This observation

contrasts with the lack of HLA-DR surface antigens expressed by Hofbauer cells in the placenta (Edwards et. al., 1985; Zaccheo et. al., 1989). However, HLA-DR antigens are now generally believed not to be obligatory markers of monocytes / macrophages (Unanue et. al., 1984). Rather, they are expressed under particular physiological conditions which may depend in turn upon a) the anatomical site of the cells (Unanue et. al., 1984), b) encounter with products like lymphokines or certain chemicals that induce or enhance HLA-DR antigen expression or c) the maturational stage of the cells (younger macrophages appear to have more DR antigen; Scher et. al., 1982; Beller and Ho, 1982). In addition, a consistent lack of HLA-DR antigens has been reported in macrophages from fetal tissues with the remarkable exception of thymic macrophages and of circulating monocytes (Raff et. al., 1980; Lu et. al., 1980). After investigation with a battery of monoclonal antibodies Zaccheo et. al. (1989) conclude that Hofbauer cells share a number of features with cells of the monocyte-macrophage lineage and yet have some distinctive properties. It is not clear if Hofbauer cells represent a particular maturational step of the macrophage lineage or if they follow a specialised pattern of differentiation related to the local environment. Observations with MAC 387 in the present study suggest that circulating leucocytes in the placenta possess immunoreactivity with this monocyte marker but that Hofbauer cells (connective tissue macrophages) do not, thus further establishing the unique phenotype of these cells.

CHAPTER 6: Ultrastructural Immunocytochemistry.

6.1 INTRODUCTION.

We have seen in chapter 3 that the major development in immunocytochemical studies of cells and tissues at the light microscope level was the introduction by Coons et. al. (1941) of the use of fluorescently labelled antibodies to identify immunoreactive sites. The introduction by Singer (1959) of the iron-containing protein ferritin, as an electron-dense marker which could be conjugated to antibodies, paved the way for a new field of study, immunolabelling for electron microscopy. This technique made a significant advance in the study of the molecular structure of cells since labelled antibodies could be individually located at their site of interaction with the antigen.

Nakane and Pierce (1966) applied the reaction of horseradish peroxidase (HRP) and diaminobenzidine (DAB), previously introduced as a histochemical marker by Graham and Karnovsky (1966), to localise antigens at the ultrastructural level by conjugating antibodies to HRP. Thus the introduction of the enzyme-labelled antibody technique became a second landmark in immunolabelling for electron microscopy. Feldherr and Marshall (1962) introduced colloidal gold markers as a tracer for electron microscopy but they were only applied as specific markers for antisera by Faulk and Taylor (1971) and for isolated antibodies by Romano et. al. (1974). In subsequent years the immunogold labelling technique has become very popular for identifying antigens at the ultrastructural level.

Colloidal gold offers many advantages as a marker for electron microscopy. Gold colloids are particulate, very distinct and, due to their high electron density, they may be easily detected in the electron microscope. Furthermore, because of the granular nature of gold particles, quantification of the degree of labelling may be made by directly counting the number of particles in a given area. This cannot be done with the homogeneous reaction product of the immunoperoxidase technique. Colloidal gold may be easily prepared by a number of methods (Roth, 1982) and the conjugation of these particles to macromolecules such as immunoglobulins or protein A, although poorly understood, is a simple matter of adsorption at the correct pH, reagent concentration and ionic strength. This method is easy, quick and economical since it requires only small amounts of specific macromolecules. As described in section 4.1 protein A from S. aureus binds to the Fc domain of the immunoglobulins from many species. This affinity may be exploited in a pseudo-immunological fashion. Protein A has been described as 'natures universal anti-antibody' (Surolia et. al., 1982) and when conjugated to colloidal gold it may be used as a secondary reagent capable of recognising a variety of primary antibodies in an indirect labelling protocol. This protein A-gold (pAg) technique has been

comprehensively reviewed elsewhere (Roth, 1982). Since colloidal gold may be produced in a variety of sizes ranging from 1nm to 150nm, dual or multiple labelling studies may be performed by adsorption of different antibodies to different sized colloids of gold. This is analogous to the dual labelling that may be achieved with the fluorescence microscope using antibodies conjugated to different fluorophores.

In order to preserve fine structural details for immunoelectron microscopical studies, it was natural in the early days to expect the epoxy resins to play a role as important as they had for routine ultrastructural studies. This did not prove to be the case, however, and the use of Epon sections had only limited success for antibody labelling studies. The major difficulty has been that the specimen preparation procedures for this approach prevent a significant fraction of the antigens in the section from being recognised by antibodies. There are very few antigens, for example, that are still antigenic in Epon sections after conventional osmium tetroxide fixation. Therefore osmium tetroxide, which greatly enhances specimen contrast in the electron microscope, must usually be omitted in the preparation of tissue for immunoelectron microscopy on Epon sections. However, there are a few notable exceptions to this generalisation (Singer, 1959; Bendayan and Zollinger, 1983). The denaturing effects of dehydration, infiltration and polymerisation are further tissue-processing steps that are detrimental to antigenicity. These steps are unavoidable for routine Epon embedding and thus those studies in which epoxy resins have been employed to give successful immunocytochemical results have been limited to those in which the target molecules are abundant in the tissue.

The problem of labelling intracellular structures for electron microscopy has been approached in two ways. The first way was to find alternative embedding media to the epoxy resins, particularly water-soluble ones which could facilitate labelling of thin sections. The second approach involved pre-embedding techniques in which labelled antibodies are introduced prior to conventional embedding procedures. In this approach solvents or detergents are applied to the tissue to facilitate access of the labelled antibodies to intracellular antigens. The tissues are then fixed with aldehyde, treated with osmium, dehydrated and conventionally embedded in epoxy resins. Labelling on sections, traditionally referred to as post-embedding labelling, was plagued by technical difficulties for many years. However, in the 1970's, two excellent sectioning approaches appeared for labelling both intra- and extracellular antigens. These techniques relied upon either the cryo-section technique in which ultrathin frozen sections are labelled, or the use of a new generation of acrylate or methacrylate, low-viscosity resins capable of withstanding polymerisation at low temperatures.

Almost all methods use fixation of the tissue and thus loss of antigenicity is a common problem. However, post fixation in osmium, commonly used in pre-embedding methods, is usually avoided in post-embedding systems because of its adverse effects on antigenicity. This leaves the tissue, lipids in particular, unprotected during processing and embedding. Therefore, to minimise tissue extraction, post embedding systems usually require a greater strength of fixation to preserve morphology. This is achieved using more reactive aldehydes, higher concentrations of fixative or longer times of fixation. However, a compromise has to be reached so that cross-linking of proteins is minimised, leaving them recognisable to antibodies. Therefore it is desirable to assess a range of different fixatives for the retention of antigenicity of the target molecule in question whilst maintaining an acceptable level of tissue morphology.

The major disadvantage of the epoxy resins, both for their high resolution structural preservation and especially for immunocytochemistry, is their extremely hydrophobic nature. Tissues must, therefore, be completely dehydrated in protein-denaturing solvents before infiltration. Furthermore, these resins may only be polymerised by heating above 50°C. An additional problem of their high viscosity was overcome by the development of Spurr's medium (Spurr, 1960) but the high degree of covalent interactions between these resins and the biological material is also a problem for immunocytochemistry (Kellenberger, 1987).

In the past 5-10 years there have been concerted attempts to develop hydrophilic acrylic-type resins for electron microscopy. Although not water miscible, these resin mixtures are designed so that they combine at least a degree of hydrophilicity with good cutting properties and electron-beam stability. These mixtures are rapidly proving to be powerful tools for immunocytochemistry. The major breakthrough in the use of acrylic resins has come by designing resins that may be polymerised at low temperature. The theoretical background for this idea was derived from studies by physical chemists on the effects of solvents at low temperature on the structure and function of proteins (Petsko, 1975; Douzou, 1977). These studies revealed that low temperatures stabilised proteins during the removal of water by dehydration. At temperatures above 0°C removal of this outer water shell denatured proteins but these effects could be reduced or avoided completely at temperatures significantly below 0°C. Based on this knowledge, Kellenberger's group at Basel have developed embedding media which can infiltrate tissue and be polymerised at temperatures below 0°C. These new resins, known commercially as the Lowicryl resins, have obtained a wide popularity for immunocytochemical studies.

This class of resin is made up of mixtures of aliphatic acrylate and methacrylate esters. The chemical rationale behind their design was that the resin 'backbone' and polymerisation reaction was left unaltered, but the physical and chemical nature of the resin could be altered by modification of the sidechains (Carlemalm et. al., 1982). Of the best known of these resins, which became commercially available, HM20 shows water-like viscosity even at -35°C, whereas K4M is more viscous. Both of these resins have low freezing points and may be polymerised at low temperatures by ultraviolet light. The side chains of these molecules may be modified to vary the hydrophilicity. Lowicryl K4M is relatively more hydrophilic and blocks may be polymerised in the presence of up to 5% water at temperatures down to -40°C. HM20, while more hydrophobic than K4M, can still accept up to 0.5% water in the blocks and may be polymerised down to -50°C. The London Resin Company has also introduced a resin analogous to Lowicryl K4M called LR Gold (Causton, 1984). This is a hydrophilic aromatic acrylic resin which can be cross-linked at low temperatures by blue light.

Two new Lowicryl resins, the polar K11M and the less polar HM23, may be polymerised down to about -60°C and -80°C respectively (Acetarin et. al., 1987). The crucial factor for these resins is their extremely low viscosity, enabling infiltration at very low temperatures. There are two major reasons why these modifications are potentially very important. First, the adverse effects of dehydration on structural preservation should be significantly reduced at these low temperatures (Hobot et. al., 1984; Kellenberger et. al., 1986; Kellenberger, 1987). From a theoretical consideration it is argued that despite the presence of a chemical solvent the water of hydration around macromolecules may be completely intact at these low temperatures (Kellenberger, 1987). Further lipid extraction should be negligible at these low temperatures (Weibull et. al., 1983a; 1983b). Clearly these phenomena are desirable for both high resolution structural preservation and for immunolabelling. For these resins the polymerisation reaction is initiated by benzoyl methylether and long wave (360nm) ultra-violet irradiation. Within the temperature range 0°C to -40°C the activator initiates a free radical reaction uniformly when added (0.5-0.6% w/w) to the liquid resin.

Besides the universal problem of fixation, the most critical step with respect to preserving molecular structure, and therefore antigenicity in Lowicryl embedding, is the dehydration step. For the theoretical reasons mentioned this is best performed at lowered temperatures since the potential of this step to denature proteins appears to be far greater than the infiltration and polymerisation steps in the resins themselves. Following routine fixation in aldehyde, tissues are dehydrated in an ascending series of ethanol while the temperature is progressively lowered. This protocol is referred

to as the PLT (progressive lowering of temperature) method (Roth, 1989). The tissue is subsequently introduced into resin:ethanol mixtures and finally into pure resin prior to polymerisation at low temperature.

The second type of post-embedding labelling is performed upon ultrathin frozen sections, the origin of which may be traced back to Fernándes-Morán (1952). The founder of this technique as we know it today was undoubtedly Tokuyasu (1973). Tokuyasu utilised the cryosectioning bowl attached to an ultramicrotome that had previously been described by Christensen (1971) and used aldehyde-fixed tissue and a cryoprotectant to avoid ice-crystal damage to the tissue. The striking innovations introduced by Tokuyasu were the use of sucrose as a cryoprotectant and a novel method of picking up sections, stretching them in the process, and applying them to the grids. In this 1973 paper, Tokuyasu showed that it was possible to cryosection, and then contrast by negative stain, a wide variety of aldehyde-fixed cells and tissues. In later years, the employment of methyl cellulose to protect thawed frozen sections against the surface tension damage caused by air-drying the sections (Tokuyasu and Singer, 1976) was an essential step in the development of the technique (Tokuyasu, 1978). The subsequent introduction of colloidal gold labelling to sections prepared with this methodology (Slot and Geuze, 1983) has rendered this an extremely powerful ultrastructural immunocytochemical technique.

The aim of the work presented in this chapter is to determine the ultrastructural distribution of endogenous immunoglobulin G in the cells and tissues of the human placenta and fetal membranes. A knowledge of this may provide valuable insights into the method by which maternal IgG traverses the syncytiotrophoblast and interstitial tissues to gain access to the fetal circulation.

6.2 MATERIALS AND METHODS.

6.2.1 Tissue collection.

Freshly dissected samples of 1st trimester villi (n=3), term villi (Cesarean section, n=3; routine delivery, n=10) and term amniochorion (Cesarean section, n=3; routine delivery, n=10) were obtained from the Leicester Royal Infirmary as previously described in section 2.2.1. The tissue was rinsed briefly with two changes of 0.1M PBS to remove maternal blood.

6.2.2 Fixation.

The tissue samples were immersion fixed for 3 hours at room temperature with one of the following fixatives: i) 3% formaldehyde in 0.1M PBS, ii) 3% formaldehyde + 0.1% glutaraldehyde in 0.1M PBS, iii) 4% paraformaldehyde in 0.1M phosphate buffer or iv) 4% paraformaldehyde + 0.1% glutaraldehyde in 0.1M phosphate buffer. These were prepared as described in appendix VII and contained 0.5mM $CaCl_2$ additive. The aldehyde reaction was then quenched using 50mM NH_4Cl in 0.1M PBS or 0.1M phosphate buffer to amidinate free reactive groups for 30 minutes at 4°C. The tissue was subsequently washed with 0.1M PBS or phosphate buffer (3 x 20 minutes, then overnight at 4°C). Finally the tissue was trimmed further with a fine pair of dissecting scissors to a size and shape (approximately $2mm^3$) suitable for resin embedding in blocks for electron microscopy. Osmium tetroxide (OsO_4), used for obtaining tissue contrast in conventional electron microscopy (see appendix III), was routinely omitted from this protocol due to its harsh effects on antigenicity.

6.2.3. Low temperature embedding.

Specimens were dehydrated in a graded series of ethanol using the progressive lowering of temperature (PLT) technique and low temperature embedded at -42°C in Lowicryl HM23 methacrylate resin (Chemische Werke Lowi GmbH) or at -23°C in Lowicryl K4M or LR Gold (London Resin Company) according to the manufacturers guide-lines. The dehydration and resin infiltration protocols are described in appendix VIII (HM23), appendix IX (K4M) and appendix X (LR Gold). The dehydration and resin infiltration procedures were performed using a high thermal capacity aluminium block possessing chambers which accommodate the tissue sample vials. By using this apparatus it was possible to draw pre-cooled solutions from the adjacent chamber into the sample vial by using a syringe. Thus it

was possible to maintain a steady temperature and prevent temperature 'shocks' to the tissue. This apparatus is illustrated in figure 6.1.

Dehydrating agent in

Dehydrating agent out

Aluminium block

Specimen

70% ethanol (-20°C)

50% ethanol (-20°C)
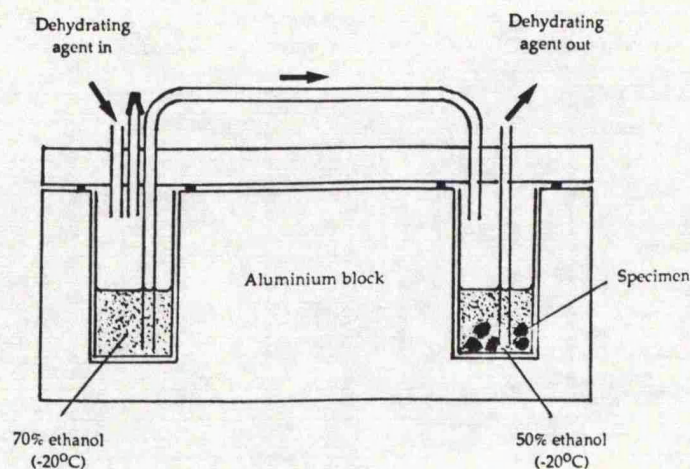
Figure 6.1. Schematic illustration demonstrating the design of the aluminium low-temperature embedding apparatus.

6.2.4 Achieving low temperatures.

The low temperatures used for conducting the progressive lowering of temperature technique were achieved by transferring the aluminium chamber containing the tissue samples from a Lec (-18°C) freezer to a Lerose (-42°C) freezer. Temperatures of -70°C were achieved by embedding the aluminium block in solid CO_2 (dry ice) in a polystyrene container in the Lerose freezer. Temperatures of -23°C were achieved with a household chest-type freezer (Lec).

6.2.5 Polymerisation at low temperature.

The tissue was removed from the sample vial of the aluminium block used to dehydrate and infiltrate it with resin. It was then transferred to fresh de-gassed, pre-cooled resin (prepared as described in appendices VIII-X) in gelatin capsules with a fine pair of cold dissecting forceps. These gelatin capsules were placed into a fine wire-loop holder contained in a highly reflective, high thermal capacity aluminium U.V. polymerisation chamber. This chamber was then placed into the Lerose (-42°C) freezer (for HM23 embedded samples) or the Lec (-23°C) freezer (for K4M and LR Gold embedded samples) and the temperature allowed to equilibriate for 1 hour.

The power supply was subsequently connected and the blocks were photopolymerised with U.V. irradiation of 360nm emitted by a Phillips TLD ISW/05 fluorescent tube (mounted 20cm from the specimens) for 24 hours. The lower third

of the gelatin capsules were immersed in ethanol to ensure adequate dissipation of heat, since polymerisation of the blocks gives rise to an exothermic reaction. Local temperature increases in the tissue blocks during photopolymerisation could have potentially deleterious effects on antigenicity. The polymerisation chamber was then removed to room temperature and the resin further cured for 48 hours to improve the sectioning qualities of the blocks. Finally the gelatin capsules were removed and the tissue blocks were stored at room temperature. The U.V. polymerisation chamber used to conduct these procedures is illustrated in figure 6.2.
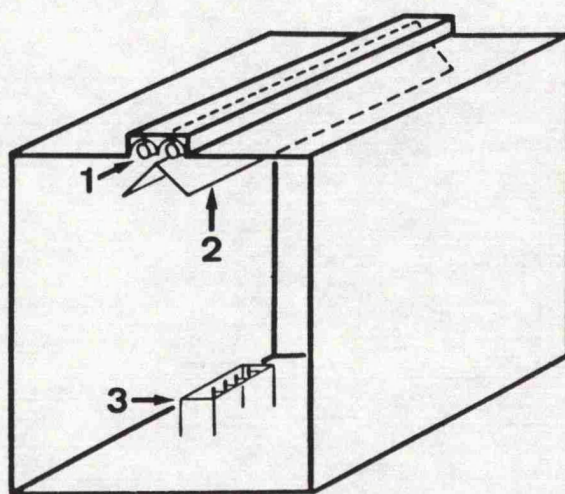
Figure 6.2. The polymerisation chamber used for U.V. irradiation of samples including (1) the U.V. source, (2) a diffuse right-angle reflector and (3) the specimen holder.

6.2.6 Sectioning.

Ultrathin sections (80-100nm; silver to gold in interference colour) of the resin embedded material were cut using a Diatome or Dupont diamond knife mounted on a Reichert OMU-3 or OMU-4 ultramicrotome. The sections were collected on 200 mesh hexagonal nickel electron microscopy grids (Agar Aids) and stored in a desiccator at room temperature until required for immunolabelling.

Lowicryl K4M is a hydrophilic resin and thus, as with other polar (water-miscible) resins, precautions were taken to ensure that the block face did not become wet during sectioning. This was best accomplished by sectioning with a level of fluid in the trough which was slightly below normal. However, the fluid was not lowered so much that the knife edge became dry (this is particularly important with diamond knives due to the hydrophobic nature of most diamond knife edges). The fluid level was routinely lowered so that the reflection from the fluid along the knife edge was

slightly darker than the normal bright silver colour. The most suitable procedure was to orient the trimmed block with the knife edge before the trough was filled. The trough was then overfilled to form a 'reverse meniscus' along the knife edge and left for 10-15 minutes. Immediately before sectioning the fluid was lowered to give a dark silver reflection along the knife edge. The final advance of the knife was then made and sectioning commenced.

6.2.7 Immunolabelling for electron microscopy.

Immunolabelling of antigens exposed at the surface of ultrathin sections was achieved by floating the grids on $20\mu l$ droplets of the solutions containing specific antisera. This was performed on clean, de-greased dental wax or Nescofilm in a humid Petri-dish (containing saturated filter paper). The grids were washed by transferring them across droplets containing the wash buffer with a fine pair of E.M. forceps.

The grids were first floated on a droplet of 50mM NH_4Cl in 0.1M PBS or tris-buffered saline (TBS; appendix XI) for 10 minutes at room temperature to ensure that any unreacted aldehydes were amidinated. The aim of this procedure was to prevent any unreacted aldehydes from effectively 'fixing' specific antisera to the sections, thus giving rise to 'false-positive' immunolabelling. The grids were then transferred to a 1% solution of bovine serum albumin (BSA), diluted in 0.1M PBS or 50mM TBS for 10 minutes at room temperature, to act as block for non-specific protein adsorption. In indirect immunogold labelling protocols, using specific primary antibodies and gold-labelled secondary antibodies, this block also included 5% non-immune serum appropriate to the second stage species. In protocols utilising gold-conjugated protein A, the use of non-immune serum was avoided to prevent interaction with immunoglobulins contained in these sera.

6.2.7.1 Primary immunological reagents.

Monoclonal antibodies to the three subtypes of human Fcγ receptor were diluted 1/50 in 0.1M PBS, containing 1% BSA and 5% NGS, and immunoreacted with the sections for 1 hour at 37°C or 24 hours at 4°C. These antibodies were purchased from Serotec (see section 5.2.2.1) and were stored at -18°C until required and subsequently at 4°C for up to 1 month.

A number of immunological reagents were utilised to identify endogenous IgG immunoreactive sites at the exposed surface of the ultrathin sections. Two methods were used, a direct method (see section 6.2.7.3) and an indirect method.

Indirect localisations of endogenous IgG were performed by incubating the tissue sections with the following reagents: i) A 1/50 dilution (range tested: 1/20 - 1/500) of goat anti-human IgG (whole molecule; Sigma, Code No.: I-1886, Batch No.: 29F-4897) in 0.1M PBS containing 1% BSA and 5% NRS for 1 hour at 37°C. ii) A 1/50 dilution (range tested: 1/20 - 1/400) of biotinylated F(ab')$_2$ fragments of goat anti-human IgG (γ-chain specific; Sigma, Code No.: B1518, Lot No.: 88F8985) in 0.1M PBS containing 1% BSA and 5% NGS for 1 hour at 37°C. These reagents were stored as described in section 4.2.2.1.

To assess the validity of the low-temperature embedding techniques positive control experiments were performed using an antibody directed against an antigen of known distribution within the tissues. This was performed by immunoreacting tissue sections with a 1/50 dilution of monoclonal mouse anti-human collagen IV (Dako, Code No.: M785; Clone, CIV 22; Mouse IgG$_1$ subclass) in 0.1M PBS containing 1% BSA and 5% NGS. This product was stored at -18°C and subsequently at 4°C when required. In addition a 1/100 dilution of rabbit polyclonal anti-type IV collagen (ICN, Code No.:68-124) containing 1% BSA was used (1h, 37°C).

The grids were rinsed by transferring them across 20µl droplets of 0.1M PBS containing 1% BSA (plus 5% NRS in experiment (i)) for 5 x 3 minutes. They were then transferred to the secondary antibody.

6.2.7.2 Secondary immunological reagents.

Primary mouse antibodies were detected with either i) a 1/100 dilution of goat anti-mouse IgG conjugated to 10nm colloidal gold (Dako, Code No.: G441, Lot No.: 061) diluted in 0.1M PBS containing 1% BSA and 5% NGS for 1 hour at 37°C or ii) a 1/100 dilution of biotinylated goat anti-mouse IgG (Amersham, Code No.: RPN 1177) diluted in 0.1M PBS containing 1% BSA and 5% NGS for 1 hour at 37°C. The dilution ranges tested for these reagents were 1/50 - 1/500 and they were stored in 10µl aliquots at -18°C prior to use and subsequently at 4°C.

Primary goat antibodies were detected using a 1/100 dilution (range tested: 1/50 - 1/500) of 10nm gold-conjugated rabbit anti-goat IgG (Sigma, Code No.: G-5402, Lot No.: 101H8844) diluted in 0.1M PBS containing 1% BSA and 5% NRS. This antibody was stored in 10µl aliquots at -18°C until required. Primary rabbit antibodies were detected using protein A conjugated to 10nm colloidal gold (Sigma, Code No.: P-1039, Lot No.: 98F-8105).

Biotinylated immunological reagents were localised by floating the grids on droplets of a 1/100 dilution (range tested: 1/50 - 1/500) of ExtrAvidin conjugated to 10nm colloidal gold (Sigma, Code No.: E-4259, Lot No.: 21H-8210). This reagent was diluted in 0.1M PBS containing 1% BSA and was immunoreacted with the tissue sections for 1 hour at 37ºC. It was stored in 10μl aliquots at -18ºC until required.

All dilutions of gold-conjugated reagents were first pelleted by centrifugation at 13000 RPM for 10 minutes in an MSE Microcentaur microcentrifuge. The supernatant, containing any unconjugated antibodies, was then discarded and the gold-conjugates re-suspended with buffer and thoroughly mixed. Finally, the solution was centrifuged at 6500 RPM for 5 minutes to pellet any large aggregations of gold. The grids containing tissue sections were immediately applied to 20μl droplets of the supernatant from this solution.

After incubation with the secondary antibody the sections were washed by transferring the grids across 20μl droplets of 0.1M PBS containing 1% BSA (3 x 3 minutes), 0.1M PBS (3 x 3 minutes) and distilled water (3 x 3 minutes). The antibody-antigen complexes were then stabilised by floating the grids for 5 minutes on a 1% aqueous solution of glutaraldehyde. The grids were subsequently washed with distilled water (3 x 3 minutes) and, finally, rinsed with 100% methanol and dried with Velin tissue (Agar Aids). The grids were stored at room temperature until required. A schematic example of a typical indirect immunogold labelling protocol is given in appendix XII.

6.2.7.3 Direct gold-labelling method.

Direct gold-labelling of endogenous immunoglobulin G was attempted by using a modification of the protein A-gold (pAg) technique. Briefly, the tissue sections were incubated with a 1/100 dilution (range tested: 1/10 - 1/500) of protein A conjugated to 10nm colloidal gold (Sigma, Code No.: P-1039, Lot No.: 98F-8105; Biocell, Code No.: EM.PAG10, Batch No.: 8768) diluted in 50mM TBS or 0.1M PBS containing 1% BSA for 1 hour at 37ºC. These reagents were tested at 4ºC, 20ºC and 37ºC for time periods ranging from 10 minutes to 24 hours. Optionally, endogenous IgG was localised with a 1/100 dilution of protein G conjugated to 10nm colloidal gold (Biocell, Code No.: EM.PGG10, Batch No. 8808) diluted and applied as described for protein A: gold. These reagents were stored for extended durations at –18ºC in 10μl aliquots and subsequently at 4ºC when required. The gold conjugates were centrifuged as described in the previous section (6.2.7.2) to remove any unconjugated proteins and large gold complexes from the solution.

After immunolabelling with the direct technique the tissue sections were washed with buffer containing 1% BSA (3 x 3 minutes), buffer alone (3 x 3 minutes) and distilled water (3 x 3 minutes). The gold-conjugated antigen-protein A/G complexes were subsequently stabilised with an aqueous solution of 1% glutaraldehyde (5 minutes), washed with distilled water (3 x 3 minutes), rinsed with 100% methanol and dried.

6.2.7.4 Control experiments.

Negative control experiments were performed on separate grids containing (serial) sections of the same tissue block. Experiments to localise Fcγ receptors were controlled by replacing the primary mouse monoclonal antibody with an equivalent (1/50) dilution of purified mouse IgG isotypes (IgG$_1$ and IgG$_{2a}$) as described in section 5.2.2.6 or by omitting the primary antibody from the solution.

Indirect localisations of endogenous human IgG immunoreactivity with the goat anti-human IgG antibody were controlled by incubating the tissue sections with an equivalent dilution (1/50) of non-immune (goat) serum diluted in 0.1M PBS containing 1% BSA and 5% NRS. An additional control was performed by incubating the tissue sections with the blocking reagents only (a 20μl droplet of 0.1M PBS containing 1% BSA and 5% NRS). Indirect localisations with the biotinylated F(ab')$_2$ goat anti-human IgG (γ-chain) were performed by omitting this primary antibody and incubating sections with 0.1M PBS containing 1% BSA and 5% NGS only. The control sections were treated in an identical way to experimental sections at all subsequent stages.

Direct localisations of endogenous IgG were controlled by incubating the protein A or protein G gold-conjugated reagents with 1×10^{-6} to 1×10^{-4}g ml^{-1} of exogenous human polyclonal IgG as a challenge (as described in section 4.2.2.5). The control grids, treated in this fashion, were subsequently treated in an identical way to experimental grids at all subsequent stages.

6.2.7.5 Non-immune sera.

A 5% non-immune serum was included in dilutions, where applicable, to act as a block to non-specific protein adsorption (as described in section 4.2.2.4). The use of non-immune sera in direct labelling experiments with gold-conjugated protein A or protein G was avoided. This was to prevent interaction of these reagents with immunoglobulins present in the sera.

6.2.8 Microscopy and photography.

The tissue sections were contrasted with 2% aqueous uranyl acetate for 5 minutes and 1% lead citrate for 6 minutes in an atmosphere of sodium hydroxide. To stabilise the resin sections in the electron beam the grids were coated with a 0.3% celloidin film. The tissue was examined in a JEM 100CX electron microscope with a liquid nitrogen-cooled specimen stage at an operating voltage of 80kV. Micrographs were taken according to conventional procedures.

6.2.9 Cryosectioning techniques for immunolabelling.

Immunolabelling of ultrathin frozen sections (Tokuyasu, 1973) was performed to localise endogenous IgG in the human placenta and fetal membranes. Type IV and type VII collagen distribution was also investigated using these techniques.

6.2.9.1 Tissue collection.

First trimester chorionic villi (n=3) were collected within 3 minutes of evacuation termination of pregnancy from the Leicester General Hospital. Term chorionic villi and amniochorion were dissected from the placentae of routine deliveries (n=3) at the Leicester Royal Infirmary. These tissues were rinsed briefly with two changes of 0.1M PBS to remove maternal blood.

6.2.9.2 Fixation.

Fixation was accomplished by immersing the tissue specimens into fixatives at room temperature for 2 hours. The following range of fixatives was used: i) 4% paraformaldehyde (PFA) in 0.1M PBS; ii) 4% PFA + 0.1% glutaraldehyde (GA) in 0.1M PBS; iii) 4% PFA + 0.5% GA in 0.1M PBS. Amniochorion specimens for use in anti-type VII collagen immunolabelling experiments were fixed by immersion into a saturated picric acid solution (15ml) made up to 100ml with 0.1M PBS (Heinz Schwartz; personal communication). The tissue specimens were subsequently washed with 0.1M PBS (3 x 20 mins).

6.2.9.3 Infusion with cryoprotectant.

The tissue was infused with cryoprotectant to prevent ice crystal damage during freezing. This was accomplished by immersing the tissue into a solution of 2.1M sucrose in 0.1M PBS. The tissue was infused for 3 x 20 mins at room temperature. The samples, contained in Eppendorf tubes, were then rapidly frozen

in liquid nitrogen and stored in a dewar containing liquid nitrogen until required. They were then transported to the European Molecular Biology Laboratory, Heidelberg, on dry ice. On arrival the tissue was thawed and small pieces (approximately 1mm^3) were mounted on copper stubs and rapidly frozen in liquid nitrogen.

6.2.9.4 Cryosectioning.

The mounted tissue specimens were transferred to an FCS cryochamber of a 'Reichert ultracut S' cryoultramicrotome (Leica) and the temperature allowed to equilibriate for 10 mins. The temperature of the specimen arm was maintained at −100°C, the knife at -90°C and the chamber at -90°C. The sample was then mounted on the specimen arm and advanced to the knife edge. Cryosectioning was performed using tungsten-coated glass knives to cut sections with a blue / gold interference colour. Sections were manipulated using a frozen eyelash.

The sections were collected and thawed using a droplet of 2.3M sucrose in 0.1M PBS suspended in a thin wire loop. This process also stretched the sections. They were then transferred to a G200-mesh copper electron microscope grid coated with (1%) formvar and a thin carbon film. These grids had previously been glow discharged to ensure hydrophilic properties (Dubochet et. al., 1982). The grids containing the sections were subsequently transferred to 0.1M PBS prior to immunolabelling or to triple-distilled water for direct observation.

Tissue sections were contrasted and protected from air-drying artefacts by embedding them in freshly prepared methyl cellulose containing uranyl acetate (Tokuyasu, 1978). This was prepared with 900μl of a 2% aqueous solution of methyl cellulose (Sigma) and 100μl of 3% aqueous uranyl acetate to give a 0.3% uranyl acetate solution. The grids were floated on drops of this solution for 10 mins on ice. They were then retrieved using thin wire loops and excess solution was blotted onto hardened filter paper (Whatman). The methyl cellulose film was allowed to air-dry. Films of yellow / blue interference colour were optimum for observation under the transmission electron microscope. The grids were removed from the loop by carefully piercing the methyl cellulose film around the edges of the suspended grid. They were stored at room temperature prior to observation in a Zeiss EM10 transmission electron microscope. Micrographs were taken according to conventional procedures.

6.2.9.5 Immunolabelling of (Tokuyasu) frozen tissue sections.

Immunolabelling of the thawed frozen sections was essentially the same as described in section 6.2.7. Briefly, the grids containing the tissue sections were transferred from the PBS to 20μl droplets of 50mM NH_4Cl in 0.1M PBS for 10 minutes at room temperature to quench unreacted aldehydes. The grids were then transferred to 20μl droplets of 10% fetal calf serum (FCS) for 10 minutes at room temperature and subsequently floated on 5μl droplets of the primary antibody solution, containing 5% FCS diluted in 0.1M PBS, for 1 hour at room temperature. The following primary antibodies were used in these investigations:

i) Rabbit anti-human IgG (Serotec, Code No.: STAR 33, Batch 012) was used at an optimum dilution of 1/100 (Range tested 1/20 - 1/200).

ii) Mouse anti-human type VII collagen (Serotec, Clone 8/LH7.2, IgG_1) was used at an optimum dilution of 1/50 (range tested 1/10-1/200).

iii) Mouse monoclonal anti-FcγR antibodies were as described in section 5.2.2.1.

The grids were washed using 20μl droplets of 0.1M PBS (5 x 3 min), blocked using 10% FCS in PBS and transferred to the secondary antibody or colloidal gold solution. Primary monoclonal mouse antibodies were detected with a 1/75 dilution of rabbit anti-mouse IgG (Serotec, Code No.: STAR 26B) for 30 mins at room temperature. These grids were washed and blocked as described above. Finally, rabbit antibodies were detected with a 1/60 dilution of protein A conjugated to 10nm colloidal gold for 30 mins at room temperature (Protein A-gold, prepared by Jan Slot, was a generous gift from Dr. Gareth Griffiths). All labelling procedures were performed using 5μl droplets. Finally the grids were transferred across droplets of 0.1M PBS (5 x 3 mins) and rinsed with triple distilled water (5 x 3 mins) before embedding in methyl cellulose as described above. Control experiments were performed by replacing specific primary rabbit antibodies with an equivalent dilution of non-immune rabbit serum. For control experiments utilising monoclonal antibodies, IgG isotype controls were performed using an equivalent concentration of purified mouse IgG_1 (Serotec; Code No.: MCA 928).

6.2.9.6 Quantitation of gold labelling.

Areas on micrographs of labelled frozen tissue sections were circumscribed using a DigiCad Plus graphics tablet and measured using a Kontron Videoplan Image-processing system. Counts of gold particles within these areas were used to deduce the number of gold particles per $μm^2$ associated with defined structures.

6.3 RESULTS.

Ultrastructural immunocytochemistry has been performed on low-temperature resin embedded tissue sections and on ultrathin frozen sections (Tokuyasu technique). These methods have been applied to demonstrate the distribution of endogenous IgG in the human placenta and fetal membranes. In addition this technique has been used to further characterise the novel extracellular matrix structures in term amniochorion ('microtrabeculae' and 'anchoring rivets') observed during the course of the routine ultrastructural studies performed in this investigation. This has been assessed using immunoreactivity to anti-type IV collagen and anti-type VII collagen.

6.3.1 Type IV and type VII collagen immunoreactivity in term amniochorion.

The results presented in chapter 2 documented the presence of novel short segments of 'homogeneous electron-dense substance' in the extracellular matrix of the compact layer, fibroblast layer, spongy layer and reticular layer of human term amniochorion (Malak et. al., 1993). These short segments appeared to be morphologically similar to the lamina densa of a typical basement membrane. The current experiments were performed to identify if these trabeculae contained type IV collagen which is present in typical basement membranes.

Ultrastructural immunocytochemistry using low denaturation embedding protocols preserved the ultrastructural morphology of the basal laminae and its anti-type IV collagen immunoreactivity (Figures 6.3-6.10). Thus colloidal gold labelling was concentrated over medium electron density structures with a texture typical of that seen in other basal laminae in the electron micrographs. The distribution of the colloidal gold particles marking the location of type IV collagen at the ultrastructural level parallels the distribution of type IV collagen immunofluorescence observed in the light microscope (Ockleford et. al., 1993b). Labelling of the amniotic epithelial basement membrane is shown in figures 6.3 and 6.8. Labelling of the chorion laeve (pseudo basement membrane) is shown in figures 6.4-6.6. Labelling of the extracellular matrix between cytotrophoblast cells of this layer also occurred. In all these cases the underlying texture of the labelled structures was of similar electron density to the lamina densa of typical basal laminae. Decidual layer blood vessels were also associated with a basement membrane which was immunoreactive with anti-type IV collagen antibodies (Figure 6.7). The specific immunolocalisations with colloidal gold frequently resulted in small clusters of electron dense particles over features with similar ultrastructural appearance (Figures 6.3-6.7). This occurred infrequently with the protein A-gold technique (Figure 6.8). This phenomenon is

likely to relate to the pattern of exposure of antigenic sites exposed at the surface of the resin and/or the increased amplification of the signal achieved in the three-stage immunocytochemical protocol used (see discussion). Control experiments in which the primary antibody was replaced with a non-specific antibody yielded negligible background labelling (Figures 6.9-6.10).

Anti-type VII collagen immunoreactivity was investigated in an attempt to identify the novel 'rivet' structures observed with routine electron microscopy (chapter 2). These structures were first identified in the epifluorescence confocal laser scanning microscope (Ockleford et. al., 1993a; 1994). Type VII collagen immunoreactivity was only conserved using the Tokuyasu thawed ultrathin frozen section technique. Furthermore, fixation with aldehydes, routinely used in conjunction with this technique, abolished immunoreactivity of this antigen with monoclonal antibody LH7.2. Therefore term amniochorion was fixed for 1 hour with a solution of saturated picric acid (15ml) made up to 100ml with 0.1M PBS. Anti-type VII collagen immunoreactivity was conserved in tissue prepared in this way but the ultrastructural morphology was considerably compromised.

Labelling with colloidal gold reveals the same overall distribution as the immunofluorescence pattern obtained for the same antibody (Ockleford et. al., 1994). This immunoreactivity was demonstrably extracellular and associated with medium electron density components of the amniotic epithelial basal lamina (Figures 6.11-6.12). Labelling was absent from the chorion laeve trophoblast basal lamina.

The fine structure with which colloidal gold particles associated appeared to be of medium electron density. It was present in the form of irregular clusters and fibrils, many of which contacted similar fibrils bridging the gap to the basal epithelial membrane (Figure 6.12). In these cryosections the fibrous structures appeared unbanded. The labelled structures appeared to form irregular bundles which were most evident in the invaginated regions between the basal foot-processes of the amniotic epithelial cells. Within the extracellular matrix of the compact layer there were also medium electron density plaque-like structures which were strongly immunoreactive with the anti-type VII collagen specific antibodies. This was in marked contrast with the overall paucity of labelling in the surrounding tissue layer. Anti-type VII collagen immunoreactivity did not associate with cells other than those at very superficial cytoplasmic surfaces and neither did it associate with the regular banded fibrous collagens. However, the clarity of the rivets obtained using routine epoxy resin embedded samples was not achieved.

6.3.2 Endogenous immunoglobulin G.

The localisation of endogenous immunoglobulin G was investigated in first trimester chorionic villi, term chorionic villi and term amniochorion using the ultrastructural immunocytochemistry described. IgG immunoreactivity was conserved in specimens fixed with 4% paraformaldehyde and 4% paraformaldehyde + 0.1% glutaraldehyde but was abolished by fixation with 4% paraformaldehyde + 0.5% glutaraldehyde. Direct immunolocalisations of IgG in resin-embedded samples with protein A: gold or protein G: gold did not yield specific labelling.

First trimester chorionic villi.
Where the ultrastructural distribution of endogenous IgG was investigated in first trimester chorionic villi, gold particles were associated with the apical syncytial plasma membrane (Figures 6.27-6.29) coated pits (Figures 6.27-6.28) coated vesicles (Figures 6.28-6.29) endosomal compartments (6.27-6.28) and lysosomes (Figure 6.30). These observations are consistent with the receptor-mediated uptake of the ligand. Gold was also demonstrated bound to the plasma membrane of uncoated vacuoles and vesicles up to approximately 500nm in size (Figures 6.28-6.29). The Golgi apparatus was unlabelled. Nuclei and mitochondria revealed negligible background levels of binding. Furthermore cytotrophoblast cells did not demonstrate specific gold labelling (Figures 6.24-6.26 and 6.31-6.34) consistent with the immunofluorescence investigations which indicates that endogenous IgG is not present in these cells. Inconsistent labelling of endogenous IgG was achieved in the first trimester villus core indicating that there were areas that contained endogenous antibodies (Figure 6.31) and areas that were devoid of endogenous antibodies (Figure 6.32). This pattern is likely to reflect localised regions where IgG is transported across the syncytiotrophoblast to the villus core. Control experiments in which the tissue was incubated in the presence of non-immune rabbit IgG and subsequently with protein A:gold yielded background labelling only (Figure 6.34).

Term chorionic villi.
In term chorionic villi gold was associated with the capillary serum proteins and endothelial cells (Figures 6.18-6.19 and 6.39-6.42). Endothelial cell gold-labelling was demonstrated in coated pits at the apical and basal surfaces (Figure 6.18) and in coated vesicles within the cell. Occasionally immunoreactivity was associated with lysosomal structures (Figure 6.19). Gold was also observed in endothelial caveolae and in large multivesicular bodies but not in the intercellular spaces between adjacent endothelial cells (Figure 6.18 and 6.40). Intracellular gold labelled vesicles could be seen near the luminal membrane of the endothelium (Figures 6.40-6.42).

In the connective tissue stroma gold labelling was associated with mesenchymal cells, Hofbauer cells and with the extracellular matrix (Figures 6.14, 6.17-6.19, 6.37 and 6.40-6.42). Gold labelling was also associated with the trophoblast and predominantly labelled the apical plasma membrane (Figures 6.14-6.16, 6.35-6.36 and 6.38), coated pits (Figures 6.13-6.14 and 6.35) and coated vesicles (Figures 6.16 and 6.36). Gold labelling was also identified with apical endosomal (Figure 6.35) and lysosomal compartments (Figure 6.38). Gold labelling in the basolateral aspect (Figure 6.37) was less frequent and bound to uncoated vesicles and tubules and the basal plasmalemma. Nuclei, erythrocytes, mitochondria, Golgi systems, cytotrophoblast cells (Figures 6.37-6.38) and control experiments (Figure 6.20) revealed a paucity of gold labelling corresponding to background levels only.

Term amniochorion.
In term amniochorion gold labelling was restricted to the extracellular matrix. The only exception to this observation was that fibroblast cells of the fetal mesenchymal tissue (fibroblast and reticular layers) displayed IgG-specific gold labelling although the ultrastructural morphology of these cells was poorly conserved by the fixation techniques employed in this study (data not shown). Human leucocytes present within the maternal decidual layer also demonstrated IgG-specific immunolabelling.

However, amniotic epithelial cells (Figures 6.21 and 6.43-6.46) and cytotrophoblast cells of the chorion laeve (Figures 6.23 and 6.49-6.50) were not labelled with colloidal gold. Labelling of the surrounding extracellular matrix, on the other hand, was intense. IgG was also associated with the basement membrane which protruded between the basal foot-processes of the amniotic epithelial cells (Figures 6.43-6.45). This correlated with the results obtained with high resolution confocal immunofluorescence micrographs which demonstrated incursions of IgG between the amniotic epithelial cell foot processes. Furthermore, immunolabelling was observed in the intercellular spaces between amniotic epithelial cells (Figure 6.43) which suggested that IgG may penetrate between these cells to some extent. Due to the extraordinarily complex and convoluted nature of the lateral intercellular space between amniotic epithelial cells it was not apparent how IgG was prevented from gaining access to the amniotic fluid. Damaged/dead cells present within the amniotic epithelium also displayed immunoreactivity to endogenous IgG (Figures 6.22 and 6.47-6.48) suggesting that they had lost the ability to exclude IgG. The cytoplasm of healthy cells did not contain IgG. However, the nucleus of such damaged cells was frequently devoid of specific gold labelling (Figure 6.22) suggesting that the nuclear envelope remained impermeable to the diffusion of IgG for a longer duration. IgG-associated immunogold labelling was also observed in the

extracellular matrix between cytotrophoblast cells of the chorion laeve (Figures 6.23 and 6.49-6.50), consistent with the immunofluorescence micrographs.

Quantitation of gold-labelling.

The number of gold particles overlying tissue components was calculated (gold particles / μm^2) and the data was subjected to statistical analysis as described in Appendix XIV. This data is summarised in Table 6.1.

	n.	Mean gold / μm^2.	Standard deviation.
1: Control.	31	2.119	1.076
2: Background.	42	2.223	1.360
3: Erythrocytes.	21	7.295	3.988
4: Cytotrophoblast cells.	42	2.036	1.205
5: 1st trimester syncytium.	20	53.267	22.880
6: 1st trimester ECM.	19	14.897	18.025
7: Term syncytium.	20	34.907	17.659
8: Term villus ECM.	22	58.505	32.602
9: Term serum.	20	269.785	179.120
10: Amnion cells.	20	3.733	1.669
11: Dead amnion cells.	6	140.368	55.044
12: Amniochorion ECM.	29	58.668	31.258

Table 6.1: Quantitation of gold particles overlying tissue components in electron micrographs of frozen placental sections.

This data is also represented graphically in figures 6.51-6.54. Figure 6.51 illustrates gold labelling densities associated with 1st trimester chorionic villi; figure 6.52 illustrates gold labelling associated with term chorionic villi and figure 6.53 illustrates gold labelling associated with term amniochorion. These graphs are overlaid for comparison in figure 6.54.

One-way analysis of variance (ANOVA) of gold particles / μm^2 yielded an F-ratio of 49.83 (df 11) with p=0.0001 (Appendix XIV). Post-hoc comparisons between pairs of mean values of gold particles / μm^2 confirmed significant differences between tissue components. Cytotrophoblast cells (n = 42, mean = 2.036, SD = 1.205) from 1st trimester and term chorionic villi and amniochorion were not significantly different from control (n = 31, mean = 2.119, SD = 1.076) or background (n = 42, mean = 2.223, SD = 1.360) gold particle counts.

In 1st trimester chorionic villi gold labelling over the syncytiotrophoblast was significantly different (n = 20, mean = 53.267, SD = 22.880; p<0.01) from cytotrophoblast cells, background (nuclei + mitochondria) and control preparations. In addition the labelling over the syncytiotrophoblast was significantly different (p<0.05) from the extracellular matrix of the villus core. Gold labelling of the villus stroma (n = 19, mean = 14.897, SD = 18.025) was not statistically significant from control or background gold particle counts. The variation of labelling in the villus stroma at this stage of gestation is indicated by the large standard deviation. This pertains to unusual local circumstances where gold labelling is intense underlying regions of contact between the syncytiotrophoblast and the extracellular matrix.

Labelling of the syncytiotrophoblast at term (n = 20, mean = 34.907, SD = 17.659; p<0.05) is statistically significant from labelling over cytotrophoblast cells, background and control preparations. It is not significantly different from labelling associated with 1st trimester syncytiotrophoblast. The incidence of cytoplasmic organelles possessing a high density of gold labelling in some micrographs contributes to the overall standard deviation. Labelling of the villus core (n = 22, mean = 58.505, SD = 32.602; p<0.01) is significantly different from cytotrophoblast cells, background and control preparations but not significantly different from the syncytiotrophoblast. The high degree of gold labelling associated with the serum proteins of fetal capillaries at term (n = 20, mean = 269.785, SD = 179.120; p<0.01) is significantly different from all other tissue components. Erythrocytes possessed slightly elevated levels of background labelling (n = 21, mean = 7.295, SD = 3.988) but these differences were not significant from background or control preparations at this level.

In term amniochorion healthy amniotic epithelial cells revealed a paucity of labelling (n = 20, mean = 3.733, SD = 1.669) which was not significantly different from gold labelling overlying background organelles or control preparations. However, dead or damaged amniotic epithelial cells (n = 6, mean = 140.368, SD = 55.044; p<0.01) possessed significantly different gold labelling from healthy cells and the extracellular matrix of the amniochorion. The stroma of the amniochorion

possessed gold labelling (n = 29, mean = 58.668, SD = 31.258; p<0.01) which was significantly different from background, cytotrophoblast cells, amniotic epithelial cells and control preparations. It was not, however, significantly different from gold labelling associated with the extracellular matrix of the chorionic villus core at term.

Fcγ Receptors.
Experiments performed to identify the ultrastructural localisation of the Fcγ receptors did not yield specific gold-labelling beyond background levels (see discussion).

FIGURES 6.3 - 6.54.

Figures 6.3-6.8: Type IV collagen immunoreactivity in ultrathin low-temperature resin-embedded sections of term amniochorion.

Figure 6.3: Colloidal gold particles reveal sites immunoreactive with anti-type IV collagen. Labelling is restricted to the amniotic epithelial basement membrane (BM) but is not evident over the amniotic epithelium (A) or collagenous fibres of the compact layer (C). Fixative: 0.1% glutaraldehyde + 3% formaldehyde; Resin: Lowicryl HM23. Scale bar represents 200nm.

Figure 6.4: Type IV collagen immunoreactive sites over the pseudo (chorion laeve) basement membrane (PBM). Clustering of the gold particles may reflect the pattern of exposure of antigenic sites at the section surface. The trophoblast cell (T) and collagenous fibres of the reticular layer (R) are not labelled. Fixative: 0.1% glutaraldehyde + 3% formaldehyde; Resin: Lowicryl HM23. Scale bar represents 200nm.

Figure 6.5: Gold labelling associated with the chorion laeve basement membrane (arrows). Note, however, that gold labelling is also associated with a short segment of basement membrane-like material (arrowheads) at a site distant from the chorion laeve basement membrane in the reticular layer (R). The trophoblast cell (T) and banded collagenous fibres of the reticular layer are not immunoreactive. Fixative: 0.1% glutaraldehyde + 3% formaldehyde; Resin: Lowicryl HM23. Scale bar represents 400nm.

Figure 6.6: Gold labelling associated with the chorion laeve basement membrane (arrows). Note that a segment of immunoreactive basement membrane-like material (arrowheads) splinters off from the basal lamina and projects into the overlying reticular layer (R). This micrograph also illustrates type IV collagen immunoreactivity extending between processes of the enmeshed trophoblast cell (T). Fixative: 0.1% glutaraldehyde + 3% formaldehyde; Resin: Lowicryl HM23. Scale bar represents 400nm.

Figure 6.7: Gold labelling is evident over the basement membrane (BM) surrounding the endothelium of a vessel in the maternal decidua. Vessel lumen (L). Fixative: 3% formaldehyde; Resin: Lowicryl HM23. Scale bar represents 400nm.

Figure 6.8: Gold particles label the amniotic epithelial basement membrane but not the amniotic epithelium (A) or the compact layer (C). Note that in this preparation the gold particles are not clustered. Fixative: 0.1% glutaraldehyde + 3% formaldehyde; Resin: Lowicryl K4M. Scale bar represents 500nm.

6.3

6.4

6.5

6.6

6.7

6.8
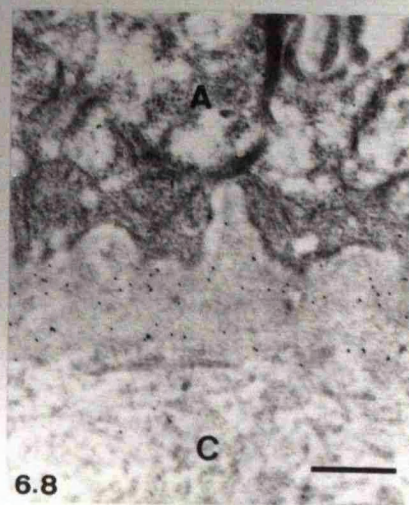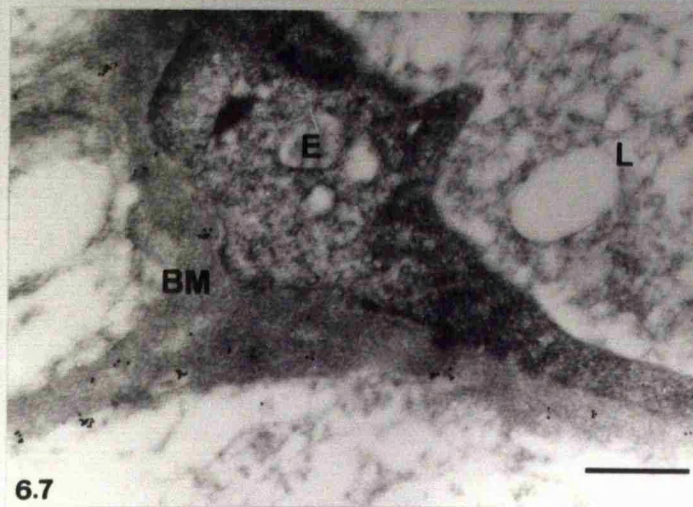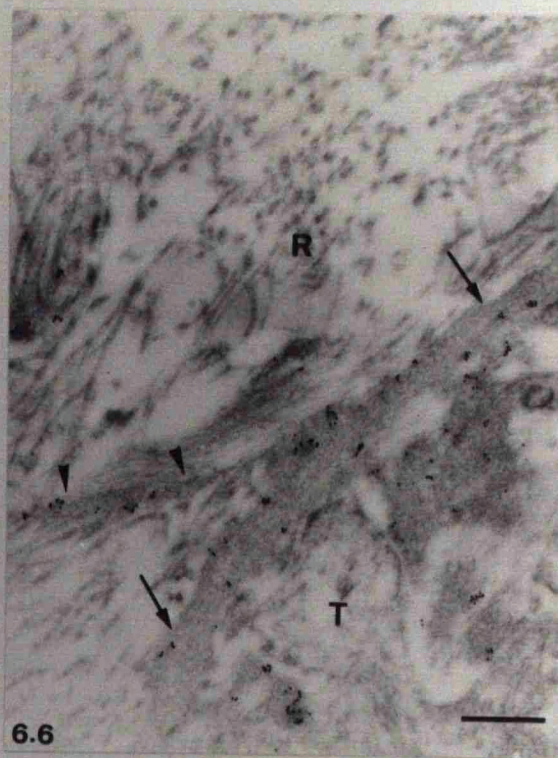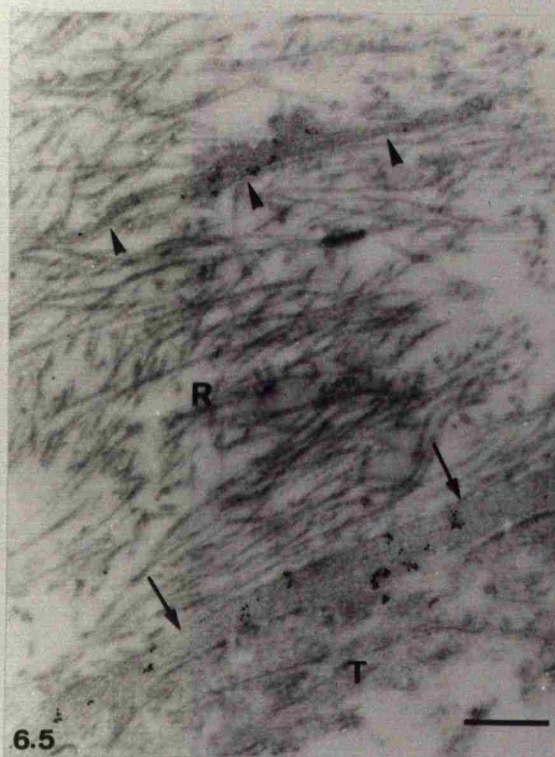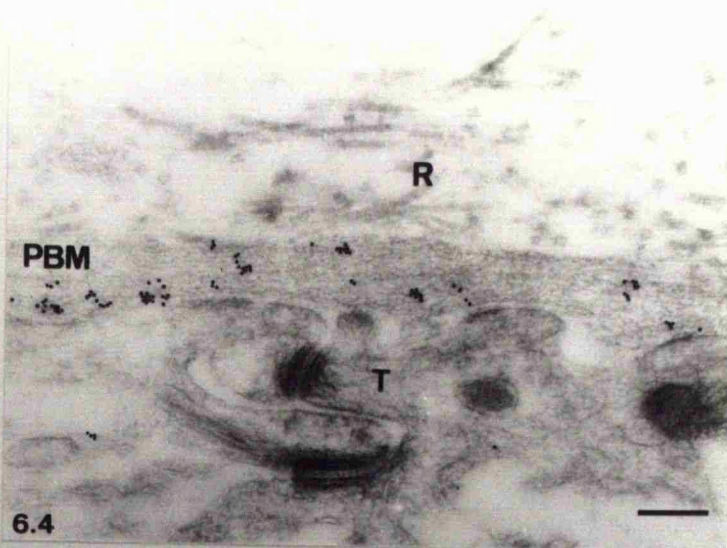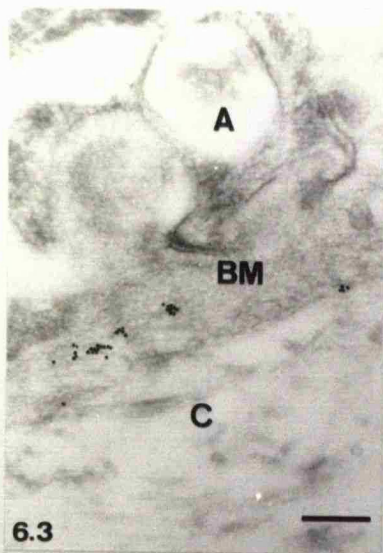
Figures 6.9-6.10: Type IV collagen control experiments in ultrathin low-temperature resin-embedded sections of term amniochorion.

Figures 6.9 and 6.10: Control preparations from similar areas of tissue to those illustrated in figures 6.3-6.8. Specific anti-collagen IV antibodies have been omitted from these preparations. Note the paucity of labelling. Amniotic epithelium (A), basement membrane (BM), compact layer (C), reticular layer (R), pseudo (chorion laeve) basement membrane (PBM) and trophoblast cell (T). Fixative: 0.1% glutaraldehyde + 3% formaldehyde; Resin: Lowicryl HM23. Scale bars represent 500nm.

Figures 6.11-6.12: Type VII collagen immunoreactivity in ultrathin frozen sections of term amnion.

Figure 6.11: Ultrathin frozen tissue section illustrating type VII collagen immunoreactivity in term amniotic epithelial basement membrane (BM). Low levels of background labelling are evident over the amniotic epithelial cell (A). Note that labelling is concentrated over the lamina densa in close apposition to the hemi-desmosomes (arrowheads). Banded collagen fibres (arrow) in the compact layer (C) are not immunoreactive. The morphology of this tissue is poorly conserved since aldehyde-fixation was omitted. Scale bar represents 400nm.

Figure 6.12: At higher magnification type VII collagen immunoreactivity overlying the lamina densa in apposition to hemi-desmosomes of the amnion (A) is clearly evident. Note the strands of material bridging the space between the hemi-desmosome and the lamina densa (arrowheads). Scale bar represents 200nm.

6.9

6.10

6.11

6.12
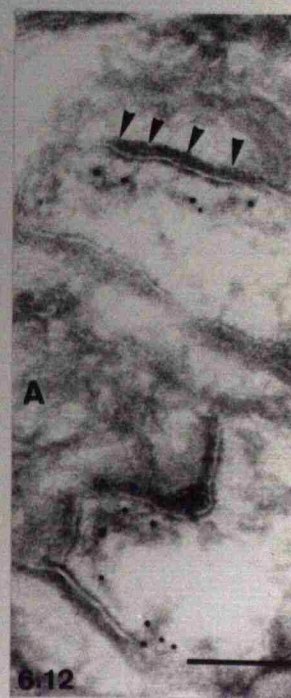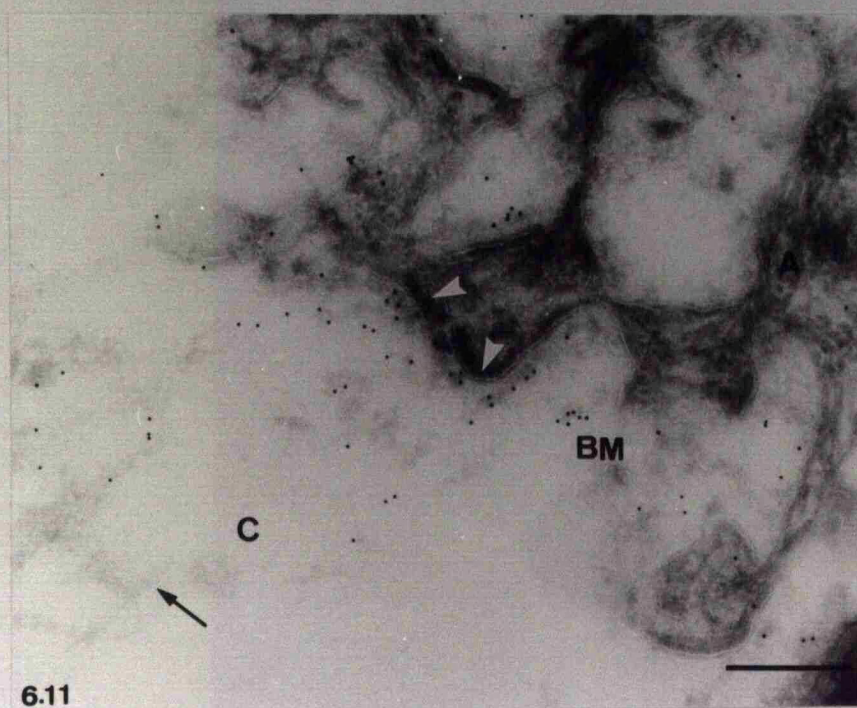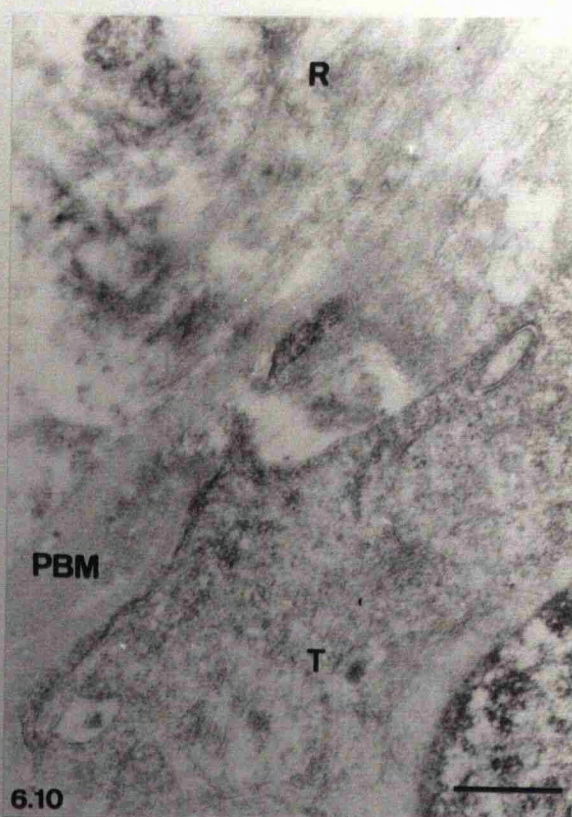
Figures 6.13-6.16: Endogenous IgG immunoreactivity in ultrathin low-temperature resin-embedded sections of term chorionic villi.

Figure 6.13: Endogenous IgG immunoreactivity in an electron micrograph of a term chorionic villus. Gold labelled IgG is associated with a coated pit (arrowhead) at the syncytiotrophoblast (Sy) apical cell surface. Nucleus (N). Fixative: 0.1% glutaraldehyde + 3% formaldehyde; Resin: Lowicryl HM23. Scale bar represents 200nm.

Figure 6.14: Endogenous IgG immunoreactivity in an electron micrograph of a term chorionic villus. Gold labelling is associated with a coated pit (arrowhead) and the plasma membrane at the syncytiotrophoblast (Sy) apical cell surface (arrow). Gold labelling is also evident in the underlying connective tissue stroma (St). Fixative: 0.1% glutaraldehyde + 3% formaldehyde; Resin: Lowicryl HM23. Scale bar represents 200nm.

Figure 6.15: Gold labelled IgG in an electron micrograph of the apical cell surface of the syncytiotrophoblast (Sy) in a term chorionic villus. Gold particles are associated with the surface of microvilli (arrows). Fixative: 0.1% glutaraldehyde + 3% formaldehyde; Resin: LR Gold. Scale bar represents 200nm.

Figure 6.16: Gold labelled IgG in an electron micrograph of the syncytiotrophoblast (Sy) in a term chorionic villus. A gold particle is associated with the surface of microvillus (arrow). A coated vesicle also contains a cluster of gold particles (arrowhead). Fixative: 3% formaldehyde; Resin: LR Gold. Scale bar represents 200nm.

6.13

6.14

6.15

6.16
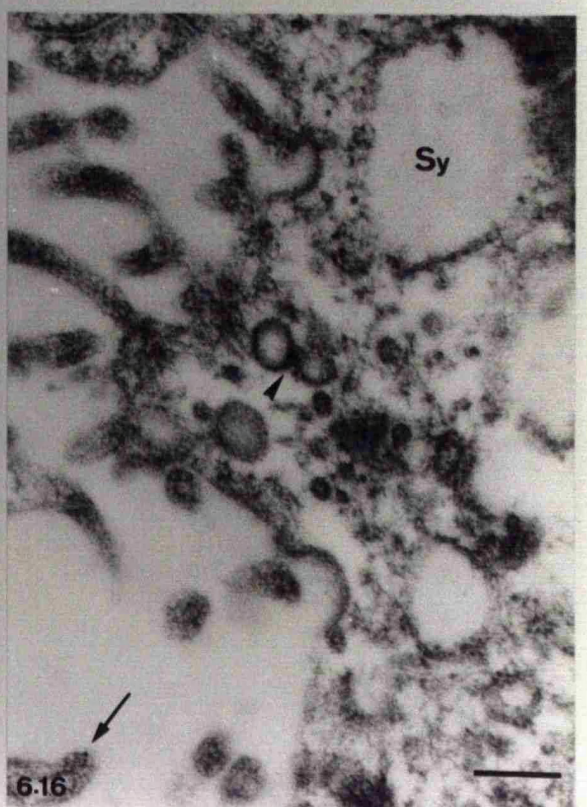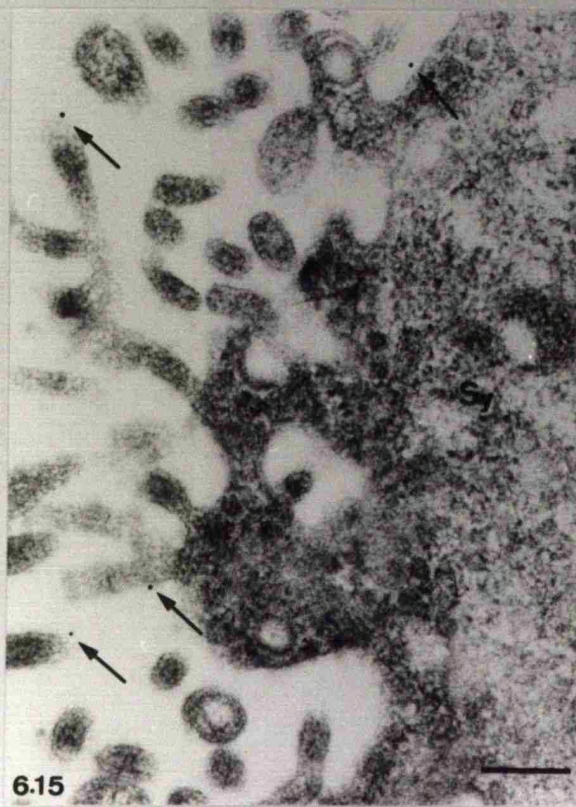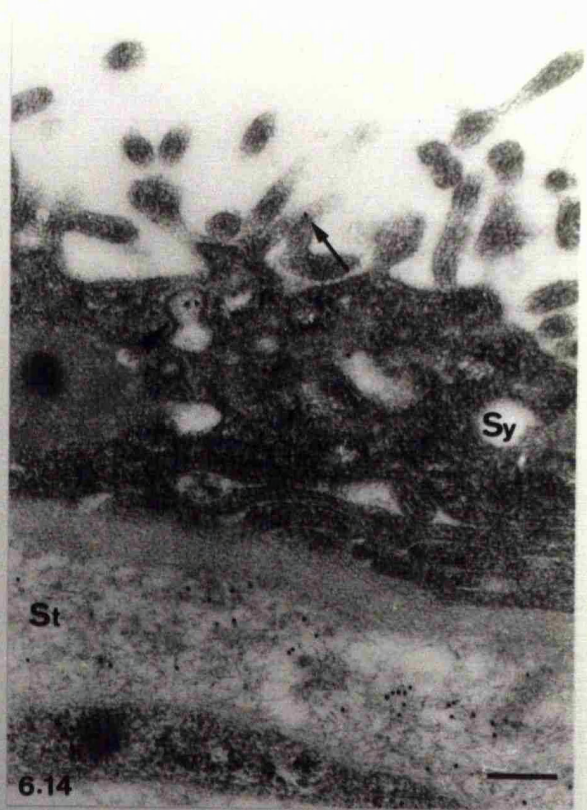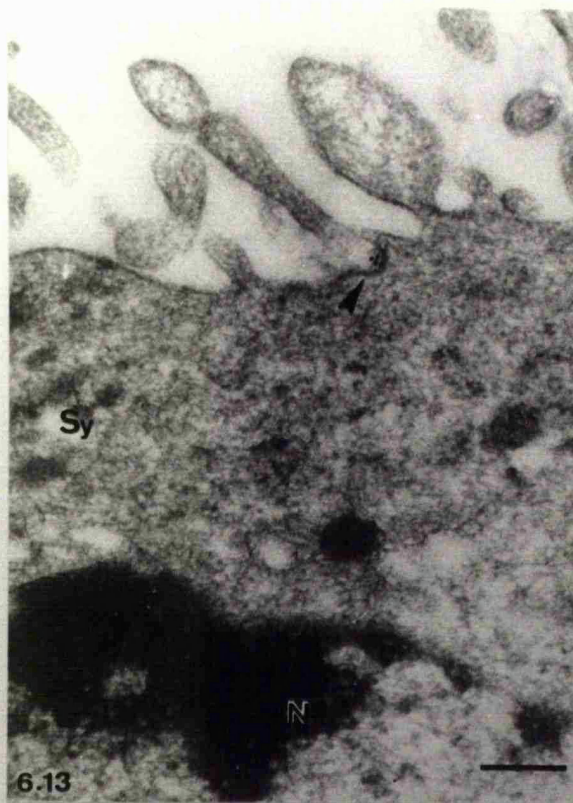
Figures 6.17-6.20: Endogenous IgG immunoreactivity in ultrathin low-temperature resin-embedded sections of term chorionic villi.

Figure 6.17: Colloidal gold labelled IgG in an electron micrograph of a term chorionic villus. Gold particles are associated with the connective tissue stroma (St). Syncytiotrophoblast (Sy). Fixative: 0.1% glutaraldehyde + 3% formaldehyde; Resin: Lowicryl HM23. Scale bar represents 200nm.

Figure 6.18: Gold labelled IgG in an electron micrograph of a term chorionic villus. Gold particles are associated with the connective tissue stroma (St) and serum proteins of the capillary lumen (L). Furthermore IgG is present in a coated pit (arrowhead) at the luminal surface of the endothelial cell (E) shown in this field. However, gold particles are not associated with intercellular channels (arrows). Fixative: 0.1% glutaraldehyde + 4% paraformaldehyde; Resin: LR Gold. Scale bar represents 200nm.

Figure 6.19: IgG immunoreactivity in an electron micrograph of a term chorionic villus.   Gold labelling is associated with the connective tissue stroma and a lysosomal-like inclusion (arrowhead) of the endothelial cell (E) shown in this field. Fixative: 0.1% glutaraldehyde + 3% formaldehyde; Resin: Lowicryl HM23. Scale bar represents 200nm.

Figure 6.20: Control electron micrograph of a term chorionic villus in which primary specific anti-human IgG antibodies have been replaced with non-immune antibodies. Note the absence of specific gold labelling. Fixative: 3% formaldehyde; Resin: LR Gold. Scale bar represents 500nm.

6.17

6.18

6.19

6.20
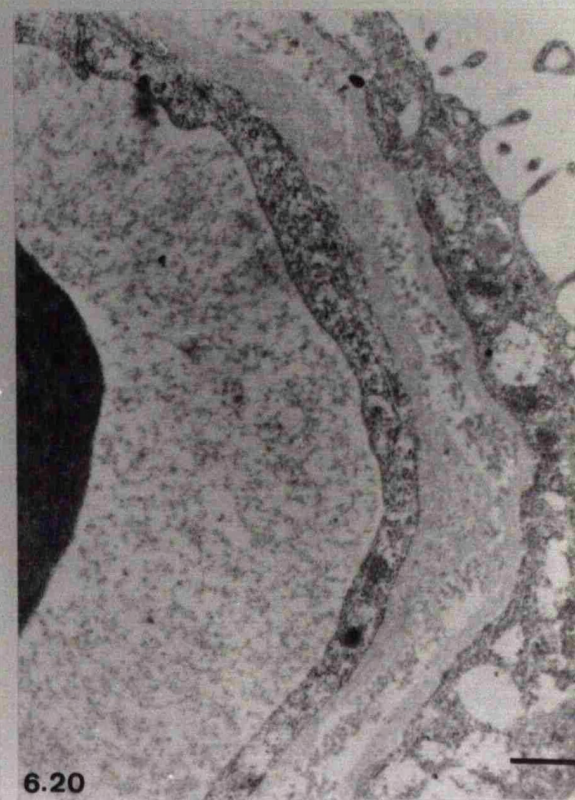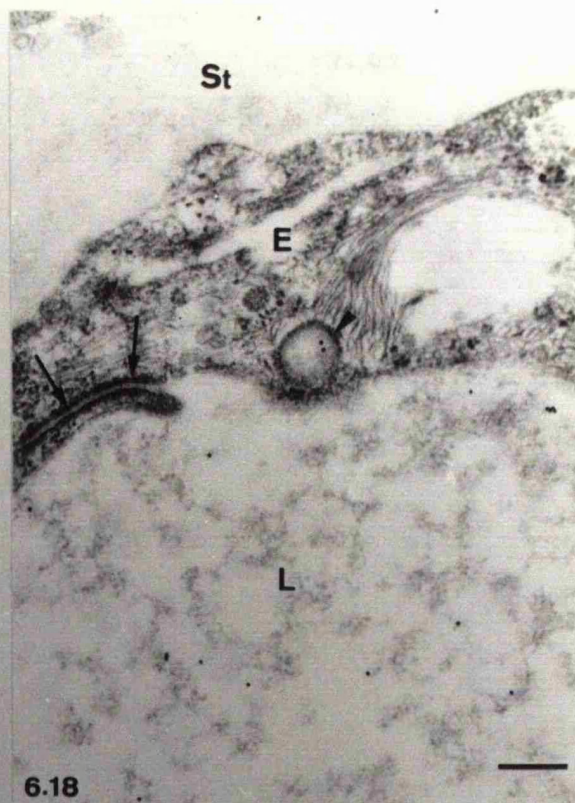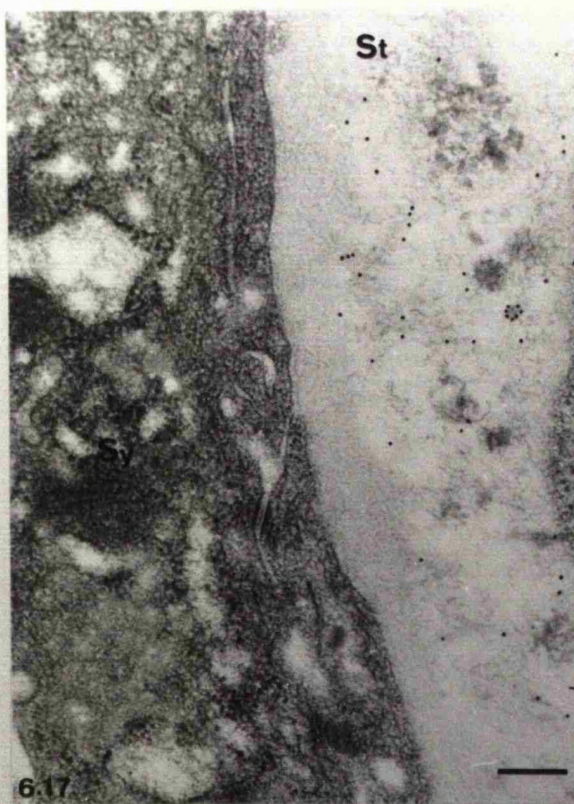
Figures 6.21-6.23: Endogenous IgG immunoreactivity in ultrathin low-temperature resin-embedded sections of term amniochorion.

Figure 6.21: Gold labelled IgG in an electron micrograph of term amnion. Gold particles are associated with the extracellular matrix of the compact layer (C) but not with the amniotic epithelial cell (A).   Fixative: 0.1% glutaraldehyde + 4% paraformaldehyde; Resin: LR Gold. Scale bar represents 200nm.

Figure 6.22: Gold labelled IgG in an electron micrograph of a damaged amniotic epithelial cell (*). Gold particles are associated with the extracellular matrix of the compact layer (C) and with the amniotic epithelial cell. However, the nucleus of this cell (N) is unlabelled. Fixative: 0.1% glutaraldehyde + 4% paraformaldehyde; Resin: LR Gold. Scale bar represents 400nm.

Figure 6.23: Gold labelled IgG in an electron micrograph of the trophoblast layer of term amniochorion. Gold particles are associated with the connective tissue stroma (St) which surrounds the trophoblast cells (T). The cytotrophoblast cells are not labelled. Fixative: 0.1% glutaraldehyde + 4% paraformaldehyde; Resin: LR Gold. Scale bar represents 400nm.

6.21

6.22

6.23
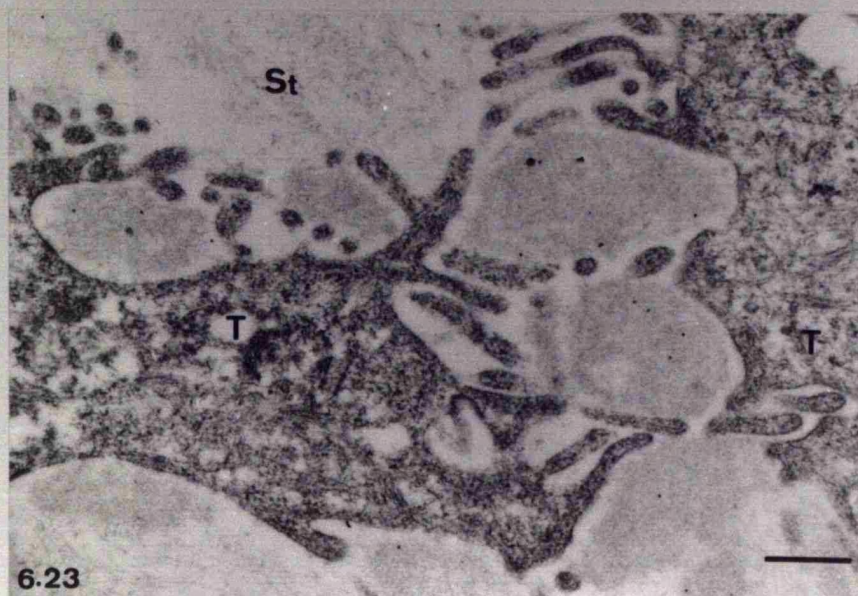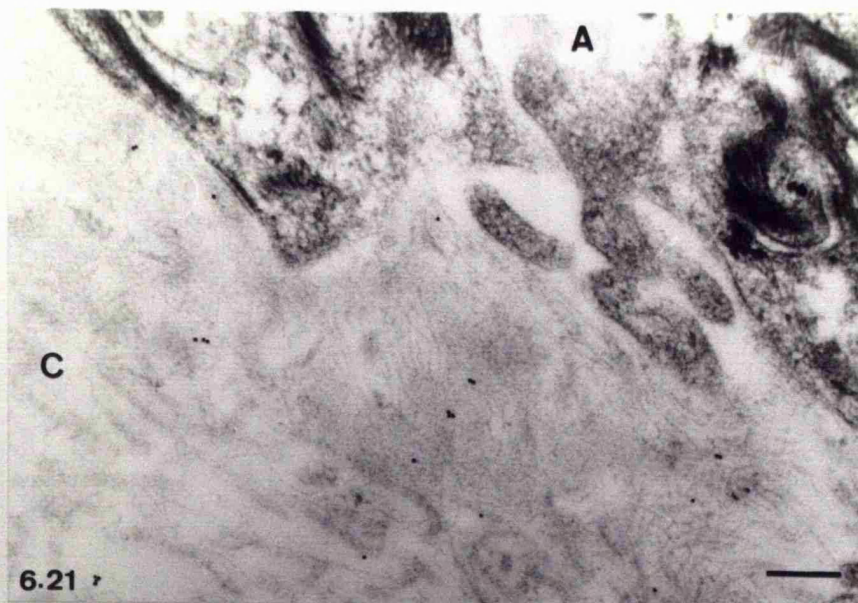
Figures 6.24-6.26: Endogenous IgG immunoreactivity in ultrathin frozen sections of 1st trimester chorionic villi.

Figure 6.24: Colloidal gold labelled IgG in a transmission electron micrograph of an ultrathin frozen section of 1st trimester trophoblast. This preparation was made using rabbit anti-human IgG subsequently localised with protein A conjugated to 10nm monodisperse gold particles. Many gold particles are associated with the syncytiotrophoblast (S) but the underlying cytotrophoblast cell (C), characterised by prominent mitochondria, does not possess specific gold labelling. A desmosome (arrowhead) is clearly apparent adjoining the syncytiotrophoblast and cytotrophoblast cell. Scale bar represents 300nm.

Figure 6.25: Gold labelled endogenous IgG in an ultrathin frozen section of 1st trimester trophoblast prepared as described above. Gold particles are associated with the plasma membrane (arrows) of basal inclusions within the syncytiotrophoblast (S) but the underlying cytotrophoblast cell (C) and nucleus are unlabelled. Scale bar represents 300nm.

Figure 6.26: Endogenous IgG immunoreactivity in an ultrathin frozen section of 1st trimester trophoblast prepared as described above. Gold particles are associated with the projection of syncytiotrophoblast (S) where it penetrates between two neighbouring cytotrophoblast cells (C). The cytotrophoblast cells are unlabelled. Note the desmosome (arrowhead) adhering the cytotrophoblast cell to the syncytiotrophoblast. Scale bar represents 400nm.

6.24

6.25

6.26
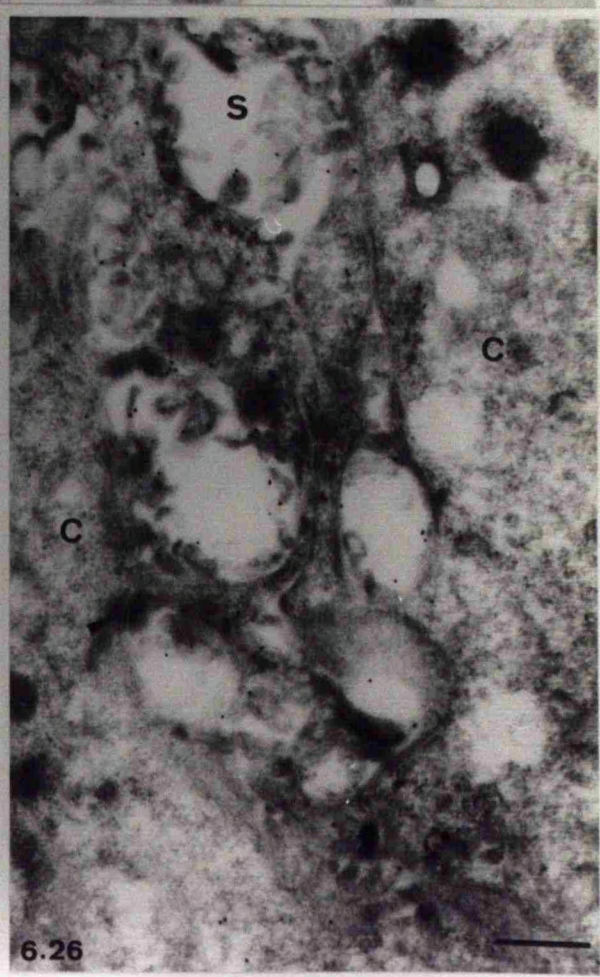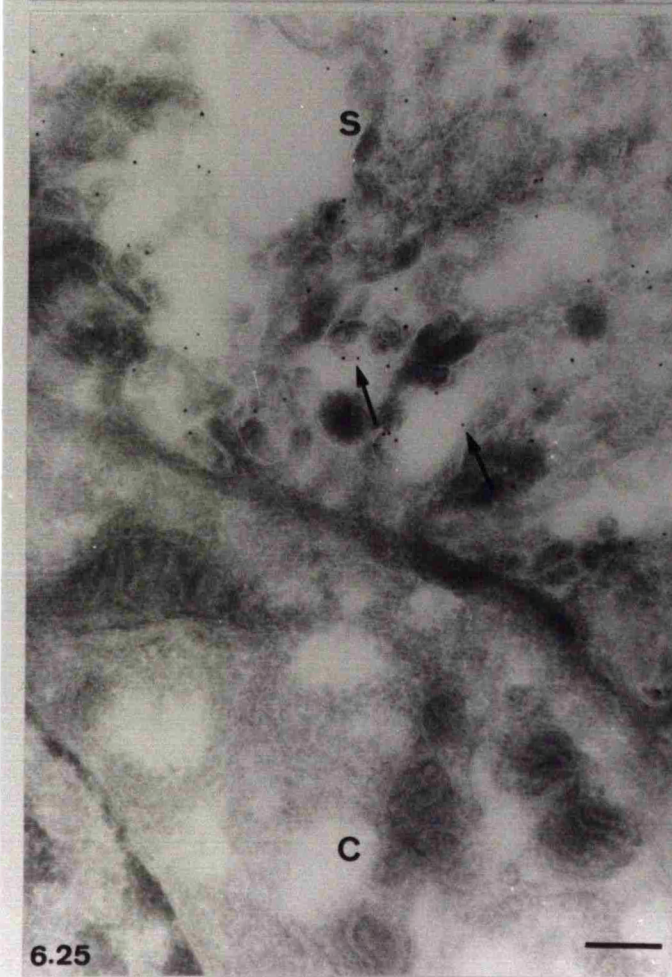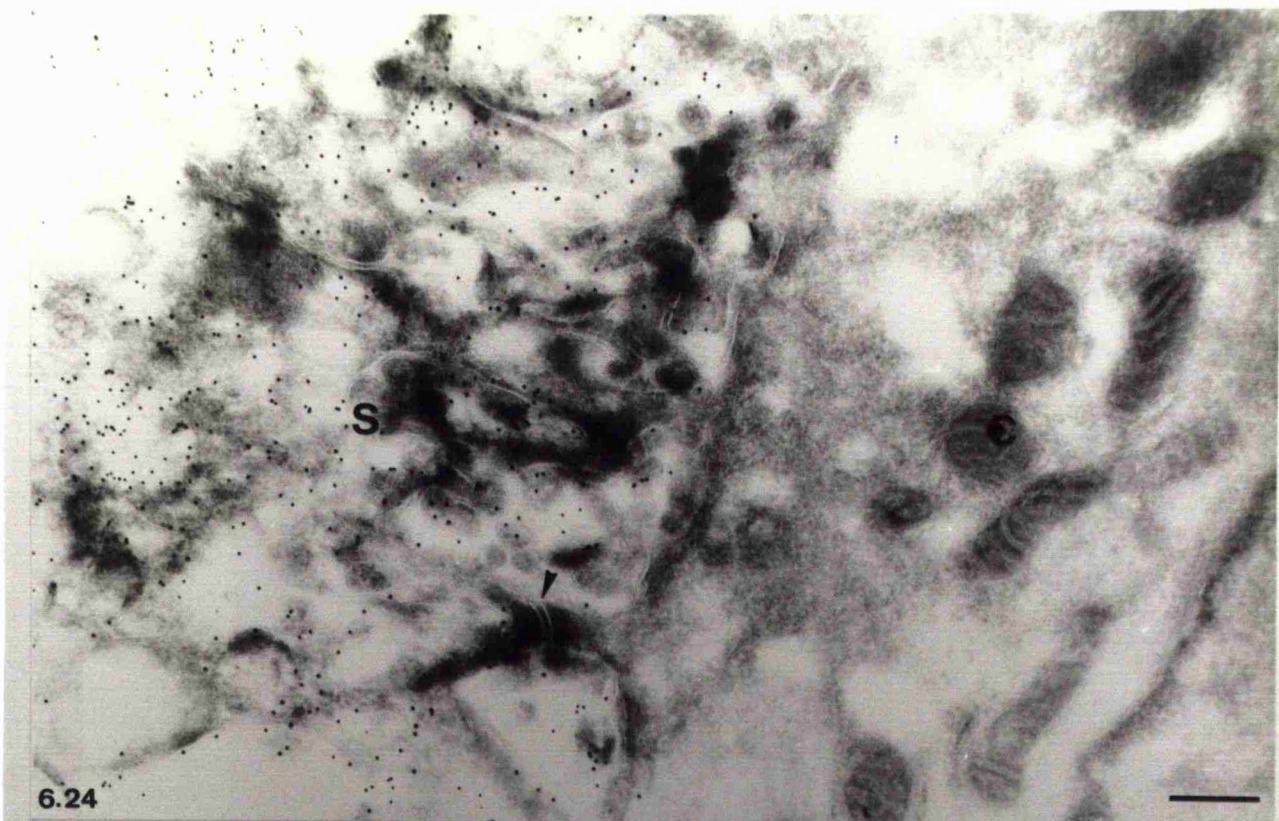
Figures 6.27-6.30: Endogenous IgG immunoreactivity in ultrathin frozen sections of 1st trimester chorionic villi.

Figure 6.27: Endogenous IgG immunoreactivity in an ultrathin frozen section of 1st trimester syncytiotrophoblast. Gold particles are associated with the apical microvilli and coated pits (arrows) at the cell surface. Apical endosome-like inclusions (arrowheads) are also labelled with numerous gold particles. The nucleus (N) present in this field exhibits a very low background level of labelling. Scale bar represents 400nm.

Figure 6.28: Gold labelled endogenous IgG in an ultrathin frozen section of 1st trimester syncytiotrophoblast. Gold particles are associated with the apical plasma membrane and a coated pit (arrow) at the cell surface. A coated vesicle (arrowhead) and numerous uncoated vacuoles (open arrow) with membrane bound gold particles may also be identified. Apical endosome-like inclusions (E) are also labelled with numerous gold particles. There is evidence of plasma membrane labelling in these compartments. Scale bar represents 400nm.

Figure 6.29: Gold labelled endogenous IgG in an ultrathin frozen section of 1st trimester syncytiotrophoblast. Gold labelling is associated with the apical plasma membrane and microvilli. A coated pit (arrowhead) at the cell surface is also labelled. Uncoated vacuoles (open arrows) with membrane bound gold particles may be identified. Scale bar represents 200nm.

Figure 6.30: Gold labelled endogenous IgG in an ultrathin frozen section of 1st trimester syncytiotrophoblast. Gold labelling is associated with medium electron density lysosome-like inclusions (arrows). These inclusions are clearly bounded by a limiting plasma membrane when sectioned in an appropriate plane (arrowhead). Scale bar represents 400nm.
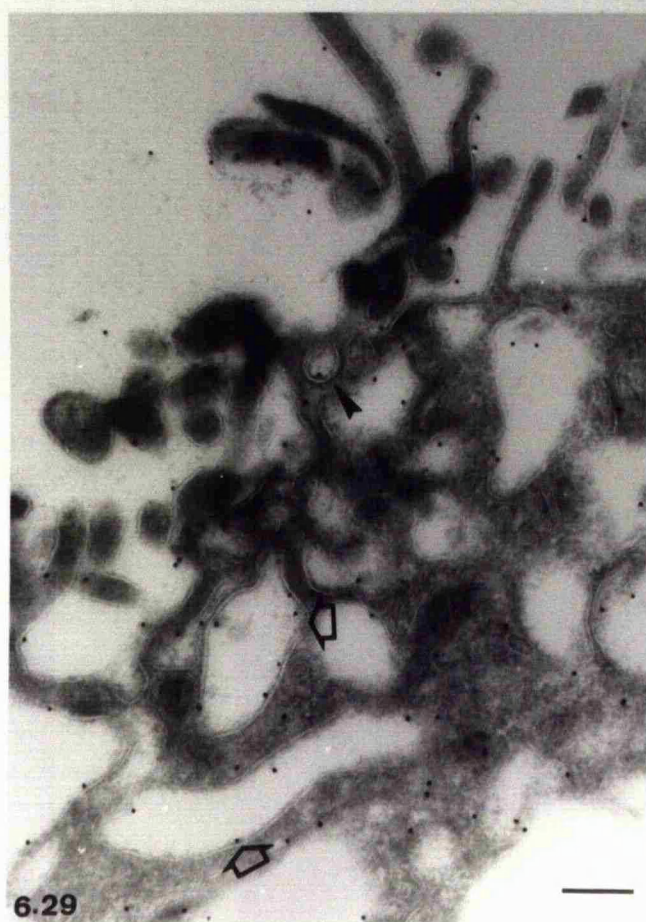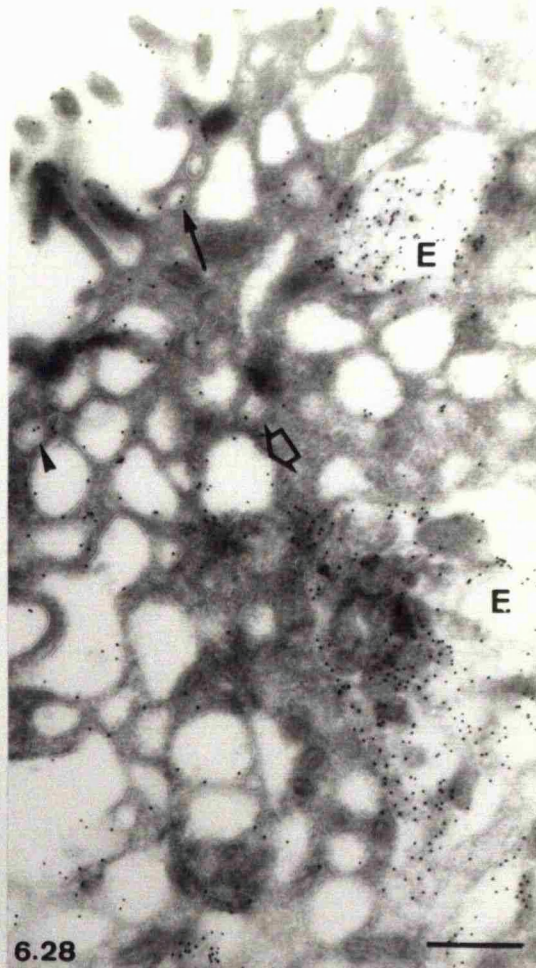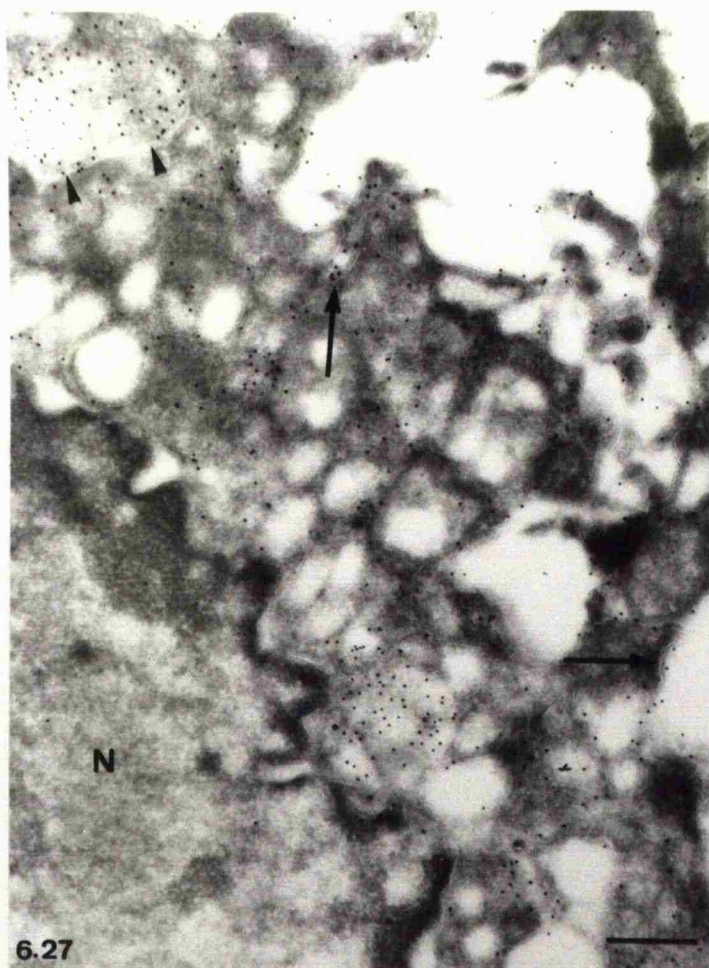
6.27

6.28

6.29

6.30

Figure 6.31: Gold labelled endogenous IgG in an ultrathin frozen section of a 1st trimester chorionic villus. Gold labelling is evident in the stroma (St) underlying a cytotrophoblast cell (C) which is not gold labelled. This indicates that IgG is able to gain access to the connective tissue core in the 1st trimester. Scale bar represents 300nm.

Figure 6.32: Gold labelled endogenous IgG in an ultrathin frozen section of a 1st trimester chorionic villus. Note the paucity of gold labelling evident in the stroma (St) of this section. A cytotrophoblast cell (C) and an endothelial cell (E) are not gold labelled. This illustrates the inconsistent labelling in the 1st trimester villus stroma which may be dependant on local circumstances, for example if the overlying syncytiotrophoblast is in direct contact with the basal lamina. Scale bar represents 300nm.

Figure 6.33: Endogenous IgG immunoreactivity in a transmission electron micrograph of an ultrathin frozen section of 1st trimester trophoblast. Gold particles are associated with the syncytiotrophoblast (Sy) but the underlying cytotrophoblast cell (C) possesses background gold labelling only. Scale bar represents 500nm.

Figure 6.34: Control transmission electron micrograph of an ultrathin frozen section of 1st trimester trophoblast. This preparation was made in an identical way to the specimen illustrated in figure 6.33 but the primary anti-human IgG antibody was replaced with an equivalent concentration of non-immune rabbit IgG. The tissue was subsequently reacted with protein A:gold. Background levels of gold particles are associated with the syncytiotrophoblast (Sy) and underlying cytotrophoblast cell (C) only. Scale bar represents 500nm.

6.31

6.32

6.33

6.34
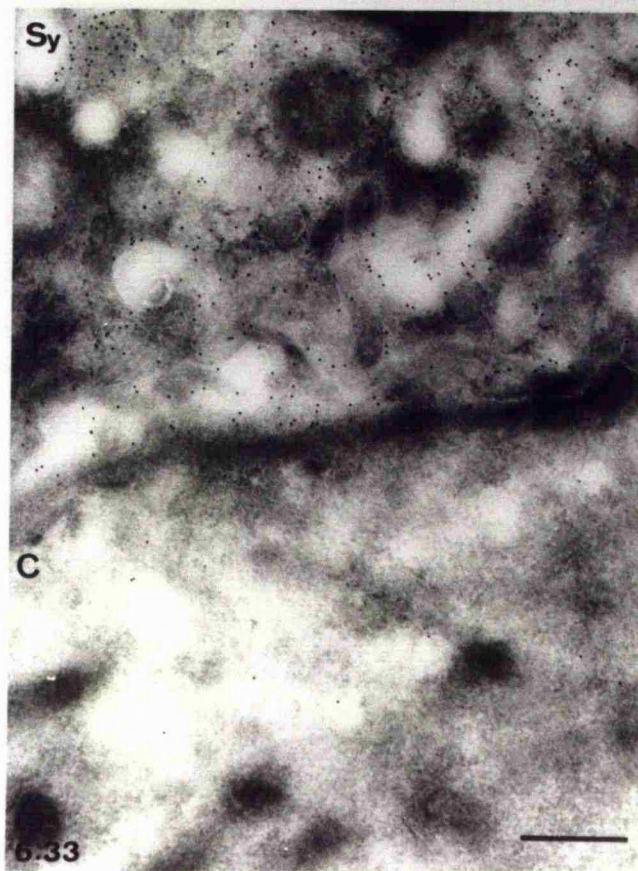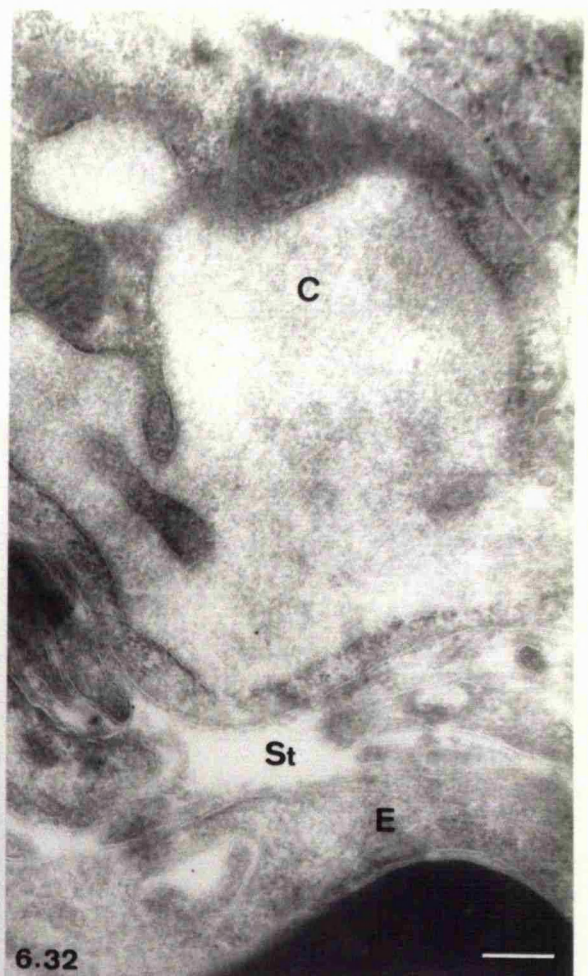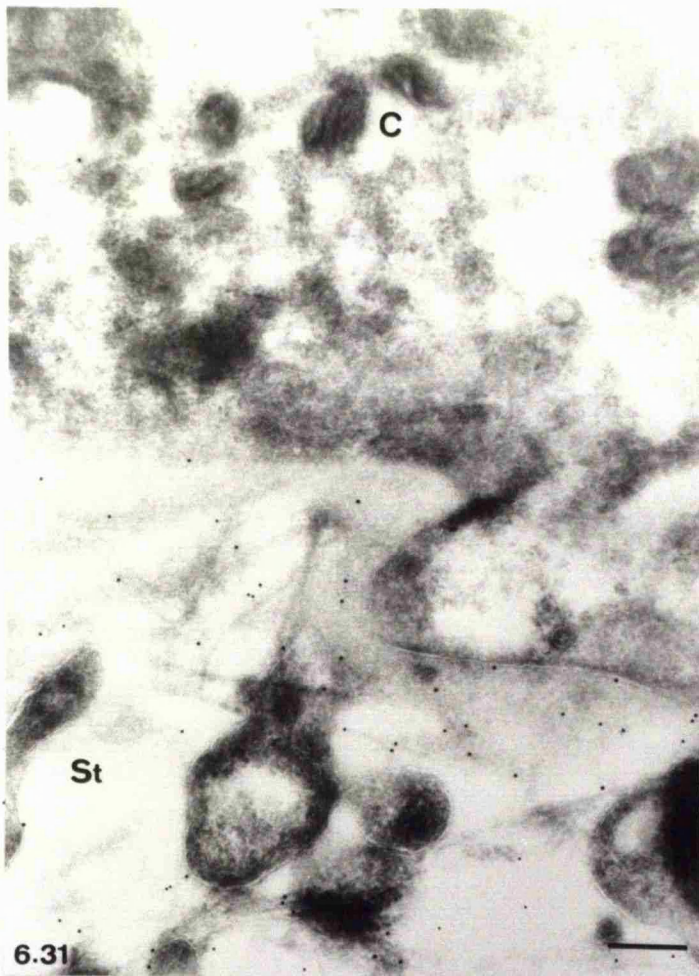
Figures 6.35-6.38: Endogenous IgG immunoreactivity in ultrathin frozen sections
of term chorionic villi.

Figure 6.35: Gold labelled endogenous IgG in an ultrathin frozen section of term
syncytiotrophoblast. Gold particles are associated with the apical plasma membrane
and microvilli (black arrowhead), coated pits (arrows) and an uncoated vacuole
(white arrowhead). Apical endosome-like inclusions (E) are also labelled with
numerous gold particles. Scale bar represents 300nm.

Figure 6.36: Gold labelled endogenous IgG in an ultrathin frozen section of term
syncytiotrophoblast. Gold labelling may be seen bound to the apical plasma
membrane and microvilli, a coated vesicle (arrow) and bound to the periphery of a
membrane bounded vesicle (arrowhead). Scale bar represents 200nm.

Figure 6.37: IgG immunoreactivity in an ultrathin frozen section of term trophoblast.
Gold labelling is evident in the syncytiotrophoblast (Sy) and in the connective tissue
stroma (St). However, the cytotrophoblast cell (C) interposed between these two
layers reveals very low levels of background labelling only as does the cell nucleus
(N). This observation is consistent with the data obtained in 1st trimester
trophoblast. Scale bar represents 400nm.

Figure 6.38: Gold labelled IgG in an ultrathin frozen section of term trophoblast.
Gold labelling is evident in the syncytiotrophoblast (Sy) but the cytotrophoblast cell
(C) reveals low levels of background labelling only as does the syncytiotrophoblast
nucleus (N). Numerous gold particles are evident in a medium electron density,
membrane bounded lysosomal-like structure (arrow). Scale bar represents 400nm.

6.35

6.36

6.37

6.38
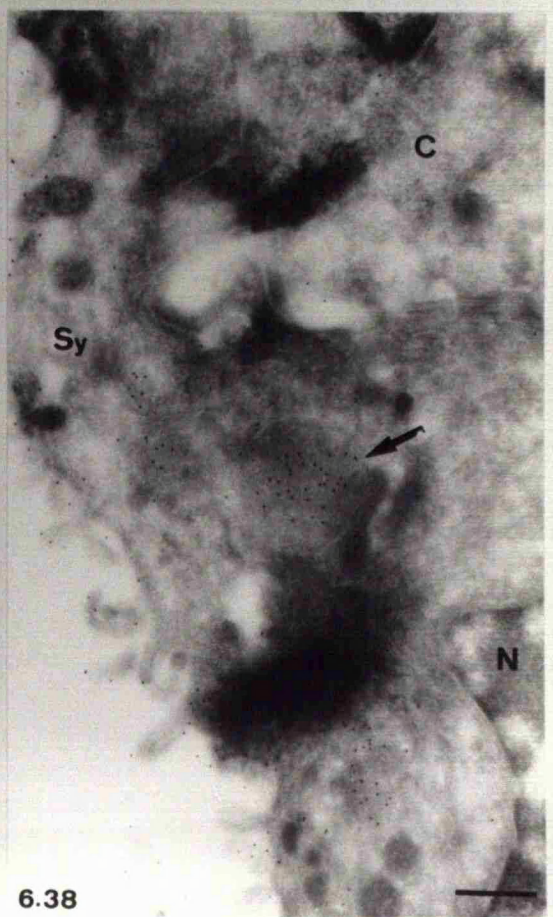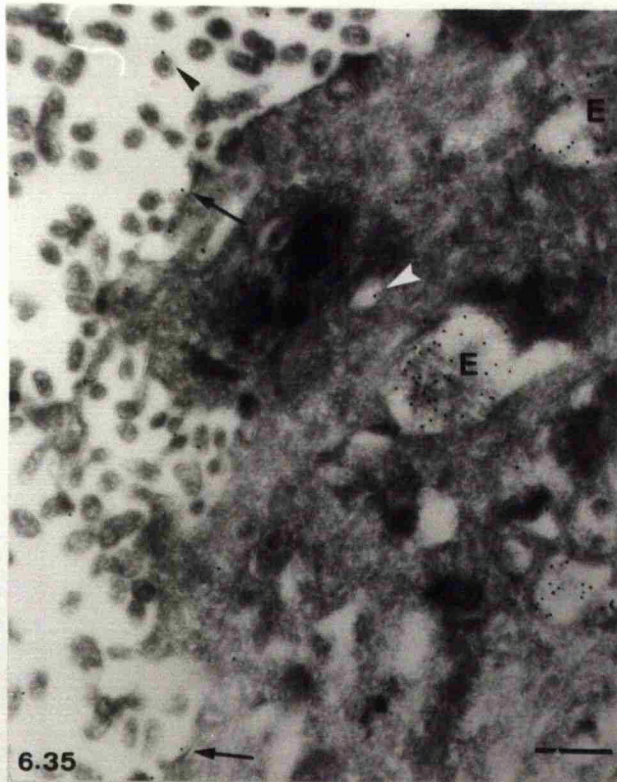
Figures 6.39-6.42: Endogenous IgG immunoreactivity in ultrathin frozen sections of term chorionic villi.

Figure 6.39: Gold labelled IgG in an ultrathin frozen section of a term chorionic villus. Extensive gold labelling is evident in the capillary lumen (L). Erythrocytes (E) and the endothelial cell nucleus (N) present in this field possess scarce background levels of labelling. Scale bar represents 1μm.

Figure 6.40: Ultrathin frozen section of a term chorionic villus. Extensive gold labelled IgG is apparent in the capillary lumen (L) and in the connective tissue stroma (St). The endothelial cell (En) present in this field possess immunogold labelling in association with membrane bound inclusions (arrowheads) but not with the intercellular cleft (arrows). Scale bar represents 300nm.

Figure 6.41: Ultrathin frozen section of a term chorionic villus. Gold labelled IgG is apparent in the capillary lumen (L) and stroma (St). The endothelial cell (En) possess labelling in association with membrane bound inclusions (arrowheads) from the luminal plasma membrane across to the abluminal membrane. The nucleus (N) and erythrocyte (E) illustrate low levels of background labelling. Scale bar represents 300nm.

Figure 6.42: Gold labelled IgG in an ultrathin frozen section of a term chorionic villus. Gold is present in the capillary lumen (L) and stroma (St). The endothelial cell (En) possesses labelling in association with membrane bounded medium electron density inclusions (arrows). Scale bar represents 400nm.
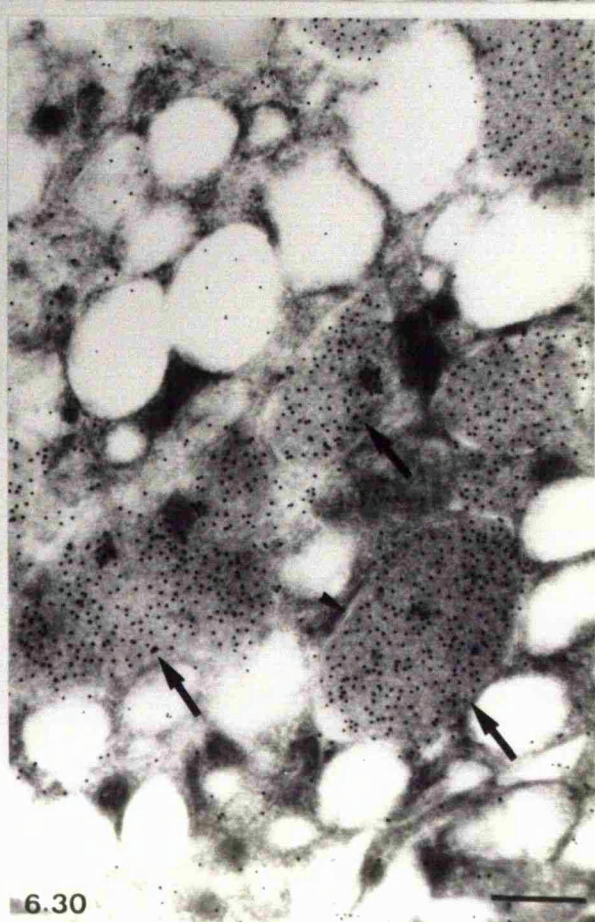
6.39

6.40

6.41

6.42
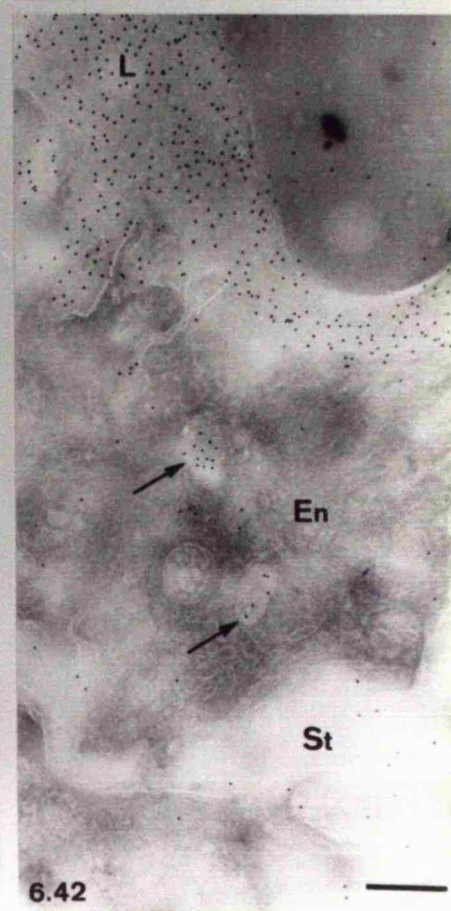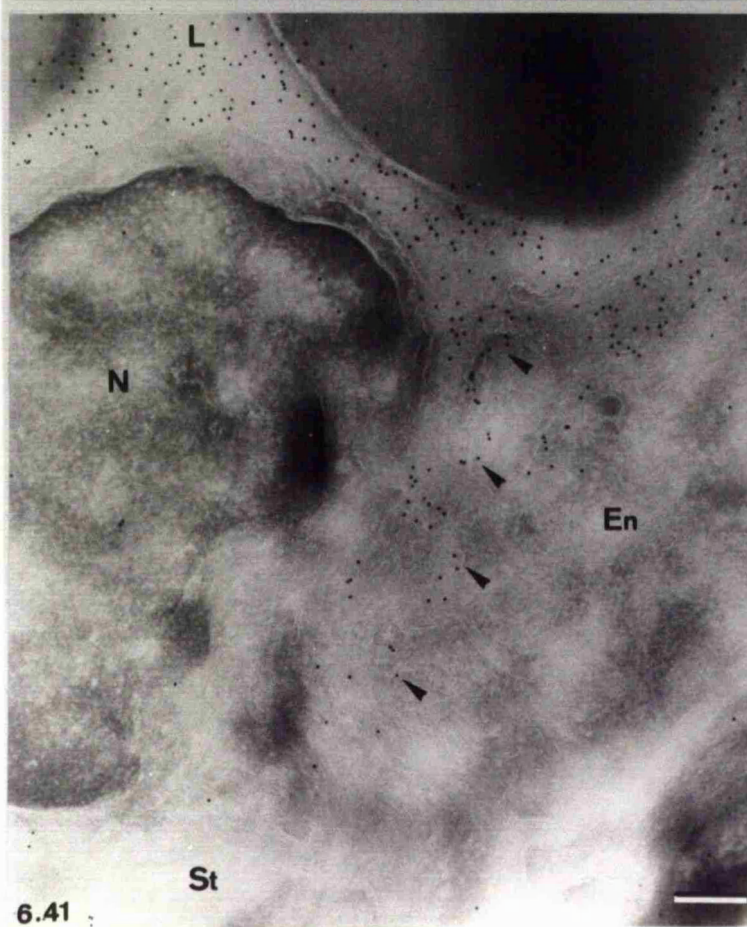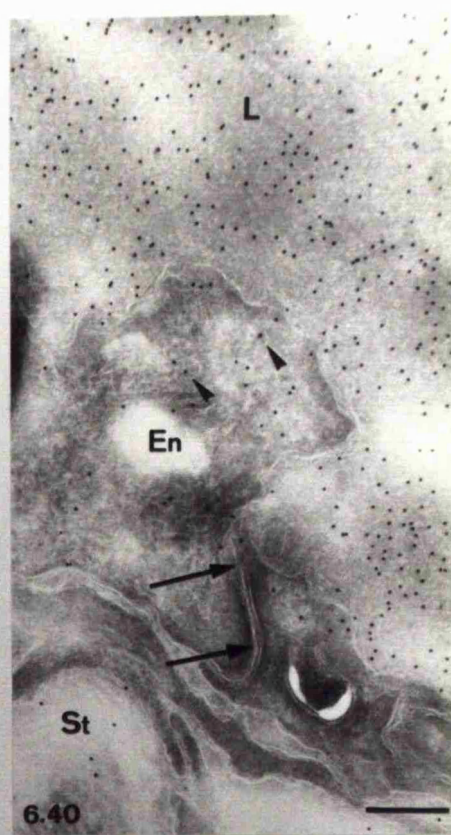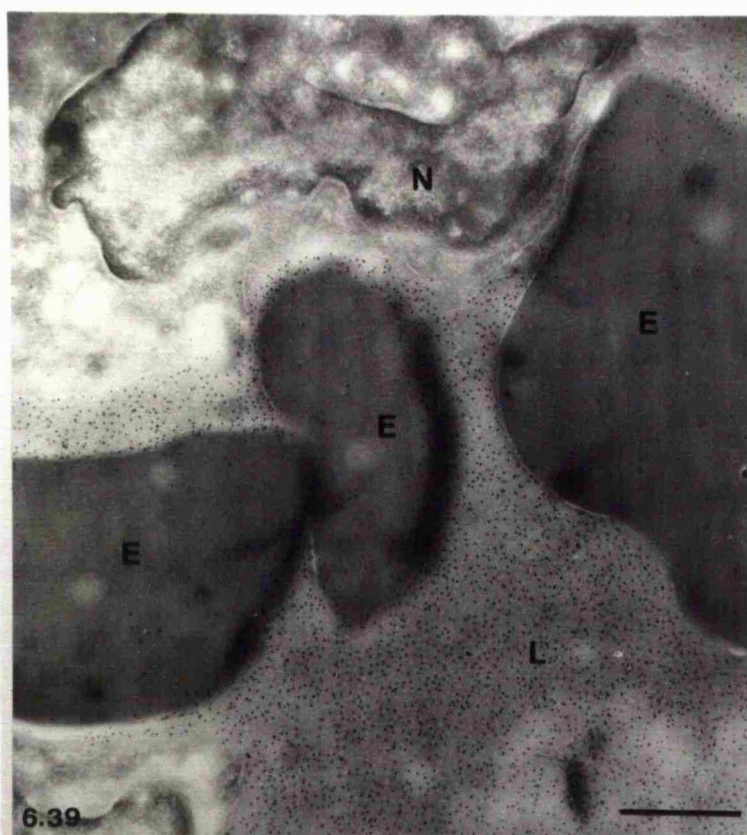
<u>**Figures 6.43-6.46: Endogenous IgG immunoreactivity in ultrathin frozen sections**</u>
<u>**of term amniochorion.**</u>

Figure 6.43: Gold labelled IgG in an ultrathin frozen section of term amniochorion. Gold is associated with the extracellular matrix of the compact layer (C) and may be observed where the connective tissue penetrates between amniotic epithelial cells. Amniotic epithelial cells (A) are unlabelled. Scale bar represents 300nm.

Figure 6.44: Endogenous IgG immunoreactivity in an ultrathin frozen section of term amniochorion. IgG is present in the compact layer (C) and penetrates between the amniotic epithelial foot processes. Gold labelling is frequently observed bound to the plasma membrane (arrows) which may indicate sites of interaction between maternal IgG molecules and (anti-) fetal antigens expressed at the cell surface. Amniotic epithelial cells (A) are unlabelled. Scale bar represents 300nm.

Figure 6.45: Endogenous IgG immunoreactivity between the foot processes of an amniotic epithelial cell in an ultrathin frozen section. The amniotic epithelial cell (A) illustrates background levels of labelling. Scale bar represents 300nm.

Figure 6.46: Background levels of labelling over the cytoplasm and nucleus (N) of an amniotic epithelial cell (A) in an ultrathin frozen section. Scale bar represents 400nm.

6.43

6.44

6.45

6.46
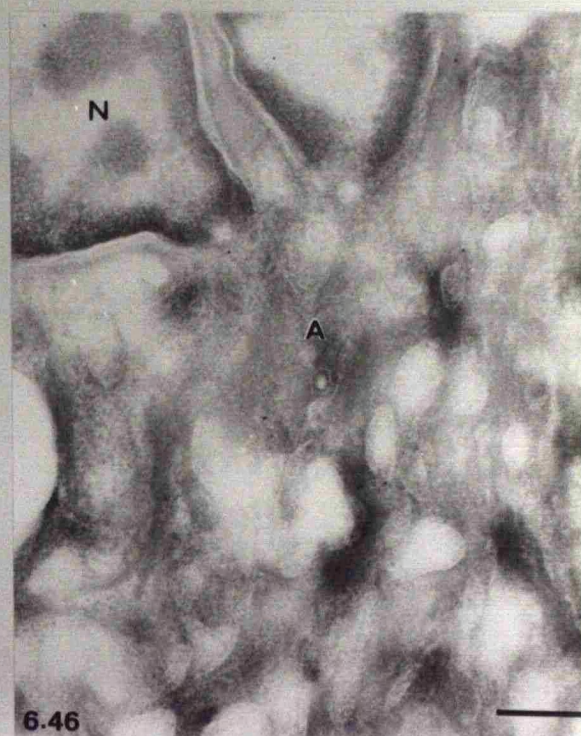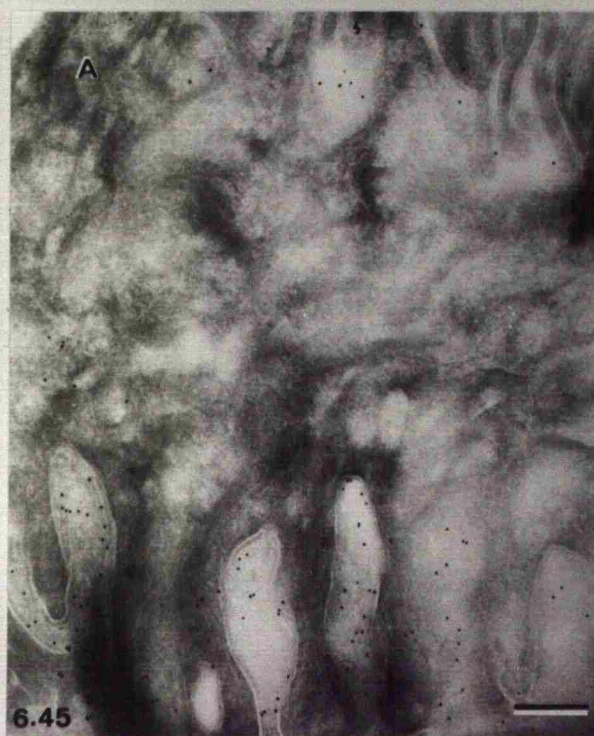
Figures 6.47-6.50: Endogenous IgG immunoreactivity in ultrathin frozen sections of term amniochorion.

Figure 6.47: IgG immunoreactivity in an ultrathin frozen section of term amnion. Gold is associated with the damaged/dead amniotic epithelial cell (D) but not with the healthy epithelial cell (A) or nucleus (N). Scale bar represents 400nm.

Figure 6.48: Gold labelled IgG in an ultrathin frozen section of term amniochorion. Gold is associated with the damaged/dead amniotic epithelial cell (D) but not with healthy epithelial cells (A). Labelling is apparent throughout the damaged cell all the way to the apical plasma membrane which would be in contact with the amniotic fluid in situ. Scale bar represents 400nm.

Figure 6.49: Immunogold labelling of endogenous IgG in an ultrathin frozen section of term amniochorion. Extensive gold labelling is associated with the connective tissue stroma (S) surrounding a cytotrophoblast cell (C). The cytotrophoblast cell cytoplasm and nucleus (N) illustrates a paucity of label. Scale bar represents 400nm.

Figure 6.50: Endogenous IgG immunoreactivity in an ultrathin frozen section of term amniochorion. Gold labelling is associated with the connective tissue stroma (S) and extracellular spaces (arrowheads) but not with the cytotrophoblast cell (C). Desmosomal attachments between adjacent cytotrophoblast cells are clearly evident. Scale bar represents 400nm.

6.47

6.48

6.49

6.50
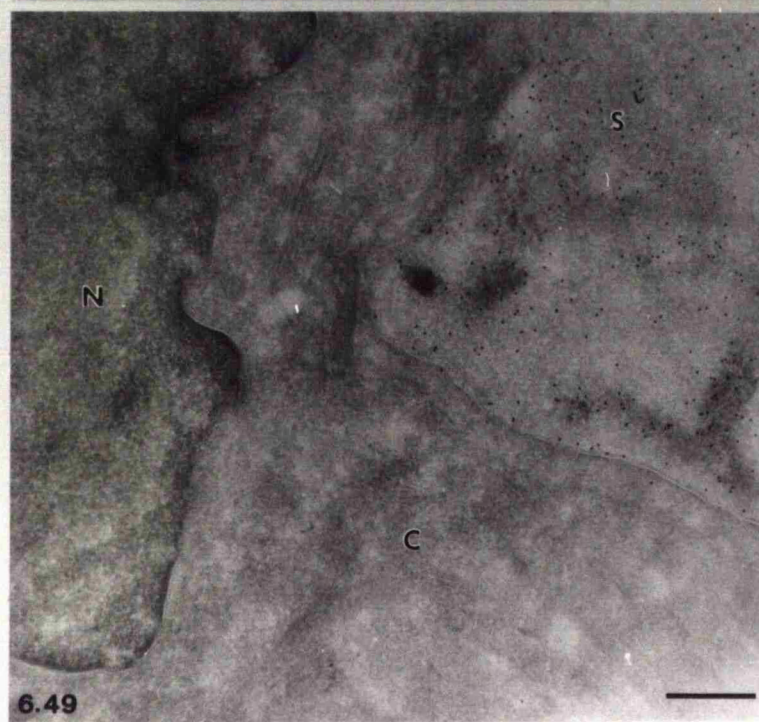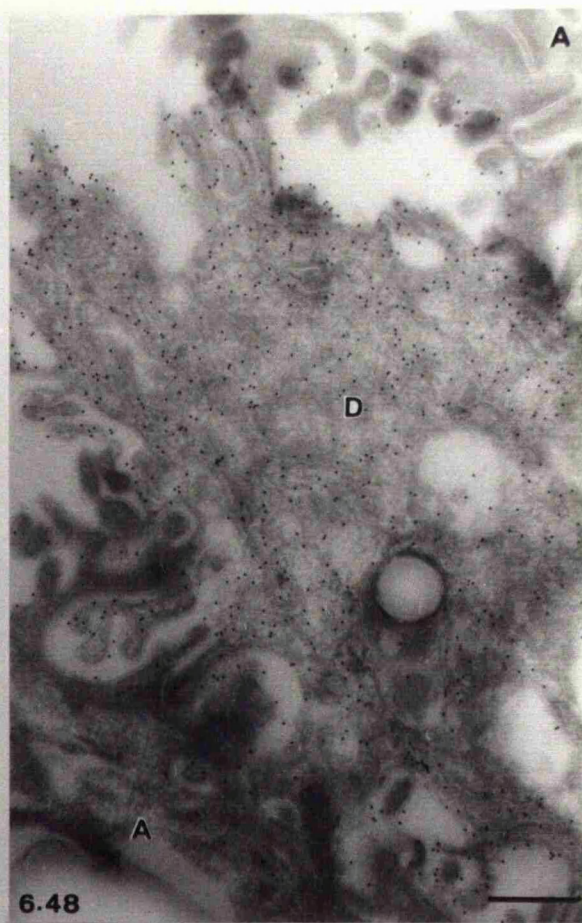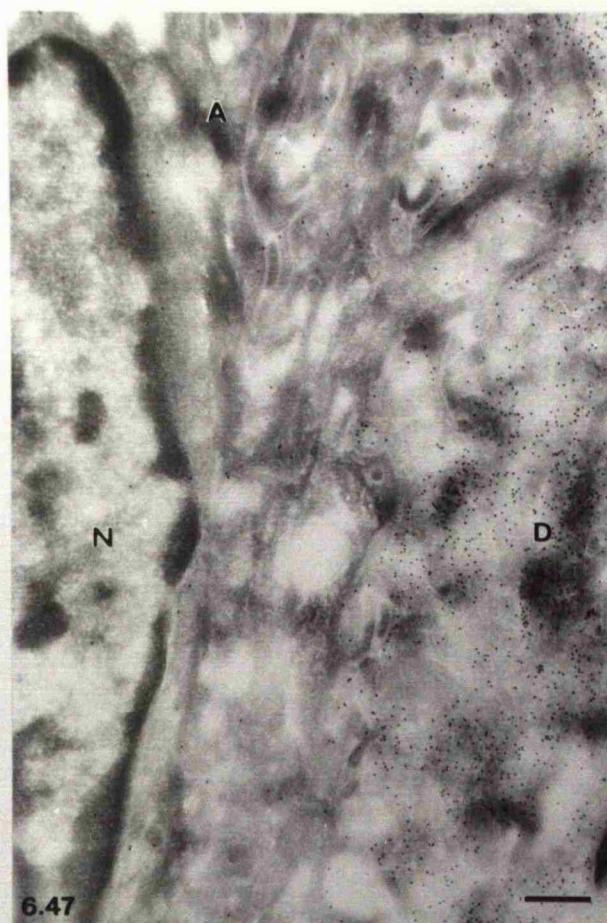
Figures 6.51-6.52: Quantitation of immunogold labelling in human placental chorionic villi.

Figure 6.51: Quantitation of immunogold labelling in 1st trimester chorionic villi. Error bars represent standard deviations.

Figure 6.52: Quantitation of immunogold labelling in term chorionic villi. Error bars represent standard deviations.

6.51: Quantitation of gold-labelling in 1st trimester chorionic villi.

Legend:
- Control
- Background
- Cytotrophoblast
- 1st trim syncytium
- 1st trim ECM

X-axis: Tissue component.
Y-axis: Mean gold particles per square micron.

6.52: Quantitation of gold-labelling in term chorionic villi.

Legend:
- Control
- Background
- Erythrocytes
- Cytotrophoblast
- Term syncytium
- Term ECM
- Term serum

X-axis: Tissue component.
Y-axis: Mean gold particles per square micron.
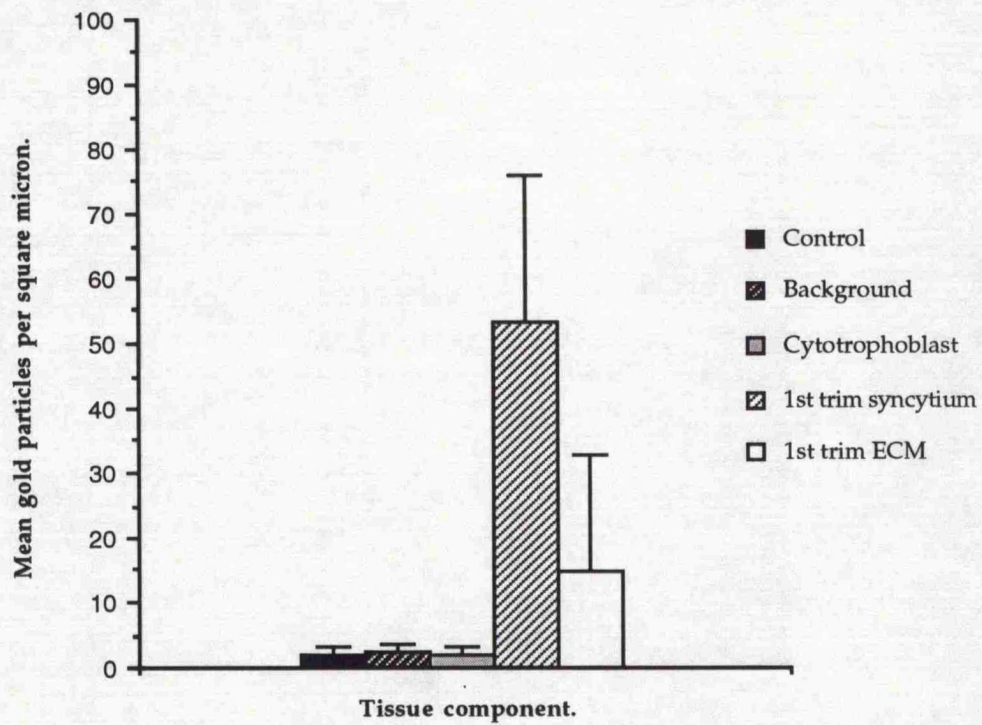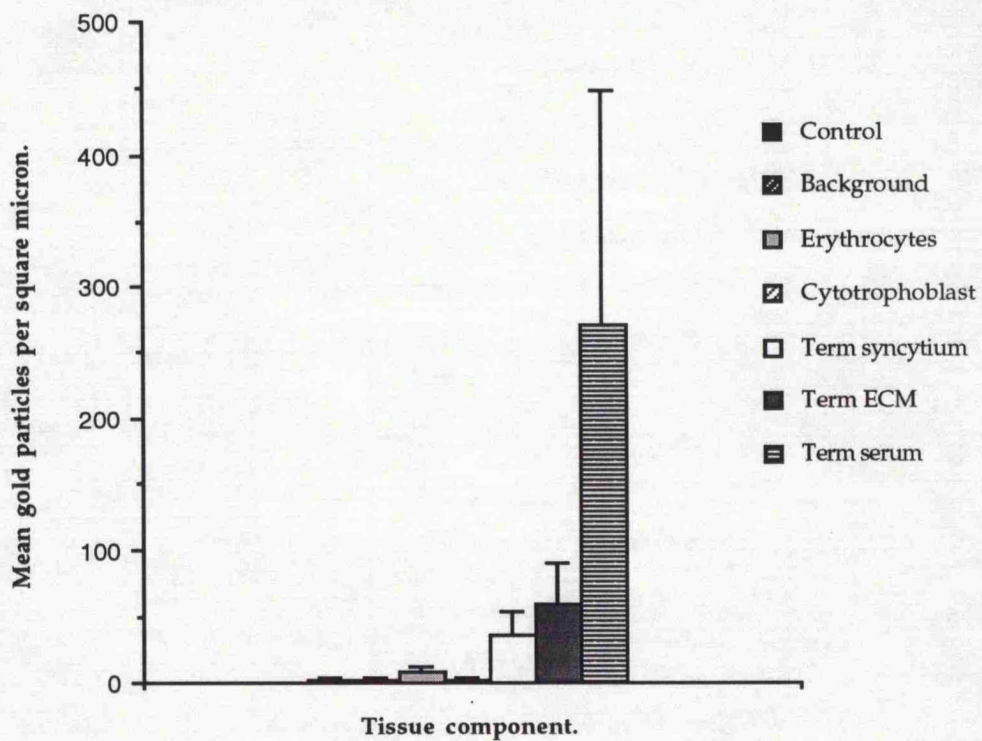
Figures 6.53-6.54: Quantitation of immunogold labelling in human amniochorion and chorionic villi.

Figure 6.53: Quantitation of immunogold labelling in term amniochorion. Error bars represent standard deviations.

Figure 6.54: Overlay graph of Figures 6.51-6.53 illustrating comparative levels of gold labelling throughout the placental tissues. Error bars represent standard deviations.

6.53: Quantitation of gold-labelling in term amniochorion.

Mean gold particles per square micron. (y-axis)

Tissue component. (x-axis)

Legend:
- ■ Control
- ▨ Background
- ▨ Cytotrophoblast
- ▨ Amnion cells
- □ Dead amnion cells
- ■ Amniochorion ECM
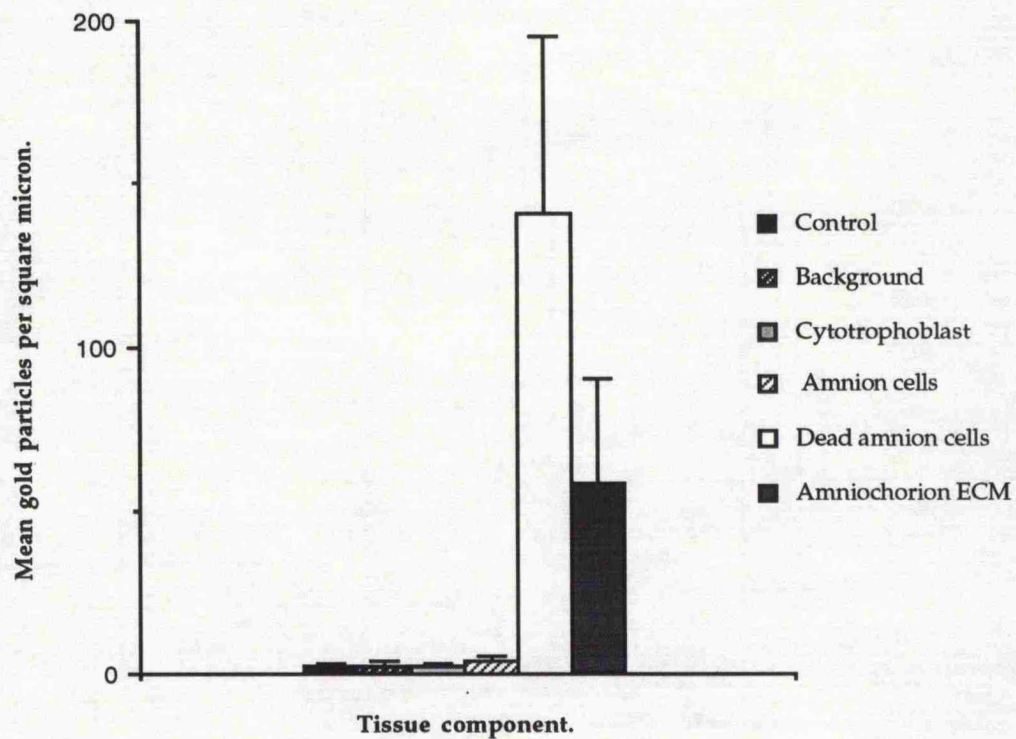
6.54: Quantitation of gold-labelling in placental tissues.

Mean gold particles per square micron. (y-axis)

Tissue component. (x-axis)

Legend:
1. ■ Control
2. ▨ Background
3. ▨ Erythrocytes
4. ▨ Cytotrophoblast
5. □ 1st trim syncytium
6. ■ 1st trim ECM
7. ▤ Term syncytium
8. ▨ Term ECM
9. ▨ Term serum
10. □ Amnion cells
11. ▨ Dead amnion cells
12. ▨ Amniochorion ECM
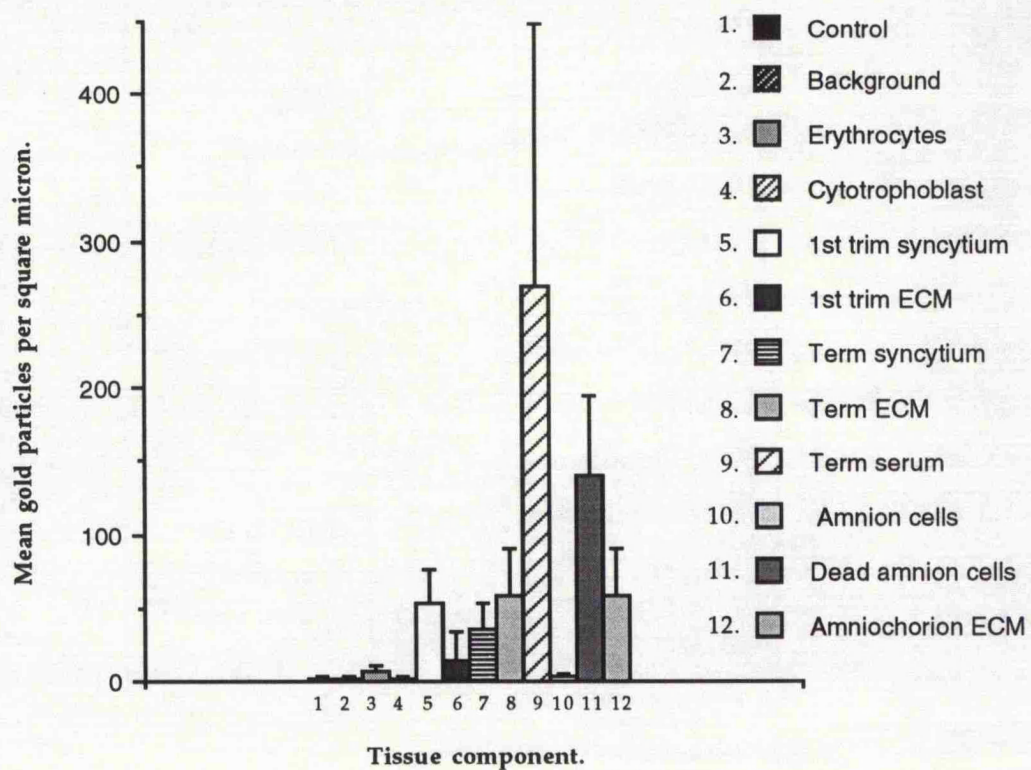
6.4 DISCUSSION.

The techniques described in this chapter have been used to i) characterise the nature of novel morphological structures in human term amniochorion and ii) localise the ultrastructural distribution of endogenous IgG in human chorionic villi and amniochorion, in an attempt to assess the ultrastructural route used to transport IgG across these tissues.

Microtrabeculae and anchoring rivets in term amniochorion.
Routine investigation into the ultrastructural morphology of the human term amniochorion using osmium fixed and resin embedded tissues has disclosed the presence of novel lamina densa-like segments distant from the sites of the epithelial basement membranes (Chapter 2; Malak et. al., 1993). In order to establish the suspected 'basement membrane-like' nature of these structures low denaturation, low-temperature resin embedded sections were used in conjunction with colloidal gold labelling to localise type IV collagen immunoreactivity.

The conventional view of type IV collagen is that it is a molecular form restricted in its distribution to basal laminae (Sage, 1982; Modesti et. al., 1989). Recent evidence, however, shows that smaller amounts of these molecules also exist in sites distant from basal laminae (Pratt and Madri, 1985; Nanaev et. al., 1991). The present study demonstrates that this protein is distributed classically in near continuous form in the basement membrane underlying the amniotic epithelium and the chorion laeve basement membrane. Type IV collagen also extends between the cytotrophoblast cells of the amniochorion. The third type of collagen IV containing component of the tissue, the spongy layer, is thought to be a remnant of the extraembryonic coelom which becomes trapped between the chorion and the expanding amnion. The type IV collagen-containing structures we call microtrabeculae are described here for the first time (Ockleford et. al., 1993b).

These studies also provide an internal 'positive control' for the methodology since an antigen of known distribution maintains its immunoreactivity when processed for electron microscopy using the techniques described. However, one must be careful not to assume that other antigens will be conserved in the same way. The clustering of the gold particles observed in the three-step immunocytochemical procedures is interesting. It is clearly not the well known artefact of this technique called flocculation since in this situation the gold would no longer be particulate. Overall the labelling in the resin embedded tissue appears relatively sparse. This may reflect the fact that only antigen exposed at the sectioned surface of the ultrathin section is accessible to the first stage antibody and this label is visualised against the

summated image of the full depth of the tissue section. Gold clusters are likely to result from amplification of the primary antibodies bound to these exposed epitopes by multiple secondary antibodies which are individually recognised by the gold-conjugated probes. In the protein A-gold technique polyclonal antibodies recognise a diversity of epitopes which are subsequently detected by the protein A-gold conjugate. Each polyclonal rabbit antibody possesses a single binding site for protein A only and thus the phenomenon of gold clustering is not observed. Thus each gold particle observed using this technique corresponds to a single exposed type IV collagen epitope.

Type VII collagen immunoreactivity was investigated in human term amniochorion to identify the sites of the novel anchoring rivets observed with routinely embedded osmium-fixed preparations (chapter 2; Ockleford et. al., 1994). Type VII collagen is usually restricted in its distribution to the basal laminae of stratified epithelium. The amniotic epithelium basement membrane in the human placenta is unique with respect to its type VII collagen immunoreactivity. However, antigenicity is destroyed in preparations fixed with aldehyde. Therefore, to conserve type VII collagen immunoreactivity tissue specimens were fixed with picric acid. This procedure conserved immunoreactivity with the monoclonal antibody used in this investigation but the ultrastructural morphology of the amniochorion was not well preserved. However, it was possible to identify gold labelling in association with the lamina densa in apposition to the hemidesmosomes of the amniotic epithelium. It was also possible to demonstrate immunoreactivity with this antibody at sites distant from the basement membrane which correlates with the fluorescence microscopy and morphology (Ockleford et. al., 1994).

Immunoglobulin G.
Attempts to label endogenous IgG with a direct application of protein A: gold or protein G: gold were unsuccessful. This may indicate that the Fc portion of the IgG molecule is unavailable for interaction in the section. This may be a consequence of fixation, steric hindrance caused by the embedding media or the presence of a bound molecule, for example an Fcγ receptor, preventing interaction with the Fc domain.

Current models of receptor-mediated endocytosis propose that ligands bind to receptors which may be either randomly distributed on the cell surface or localised in clathrin-coated pits (Wileman et. al., 1985; Goldenthal et. al., 1988). Soon after clustering in coated pits, receptor-ligand complexes appear in coated vesicles. These vesicles lose their clathrin coats to form endosomes which move to the interior of the cell. Subsequent fusion of the endosomes with other vesicles results in multivesicular bodies which have an acidic pH (Hopkins, 1983). Dissociation of

ligands from receptors occurs either in these vesicles or in the endosomes once they come into contact with elements of the trans Golgi system (Goldenthal et. al., 1988) or the compartment of uncoupling of receptors and ligands (CURL) system (Geuze et. al., 1983). Receptors may then be directed to the lysosomes or recycled back to the cell surface, whilst ligands can either be degraded or transcytosed.

Immunolabelling of IgG was demonstrated at the syncytiotrophoblast apical surface and was associated with microvilli as well as in pits, many of which possessed a coat. This suggests that receptors to which IgG bind are dispersed over the entire microvillous membrane and are not merely confined to coated pits. The demonstration of IgG immunoreactivity in coated pits and vesicles at the apical side of the syncytium and in apical endosomal compartments correlates with observations in the fluorescence microscope where a punctate apical pattern of immunoreactivity was revealed. These findings also concur with those of King (1982a) and Griffiths et. al. (1985) but not with those of Lin (1980) who observed IgG-like immunoreactivity in lysosomes and multivesicular bodies fusing with the basal membrane of the syncytiotrophoblast. The apical endosomal compartments demonstrated in this study using ultrathin frozen sections possessed a high degree of peripheral membrane-associated gold labelling suggesting that IgG was still bound to its receptor. Therefore these organelles are likely candidates for receptor sorting and/or release of the ligand. Vesicles were frequently observed fusing with these organelles. However, it is not clear if IgG which is transcytosed by-passes these organelles or is sorted from them. Labelling was observed in remote vesicles in the basal aspect of the syncytiotrophoblast suggesting that only small amounts are transported and released at the fetal side.

The interstitial space between the trophoblast and the fetal endothelium was found to contain endogenous IgG. Similarly invaginations of the abluminal (basal) plasma membrane of endothelial cells appeared to be immunoreactive in agreement with the observations of King (1982a) but not with those of Lin (1980) who found evidence for a paracellular route across the endothelium. Gold was demonstrated in coated pits and coated vesicles within the endothelium and in caveolae, but not in intercellular clefts. The pattern of localisation within the fetal endothelium indicates vesicular routing of IgG across the cells rather than a paracellular route. It is not clear if the endothelial vesicles reflect individual vesicles acting as 'shuttles' or if they subsequently fuse with other vesicular structures. In addition the fetal capillary serum proteins were intensely gold labelled as one may expect. However, it is not certain whether the high degree of gold labelling at the luminal plasma membrane of endothelial cells was a reflection of the true in vivo situation or a consequence of IgG being fixed to the endothelial cell surface in the preparations used in this study.

In first trimester chorionic villi trophoblast-associated immunogold labelling was restricted in its distribution to the syncytiotrophoblast surrounding the villi. Cytotrophoblast cells underlying the syncytium were not gold labelled. These results correlate with the immunofluorescence preparations which indicate that cytotrophoblast cells do not possess endogenous immunoglobulin. Labelling of the underlying connective tissue core of first trimester villi was not consistent. This indicates that there may be local circumstances in which IgG is able to gain access to the villus stroma, particularly in regions where the overlying syncytiotrophoblast is in direct contact with the basal lamina. Other regions of the stroma were unlabelled.

In the syncytiotrophoblast gold labelling was associated with the apical plasma membrane, coated pits and vesicles, uncoated vesicles and apical endosomal compartments. It is not clear if gold targeted for transcytosis is protected from fusing with these endosomal compartments. A high density of gold labelling was also observed in lysosomal compartments which indicates that a large proportion of IgG taken up by the syncytiotrophoblast is targeted for lysosomal destruction. This would evidently be a rich source of amino acids for the proliferating trophoblast. IgG immunoreactivity was prominent in the basal regions of the syncytiotrophoblast, in contrast to the situation at term. This may indicate that transport is blocked and that IgG is 'backing up' rather than being efficiently released at the basal plasma membrane. However, where the syncytiotrophoblast penetrated between the cytotrophoblast cells gold labelled IgG could be identified in vesicular structures extending to the basal plasma membrane. Gold was also associated with the basal plasmalemma and, intriguingly in these circumstances, in the connective tissue stroma underlying regions of contact. These observations suggest that IgG is released from the syncytiotrophoblast at these regions of contact with the basement membrane.

In term amniochorion the findings of the ultrastructural investigations parallel those of the fluorescence microscopy immunocytochemical experiments. IgG was concentrated in the extracellular matrix of this tissue and was also associated with fibroblast cells of the fetal mesenchymal layers and leucocytes present in the maternal decidua. However, the ultrastructural morphology of the mesenchymal cells was poorly conserved using these fixation conditions and thus a precise ultrastructural assignment in these cells was not possible. Cytotrophoblast cells of the chorion laeve were not labelled using these techniques suggesting that they exclude immunoglobulin. These findings are consistent with the absence of labelling observed in first trimester and term chorionic villi. The extracellular matrix surrounding these cells, however, was labelled with gold suggesting that IgG is not prevented from diffusing across the chorion laeve. Similarly amniotic epithelial cells

were not labelled, with the exclusion of dead or damaged cells. This suggests that healthy amniotic epithelial cells exclude IgG and are thus not responsible for the presence of antibody in the amniotic fluid. A high degree of gold labelling was associated with dead cells, however, suggesting that IgG may freely diffuse between the amniotic fluid and fetal connective tissues via these cells. The high concentration of IgG in these cells may also be attributable to maternal antibodies binding to anti-fetal intracellular antigens which would not be exposed by a healthy, intact cell. IgG-specific gold labelling was observed at the apical cell surface of amniotic epithelial cells which may indicate that immunoglobulins present within the amniotic fluid have become adsorbed to the surface of the cells during processing of the tissue for electron microscopy. Conversely this may again be indicative of maternal antibodies recognising (anti) fetal antigens expressed at the cell surface.

The high intensity of gold-labelling observed in the present study appears to be a direct consequence of the low-denaturation, low temperature embedding methodology used and, in particular, the cryoultramicrotomy used to prepare ultrathin frozen tissue sections. Major advantages of this latter technique for studying the human placenta include good accessibility of antigens in the tissue section, the omission of harsh dehydrating agents and excellent delineation of structural details. The use of a particulate probe such as colloidal gold allows accurate localisation of binding sites with high resolution. In conclusion, the ultrastructural data presented in this chapter indicates that IgG is transcytosed across placental syncytiotrophoblast via receptor-mediated endocytosis and transport vesicles. It is subsequently released into the fetal stroma at the basal plasma membrane. These investigations confirm the light microscopical observations that IgG is excluded from cytotrophoblast cells and thus support the hypothesis that these cells may act as a barrier to transmission of passive immunity, thus causing IgG to accumulate in the syncytiotrophoblast. The results from this study also correlate with the findings using fluorescence microscopy that IgG is present in the extracellular spaces between cytotrophoblast cells in human term amniochorion and thus this is conceivably a route which is available for diffusion of IgG molecules into the fetal compartments.

Quantitation of gold labelling.
Quantitation of gold particles associated with tissue components in the human placenta confirmed qualitative observations of the heterogeneity of labelling.

Cytotrophoblast cells demonstrated a paucity of labelling which was not statistically significant from background levels or control preparations. This is in accordance with observations using the fluorescence microscope and supports the

hypothesis that these cells exclude IgG. The syncytiotrophoblast of 1st trimester chorionic villi is densely labelled and, although not statistically different from labelling associated with the syncytiotrophoblast of term chorionic villi, the higher degree of labelling may reflect that IgG accumulates as a consequence of cytotrophoblast cells inhibiting transcytosis to the underlying stroma at this stage of gestation. The heterogeneity of gold labelling associated with the 1st trimester villus stroma parallels immunofluorescence observations and illustrates regions devoid of endogenous antibody and areas underlying the syncytium which possess a high degree of labelling. However, gold labelling in the villus stroma at term is significantly higher than in the first trimester.

The density of gold labelling associated with the serum proteins of blood capillaries at term reflects the high concentration of circulating antibody. The quantity of gold particles associated with the extracellular matrix of term chorionic villi is not significantly different from the amniochorion extracellular matrix. This is an interesting observation and supports the hypothesis that IgG may be able to freely diffuse through the mesenchyme between the placenta and the amniochorion.

Amniotic epithelial cells exhibit a paucity of labelling corresponding to background levels only, thus supporting the hypothesis that these cells prevent the exchange of IgG between the amniotic fluid and fetal mesenchyme. However, damaged cells possess significantly higher labelling than their healthy counterparts and the extracellular matrix of the amniochorion. Therefore simple diffusion through these damaged cells does not account for the statistical significance. This is likely to be caused by maternal antibodies binding to intracellular fetal antigens not normally exposed by the intact cell.

Fcγ Receptors
Experiments performed to identify the ultrastructural localisation of the Fcγ receptors did not yield successful results. Specific gold-labelling was not observed beyond background levels. The likely reason for the inability to detect these receptors may be their sensitivity to the fixatives used in this study or low levels of expression of these molecules. Griffiths (1993) asserts that the labelling efficiency of the colloidal gold-labelling technique is likely to be as low as 15% and thus it is difficult to ascertain specific labelling beyond background levels where the concentration of antigen is low. In future attempts to localise these receptors at the ultrastructural level their individual sensitivities to aldehyde fixatives need to be thoroughly screened using immunofluorescence. Furthermore, the use of immunological reagents and gold conjugated probes which do not cross-react with Fcγ receptors and endogenous IgG, such as F(ab')$_2$ fragments and ExtrAvidin, are to be recommended.

CHAPTER 7: General Discussion.

GENERAL DISCUSSION.

This study has investigated the distribution of endogenous IgG and Fcγ receptors in the human placenta and fetal membranes. This was performed using the technique of immunocytochemistry at both the light (fluorescence and confocal) microscope level and the ultrastructural level. These techniques have provided valuable insights as to how the human fetus acquires maternally derived passive immunity. By using tissue acquired from therapeutic terminations of pregnancy and term deliveries (both Cesarean and routine vaginal deliveries) it has been possible to assess the developmental changes that occur during immunoglobulin transmission. The novel use of the amniochorion from term deliveries in these experiments has contributed to our understanding of its role in the immunological protection of the fetus.

Immunocytochemistry and electron microscopy of the human placental tissues have demonstrated that the protein clathrin, the major constituent of coated pits and vesicles, is a ubiquitous protein in the human placenta. Immunofluorescence microscopy has not previously been utilized to localise this protein in the placenta. The results obtained in this study suggest that all cell types possess coated pits and coated vesicles which may therefore contribute to receptor-mediated uptake of ligands.

The results of the immunofluorescence investigations to localise the three characterised subtypes of human Fcγ receptor are consistent with the results of immunocytochemical experiments of other groups published during the course of this study (Kristoffersen et. al., 1990; Kameda et. al., 1991). However, the increased sensitivity of detection achieved with the immunofluorescence and confocal microscopy techniques employed in the current study demonstrated several features not previously reported for human chorionic villi. FcγRI, the high affinity immunoglobulin receptor, was consistently present on connective tissue core mesenchymal cells as well as Hofbauer cells, indicating that they may possess a hitherto unsuspected immunoregulatory role. Immunoreactivity to FcγRII, a low affinity receptor for monomeric IgG, was demonstrated on capillary endothelial cells of both first trimester and term chorionic villi extending the observations of Kristoffersen et. al. (1990) and Kameda et. al. (1991) who demonstrated immunoreactivity in term endothelium only. Furthermore the increased sensitivity of the techniques used in the current study revealed the presence of a punctate pattern of immunoreactivity in endothelial cells which indicates that the receptor and its ligand may be incorporated into subcellular vesicular structures.

Both of these previous two groups have demonstrated immunoreactivity to FcγRIII in the trophoblast surrounding chorionic villi. The current study has demonstrated several additional novel features. This receptor is associated with the margins of large vesicular inclusions in first trimester trophoblast and is often concentrated at a pole of these organelles suggesting that other vesicles rich with Fcγ receptors may fuse to the larger structures or it may reflect sorting of the receptors in these organelles. It is clear that the receptor remains bound to the periphery in its immunoreactive form in these organelles. Furthermore immunoreactivity extends to the basal plasmalemma in the syncytiotrophoblast suggesting that this receptor may have a potential role in transcytosis of its ligand. In addition, the techniques used in this study were sufficient to resolve the fact that cytotrophoblast cells do not possess this receptor extending the findings of the previous two groups. In term chorionic villi this receptor is predominantly associated with the apical syncytiotrophoblast. It is not clear, therefore, if this receptor directs most of its ligand into an apically-associated catabolic pathway. It is conceivable that low levels of FcγRIII-bound ligand may escape lysosomal degradation and become transcytosed to the basal plasmalemma.

The distribution of Fcγ receptors in the amniochorion has not previously been investigated. This study has demonstrated that FcγRI, FcγRII and FcγRIII are expressed by cells of the maternal decidual layer associated with the amniochorion. These cells are likely to represent immunocompetent maternal leucocytes. Furthermore, cells of the fetal mesenchyme have been demonstrated to express these receptor subtypes. Quantitation of receptor-positive cells indicated that FcγRII was predominantly expressed and that a smaller population of cells expressed FcγRI and FcγRIII. Immunoreactivity with the latter two receptors was only detected by employing more sensitive three-step immunocytochemical techniques suggesting that these cells possess only a low level of expression. These results indicate that fetal cells, of mesenchymal origin, may possess an as yet unsuspected role in the immunological protection of the fetus. It is not clear if the existence of receptor-positive and receptor-negative cells in these layers is indicative of cells in different developmental stages or if these cells are of a different type. The latter is a possibility since the results are consistent with our previous observations that the cells of these layers possess anti-vimentin immunoreactivity only or co-express desmin and vimentin indicating that there may be two cell types (Ockleford et. al., 1993c).

It is particularly intriguing that amniotic epithelial cells and cytotrophoblast cells of the chorion laeve, a cellular layer which is in lateral continuity with the trophoblast of the placental chorionic villi, do not express any of the characterised Fcγ receptor subtypes investigated here. It is possible that these cells express a

distinct Fcγ receptor which has not, as yet, been characterised and which may interact with IgG. However, the observation that these cell types do not contain any endogenous immunoglobulin G suggests that this is not, in fact, the case. These results are consistent with the inability to detect a receptor or its ligand in cytotrophoblast cells present in chorionic villi of various gestational age.

Wood et. al. (1982) were the first to detect IgG in the human trophoblast at the light microscope level. The present study has investigated the distribution of IgG throughout the placental tissues. It has been possible to demonstrate endogenous IgG predominantly in the apical aspect of the syncytiotrophoblast in term villi. The confocal microscopy techniques used were capable of resolving punctate sub-apical compartments suggestive of endosomal or lysosomal inclusions. Low levels of immunoreactivity were associated with the basal trophoblast which suggests that only a small percentage of the IgG taken up at the apical cell surface escapes lysosomal degradation to become transcytosed. However, it may reflect rate-limited transport dynamics at the apical cell surface resulting in an accumulation of IgG and subsequent rapid transport to the basal plasmalemma.

IgG is concentrated in the mesenchymal core of term chorionic villi suggesting that it is efficiently transported to the fetal compartments. Immunoreactivity may be demonstrated in association with mesenchymal cells, Hofbauer cells, and endothelial cells of the core. Intense immunoreactivity was associated with the serum proteins of fetal capillaries suggesting that there are high concentrations of circulating antibodies contributing to the immunological protection of the fetus. In first trimester placentae IgG immunoreactivity is almost completely confined to the syncytiotrophoblast surrounding chorionic villi. The striking observation in these investigations is that cytotrophoblast cells underlying the syncytium do not contain endogenous antibody. Indeed, on occasions where the syncytiotrophoblast may be observed to penetrate between cytotrophoblast cells and contact the basal lamina only the syncytium is immunoreactive with anti-IgG antibodies. It is fascinating in these instances that low levels of IgG immunoreactivity may also be detected in the villus stroma underlying the trophoblast. These observations suggest that the syncytiotrophoblast is responsible for transmission of IgG from maternal blood to the fetal connective tissue stroma and that cytotrophoblast cells may represent a barrier layer to this transport (Bright and Ockleford, 1994b). Thus, as the continuity of this layer degenerates with increasing gestational age there may be potential for increased IgG transport accounting for the paradox that IgG transmission is not rate-limited by a lack of Fc receptors in the early stages of gestation (Morphis and Gitlin, 1970) and the increase in antibody transport observed around 22 weeks of gestation (Gitlin and Biasucci, 1969). It is tempting to speculate that an FcγRIII isoform,

recognised by the monoclonal antibody used in the present study, is responsible for the observed transmission of IgG since the receptor and its ligand co-localise in the syncytiotrophoblast. However, it is not possible to resolve the ultrastructural compartments in which these molecules are localised using the light microscopical techniques used in this study.

The distribution of endogenous immunoglobulin G in human term amniochorion has not previously been demonstrated. This study has revealed that IgG is present throughout the extracellular matrix of the tissue. In addition, IgG is associated with the FcγR-bearing cells of the maternal decidua and fetal mesenchymal layers as demonstrated by dual-labelling immunocytochemical experiments. This observation offers further evidence that undifferentiated fetal mesenchymal cells or fibroblast cells possess an immunoregulatory role. The most intriguing aspect of this study comes from negative results. Amniotic epithelial cells and cytotrophoblast cells do not contain any detectable endogenous antibodies. This suggests that the amniotic fluid, which has been demonstrated to contain maternal IgG class antibodies, does not acquire these antibodies via a paraplacental transamniochorion route. The implications of this study are that the amniotic epithelial cells represent a barrier to IgG gaining access to the amniotic fluid. However, the concession must be made that if the amniotic epithelium loses its integrity for any reason, for example by fetal scratching, then soluble antibody may be capable of diffusing through dead or damaged cells from the associated fetal mesenchyme and thus contribute to the contents of the amniotic fluid. It is particularly interesting that damaged cells display such intense immunolabelling. This may be a consequence of maternal antibodies binding to allogeneic epitopes expressed by fetal intracellular antigens that would not normally be exposed by the intact cell.

However, it appears that IgG may be able to diffuse, non-specifically, from the maternal decidua to the fetal connective tissues or vice versa. This study has revealed the presence of IgG immunoreactivity between the cytotrophoblast cells of the amniochorion. This indicates that IgG may gain access to the fetal connective tissues via a non-specific paracellular route. It is not clear at present what quantity of IgG molecules, if any, gain access to the fetal extracellular tissues via this route. It is clear, however, that if this is the case IgG which gains access through the chorion may conceivably undergo lateral diffusion and encounter the mesenchyme of the placenta itself, thus contributing to the passive immunity of the fetus. This hypothesis implies, therefore, that Fcγ receptors expressed by placental endothelial cells would be responsible for discriminating between immunoglobulin classes and IgG subclasses. Furthermore, this hypothesis would account for the observations of

Kulangara et. al. (1965) who demonstrated that labelled BSA could be detected in the fetal blood stream after having been deposited over the extraplacental chorion in the uterine lumen. Therefore, this hypothetical route for the acquisition of some maternal antibodies may also help to account for the increased rate of transmission observed in the last trimester of pregnancy. As cytotrophoblast cells present in the chorion laeve become attenuated with advanced gestational age, so the continuous barrier of cells becomes removed allowing IgG access to the fetal placental connective tissues.

It is clear from the findings presented in this study that we must not fail to consider the placenta as a whole when addressing the issue of transport of immunoglobulins. The fetal membranes are now strongly implicated in possessing an important role in this context and in the immunological protection of the fetus. Many studies concentrate on the trophoblast surrounding chorionic villi when investigating the transmission of IgG. Whilst the trophoblast is undoubtedly of foremost importance it is important to recognise that transport does not end here. Immunoglobulins are likely to encounter Fcγ receptors expressed by mesenchymal cells, Hofbauer cells and endothelial cells of the connective tissue core in addition to fetal antigens. Models which contemplate transmission of IgG across the trophoblast only are too simplistic and it is now evident that we must discriminate between cytotrophoblast and syncytiotrophoblast since it appears that cytotrophoblast cells may not now be considered to participate in the transport of antibodies.

Future study.
There are many questions which remain to be answered concerning the phenomenon of passive immunity. The present study has demonstrated the presence of the three characterised Fc receptor subtypes in the placental tissues. However, it has not been possible to assert unequivocally that these are the receptors that are responsible for the observed transmission of antibody or if they possess other immunoregulatory roles. Furthermore, it is not clear if the receptors identified in this study are identical to the native molecules expressed by human leucocytes or if they represent a new family of molecules which share some features (epitopes) with the characterised molecules.

i) Biochemical purification would provide valuable information concerning the structure and function of these receptors.

ii) Localisation of the receptors at the ultrastructural level remains a vitally important experiment, particularly if dual labelling with endogenous human IgG is

performed. Ultrathin frozen sections are the ideal vehicle with which to perform these investigations.

iii) Uptake of gold-labelled or DNP-labelled IgG by chorionic villi in culture may be investigated using different times of exposure to the labelled molecule. By fixing this tissue and preparing it for ultrastructural immunocytochemistry using ultrathin frozen sections it would be possible to see what molecules are involved and at what times using a different sized colloidal gold.

iv) Inhibition of uptake of labelled immunoglobulin by chorionic villi in culture may be attempted by including anti-FcγRIII antibodies.

v) Immunocytochemical localisation of the four IgG subclasses may be performed to identify the point at which the subclasses are discriminated.

vi) Immunocytochemistry may be performed to localise other immunoglobulin classes, particularly in term amniochorion. Such studies may resolve if these are capable of penetrating between cytotrophoblast cells of the chorion laeve. Thus the point of discrimination of these molecules may be assessed.

vii) In situ hybridisation may be performed to look for FcγR expression using light and electron microscopy.

viii) Monoclonal antibody 4IHI6 recognises the HR form of FcγRIIa and thus immunocytochemistry could be performed to localise this form of the molecule. This may help to explain why IgG_2 is discriminated against.

APPENDICES.

I.   Recipe for 0.1M phosphate buffered saline (PBS).

II.   Recipe for 0.1M phosphate buffer.

III.   Processing schedule for examination of placental tissue by transmission electron microscopy (TEM).

IV.   Processing schedule for examination of placental tissue by scanning electron microscopy (SEM).

V.   Fluorescence nuclear counterstaining.

VI.   Slide subbing.

VII.   Preparation of fixatives for use with immunogold electron microscopy.

VIII.   Low temperature embedding protocol for Lowicryl HM23 resin.

IX.   Low temperature embedding protocol for Lowicryl K4M resin.

X.   Low temperature embedding protocol for LR Gold resin.

XI.   Recipe for 50mM tris-buffered saline (TBS).

XII.   Immunogold labelling protocol for electron microscopy of resin embedded tissue samples.

XIII.   Immunofluorescence labelling protocol for epifluorescence light microscopy of frozen sections.

XIV.   Quantitation of gold labelling.

APPENDIX I.

Recipe for 0.1M phosphate buffered saline (PBS).

PBS was prepared according to the method of Osborn and Weber (1982) and the chemicals were all analytical reagent (AR) grade purchased from Fisons. The composition of 1 litre of PBS was as follows:

NaCl	8.0g
KCl	0.2g
KH_2PO_4	0.2g
Na_2HPO_4	1.15g

These chemicals were dissolved in a solution made up to 1 litre with distilled water and the pH was adjusted to 7.4 with NaOH. The pH values were checked with a Pye Unicam (PW 9409) digital pH meter calibrated with pH standards.

APPENDIX II.

Recipe for 0.1M phosphate buffer.

0.1M Sörensens phosphate buffer was prepared according to methods detailed in Glauert (1975). A 0.1M solution of monobasic sodium ions (sodium dihydrogen orthophosphate; NaH_2PO_4; M. Wt. 156.01) was prepared with distilled water (solution A). A 0.1M solution of dibasic sodium ions (disodium hydrogen orthophosphate; Na_2HPO_4; M. Wt. 141.96) was also prepared with distilled water (Solution B). These solutions were stored at 4°C in the dark.

To make a 0.1M working solution (pH 7.4) the solutions were mixed in the ratio of 1 volume of solution A with 4 volumes of solution B when required. The pH was checked with a Pye Unicam (PW 9409) digital pH meter calibrated with pH standards.

APPENDIX III.

Processing schedule for examination of tissue by transmission electron microscopy (TEM).

Small pieces (approximately 2mm^3) of freshly dissected placental tissue were fixed for 3 hours at room temperature with 3% glutaraldehyde in 0.1M phosphate buffer (pH 7.4). The sample was then washed (1 hour, then overnight) at 4°C with phosphate buffer. Tissue was post-fixed with aqueous 2% OsO_4 at 4°C for 1 hour, washed (1 hour, then overnight) with phosphate buffer and exposed to the following dehydration and embedding regime:

SOLUTION.	TIME.
50% ethanol in distilled H_2O.	10 mins.
70% ethanol in distilled H_2O.	10 mins.
90% ethanol in distilled H_2O.	10 mins.
100% ethanol.	10 mins.
100% ethanol (dried over Na_2SO_4).	10 mins.

The tissue was then passed into Propylene Oxide (1,2-Epoxy Propane) as an exchange medium and infiltrated with Araldite resin (Agar Aids) according to the following schedule:

SOLUTION.	TIME.
1,2-Epoxy propane.	20 mins.
1,2-Epoxy propane.	20 mins.
50:50 1,2-Epoxy propane : Araldite.	24 hours.

The 1,2-Epoxy propane was then allowed to evaporate for at least 3 hours prior to embedding in a further change of pure Araldite resin (24 hours) containing 1 drop of benzyldimethylamine (BDMA) catalyst per gram of Araldite. The tissue was then embedded in fresh Araldite resin containing BDMA catalyst in BEEM or gelatin capsules (Agar Aids) and polymerised at 60°C for 48 hours. The hardened blocks were subsequently stored at room temperature.

APPENDIX IV.

Processing schedule for examination of placental tissue by scanning electron microscopy (SEM).

Small pieces of tissue (approximately 5mm^3) were dissected and fixed for 3 hours at room temperature with 3% glutaraldehyde in 0.1M phosphate buffer (pH 7.4). The tissue was then washed at 4°C in phosphate buffer (1 hour, then overnight). The samples were post-fixed with aqueous 2% OsO_4 for 1 hour, washed with phosphate buffer at 4°C (1 hour, then overnight) and processed for SEM according to the protocol described below:

SOLUTION.	TIME.
50% ethanol in distilled H_2O.	10 mins.
70% ethanol in distilled H_2O.	10 mins.
90% ethanol in distilled H_2O.	10 mins.
100% ethanol.	10 mins.
100% ethanol.	10 mins.

The samples were then passed into 100% acetone as an exchange medium and transferred to the critical point drier (Polaron). The acetone was replaced with 2 flushes of liquid CO_2 and allowed to impregnate for 1 hour. The samples were then critical point dried at a pressure of 1200 PSI and a temperature of 31.5°C. Finally, the samples were mounted onto aluminium stubs with Scotch double-sided adhesive tape and coated with 25nm of gold in a Polaron (E5150) sputter coating unit.

APPENDIX V.

Fluorescence nuclear counterstaining.

A solution of propidium iodide was prepared as described by Ockleford et. al. (1981). 5mg of propidium iodide (Sigma) was added to 100ml of 0.1M trisodium citrate and dissolved to make a stock solution. To counterstain cell nuclei, one part of the stock solution was added to 3 parts of 0.1M PBS. The tissue sections were rinsed with this solution for 5 minutes at 4°C half way through the penultimate wash, with 2 extra washes afterwards. Propidium iodide is a carcinogen and was handled with great care and applied in a fume cupboard.

APPENDIX VI.

Slide subbing.

Subbed 10-well immunofluorescence slides were prepared, to insure that pre-fixed tissue sections adhered firmly to the slide, according to the following protocol:

1)   Rack up Dispo or Flow Labs immunofluorescence slides and soak with 5% 'Decon' overnight.

2)   Leave slides under hot running water for 30 minutes with occasional agitation.

3)   3 washes with distilled water.

4)   2 washes with deionised water.

5)   Dry in a glassware oven.

6)   Prepare a subbing solution of 2% 3-Aminopropyltriethoxysilane (Sigma) in acetone and rinse with the following solutions:

	SOLUTION.	TIME.
7)	2% 3-aminopropyltriethoxysilane in acetone.	1 min.
8)	100% acetone.	1 min.
9)	100% acetone.	1 min.
10)	Deionised water.	1 min.
11)	Deionised water.	1 min.

The slides were then dried in a glassware oven, covered to prevent dust from adhering to the surface and stored until required.

APPENDIX VII.

Preparation of fixatives fo use with immunogold electron microscopy.

i)   3% formaldehyde in 0.1M PBS (pH 7.4) was prepared from a stock 40% formaldehyde solution (7.5ml formaldehyde made up to 100ml with PBS prepared according to appendix I).

ii)   3% formaldehyde + 0.1% glutaraldehyde was prepared from stock 40% formaldehyde and 25% glutaraldehyde solutions (7.5ml formaldehyde + 0.4ml glutaraldehyde made up to 100ml with 0.1M PBS prepared according to appendix I).

iii)   4% paraformaldehyde in 0.1M phosphate buffer was freshly prepared from powdered paraformaldehyde according to Glauert (1975). 8g of paraformaldehyde was added to distilled water and heated to 65°C with occasional stirring. This resulted in a cloudy solution which was cleared with the addition of a few drops of 1M NaOH. The solution was then allowed to cool to room temperature and made up to 100ml with distilled water. This solution was then added to 100ml of 0.2M phosphate buffer.

iv)   4% paraformaldehyde + 0.1% glutaraldehyde was made as above except that 0.8ml of stock 25% glutaraldehyde solution was also added prior to making the solution up to 100ml with distilled water and the addition of 100ml 0.2M phosphate buffer.

APPENDIX VIII.

Low temperature embedding protocol for Lowicryl HM23 resin.

Small pieces of tissue (approximately 2mm^3) were fixed and washed as described in section 6.2.2. The specimens were then dehydrated using the PLT method as outlined below:

SOLUTION.	TEMPERATURE.	TIME.
50% ethanol in distilled H$_2$O.	-18°C.	60 mins.
70% ethanol in distilled H$_2$O.	-42°C.	60 mins.
90% ethanol in distilled H$_2$O.	-70°C.	60 mins.
100% ethanol.	-70°C.	60 mins.
100% ethanol.	-70°C.	60 mins.

Lowicryl HM23 low temperature methacrylate resin was prepared, according to the manufacturers instructions, as follows:

Crosslinker F.	1.1g.
Monomer G.	18.9g.
Initiator C.	0.1g.

The resin was carefully prepared in a fume cupboard using protective clothing and the components mixed with a steady stream of nitrogen gas. This also had the effect of degassing the resin since the incorporation of oxygen into the resin may interfere with polymerisation. Infiltration of the tissue by the resin was achieved as follows:

SOLUTION.	TEMPERATURE.	TIME.
1:1 HM23 : 100% ethanol.	-70°C.	60 mins.
2:1 HM23 : 100% ethanol.	-70°C.	60 mins.
Pure HM23.	-70°C.	60 mins.
Pure HM23.	-70°C.	Overnight.
Pure HM23.	-70°C.	8 hours.

The tissue was transferred to fresh, pre-cooled resin in gelatin capsules and photopolymerised for 24 hours at -42°C and 48 hours at room temperature as described in section 6.2.5. The cured blocks were stored at room temperature.

APPENDIX IX.

Low temperature embedding protocol for Lowicryl K4M resin.

Small pieces of tissue (approximately 2mm^3) were fixed and washed as described in section 6.2.2. The specimens were then dehydrated using a graded series of ethanol as follows:

SOLUTION.	TEMPERATURE.	TIME.
50% ethanol in distilled H$_2$O.	-18°C.	60 mins.
70% ethanol in distilled H$_2$O.	-18°C.	60 mins.
90% ethanol in distilled H$_2$O.	-18°C.	60 mins.
98% ethanol in distilled H$_2$O.	-18°C.	60 mins.
98% ethanol in distilled H$_2$O.	-18°C.	60 mins.

The Lowicryl K4M resin was then prepared, according to the manufacturers instructions, as follows:

Crosslinker A.	2.7g.
Monomer B.	17.3g.
Initiator C.	0.1g.

The resin, having been carefully prepared in a fume cupboard using protective clothing, was mixed with a steady stream of nitrogen gas. This also prevents incorporation of oxygen into the resin which may interfere with polymerisation. A total of 2% H$_2$O by weight (indicated in parentheses) was added to the final mixture since this resin may tolerate up to 5% H$_2$O by weight in the polymerised block. Infiltration of the tissue by this resin was achieved as follows:

SOLUTION.	TEMPERATURE.	TIME.
1:1 K4M : 100% ethanol (2% H$_2$O).	-18°C.	60 mins.
2:1 K4M : 100% ethanol (2% H$_2$O).	-18°C.	60 mins.
Pure K4M (2% H$_2$O).	-18°C.	60 mins.
Pure K4M (2% H$_2$O).	-18°C.	Overnight.
Pure K4M (2% H$_2$O).	-18°C.	8 hours.

The tissue was then transferred to fresh resin (+ 2% H$_2$O) in gelatin capsules and photopolymerised at -23°C for 24 hours as described in section 6.2.5.

APPENDIX X.

Low temperature embedding protocol for LR Gold resin.

Small pieces of tissue (approximately 2mm^3) were fixed and washed as described in section 6.2.2. The specimens were then dehydrated in a graded series of ethanol as follows:

SOLUTION.	TEMPERATURE.	TIME.
50% ethanol in distilled H$_2$O.	-18°C.	60 mins.
70% ethanol in distilled H$_2$O.	-18°C.	60 mins.
90% ethanol in distilled H$_2$O.	-18°C.	60 mins.
100% ethanol in distilled H$_2$O.	-18°C.	60 mins.
100% ethanol in distilled H$_2$O.	-18°C.	60 mins.

The tissue was then infiltrated with LR Gold resin according to the following protocol:

SOLUTION.	TEMPERATURE.	TIME.
1:1 LR Gold : 100% ethanol.	-18°C.	60 mins.
7:3 LR Gold : 100% ethanol.	-18°C.	60 mins.
Pure LR Gold (+0.5% catalyst).	-18°C.	60 mins.
Pure LR Gold (+0.5% catalyst).	-18°C.	Overnight.
Pure LR Gold (+0.5% catalyst).	-18°C.	8 hours.

0.5% by weight of the catalyst (Benzoin ethyl ether; Aldrich Chemical Co.) was added to the LR Gold resin to initiate the photopolymerisation reaction. The tissue was then transferred to fresh pre-cooled resin (+0.5% catalyst) in gelatin capsules. The resin was then photopolymerised with 360 nm irradiation for 24 hours at -23°C, and a further 48 hours at room temperature as described in section 6.2.5. The cured blocks were stored at room temperature.

APPENDIX XI.

Recipe for 50mM tris-buffered saline (TBS).

TBS was prepared according to Berryman and Rodewald (1990) and the chemicals were all AR grade purchased from Fisons. The composition of solute in 100ml of aqueous solution was as follows:

Tris-hydroxymethylamine.	0.606g.
NaCl.	0.877g.

This gave a 50mM solution of tris buffer and 150mM NaCl dissolved in distilled water. The pH was adjusted to either 8.0 or 7.4 with HCl and checked with a Pye Unicam (PW 9409) digital pH meter calibrated with pH standards.

Immunogold labelling protocol for electron microscopy of resin embedded tissue samples.

The following is an example of a typical gold-labelling protocol for localisation of an antigen on sections of low temperature resin embedded material:

SOLUTION.	TIME.	TEMP.
1) 50mM NH_4Cl in 0.1M PBS.	10 mins.	20°C.
2) 1% BSA + 5% NRS in 0.1M PBS.	10 mins.	20°C.
3) 1° goat anti-human IgG (1/50) in 0.1M PBS containing 1% BSA + 5% NRS. Control: 1/50 NGS in 0.1M PBS containing 1% BSA + 5% NRS.	60 mins.	37°C.
4) 0.1M PBS containing 1% BSA + 5% NRS.	5 x 3 mins.	20°C.
5) 2° 10nm gold-conjugated rabbit anti-goat IgG (1/100) in 0.1M PBS containing 1% BSA + 5% NRS.	60 mins.	37°C.
6) 1% BSA in 0.1M PBS.	3 x 3 mins.	20°C.
7) 0.1M PBS.	3 x 3 mins.	20°C.
8) Distilled H_2O.	3 x 3 mins.	20°C.
9) 1% glutaraldehyde in distilled H_2O.	5 mins.	20°C.
10) Distilled H_2O.	3 x 3 mins.	20°C.

The grids were then rinsed briefly in 100% methanol, dried with Velin tissue (Agar Aids) and stored in a grid holder. The sections were subsequently contrasted with 2% aqueous uranyl acetate for 5 minutes and 1% lead citrate for 6 minutes in an atmosphere of sodium hydroxide.

Immunofluorescence labelling protocol for epifluorescence light microscopy of frozen tissue samples.

A typical immunofluorescence labelling protocol for localising antigens in frozen tissue sections is outlined below (* optional steps):

SOLUTION.	TIME.	TEMP.
1) 0.1M PBS.	2 x 2 mins.	20°C.
2) 3% formaldehyde in 0.1M PBS.*	10 mins.	20°C.
3) 0.1M PBS.*	3 x 5 mins.	20°C.
4) 0.05% Triton X-100 in 0.1M PBS.*	10 mins.	20°C.
5) 0.1M PBS.*	3-4 x 30 secs.	20°C.
6) 1° goat anti-clathrin (1/50) in 0.1M PBS containing 5% NRS. Control: 1/50 NGS in 0.1M PBS containing 5% NRS.	60 mins.	37°C.
7) 0.1M PBS.	3 x 30 secs.	20°C.
8) 0.1M PBS.	60 mins.	4°C.
9) 2° FITC-conjugated rabbit anti-goat IgG (1/500) in 0.1M PBS containing 5% NRS.	60 mins.	37°C.
10) 0.1M PBS.	3 x 30 secs.	20°C.
11) 0.1M PBS.	30 mins.	4°C.

The slides were subsequently mounted with photobleach retardant mountant (Citifluor) under Chance Propper Ltd. No. 0 thickness glass coverslips, sealed with nail-varnish and viewed.

Quantitation of gold labelling.

Areas on micrographs of labelled frozen tissue sections were circumscribed using a DigiCad Plus graphics tablet and measured using a Kontron Videoplan Image-processing system. Counts of gold particles within these areas were used to deduce the number of gold particles per μm^2 associated with defined cellular components. The tissue was immunoreacted, in each instance, with 1/100 rabbit anti-human IgG and 1/60 protein A conjugated to 10nm colloidal gold. Control counts were taken from areas of 1st trimester syncytiotrophoblast treated with 1/100 non-immune rabbit serum and subsequently with 1/60 protein A:gold. Background counts were taken using gold particles overlying nuclei and mitochondria. The following categories were used:

Group 1: Control.
Group 2: Background (nuclei + mitochondria).
Group 3: Erythrocytes.
Group 4: Cytotrophoblast cells.
Group 5: 1st trimester syncytium.
Group 6: 1st trimester extracellular matrix (ECM).
Group 7: Term syncytium.
Group 8: Term extracellular matrix (ECM).
Group 9: Term serum.
Group 10: Amniotic epithelial cells (amnion cells).
Group 11: Dead amniotic epithelial cells (dead AE cells).
Group 12: Amniochorion extracellular matrix (AC: ECM).

The number of gold particles overlying particular tissue components in each electron micrograph was then calculated (gold particles / μm^2) and incorporated into Super Anova Software (Abacus Concepts Inc., version 1.11) to test for statistical significance. One way analysis of variance (ANOVA) of gold particles / μm^2 within the placental tissue components yielded an F ratio of 49.83 (df 11) with p=0.0001. Post-hoc comparisons between pairs of mean values of gold particles / μm^2 using Fisher's Protected least significant difference at the 0.05 and 0.01 significance value confirmed significant differences between tissue components:

Source	df	Sum of Squares	Mean Square	F-Value	P-value
Column 2	11	1363823.638	123983.967	49.830	0.0001
Residual	280	696685.789	2488.164		

Fisher's Protected LSD
Effect: Column 2
Dependent: Column 1
Significance level: 0.01

	1	2	3	4	5	6	7	8	9	10	11	12
1. Cytotrophoblast	-											
2. Control	-	-										
3. Background	-	-	-									
4. Amnion cells	-	-	-	-								
5. Erythrocytes	-	-	-	-	-							
6. 1st trim ECM	-	-	-	-	-	-						
7. Term syncytium	-	-	-	-	-	-	-					
8. 1st trim syncytium	S	S	S	S	S	-	-	-				
9. Term ECM	S	S	S	S	S	S	-	-	-			
10. AC: ECM	S	S	S	S	S	S	-	-	-	-		
11. Dead AE cells	S	S	S	S	S	S	S	S	S	S	-	
12. Term serum	S	S	S	S	S	S	S	S	S	S	S	-

Significance level: 0.05

	1	2	3	4	5	6	7	8	9	10	11	12
1. Cytotrophoblast	-											
2. Control	-	-										
3. Background	-	-	-									
4. Amnion cells	-	-	-	-								
5. Erythrocytes	-	-	-	-	-							
6. 1st trim ECM	-	-	-	-	-	-						
7. Term syncytium	S	S	S	S	-	-	-					
8. 1st trim syncytium	S	S	S	S	S	S	-	-				
9. Term ECM	S	S	S	S	S	S	-	-	-			
10. AC: ECM	S	S	S	S	S	S	-	-	-	-		
11. Dead AE cells	S	S	S	S	S	S	S	S	S	S	-	
12. Term serum	S	S	S	S	S	S	S	S	S	S	S	-

S = Significantly different at this level.

Appendix XIV (gold particles per square micron).

	Control	Background	Erythrocytes	Cytotrophoblast
	1.675	3.902	4.025	2.153
	2.388	3.122	5.931	4.330
	4.256	1.338	1.873	.975
	1.924	3.366	13.054	2.536
	1.608	2.288	12.486	4.562
	3.674	.851	15.998	2.479
	2.902	.567	13.657	1.695
	2.134	1.821	10.256	2.883
	2.924	1.756	6.963	2.341
	1.289	2.809	4.509	1.561
	3.851	3.815	4.905	1.665
	3.212	.761	9.365	2.051
	2.106	4.566	7.804	1.357
	1.387	2.081	3.602	1.826
	2.749	.624	2.521	2.029
	1.289	2.601	4.856	1.086
	2.485	3.126	4.058	2.601
	.393	3.746	8.083	2.854
	1.608	1.041	4.566	3.122
	.706	5.029	9.784	2.497
	2.766	3.876	4.896	2.676
	1.195	2.142		1.873
	3.952	.960		1.951
	1.805	3.122		1.892
	3.212	1.561		3.529
	3.106	1.338		3.736
	1.506	.457		.702
	.448	.415		1.249
	.537	1.338		1.218
	1.530	1.419		.816
	1.063	1.734		1.683
		1.301		.651
		1.561		5.141
		1.041		1.058
		1.456		.760
		2.283		.878
		4.566		1.410
		4.566		.163
		.612		.127
		3.518		1.736
		4.234		1.018
		.651		4.649
n	31	42	21	42
total	65.680	93.361	153.192	85.519
mean	2.119	2.223	7.295	2.036
std	1.076	1.360	3.988	1.205

Appendix XIV (gold particles per square micron).

	1st Syncytium	1st ECM	Term Syncytium	Term ECM
	61.785	2.341	18.351	51.505
	20.574	5.128	41.285	100.669
	47.686	.390	35.004	36.210
	7.427	.568	17.181	54.332
	65.014	58.269	49.169	20.650
	33.175	34.337	38.293	15.301
	50.798	55.147	27.146	87.200
	43.759	30.884	18.628	48.885
	33.947	26.580	19.333	39.405
	71.594	6.522	25.649	40.380
	37.378	16.538	66.977	34.469
	55.938	11.415	26.877	30.148
	61.130	1.701	24.117	45.887
	57.436	2.138	42.512	101.623
	68.153	1.344	18.879	76.099
	54.106	.942	34.342	47.770
	59.982	12.620	73.451	65.678
	117.970	5.877	32.338	81.226
	74.117	10.306	69.148	71.725
	43.374		19.457	157.640
				41.251
				39.063
n	20	19	20	22
total	1065.343	283.047	698.137	1287.116
mean	53.267	14.897	34.907	58.505
std	22.880	18.025	17.659	32.602

	Term Serum	Amnion cells	Dead AE Cells	AC: ECM
	306.690	6.243	59.309	19.007
	705.465	3.746	84.832	66.861
	711.708	5.283	170.950	36.724
	399.555	2.775	179.488	69.670
	393.312	2.986	153.923	89.137
	380.046	4.958	193.705	34.337
	133.128	2.554		45.782
	330.102	2.861		37.235
	125.307	3.943		49.661
	160.759	1.530		118.261
	182.832	4.423		126.734
	165.441	4.353		71.795
	181.829	2.283		79.222
	152.294	4.197		46.547
	302.788	4.957		53.066
	170.818	5.250		10.405
	127.840	7.414		28.094
	246.548	1.999		72.621
	131.101	1.852		83.324
	88.131	1.058		94.475
				71.184
				12.393
				70.518
				111.204
				16.723
				20.745
				55.208
				46.571
				63.869
n	20	20	6	29
total	5395.694	74.665	842.207	1701.373
mean	269.785	3.733	140.368	58.668
std	179.120	1.669	55.044	31.258

BIBLIOGRAPHY.

Acetarin, J. D., Carlemalm, E., Kellenberger, E. and Villiger, W. (1987). Correlation of some mechanical properties of embedding resins with their behaviour in microtomy. *Journal of Electron Microscopy Techniques*, **6**, 63-79.

Aderem, A. A, Rosen, A. and Barker, K. A. (1988). Modulation of prostaglandin and leukotriene biosynthesis. *Current Opinions in Immunology*, **1**, 56-62.

Åkerström, B., Brodin, T., Reis, K. and Björck, L. (1985). Protein G: a powerful tool for binding and detection of monoclonal and polyclonal antibodies. *Journal of Immunology*, **135**, 2589-2598.

Åkerström, B. and Björck, L. (1986). A physiochemical study of protein G, a molecule with unique immunoglobulin G-binding properties. *Journal of Biological Chemistry*, **262**, 10240-10247.

Alberts, B., Bray, D., Lewis, J., Raff, M., Roberts, K. and Watson J. D. (1983). Molecular biology of the cell. pp. 1-1146. Garland, New York.

Alger, L. S. and Pupkin, M. J. (1986). Aetiology of preterm premature rupture of the membranes. *Clinical Obstetrics and Gynaecology*, **29**, 758-770.

Allansmith, M. and Buell, D. N. (1964). The relationship of gamma-1A globulin and reagin in cord sera. *Journal of Allergy*, **35**, 339-345.

Allansmith, M., McClennan, B. H., Butterworth, M. and Moloney, J. R. (1968). The development of immunological levels in man. *Journal of Pediatrics*, **72**, 276-289.

Allen, R. D., David, G. B. and Nomarski, G. (1969). The Zeiss - Nomarski differential interference equipment for transmitted light microscopy. *Zeitschrift für Wissenschaftliche-mikroskopie und mikroskopische Technik*, **69**, 193-221.

Allen, J. M. and Seed, B. (1989). Isolation and expression of functional high-affinity Fc receptor complementary DNAs. *Science*, **243**, 378-381.

Amigorena, S., Drake, J. R., Webster, P. and Mellman, I. (1994). Transient accumulation of new class II MHC molecules in a novel endocytic compartment in B lymphocytes. *Nature*, **369**, 113-120.

Anderson, T. F. (1950). The use of critical point phenomena in preparing specimens for the electron microscope. *Journal of Applied Physiology*, **21**, 724.

Anderson, C. L. (1982). Isolation of the receptor from human monocyte cell line (U937) and from human peripheral blood monocytes. *Journal of Experimental Medicine*, **156**, 1794-1805.

Anderson, C. L. and Looney, R. J. (1986). Human leukocyte IgG Fc receptors. *Immunology today*, **7**, 264-266.

Anderson, J. M. and Ferguson Smith, M. A. (1971). Nature's transplant. *British Medical Journal*, **2**, 166-171.

Anderson, P., Caligiuri, M., O'Brien, C., Manley, T., Ritz, J. and Schlossman, S. F. (1990). Fcγ receptor type III (CD16) is included in the ζ NK receptor complex expressed by human killer cells. *Proceedings of the National Academy of Sciences of the USA*, **87**, 2274-2278

Anderson, R. G. W., Goldstein, J. L. and Brown, M. S. (1977). A mutation that impairs the ability of lipoprotein receptors to localise in coated pits on the cell surface of human fibroblasts. *Nature*, 270, 695-699.

Anderson, R. G. W., Vasile, E., Mello, R. J., Brown, M. S. and Goldstein, J. L. (1978). Immunocytochemical visualisation of coated pits and vesicles in human fibroblasts: relation to low density lipoprotein receptor distribution. *Cell*, 15, 919-933.

Ashwell, J. and Klausner, R. (1990). Genetic and mutational analysis of the T-cell-antigen receptor. *Annual Review of Immunology*, 8, 139-168.

Baker, B. L., Hook, S. J. and Severinghaus, A. E. (1944). The cytological structure of the human chorionic villus and decidua parietalis. *American Journal of Anatomy*, 74, 291-326.

Balfour, A. H. and Jones, E. A. (1976). The binding of IgG to human placental membranes. In *Maternofoetal transmission of immunoglobulins*, (Ed. W. A. Hemmings), pp. 61-72. Cambridge University Press, New York.

Ballieux, R. E., Bernier, G. M., Tominaga, K. and Putnam, F. W. (1964). Gamma-globulin antigenic types defined by heavy chain determinants. *Science*, 145, 168-170.

Bangham, D. R., Hobbs, K. R. and Terry, R. J. (1958). Selective placental transfer of serum proteins in the rhesus. *Lancet*, 2, 351-354.

Barr, M., Glenny, A. T. and Randall, K. J. (1949). Concentration of diphtheria antitoxin in cord blood and rate of loss in babies. *Lancet*, 2, 324-326.

Bautzmann, H. and Schröder, R. (1955). Vergleichende studien über bau und funktion des amnions. Neue befunde am menschlichen amnion mit einschluß seiner freien bindegewebs - oder sog. Hofbauerzellen. *Zeitschrift für Anatomie und Entwicklungsgeschichte*, 199, 7-22.

Bautzmann, H. and Schröder, R. (1958). Comparative studies on the histology and function of the amnion. *Acta Anatomica* (Basel), 33, 38-49.

Bayer, E. A., Skutelsky, E. and Wilchek, M. (1979). The avidin-biotin complex in affinity cytochemistry. In 'Methods in Enzymology', (Eds. D. B. McCormick and L. D. Wright), pp. 308-315. Academic Press, New York.

Beller, D. I. and Ho, K. (1982). Regulation of macrophage population. V. Evaluation of the control of macrophage Ia expression in vitro. *Journal of Immunology*, 129, 971-976.

Berryman, M. A. and Rodewald, R. D. (1990). An enhanced method for post embedding immunocytochemical staining which preserves cell membranes. *Journal of Histochemistry and Cytochemistry*, 38, 159-170.

Bendayan, M. and Zollinger, M. (1983). Ultrastructural localisation of antigenic sites on osmium-fixed tissues applying the protein A-gold technique. *Journal of Histochemistry and Cytochemistry*, 31, 101-109.

Björck, L. and Kronvall, G. (1984). Purification and some properties of streptococcal Protein G, a novel IgG-binding reagent. *Journal of Immunology*, 133, 969-974.

Bleil, J. D. and Bretscher, M. S. (1982). Transferrin receptor and its recycling in HeLa cells. *EMBO Journal*, 1, 351-355.

Booth, A. G. and Wilson, M. J. (1981). Human placental coated vesicles contain receptor-bound transferrin. *Biochemical Journal*, 196, 355-362.

Börner, P., Deicher, H., Heide, K. and Reinecke, J. (1974). Evidence for the participation of the Fc portion of immunoglobulin G in maternofoetal immunoglobulin transfer in the human. In 'Immunology in Obstetrics and Gynaecology', (Eds. A. Centaro and N. Carretti), pp. 272-274. Excerpta Medica, Amsterdam.

Bourne, G. L. (1960). The microscopic anatomy of the human amnion and chorion. American Journal of Obstetrics and Gynaecology, 79, 1070-1073.

Bourne, G. (1962). The human amnion and chorion. pp. 1-276. Lloyd-Luke Ltd. London.

Boyd, J. D. and Hamilton, W. J. (1970). The human placenta. pp. 1-365. W. Heffer & sons, Cambridge.

Brambell, F. W. R., Hemmings, W. A. and Oakley, C. L. (1959). The relative transmission of natural and pepsin-refined homologous antitoxin from the uterine cavity to the foetal circulation in the rabbit. Proceedings of the Royal Society of London Series B, 150, 312-317.

Brambell, F. W. R. (1966). The transmission of passive immunity from mother to young and the catabolism of immunoglobulins. Lancet, 2, 1087-1093.

Brambell, F. W. R. (1970). The transmission of passive immunity from mother to young. pp. 1-385. North-Holland publishing company, Amsterdam.

Breshnihahn, B., Grigor, R. R., Oliver, M., Lewkonia, R. M., Hughes, G. R. V., Lovins, R. E. and Faulk, W. P. (1977). Immunological mechanism for spontaneous abortion in systemic lupus erythematosus. Lancet, 2, 1205-1207.

Bright, N. A. and Ockleford, C. D. (1993). Expression of Fcγ receptors by cells of the human amniochorion. Placenta, 14, A7.

Bright, N. A. and Ockleford, C. D. (1994a). Heterogeneity of Fcγ receptor bearing cells in human term amniochorion. Placenta, 15, 247-255.

Bright, N. A. and Ockleford, C. D. (1994b). Cytotrophoblast cells. A barrier to maternofetal transmission of passive immunity? Journal of Histochemistry and Cytochemistry, submitted for publication.

Bright, N. A., Ockleford, C. D. and Anwar, M. (1994). Ontogeny and distribution of Fcγ receptors in the human placenta. Transport or immune surveillance? Journal of Anatomy, 184, 297-308.

Brunhouse, R. and Cebra, J. J. (1979). Isotypes of IgG: comparison of the primary structures of three pairs of isotypes which differ in their ability to activate complement. Molecular Immunology, 16, 907-917.

Bruns, R. R. (1969). A symmetrical extracellular fibril. Journal of Cell Biology, 42, 418-430.

Bullock, G. R. and Petrusz, P. (eds.) (1982). Techniques in immunocytochemistry (Volume 1). pp. 1-306. Academic Press, London.

Bullock, G. R. and Petrusz, P. (eds.) (1983). Techniques in immunocytochemistry (Volume 2). pp. 1-290. Academic Press, London.

Bullock, G. R. and Petrusz, P. (eds.) (1985). Techniques in immunocytochemistry (Volume 3). pp. 1-241. Academic Press, London.

Burton, D. R., Gregory, L. and Jefferis, R. (1986). Aspects of the molecular structure of the IgG subclasses. *Monographs in Allergy*, **19**, 7-35.

Byrd, N. A., Bright, N. A. and Ockleford, C. D. (1994). Dual channel localisation of $\alpha6\beta4$ integrin and type VII collagen in human term amniochorion. *Journal of Anatomy*, In the press.

Carlemalm, E., Garavito, R. M. and Villiger, W. (1982). Resin development for electron microscopy and an analysis of embedding at low temperature. *Journal of Microscopy*, **126**, 123-143.

Castellucci, M., Zaccheo, D. and Pescetto, G. (1980). A three-dimensional study of the normal human placental villous core. I. The Hofbauer cells. *Cell and Tissue Research*, **210**, 235-247.

Castellucci, M. and Kaufmann, P. (1982). A three-dimensional study of the normal human placental villous core. II. Stromal architecture. *Placenta*, **3**, 269-286.

Castellucci, M. and Kaufmann, P. (1990). Hofbauer cells. In *'Pathology of the human placenta'*, (Eds. K. Benirschke and P. Kaufmann), pp. 71-80. Springer, New York.

Causton, B. E. (1984). The choice of resins for immunocytochemistry. In *'Immunolabelling for electron microscopy'*, (Eds. J. M. Polak and I. M. Varndell), pp. 29-37. Elsevier, Amsterdam.

Caux, C., Dezutter-Dambuyant, C., Schmitt, D. and Bancherean, J. (1992). GM-CSF and TNF-α cooperate in the generation of dendritic Langerhans cells. *Nature*, **360**, 258-261.

Cederqvist, L. L., Queenan, J. T. and Gadow, E. C. (1972). The origin of gamma G globulins in human amniotic fluid. *American Journal of Obstetrics and Gynaecology*, **113**, 838-840.

Chandra, R. K. (1976). Levels of IgG subclasses, IgA, IgM and tetanus antitoxin in paired maternal and foetal sera findings in healthy pregnancy and placental insufficiency. In *Maternofoetal transmission of immunoglobulins*, (ed. W. A. Hemmings), pp. 77-87. Cambridge University Press, New York.

Christensen, A. K. (1971). Frozen thin sections of fresh tissue for electron microscopy, with a description of pancreas and liver. *Journal of Cell Biology*, **51**, 772-804.

Chudwin, D. S., Wara, D. W., Schiffman, G., Artrip, S. G. and Ammann, A. J. (1985). Maternal-fetal transfer of pneumococcal capsular polysaccharide antibodies. *American Journal of Diseases of Children*, **139**, 378-380.

Cohen, L., Sharp, S. and Kulczycki, A. Jr. (1983). Human monocytes, B lymphocytes and non-B lymphocytes each have structurally unique Fc gamma receptors. *Journal of Immunology*, **131**, 378-382.

Colman, P. M., Deisenhofer, J. and Huber, R. (1976). Structure of the human antibody molecule Kol (immunoglobulin G1): an electron density map at 5.0 Å resolution. *Journal of Molecular Biology*, **100**, 257-282.

Coons, A. H., Creech, H. J. and Jones, R. N. (1941). Immunological properties of an antibody containing a fluorescent group. *Proceedings of the Society for Experimental Biology and Medicine*, **47**, 200-202.

Coons, A. H., Leduc, E. H. and Connolly, J. M. (1955). Studies on antibody production. I. A method for the histochemical demonstration of specific antibody

and its application to a study of the hyperimmune rabbit. *Journal of Experimental Medicine*, 102, 49-60.

Dancis, J., Lind, J., Oratz, M., Smolens, J. and Vara, P. (1961). Placental transfer of proteins in human gestation. *American Journal of Obstetrics and Gynaecology*, 82, 167-171.

Dearden, L., Ockleford, C. D. and a contribution from Gupta, M. (1983). Structure of human trophoblast: Correlation with function. In *'Biology of trophoblast'*, (Eds. Y. W. Loke and A. Whyte), pp. 69-110. Elsevier, Oxford.

Desai, R. G. and Creyer, V. P. (1963). Maternal-fetal passage of leucocytes and platelets in man. *Blood*, 21, 665-670.

Douzou, P. (1977). Enzymology at sub-zero temperatures. *Advances in Enzymology*, 45, 157-272.

Dray, S. (1960). Three γ-globulins in normal human serum revealed by monkey precipitins. *Science*, 132, 1313-1314.

Duance, V. C. and Bailey, A. J. (1983). Structure of the trophoblast basement membrane. In *'Biology of trophoblast'*, (Eds. Y. W. Loke and A. Whyte). pp. 597-625. Elsevier.

Dubochet, J., Lepault, J., Freeman, R., Berriman, J. A. and Homo, J. K. (1982). Electron microscopy of frozen water and aqueous solutions. *Journal of Microscopy*, 128, 219-237.

Edelman, G. M. (1959). Dissociation of γ-Globulin. *Journal of the American Chemical Society*, 81, 3155-3156.

Edelman, G. M. and Poulik, M. D. (1961). Studies on structural units of the γ-globulins. *Journal of Experimental Medicine*, 113, 861-884.

Edelman, G. M. and Gally, J. A. (1962). The nature of Bence-Jones proteins. *Journal of Experimental Medicine*, 116, 207-227.

Edelman, G. M. (1973). Antibody structure and molecular immunology. *Science*, 180, 830-840.

Edwards, J. A., Jones, D. B., Evans, P. R. and Smith, J. L. (1985). Differential expression of HLA class II antigens on human fetal and adult lymphocytes and macrophages. *Immunology*, 55, 489-500.

Einhorn, M. S., Granoff, D. M., Nahm, M. H., Quinn, A. and Shackelford, P. G. (1987). Concentration of antibodies in paired maternal and infant sera : relation to IgG subclass. *Journal of Pediatrics*, 111, 783-788.

Enders, A. C. and King, B. F. (1970). The cytology of the Hofbauer cell. *Anatomical Record*, 167, 231-252.

Engvall, E. and Perlmann, P. (1971). Enzyme-linked immunosorbent assay (ELISA). Quantitative assay of immunoglobulin G. *Immunochemistry*, 8, 871-874.

Fan, J., Carpentier, J., Gorden, P., Van Obberghen, E., Blackett, N., Grunfeld, C. and Orci, L. (1982). Receptor-mediated endocytosis of insulin: role of microvilli, coated pits and coated vesicles. *Proceedings of the National Academy of Sciences of the USA*, 79, 7788-7791.

Faulk, W. P. and Taylor, G. M. (1971). An immunocolloid method for the electron microscope. *Immunochemistry*, 8, 1081-1083.

Fawthrop, R. K. and Ockleford, C. D. (1994). Cryofracture of human term amniochorion. *Cell and Tissue Research*, In the press.

Fawcett, D. W. (1965). Surface specialisations of absorbing cells. *Journal of Histochemistry and Cytochemistry*, 13, 75-91.

Feinstein, A., Richardson, N. and Taussig, M. J. (1986). Immunoglobulin flexibility in complement activation. *Immunology Today*, 7, 169-174.

Feldherr, C. M. and Marshall, J. M. (1962). The use of colloidal gold for studies of intracellular exchange in amoeba *Chaos chaos*. *Journal of Cell Biology*, 12, 640-645.

Fernándes-Morán (1952). Application of the ultrathin freezing-sectioning technique to the study of cell structures within the electronmicroscope. *Arkiv for Fysik*, 4, 471-491.

Flavell, D. J., Jones, D. B. and Wright, D. H. (1987). Identification of tissue histiocytes on paraffin sections by a new monoclonal antibody. *Journal of Histochemistry and Cytochemistry*, 35, 1217-1226.

Fleit, H. B., Wright, S. D. and Unkeless, J. C. (1982). Human neutrophil Fc receptor distribution and structure. *Proceedings of the National Academy of Sciences of the USA*, 79, 3275-3279.

Fleming, T. P. and Johnson, M. H. (1988). From egg to epithelium. *Annual Review of Cell Biology*, 4, 459-485.

Fox, H. (1967). The incidence and significance of Hofbauer cells in mature human placenta. *Journal of Pathology and Bacteriology*, 93, 710-717.

Frangione, B., Milstein, C. and Pink, J. R. L. (1969). Structural studies of immunoglobulin G. *Nature*, 221, 145-148.

Franklin, E. C. and Kunkel, H. G. (1958). Comparative levels of high molecular weight (19S) gamma globulin in maternal and umbilical cord sera. *Journal of Laboratory and Clinical Medicine*, 52, 724-727.

French, M. (1986). Serum IgG subclasses in normal adults. *Monographs in Allergy*, 19, 100-107.

Fulginiti, V. A., Sieber, O. F., Jr., Claman, H. N. and Merrill, D. (1966). Serum immunoglobulin measurement during the first year of life and in immunoglobulin deficiency states. *Journal of Pediatrics*, 68, 723-730.

Gadow, E. C., Floriani, F. A. and Florin, A. (1974). IgG levels in amniotic fluid. *American Journal of Obstetrics and Gynaecology*, 119, 849-851.

Galton, M. (1962). DNA content of placental nuclei. *Journal of Cell Biology*, 13, 183-203.

Gaunt, M., Addai, F. and Ockleford, C. D. (1986). Microinjection of human placenta. I: Techniques. *Placenta*, 7, 315-324

Gaunt, M. and Ockleford, C. D. (1986). Microinjection of human placenta. II: Biological application. *Placenta*, 7, 325-331.

Gazaway, P. and Mullins, C. L. (1986). Prevention of preterm labour and premature rupture of the membranes. *Clinical Obstetrics and Gynaecology*, 29, 835-849.

Geuze, H. J., Slot, J. W., Strous, G. J. A. M., Lodish, H. F. and Schwartz, A. L. (1983). Intracellular site of asialoglycoprotein receptor-ligand uncoupling: double-label immunoelectron microscopy during receptor mediated endocytosis. *Cell*, 32, 277-287.

Gitlin, D., Kumate, J., Urrusti, J. and Morales, C. (1964a). The selectivity of the human placenta in the transfer of plasma proteins from mother to fetus. *Journal of Clinical Investigation*, 43, 1938-1951.

Gitlin, D., Kumate, J., Urrusti, J. and Morales, C. (1964b). Selective and directional transfer of 7s γ₂-globulin across the human placenta. *Nature*, 203, 86-87.

Gitlin, D. and Biasucci, A. (1969). Development of IgG, IgA, IgM, BIC/BIA, C1 esterase inhibitor, ceruloplasmin, transferrin, hemopexin, haptoglobulin, fibrinogen, plasminogen, α 1-antitrypsin, orosomucoid, B-lipoprotein, α₂-macroglobulin and prealbumin in the human conceptus. *Journal of Clinical Investigation*, 48, 1433-1446.

Gitlin, D., Kumate, J. and Morales, C., Noriega, L. and Arévalo, N. (1972). The turnover of amniotic fluid protein in the human conceptus. *American Journal of Obstetrics and Gynaecology*, 113, 632-645.

Gitlin, J. D. and Gitlin, D. (1976). Protein binding by cell membranes and the selective transfer of proteins from mother to young across tissue barriers. In *'Maternofoetal transmission of immunoglobulins'*, (ed. W. A. Hemmings), pp. 113-123. Cambridge University Press, New York.

Glauert, A. M. (Ed.) (1975). Fixation, dehydration and embedding of biological specimens. pp. 1-207. North-Holland/American Elsevier.

Goldenthal, K. L., Hedman, K., Chen, J. W., August, J. T., Vihko, P., Pastan, I. and Willingham, M. C. (1988). Pre-lysosomal divergence of alpha-2-macroglobulin and transferrin: a kinetic study using monoclonal antibody against a lysosomal membrane glycoprotein (LAMP-1). *Journal of Histochemistry and Cytochemistry*, 36, 391-400.

Goldstein, J. L., Anderson, R. G. W. and Brown, M. S. (1979). Coated pits, coated vesicles and receptor-mediated endocytosis. *Nature*, 279, 679-684.

Good, R. A. and Zak, S. J. (1956). Disturbances in gamma-globulin synthesis as 'experiments of nature'. *Pediatrics*, 18, 109-149.

Goodman, J. W. (1987). Immunoglobulins I: Structure and function. In *'Basic and Clinical Immunology'*, (Eds. D. P. Stites, J. D. Stobo, H. H. Fudenberg and J. V. Wells), pp. 30-42. Lange Medical Publications, Los Altos, California.

Gough, N. (1981). The rearrangement of immunoglobulin genes. *Trends in Biochemical Sciences*, 6, 203-205.

Graham, R. C. and Karnovsky, M. J. (1966). The early stages of absorption of injected horseradish peroxidase in the proximal tubules of mouse kidney: ultrastructural cytochemistry by a new technique. *Journal of Histochemistry and Cytochemistry*, 14, 291-302.

Green, S. A., Plutner, H. and Mellman, I. (1985). Biosynthesis and intracellular transport of the mouse macrophage Fc receptor. *Journal of Biological Chemistry*, 260, 9867-9874.

Grey, A. M. and Kunkel, H. G. (1964). H chain subgroups of myeloma proteins and normal 7S gamma globulin. *Journal of Experimental Medicine*, 120, 253-263.

Griffin, R. L. (1972). Ultramicrotomy. pp. 1-93. Baillere-Tindall, London.

Griffiths, G. D., Kershaw, D. and Booth, A. G. (1985). Rabbit peroxidase-anti peroxidase complex (PAP) as a model for uptake of Immunoglobulin G by the human placenta. *Histochemical Journal*, 17, 867-881.

Griffiths, G. (1993). Fine structure immunocytochemistry. pp. 1-459. Springer-Verlag, Berlin.

Grosser, O. (1927). Frühentwicklung, eihautbildung und placentation des menschen und der saügetiere. *Deutsche Frauenheilkunde* (5). Bergmann, Munich.

Grubb, R. and Laurell, A. B. (1956). Hereditary serological human serum groups. *Acta Pathologica et Microbiologica Scandinavica*, 39, 390-398.

Grundy, H. O., Peltz, G., Moore, K. W., Golbus, M. S., Jackson, L. G. and Lebo, R. V. (1989). The polymorphic Fcγ receptor II gene maps to human chromosome 1q. *Immunogenetics*, 29, 331-339.

Hamilton, R. G. (1987). The human IgG subclasses. pp. 1-76. Calbiochem Corporation, San Diego.

Hamilton, W. J., Boyd, J. D. and Mossman, H. W. (1952). Human Embryology (2nd Edition). pp. 1-646. W. Heffer & sons Ltd., Cambridge; The Williams and Wilkins Co., Baltimore.

Hamilton, W. J., Boyd, J. D. and Mossman, H. W. (1966). Human Embryology (3rd Edition). pp. 1-646. W. Heffer & sons Ltd., Cambridge; The Williams and Wilkins Co., Baltimore.

Hartley, P. (1951). The effect of peptic digestion on the properties of diphtheria antitoxin. *Proceedings of the Royal Society of London Series B*, 138, 499-513.

Hay, F. C., Hull, M. S. and Torringians, G. (1971). The transfer of human IgG subclasses from mother to fetus. *Clinical and Experimental Immunology*, 9, 355-358.

Hemmings, W. A. and Williams, E. W. (1976). The attachment of IgG to cell components of transporting membranes. In 'Maternofoetal transmission of immunoglobulins', (Ed. W. A. Hemmings), pp. 91-111. Cambridge University Press, New York.

Hempel, E. (1972). Die ultrastructurelle differenzierung des menschlichen amnionepithels unter besonderer berücksichtigung des Nabelstranges. *Anatomischer Anzeiger*, 132, 356-370.

Hertig, A. T. and Rock, J. (1943). On the seven and one-half day human ovum (Carnegie No. 8020). *Anatomical Record*, 85, 317.

Hertig, A. T. (1945). On the development of the amnion and exocoelomic membrane in the pre-villous human ovum. *Yale Journal of Biological Medicine*, 18, 107-115.

Hertig, A. T. and Rock, J. (1945). Two human ova of the pre-villous stage, having a developmental age of about seven and nine days respectively. *Contributions to Embryology of the Carnegie Institute of Washington*, 31, 65-84.

Hertig, A. T., Rock, J. and Adams, E. C. (1956). A description of 34 human ova within the first 17 days of development. *American Journal of Anatomy*, 98, 435-494.

Heuser, C. H. (1932a). A presomite human embryo with a definite chorda canal. *Contributions to Embryology of the Carnegie Institute of Washington*, **23**, 251-267.

Heuser, C. H. (1932b). An intrachorionic mesothelial membrane in young stages of the monkey (Macacus rhesus). *Anatomical Record*, **52** (suppl), 15-16.

Heuser, C. H. (1938). Early development of primitive mesoblast in embryos of the rhesus monkey. Carneg. Instn. (Pub. sol.) Cooperation in Research, 383.

Heuser, J. (1980). Three dimensional visualisation of coated vesicle formation in fibroblasts. *Journal of Cell Biology*, **84**, 560-583.

Hibbs, M. L., Walker, I. D., Kirszbaum, L., Pietersz, G. A., Deacon, N. J., Chambers, G. W., McKenzie, I. F. C. and Hogarth, P. M. (1986). The murine Fc receptor for immunoglobulin: purification, partial amino acid sequence, and isolation of cDNA clones. *Proceedings of the National Academy of Sciences of the USA*, **83**, 6980-6984.

Hibbs, M. L., Classon, B. J., Walker, I. D., McKenzie, I. F. C. and Hogarth, P. M. (1988). The structure of the murine Fc receptor for IgG. Assignment of intrachain disulphide bonds, identification of N-linked glycosylation sites, and evidence of a fourth form of Fc receptor. *Journal of Immunology*, **140**, 544-550.

Hibbs, M., Selvaraj, P., Carpén, O., Springer, T. A., Kuster, H., Jouvin, M. -H. E. and Kinet, J. -P. (1989). Mechanisms for regulating expression of membrane isoforms of FcγRIII (CD16). *Science*, **246**, 1608-1611.

Hill, R. L., Delaney, R., Fellows, R. E. Jr. and Lebovitz, H. E. (1966). The evolutionary origins of the immunoglobulins. *Proceedings of the National Academy of Sciences of the USA*, **56**, 1762-1769.

Hilschmann, N. and Craig, L. C. (1965). Amino acid sequence studies with Bence-Jones proteins. *Proceedings of the National Academy of Sciences of the USA*, **53**, 1403-1409.

Hobot, J. A., Carlemalm, E., Villiger, W. and Kellenberger, E. (1984). Periplasmic gel: New concept resulting from the reinvestigation of bacterial cell envelope ultrastructure by new methods. *Journal of Bacteriology*, **160**, 143-152.

Hofbauer, J. (1905). Grundzüge einer biologie der menschlichen plazenta. Leipzig: Braumuller.

Hopkins, C. R. (1983). The importance of the endosome in intracellular traffic. *Nature*, **304**, 684-685.

Howe, C. L., Granger, B. L., Hull, M., Green, S. A., Gabel, C. A., Helenius, A. and Mellman, I. (1988). Derived protein sequence, oligosaccharides, and membrane insertion of the 120kDa lysosomal membrane protein Igp120: Identification of a highly conserved family of lysosomal membrane glycoproteins. *Proceedings of the National Academy of Sciences of the USA*, **85**, 7577-7581.

Hoyes, A. D. (1970). Ultrastructure of the mesenchymal layers of the human amnion in early pregnancy. *American Journal of Obstetrics and Gynaecology*, **106**, 557-566.

Huizinga, T. W. J., Van der Schoot, C. E., Jost, C., Klaassen, R., Kleijer, M., Von dem Borne, A. E. G. Kr., Roos, D and Tetteroo, P. A. T. (1988). The PI-linked receptor FcRIII is released on stimulation of neutrophils. *Nature*, **333**, 667-669.

Humphreys, W. J., Spurlock, B. O. and Johnson, J. S. (1974). Critical point drying of ethanol-infiltrated, cryofractured biological specimens for scanning electron

microscopy. In 'Scanning electron microscopy', (Eds. O. Johari and J. Corvin), pp. 275-282. IIT Inst., Chicago.

Hunziker, W. and Mellman, I. (1989). Expression of macrophage-lymphocyte Fc receptors in Madin-Darby canine kidney cells: polarity and transcytosis differ for isoforms with or without coated pit localisation domains. *Journal of Cell Biology*, 109, 3291-3302.

Huxham, I. M. and Beck, F. (1981). Receptor-mediated coated vesicle transport of rat IgG across the 11.5 day in vitro rat yolk sac endoderm. *Cell Biology International Reports*, 5, 1073-1081.

Huxham, I. M. (1982). Yolk-sac receptors: their association with coated vesicles and transport of specific proteins in vitro in the early post-implantation rat conceptus. Ph.D thesis: University of Leicester.

Ishizaka, K. and Ishizaka, T. (1967). Identification of γE-antibodies as a carrier of reaginic activity. *Journal of Immunology*, 99, 1187-1198.

Ishizaka, T., Ishizaka, K., Salmon, S. and Fudenberg, H. (1967). Biologic activities of aggregated γ-globulin. VIII. Aggregated immunoglobulins of different classes. *Journal of Immunology*, 99, 82-91.

Jacobs, P. A., Wilson, C. M., Sprenkle, J. A., Rosenhein, N. B. and Migeon, B. R. (1980). Mechanism of origin of complete hydatidiform moles. *Nature*, 286, 714-716.

Jacobs, P. A., Szulman, A. E., Funkhouser, J., Matsuura, J. S. and Wilson, C. C. (1982). Human triploids: relationship between parental origin of the additional haploid complement and the development of partial hydatidiform mole. *Annals of Human Genetics*, 46, 223-231.

Jenkinson, E. J., Billington, W. D. and Elson, J. (1976). Detection of receptors for immunoglobulin on human placenta by E.A. rosette formation. *Clinical and Experimental Immunology*, 23, 456-461.

Johnson, P. M., Trenchev, P. and Faulk, W. P. (1975). Immunological studies of human placental binding of complexed immunoglobulin by stromal endothelial cells. *Clinical and Experimental Immunology*, 22, 133-138.

Johnson, P. M., Faulk, W. P. and Wang, A. C. (1976). Immunological studies of human placentae: subclass and fragment specificity of binding of aggregated IgG by placental endothelial cells. *Journal of Immunology*, 31, 659-664.

Johnson, P. M., Brown, P. J. and Slade, M. B. (1982). Identification of syncytiotrophoblast-associated IgG in term human placentae. *Journal of Reproductive Immunology*, 4, 1-9.

Johnson, M. H., Chisholm, J. C., Fleming, T. P. and Houliston, E. (1986). A role for cytoplasmic determinants in the development of the mouse early embryo. *Journal of Embryology and Experimental Morphology*, 97 (Supplement), 97-121.

Jones, C. J. P. and Fox, H. (1991). Ultrastructure of the normal human placenta. *Electron Microscopy Reviews*, 4, 129-178.

Jones, E. A. and Waldmann, T. A. (1972). The mechanism of intestinal uptake and transcellular transport of IgG in the neonatal rat. *Journal of Clinical Investigation*, 51, 2916-2927.

Jones, G. E. S., Gey, G. O. and Gey, M. K. (1943). Hormone production by placental cells maintained in continuous culture. *Johns Hopkins Hospital Bulletin*, 72, 26-38.

Jones, W. R. (1979). Tissue specific autoimmune disease in pregnancy. *Clinical Obstetrics and Gynaecology*, 6, 473-483.

Kajii, T. and Ohama, K. (1977). Androgenetic origin of hydatidiform mole. *Nature*, 268, 633-634.

Kaneseki, T. and Kadota, K. (1969). The 'vesicle in a basket'- a morphological study of the coated vesicle isolated from nerve endings of guinea pig brain with special reference to mechanisms of membrane movement. *Journal of Cell Biology*, 42, 202-220.

Kameda, T., Koyama, M., Matsuzaki, N., Taniguchi, T., Saji, F. and Tanizawa, O. (1991). Localisation of three subtypes of Fcγ receptors in human placenta by immunohistochemical analysis. *Placenta*, 12, 15-26.

Kaplan, K. C., Catsoulis, E. A. and Franklin, E. C. (1965). Maternal-foetal transfer of human immune globulins and fragments in rabbits. *Immunology*, 8, 354-359.

Kaufmann, P. and King, B. F. (Eds.) (1981). Structural and functional organisation of the placenta. *Bibliotheca Anatomica*, 22. Karger, Basel.

Kaufmann, P. and Burton, G. (1994). Anatomy and genesis of the placenta. In 'The Physiology of Reproduction', (Eds. E. Knobil and J. D. Neill), pp. 441-484. Raven Press Ltd., New York.

Karnovsky, M. J. (1967). The ultrastructural basis of capillary permeability studied with peroxidase as a tracer. *Journal of Cell Biology*, 35, 213-236.

Keene, D. R., Sakai, L. Y., Lunstrum, G. P., Morris, N. P. and Burgeson, R. E. (1987). Type VII collagen forms an extended network of anchoring fibrils. *Journal of Cell Biology*, 104, 611-621.

Kellenberger, E., Carlemalm, E. and Villiger, W. (1986). Physics of specimen preparation and observation of specimens that involve cryoprocedures. In 'Science of biological specimen preparation', (Eds. M. Müller, R. P. Becker, A. Boyles and J. J. Wolosewick), pp. 1-20. SEM Inc., AMF O'Hare, Chigago.

Kellenberger, E. (1987). The response of biological macromolecules and supramolecular structures to the physics of specimen cryopreparation. In 'Cryotechniques in biological electron microscopy', (Eds. R. A. Steinbrecht and K. Zierold), pp. 35-63. Springer-Verlag, Berlin.

Kelton, J. G., Blanchette, V. S., Wilson, W. E., Powers, P., Pai, K. R., Effer, S. B. and Barr, R. D. (1980). Neonatal thrombocytopenia due to passive immunisation: prenatal diagnosis and the distinction between maternal platelet alloantibodies and autoantibodies. *New England Journal of Medicine*, 302, 1401-1403.

Kempe, C. H. and Benenson, A. S. (1953). Vaccinia. Passive immunity in newborn infants. I. Placental transmission of antibodies. II. Response to vaccination. *Journal of Pediatrics*, 43, 525-531.

King, B. F. and Enders, A. C. (1970). Protein absorption and transport by the guinea pig visceral yolk-sac placenta. *American Journal of Anatomy*, 129, 261-289.

King, B. F. (1977). In vitro absorption of peroxidase-conjugated IgG by human placental villi. *Anatomical Record*, 187, 624-625.

King, B. F. (1982a). Absorption of peroxidase-conjugated immunoglobulin G by human placenta: an in vitro study. *Placenta* 3, 395-406.

King, B. F. (1982b). Cell surface specialisations and intercellular junctions in human amniotic epithelium. An electron microscopic and freeze-fracture study. *Anatomical Record*, 203, 73-82.

Kitzmiller, J. C. (1978). Autoimmune disorders: maternal, fetal and neonatal risks. *Clinical Obstetrics and Gynaecology*, 21, 385-396.

Klima, G., Zerlauth, B., Richeter, J. and Schmidt, W. (1989). Die mikrotextur von amnion - und chorionbindegewebe. *Anatomischer Anzeiger*, 168, 395-400.

Kohler, G. and Milstein, C. (1975). Continuous cultures of fused cells secreting antibodies of predefined specificity. *Nature*, 256, 495-497.

Kohler, P. F. and Farr, R. S. (1966). Elevation of cord over maternal IgG immunoglobulins. *Nature*, 210, 1070-1071.

Koshland, M. E. and Englberger, F. M. (1963). Differences in the amino acid composition of two purified antibodies from the same rabbit. *Proceedings of the National Academy of Science of the USA*, 50, 61-68.

Kristoffersen, E. K., Ulvestad, E., Vedeler, C. A. and Matre, R. (1990). Fcγ receptor Heterogeneity in the human placenta. *Scandinavian Journal of Immunology*, 31, 561-564.

Kronvall, G. and Williams, R. C. Jr. (1969). Differences in anti-Protein A activity among IgG subgroups. *Journal of Immunology*, 103, 828-833.

Kronvall, G. and Frommel, D. (1970). Definition of staphylococcal protein A reactivity for human immunoglobulin G fragments. *Immunochemistry*, 7, 124-127.

Kulangara, A. C., Menon, M. K. K. and Willmott, M. (1965). Passage of bovine serum albumin from the uterine lumen to the human foetus. *Nature*, 206, 1259-1260.

Kurosaki, T. and Ravetch, J. V. (1989). A single amino acid in the glycosyl phosphatidylinositol attachment domain determines the membrane topology of FcγRIII. *Nature*, 342, 805-807.

Lanier, L. L., Cwirla, S., Yu, G., Testi, R. and Phillips, J. H. (1989). Membrane anchoring of a human IgG Fc receptor (CD16) determined by a single amino acid sequence. *Science*, 246, 1611-1613.

Lanzavecchia, G. and Moranno, E. (1959). Ultrastruttura dell' epitelio amniotico umano, osservato al microscopio elettronico. *Archives dell Italia Anatomie e Embriologie*, 64, 74-86.

Lawler, S. D., Pickthall, V. J., Fisher, R. A., Povey, S., Wyn Evans, M. and Szulman, A. E. (1979). Genetic studies of complete and partial hydatidiform moles. *Lancet*, 2, 580.

Lawler, S. D., Fisher, R. A., Pickthall, V. J., Povey, S. and Evans, M. W. (1982a). Genetic studies on hydatidiform moles. I. The origin of partial moles. *Cancer Genetics and Cytogenetics*, 5, 309-320.

Lawler, S. D., Povey, S., Fisher, R. A. and Pickthall, V. J. (1982b). Genetic studies on hydatidiform moles. II. The origins of complete moles. *Annals of Human Genetics*, 46, 209-222.

Leslie, G. A. and Swate, T. E. (1972). Structure and biologic functions of human IgD. I. The presence of immunoglobulin D in cord sera. *Journal of Immunology*, 109, 47-50.

Leslie, R. G. Q. (1980). The binding of soluble immune complexes of guinea pig IgG_2 to homologous peritoneal macrophages. Determination of the avidity constants at 4°C. *European Journal of Immunology,* 10, 317-322.

Lewis, V. A., Koch, T., Plutner, H. and Mellman, I. (1986). Characterisation of a cDNA clone for a mouse macrophage-lymphocyte Fc receptor. *Nature,* 324, 372-375.

Lichter, E. A. and Dray, S. (1964). Immunoelectrophoretic characterisation of human serum proteins with primate antisera. *Journal of Immunology,* 92, 91-99.

Lin, C. T. (1980). Immunoelectron microscopic localisation of immunoglobulin G in human placenta. *Journal of Histochemistry and Cytochemistry,* 28, 339-346.

Linnet-Jepsen P., Galatius-Jepsen F. and Hauge, M. (1958). On the inheritance of the Gm serum group. *Acta Genetica (Basel),* 8, 164-167.

Litwin, S. D. and Balaban, S. (1972). A quantitative method for determining human gamma-G allotype antigens (Gm). II. Differences in Gm gene expression for γG_1 and γG_3 H chains in sera. *Journal of Immunology,* 108, 991-999.

Leder, P. (1982). The genetics of antibody diversity. *Scientific American,* 246, 72-83.

Loke, Y. W. (1978). Immunology and immunopathology of the human foetal-maternal interaction. pp. 1-328. Elsevier/North Holland Biomedical press, Amsterdam.

Looney, R. J., Abraham, G. N. and Anderson, C. L. (1986). Human monocytes and U397 cells bear two distinct Fc receptors for IgG. *Journal of Immunology,* 136, 1641-1647.

Lu, C. Y., Beller, D. I. and Unanue, E. R. (1980). During ontogeny, Ia-bearing accessory cells are found early in the thymus but late in the spleen. *Proceedings of the National Academy of Science of the USA,* 77, 1597-1601.

Malak, T. M., Ockleford, C. D., Bell, S. C., Dalgleish, R., Bright, N. and Macvicar, J. (1993). Confocal immunofluorescence localisation of collagen types I, III, IV, V and VI and their ultrastructural organisation in term human fetal membranes. *Placenta,* 14, 385-406.

Mantyjarvi, R., Hirvonen, T. and Toivanen, P. (1970). Maternal antibodies in human neonatal sera. *Immunology,* 18, 449-451.

Marsh, M. and Helenius, A. (1981). Adsorptive endocytosis of Semliki Forest virus. *Journal of Molecular Biology,* 142, 439-454.

Martin, B. J. and Spicer, S. S. (1973). Multivesicular bodies and related structures of the syncytiotrophoblast of human term placenta. *Anatomical Record,* 175, 15-36.

Matre, R., Tonder, O. and Endersen, C. (1975). Fc receptors in the human placenta. *Scandinavian Journal of Immunology,* 4, 741-745.

Matre, R. (1977). Similarities of Fc receptors on trophoblasts and placental endothelial cells. *Scandinavian Journal of Immunology,* 6, 953-958.

Matre, R. and Haugen, A. (1978). The placental Fc receptors studies using immune complexes of peroxidase. *Scandinavian Journal of Immunology,* 8, 187-193.

Matre, R., Kleppe, G. and Tonder, O. (1981). Isolation and characterisation of Fc receptors from the human placenta. *Acta Pathologica et Microbiologica Scandinavica Section C,* 89, 209-213.

Maxfield, F. R., Schlessinger, J., Schechter, Y., Patsan, I. and Willingham, M. C. (1978). Collection of insulin, EGF and α2 macroglobulin in the same patches on the surface of cultured fibroblasts and common internalisation. *Cell*, 14, 805-810.

Mayhew, T. M. and Burton, G. J. (1988). Methodological problems in placental morphometry: Apologia for the use of stereology based on sound sampling practice. *Placenta*, 9, 565-581.

McNabb, T., Koh, T. Y., Dorrington, K. J. and Painter, R. H. (1976). Structure and function of immunoglobulin domains. V. Binding of immunoglobulin G and fragments to placental membrane preparations. *Journal of Immunology*, 117, 882-888.

Meittinen, H. M., Rose, J. K. and Mellman, I. (1989). Fc receptor isoforms exhibit distinct abilities for coated pit localisation as a result of cytoplasmic domain heterogeneity. *Cell*, 58, 317-327.

Mellman, I. and Unkeless, J. C. (1980). Purification of a functional mouse Fc receptor through the use of a monoclonal antibody. *Journal of Experimental Medicine*, 152, 1048-1069.

Mellman, I., Plutner, H., Steinman, R. M., Unkeless, J. C. and Cohn, Z. A. (1983). Internalisation and degradation of macrophage Fc receptors during receptor-mediated phagocytosis. *Journal of Cell Biology*, 96, 887-895.

Mellman, I. and Plutner, H. (1984). Internalisation and degradation of macrophage Fc receptors bound to polyvalent immune complexes. *Journal of Cell Biology*, 98, 1170-1177.

Mellman, I., Plutner, H. and Ukkonen, P. (1984). Internalisation and rapid recycling of macrophage Fc receptors tagged with monovalent anti-receptor antibody: possible role of a pre-lysosomal compartment. *Journal of Cell Biology*, 98, 1163-1169.

Mellman, I., Kock, T., Healey, G., Hunziker, W., Lewis, V., Plutner, H., Meittinen, H., Vaux, D., Moore, K. and Stuart, S. (1988). Structure and function of Fc receptors on macrophages and lymphocytes. *Journal of Cell Science*, 9 (Suppl), 45-65.

Mellman, I. (1989). Relationships between structure and function in the Fc receptor family. *Current Opinions in Immunology*, 1, 16-25.

Michaelsen, T. E., Frangione, B. and Franklin, E. C. (1977). The amino acid sequence of a human immunoglobulin G3m(g) pFc' fragment. *Journal of Immunology*, 119, 558-563.

Midgley, A. R. Jr. and Pierce, G. B. Jr. (1962). Immunohistochemical localisation of human chorionic gonadotrophin. *Journal of Experimental Medicine*, 115, 289-294.

Milstein, C., Galfre, G., Secher, D. S. and Springer, T. (1979). Monoclonal antibodies and cell surface antigens. *Cell Biology International Reports*, 3, 1-16.

Modesti, A., Scarpa, S., D'Orazi, G., Simonelli, L. and Caramia, F. G. (1989). Localisation of type IV and type V collagens in the stroma of human amnion. *Developments in Ultrastructure of Reproduction*, 296, 459-463.

Monif, G. R. G. and Mendenhall, H. W. (1970). Immunoglobulin G levels and the titres of specific antiviral antibodies in amniotic fluid. *American Journal of Obstetrics and Gynaecology*, 108, 651-654.

Mongan, L. C. and Ockleford, C. D. (1994). The transport of IgG subclasses across the human placenta. *Journal of Anatomy*, In press.

Morell, A., Terry, W. D. and Waldmann, T. A. (1970) Metabolic properties of IgG subclasses in man. *Journal of Clinical Investigation*, 49, 673-680.

Morell, A., Skvaril, F., Hitzig, W. H. and Barandun, S. (1972a). IgG subclasses: development of the serum concentrations in "normal" infants and children. *Journal of Pediatrics*, 80, 960-964.

Morell, A., Skvaril, F., Steinberg, A. G., Van Loghem, E. and Terry, W. D. (1972b). Correlations between concentrations of the four subclasses of IgG and Gm allotypes in normal human sera. *Journal of Immunology*, 108, 195-206.

Morphis, L. G. and Gitlin, D. (1970). Maturation of the maternofoetal transport system for human γG in the mouse. *Nature*, 228, 573.

Moskalewski, S., Ptak, W. and Czarnik, K. (1975). Demonstration of cells with IgG receptor in human placenta. *Biology of the Neonate*, 26, 268-273.

Mossman, H. W. (1987). Vertebrate fetal membranes. pp. 1-383. McMillan, Basingstoke.

Moxon, L. A., Wild, A. E. and Slade, B. S. (1976). Localisation of proteins in coated micropinocytic vesicles during transport across rabbit yolk-sac endoderm. *Cell and Tissue Research*, 171, 175-193.

Nakane, P. K. and Pierce, G. B. Jr. (1966). Enzyme-labelled antibodies: preparation and application for the localisation of antigens. *Journal of Histochemistry and Cytochemistry*, 14, 929-931.

Nanaev, A. K., Rukosuev, V. S., Shirinsky, V. P., Milovanov, A. P., Domogatsky, S. P., Duance, V. C., Bradbury, F. M., Yarrow, P., Gardiner, L., d'Lacey, C. and Ockleford, C. D. (1991). Confocal and conventional immunofluorescent and immunogold electron microscopic localisation of collagen types III and IV in human placenta. *Placenta*, 12, 573-595.

Neill, J. M., Gaspari, E. L., Richardson, L. V. and Sugg, J. Y. (1932). Diphtheria antibodies transmitted from mother to child. *Journal of Immunology*, 22, 117-124.

Nevard, C. H. F., Gaunt, M. and Ockleford, C. D. (1990). The transfer of passive and active immunity. In 'The immunology of the fetus', (Ed. G. Chaouat), pp. 193-214. CRC Press, Boca Raton, Florida.

Niezgodka, M., Mikulska, J., Ugorski, M., Boratynski, J. and Lisowski, J. (1981). Human placental membrane receptors for IgG-I. Studies on properties and solubilisation of the receptor. *Molecular Immunology*, 18, 163-172.

Nisonoff, A., Wissler, F. C., Lipman, L. N. and Woernley, D. L. (1960). Separation of univalent fragments from the bivalent rabbit antibody molecule by reduction of disulphide bonds. *Archives of Biochemistry and Biophysics*, 89, 230-244.

Ockleford, C. D. (1976). A three-dimensional reconstruction of the polygonal pattern on placental coated vesicle membranes. *Journal of Cell Science*, 21, 83-91.

Ockleford, C. D. and Whyte, A. (1977). Differentiated regions of human placental cell surface associated with the exchange of materials between maternal and foetal blood. The structure, distribution, ultrastructural cytochemistry and biochemical composition of coated vesicles. *Journal of Cell Science*, 25, 293-312.

Ockleford, C. D., Whyte, A. and Bowyer, D. E. (1977a). Variation in the volume of coated vesicles isolated from the human placenta. *Cell Biology International Reports*, 1, 137-146.

Ockleford, C. D., Whyte, A. and Bowyer, D. E. (1977b). Negative staining of coated vesicles. *Micron*, 8, 233-235.

Ockleford, C. D. and Clint, J. M. (1980). The uptake of IgG by human placental chorionic villi: A correlated autoradiographic and wide aperture counting study. *Placenta*, 1, 91-111.

Ockleford, C. D. and Whyte, A. (Eds.) (1980). Coated vesicles. pp. 1-344. Cambridge University Press, Cambridge.

Ockleford, C. D., Wakely, J. and Badley, R. A. (1981). Morphogenesis of human placental chorionic villi; cytoskeletal, syncytioskeletal and extracellular matrix proteins. *Proceedings of the Royal Society of London Series B*, 212, 305-316

Ockleford, C. D., Hsi, B. -L., Wakely, J., Badley, R. A., Whyte, A. and Page Faulk, W. (1981). Propidium Iodide as a nuclear marker in immunofluorescence. I. Use with tissue and cytoskeletal studies. *Journal of Immunological Methods* 43, 261-267.

Ockleford, C. D. (1982). Coated vesicles. In *'Electron microscopy of proteins'*, (Ed. R. Harris), pp. 255-299. Academic Press.

Ockleford, C. D. and Dearden, L. (1984). The acquisition of immunity by the fetus. In *'Immunological aspects of reproduction in mammals'*, (Ed. D. B. Crighton), pp. 251-263. Butterworths, London.

Ockleford, C., Barker, C., Griffiths, J., McTurk, G., Fisher, R. and Lawler, S. (1989). Hydatidiform mole: An ultrastructural analysis of syncytiotrophoblast surface organisation. *Placenta*, 10, 195-212.

Ockleford, C. D. (1990). An atlas of antigens. pp. 1-323. MacMillan-Stockton Press, Basingstoke.

Ockleford, C. D., McCracken, S. A., Rimmington, L. A., Hubbard, A. R. D., Bright, N. A., Jefferson, T. B. and d'Lacey, C. (1993a). Vertical integration of amnion layers by type VII collagen rivets. *Journal of Pathology*, 170 (suppl), 44.

Ockleford, C., Bright, N., Hubbard, A., d'Lacey, C., Smith, J., Gardiner, L., Sheikh, T., Albentosa, M. and Turtle, K. (1993b). Micro-trabeculae, macroplaques or mini-basement membranes in human term fetal membranes? *Philosophical Transactions of the Royal Society of London Series B, Biological Sciences*, 342, 121-136.

Ockleford, C., Abdel-Malak, T., Hubbard, A., Braken, K., Burton, S.-A., Bright, N., Blakey, G., Goodliffe, J., Garrod, D. and d'Lacey, C. (1993c). Confocal and conventional immunofluorescence and ultrastructural localisation of intracellular strength giving components of human fetal membranes. *Journal of Anatomy*, 183, 483-505.

Ockleford, C. D., Bright, N. A., Hubbard, A. R. D., McCracken, S. A., Rimmington, L. A., Byrd, N. A., Byrne, S., Cockcroft, N., Jefferson, T. B. and d'Lacey, C. (1994). Type VII collagen associated with the basement membrane of a simple epithelium produces giant anchoring rivets which penetrate a massive lamina reticularis. In revision.

Ogra, S. S., Weintraub, D. and Ogra, P. L. (1977). Immunological aspects of human colostrum and milk. III fate and absorption of cellular and soluble components via the gastrointestinal tract of the newborn. *Journal of Immunology*, 119, 245-248.

Ohama, K., Kajii, T., Okamoto, E., Fukada, Y., Imaizumi, K., Tsukahara, M., Kobayashi, K. and Hagiwara, K. (1981). Dispermic origin of XY hydatidiform mole. *Nature*, **292**, 551-552.

Olding, L. (1972). The possibility of materno-foetal transfer of lymphocytes in man. *Acta Paediatrica Scandinavica*, **61**, 73-78.

Osborn, J. J., Dancis, J. and Julia, J. F. (1952). Studies on the immunology of the newborn infant. II. Interference with active immunisation by passive transplacental circulating antibody. *Pediatrics*, **10**, 328-334.

Osborn, M. and Weber, K. (1982). Immunofluorescence and immunocytochemical procedures with affinity-purified antibodies: tubulin containing structures. In *'Methods in Cell Biology'*, 24, (Ed. L. Wilson), pp. 97-132. Academic Press, Boston.

Pan, L., Mendel, D. B., Zurlo, J. and Guyre, P. M. (1990). Regulation of the steady state level of FcγRI mRNA by IFN-gamma and dexamethasone in human monocytes, neutrophils and U-937 cells. *Journal of Immunology*, **145**, 267-275.

Panigel, M. and Anh, J. N. H. (1963). Precisions sur l'evolution de l'ultrastructure des elements trophoblastiques et sur leurs modifications superficielles dans le placenta humain. *Comptes Rendus Hebdomadaires des Seances de l'Academie des Sciences. Serie D. Sciences Naturelles*, **257**, 3669-3671.

Pearse, B. M. F. (1976). Clathrin: a unique protein associated with intracellular transfer of membrane by coated vesicles. *Proceedings of the National Academy of Sciences of the USA*, **73**, 1255-1259.

Pearse, B. M. F. (1978). On the structural and functional components of coated vesicles. *Journal of Molecular Biology*, **126**, 803-812.

Pearse, B. M. F. (1980). Coated vesicles. *Trends in Biochemical Sciences*, **111**, 131-134.

Pearse, B. M. F. and Bretscher, J. (1981). Membrane recycling by coated vesicles. *Annual Review of Biochemistry*, **50**, 85-101.

Pearse, B. M. F. (1982). Coated vesicles from human placenta carry ferritin, transferrin and immunoglobulin G. *Proceedings of the National Academy of Sciences of the USA*, **79**, 451-455.

Pearse, B. M. F. (1987). Clathrin and coated vesicles. *EMBO Journal*, **6**, 2507-2512.

Peltz, G., Frederick, K., Anderson, C. L. and Peterlin, B. M. (1988). Characterisation of the human monocyte high affinity Fc receptor (hu FcRI). *Molecular Immunology*, **25**, 243-250.

Perussia, B., Acuto, O., Terhorst, C., Faust, J., Lazarus, R., Fanning, V. and Trinchieri, G. (1984). Human natural killer cells analysed by B73.1, a monoclonal antibody blocking Fc receptor functions. II. Studies of B73.1 antibody-antigen interaction on the lymphocyte membrane. *Journal of Immunology*, **130**, 2142-2148.

Peters, H. (1899). Über die Einbettung des menschlichen Eies und das früheste bisher bekante menschliche Placentationsstadium. Deutike, Leipzig und Vienna.

Petersen, O. W. and Van Deurs, B. (1983). Serial section analysis of coated pits and vesicles involved in absorptive pinocytosis in cultured fibroblasts. *Journal of Cell Biology*, **96**, 277-281.

Petsko. G. A. (1975). Protein crystallography at sub-zero temperatures: cryo-protective mother liquose for protein crystals. *Journal of Molecular Biology*, **96**, 381-392.

Pilch, P., Shia, M., Benson, R. J. and Fine, R. (1983). Coated vesicles participate in receptor-mediated endocytosis of insulin. *Journal of Cell Biology*, **96**, 133-138.

Pitcher-Wilmott, R. W., Hindocha, P. and Wood, C. B. S. (1980). The placental transfer of immunoglobulin and subclasses in human pregnancy. *Clinical and Experimental Immunology*, **41**, 303-308.

Polak, J. M. and Van Noorden, S. (Eds.) (1983). Immunocytochemistry: Practical applications in pathology and biology. pp. 1-396. Wright PSG, Bristol.

Polak, J. M. and Varndell, I. M. (Eds.) (1984). Immunolabelling for electron microscopy. pp. 1-370. Elsevier, Amsterdam.

Porter, R. R. (1959). The hydrolysis of rabbit γ-globulin and antibodies with crystalline papain. *Biochemical Journal*, **73**, 119-127.

Porter, R. R. (1960). The chemical structure of gammaglobulin and antibodies and its relation to theories of antibody formation. In 'Mechanisms of antibody formation', A symposium Holub and Jaroskova, pp. 208-210. Academic Press.

Pratt, B. and Madri, M. (1985). Immunolocalisation of type IV collagen and laminin in non basement membrane structures of murine corneal stroma. *Laboratory Investigation*, **52**, 650-656.

Pumphrey, R. (1986). Computer models of the human immunoglobulins: Shape and segmental flexibility. *Immunology Today*, **7**, 174-184.

Qiu, W. Q., de Bruin, B., Brownstein, B. H., Pearse, R. and Ravetch, J. V. (1990). Organisation of the human and mouse low affinity FcγR : duplication and recombination. *Science*, **248**, 732-735.

Raff, H. V., Picken, L. J. and Stobo, J. D. (1980). Macrophage heterogeneity in man. A subpopulation of HLA-DR bearing macrophages required for antigen-induced T-cell activation also contain stimulators for autologous-reactive T-cells. *Journal of Experimental Medicine*, **152**, 581-593.

Ravetch, J. V., Luster, A. D., Weinshank, R., Kochan, J., Pavlovec, A., Portnoy, D. A., Hulmes, J., Pan, Y. -C. E. and Unkeless, J. C. (1986). Structural heterogeneity and functional domains of murine immunoglobulin G Fc receptors. *Science*, **234**, 718-725.

Ravetch, J. V. and Perussia, B. (1989). Alternative membrane forms of FcγRIII (CD16) on human natural killer cells and neutrophils: cell-type specific expression of two genes which differ in single nucleotide substitutions. *Journal of Experimental Medicine*, **170**, 481-497.

Ravetch, J. V. and Kinet, J. P. (1991). Fc receptors. *Annual Review of Immunology*, **9**, 457-492.

Recht, B., Frangione, B., Franklin, E. and Van Loghem, E. (1981). Structural studies of a human γ3 myeloma protein (GOE) that binds Staph protein A. *Journal of Immunology*, **127**, 917-923.

Reynolds, E. S. (1963). The use of lead citrate at high pH as an electron opaque stain in electron microscopy. *Journal of Cell Biology*, **17**, 208-212.

Richart, R. (1961). Studies of placental morphogenesis. I. Radioautographic studies of human placenta utilising tritiated thymidine. *Proceedings of the Society for Experimental and Biological Medicine*, **106**, 829-831.

Riggs, J. L., Seiwald, R. J., Burckhalter, J. H., Downs, C. M. and Metcalf, T. G. (1958). Isothiocyanate compounds as fluorescent labelling agents for immune serum. *American Journal of Pathology*, **34**, 1081-1097.

Rodewald, R. (1976). Intestinal transport of peroxidase-conjugated IgG fragments in the neonatal rat. In '*Maternofoetal transmission of immunoglobulins*', (Ed. W. A. Hemmings), pp. 137-149. Cambridge University Press, New York.

Rodewald, R. (1980). Immunoglobulin transmission in mammalian young and the involvement of coated vesicles. In '*Coated vesicles*', (Eds. C. D. Ockleford and A. Whyte), pp. 69-101. Cambridge University Press, New York.

Romano, E. L., Stolinski, C. and Hughes-Jones, N. C. (1974). An antiglobulin reagent labelled with colloidal gold for use in electron microscopy. *Immunochemistry*, **11**, 521-522.

Rote, N. S. (1982). Pathophysiology of Rh isoimmunisation. *Clinical Obstetrics and Gynaecology*, **25**, 243-253.

Roth, T. F. and Porter, K. R. (1964). Yolk protein uptake in oocyte of mosquito, <u>Aedes aegypti</u>. *Journal of Cell Biology*, **20**, 313-332.

Roth, J. (1982). The protein A-gold (pAg) technique - A qualitative and quantitative approach for antigen localisation on thin sections. In '*Techniques in immunocytochemistry* (volume 1)', (Eds. G. R. Bullock and P. Petrusz), pp. 107-133. Academic Press, London.

Roth, J. (1989). Postembedding labelling on Lowicryl K4M tissue sections: detection and modification of cellular components. *Methods in Cell Biology*, **31**, 513-550.

Rothman, J. E. and Fine, R. E. (1980). Coated vesicles transport newly synthesised membrane glycoproteins from endoplasmic reticulum to plasma membrane in two successive stages. *Proceedings of the National Academy of Sciences of the USA*, **77**, 780-784.

Ryan, K.J. (1959). Metabolism of C-16 oxygenated steroids by the human placenta. The formation of estriol. *Journal of Biological Chemistry*, **234**, 2006-2008.

Sage, H. (1982). Collagens of basement membrane. *Journal of Investigative Dermatology*, **79**, 51-59.

Sakai, L. Y., Keene, D. R., Morris, N. P. and Burgeson, R. E. (1986). Type VII collagen is a major structural component of anchoring fibrils. *Journal of Cell Biology*, **103**, 1577-1586.

Salisbury, J. L., Condeelis, J. S., Maihle, N. J. and Satir, P. (1981). Calmodulin localisation during capping and receptor mediated endocytosis. *Nature*, **294**, 163-166.

Saluk, P. H. and Clem, W. (1975). Studies on the cryoprecipitation of a human IgG_3 cryoglobulin: the effects of temperature induced conformational changes on the primary interaction. *Immunochemistry*, **12**, 29-37.

Scallon, B. J., Scigliano, E., Freedman, V. H., Miedel, M. C., Pan, Y. -C. E., Unkeless, J. C. and Kochan, J. P. (1989). A human immunoglobulin G receptor exists in both polypeptide-anchored and phophatidylinositol-glycan-anchored forms. *Proceedings of the National Academy of Sciences of the USA*, **86**, 5079-5083.

Schanfield, M. S. (1976). Genetic markers of human immunoglobulins. In *Basic and Clinical Immunology*, (Eds. H. H. Fudenberg, D. P. Stites, J. I. Caldwell and J. V. Wells), pp. 59-65. Lange Medical Publications, Los Altos, California.

Scher, M. G., Unanue, E. R. and Beller, D. U. (1982). Regulation of macrophage populations. III. The immunologic induction of exudates rich in Ia-positive macrophages is a radiosensitive process. *Journal of Immunology*, **128**, 447-450.

Schmidt, W. (1965). Über den paraplacentaren, fruchtwassergebunden strofftransport beim menschen. I. Histochemische untersuchung der in den eihäuten angereicherten stroffe. *Zeitschrift für Anatomie und Entwicklungsgeschichte*, **124**, 321-334.

Schmidt, W. (1992). The amniotic fluid compartment: The fetal habitat. *Advances in Anatomy, Embryology and Cell Biology*, **127**, 1-100. Springer-Verlag, Berlin.

Schröder, J. (1974). Passage of leukocytes from mother to fetus. *Scandinavian Journal of Immunology*, **3**, 369-374.

Schur, P. H. (1972). Human gamma-G subclasses. *Progress in Clinical Immunology*, **1**, 71-104.

Schur, P. H., Alpert, E. and Alper, C. (1973). Gamma G groups in human fetal, cord and maternal sera. *Clinical Immunology and Immunopathology*, **2**, 62-66.

Schwartz, J. H. and Edelman, G. M. (1963). Comparisons of Bence-Jones proteins and L polypeptide chains of myeloma globulins after hydrolysis with trypsin. *Journal of Experimental Medicine*, **118**, 41-53.

Schwartzacher, H. G. (1960). Beitrag zur histogenese des menschlichen amnions. *Acta Anatomica*, **43**, 303-311.

Scott, J. S., Maddison, P. J., Taylor, P. V.,Esscher, E., Scott, O. and Skinner, R. P. (1983). Connective tissue disease, antibodies to ribonucleoprotein and congenital heart block. *New England Journal of Medicine*, **309**, 209-212.

Sears, D., Osman, N., Tate, B., McKenzie, I. F. C. and Hogarth, P. M. (1990). Molecular cloning and expression of the mouse high affinity Fc receptor for IgG. *Journal of Immunology*, **144**, 371-378.

Selvaraj, P., Rosse, W. F., Silber, R. and Springer, T. A. (1988). The major Fc receptor in blood has a phosphatidylinositol anchor and is deficient in paroxysomal nocturnal hemoglobinuria. *Nature*, **333**, 564-567.

Selvaraj, P., Carpén, O, Hibbs, M. L. and Springer, T. A. (1989). Natural killer cell and granulocyte Fcγ receptor III (CD16) differ in membrane anchor and signal transduction. *Journal of Immunology*, **143**, 3283-3288.

Shakib, F. and Stanworth, D. R. (1980). Human IgG subclasses in health and disease (A review). Part II. *La Ricerca In Clinica E In Laboratorio*, **10**, 561-571.

Siegenbeek van Heukelom, D. E. (1898). Über die menschliche Placentation. *Archives für Anatomie und Physiologie (Anat. Abthlg)*, 1-36.

Silverton, E. W., Navia, M. A. and Davis, D. R. (1977). Three-dimensional structure of an intact human immunoglobulin. *Proceedings of the National Academy of Sciences of the USA*, **74**, 5140-5144.

Simister, N. E. and Mostov, K. E. (1989). An Fc receptor structurally related to MHC class I antigens. *Nature*, **337**, 184-187.

Simmons, D. and Seed, B. (1988). The Fcγ receptor of natural killer cells is a phospholipid linked membrane protein. *Nature*, **333**, 568-570.

Singer, S. J. (1959). Preparation of an electron-dense antibody conjugate. *Nature*, **183**, 1523-1524.

Slot, J. W. and Geuze, H. J. (1983). The use of protein A-colloidal gold (PAG) complexes as immunolabels in ultrathin frozen sections. In *'Immunohistochemistry'*, (Ed. A. C. Cuello), pp. 323-346. John Wiley & Sons, Chichester.

Smith, J. and Ockleford, C. D. (1994). Laser scanning confocal examination and comparison of nidogen (entactin) with laminin in term human amniochorion. *Placenta*, **15**, 95-106.

Sorensen, R. U., Tomford, J. W., Gyves, M. T., Judge, N. E. and Polmar, S. H. (1984). Use of intravenous immune globulin in pregnant women with common variable hypogammaglobulinemia. *American Journal of Medicine*, **76**, 73-83.

Speigelberg, H. L. and Fishkin, B. G. (1972). The catabolism of human γG immunoglobulins of different heavy chain subclasses. III. The catabolism of heavy chain disease proteins and of Fc fragments of myeloma proteins. *Clinical and Experimental Immunology*, **10**, 599-607.

Spiegelberg, H. L. (1974). Biological activities of immunoglobulins of different classes and subclasses. *Advances in Immunology*, **19**, 259-294.

Spurr, A. R. (1969). A low-viscosity epoxy resin embedding medium for electron microscopy. *Journal of Ultrastructure Research*, **26**, 31-43.

Steigman, A. J. and Lipton, M. M. (1958). Neonatal immunity II. Poliocidal effect of human amniotic fluids. *Proceedings of the Society for Experimental Biology and Medicine*, **99**, 576-579.

Stengelin, S., Stamenkovic, I. and Seed, B. (1988). Isolation of cDNAs for two distinct human Fc receptors by ligand affinity cloning. *EMBO Journal*, **7**, 1053-1059.

Stiehm, E. R. and Fudenberg, H. H. (1966). Serum levels of immune globulins in health and disease: a survey. *Pediatrics*, **37**, 715-727.

Stiehm, R. E. (1975). Fetal defence mechanisms. *American Journal of Diseases of Children*, **129**, 438-443.

Stone, D. L., Suzuki, Y. and Wood, G. W. (1987). Human amnion as a model for IgG transport. *American Journal of Reproductive Immunology and Microbiology*, **13**, 36-43.

Stuart, S. G., Simister, N. E., Clarkson, S. B., Kacinski, B. M., Shapiro, M. and Mellman, I (1989). Human IgG Fc receptor (hFcRII; CD32) exists as multiple isoforms in macrophages, lymphocytes and IgG-transporting placental epithelium. *EMBO Journal*, **8**, 3657-3666.

Surolia, A., Pain, D. and Kahn, M. I. (1982). Protein A: nature's universal anti-antibody. *Trends in Biochemical sciences*, **7**, 74-76.

Szulman, A. E. and Surti, U. (1978). The syndromes of hydatidiform mole. II. Morphologic evolution of the complete and partial mole. *American Journal of Obstetrics and Gynaecology*, **132**, 20-27.

Ten Broeck, C. and Bauer, J. H. (1923). The transmission of tetanus antitoxin through the placenta. *Proceedings of the Society for Experimental Biology and Medicine,* 20, 399-400.

Terry, W. D. and Fahey, J. L. (1964a). Heterogeneity of the H chains of human 7S gamma-globulin. In *'48th annual meeting of the Federation of American Societies for Experimental Biology'.* Chicago.

Terry, W. D. and Fahey, J. L. (1964b). Subclasses of human γ_2 globulin based on differences in the heavy polypeptide chains. *Science,* 146, 400-401.

Thomas, C. E. (1965). The ultrastructure of human amniotic epithelium. *Journal of Ultrastructure Research,* 13, 65-84.

Tokuyasu, K. T. (1973). A technique for ultracryotomy of cell suspensions and tissues. *Journal of Cell Biology,* 57, 551-565.

Tokuyasu, K. T. (1978). A study of positive staining of ultrathin frozen sections. *Journal of Ultrastructure Research,* 63, 287-307.

Tokuyasu, K. T. and Singer, J. S. (1976). Improved procedures for immunoferritin labelling of ultrathin frozen sections. *Journal of Cell Biology,* 71, 894-906.

Tulp, A., Verwoerd, D., Dobberstein, B., Ploegh, H. L. and Pieters, J. (1994). Isolation and characterisation of the intracellular MHC class II compartment. *Nature,* 369, 120-126.

Turner, J. H., Wald, N. and Quinlivan, W. L. G. (1966). Cytogenetic evidence concerning possible transplacental transfer of leukocytes in pregnant women. *American Journal of Obstetrics and Gynaecology,* 95, 831-836.

Ukkonen, P., Lewis, V., Marsh, M., Helenius, A. and Mellman, I. (1986). Transport of macrophage Fc receptors and Fc receptor-bound ligands to lysosomes. *Journal of Experimental Medicine,* 163, 952-971.

Unanue, E. R., Beller, D. I., Lu, C. Y. and Allen, P. M. (1984). Antigen presentation: comments on its regulation and mechanism. *Journal of Immunology,* 132, 1-5.

Ungewickell, E. and Branton, D. (1981). Assembly units of clathrin coats. *Nature,* 289, 420-422.

Unkeless, J. C. (1977). The presence of two Fc receptors on murine macrophages: evidence from a variant cell line and differential trypsin sensitivity. *Journal of Experimental Medicine,* 145, 931-947.

Unkeless, J. C. (1979). Characterisation of a monoclonal antibody directed against mouse macrophage and lymphocyte Fc receptors. *Journal of Experimental Medicine,* 150, 580-596.

Unkeless, J. C., Fleit, H. and Mellman, I. S. (1981). Structural aspects and heterogeneity of immunoglobulin Fc receptors. *Advances in Immunology,* 31, 247-270.

Usategui-Gomez, M., Morgan, D. F. and Toolan, H. W. (1967). A comparative study of amniotic fluid, maternal sera and cord sera by disc electrophoresis. *Proceedings of the Society for Experimental Biology and Medicine,* 123, 547-551.

Usategui-Gomez, M. and Stearns, S. (1969). Comparative study of the Rh.D antibody titres of amniotic fluids and corresponding maternal sera in Rh.D sensitised pregnancies. *Nature,* 221, 82-83.

Vahlquist, B., Lagercrantz, R. and Nordbring, F. (1950). Maternal and fetal titres of antistreptolysin and antistaphylolysin at different stages of gestation. *Lancet*, **2**, 851-853.

Van der Meulen, J. A., McNabb, T. C., Haeffner-Cavaillon, N., Klein, M. and Dorrington, K. J. (1980). The Fcγ receptor on human placental plasma membrane. I. Studies on the binding of homologous and heterologous immunoglobulin G. *Journal of Immunology*, **124**, 500-507.

Van Loghem, E. (1978). Genetic Studies on human immunoglobulins. In *'Handbook of experimental immunology'*, (Ed. **D. M. Weir**), pp. 11.1-11.16. Blackwell scientific Publications, Oxford.

Van Loghem, E. (1986). Allotypic markers. *Monographs in Allergy*, **19**, 40-51.

Vassilakos, P., Riotton, G. and Kajii, T. (1977). Hydatidiform mole: two entities. A morphological and cytogenetic study with some clinical observations. *American Journal of Obstetrics and Gynaecology*, **127**, 167-170.

Vaughn, M., Taylor, M. and Mohanakumar, T. (1986). Characterisation of human IgG Fc receptors. *Journal of Immunology*, **135**, 4059-4065.

Virella, G., Nunes, M. A. S. and Tamagnini, G. (1972). Placental transfer of human IgG subclasses. *Clinical and Experimental Immunology*, **10**, 475-478.

Vivier, E., Ackerly, M., Rochet, N. and Anderson, P. (1992). Structure and function of the CD16:ζ:γ complex expressed on human natural-killer cells. *International Journal of Cancer*, **7** (suppl), 11-14.

Wall, D. A., Wilson, G. and Hubbard, A. L. (1980). The galactose-specific recognition system of the mammalian liver: the route of ligand internalisation in rat hepatocytes. *Cell*, **21**, 79-93.

Wang, A. C. Faulk, W. P., Struckley, M. A. and Fundenberg, H. H. (1970). Chemical differences of adult, foetal and hypogammaglobulinaemic IgG. *Immunochemistry*, **7**, 703-708.

Warmerdam, P. A. M., van de Winkel, J. G. J., Gosselin, E. J. and Capel, P. J. A. (1990). Molecular basis for a polymorphism of human Fcγ receptor II (CD32). *Journal of Experimental Medicine*, **172**, 19-27.

Warmerdam, P. A. M., van de Winkel, J. G. J., Vlug, A., Westerdaal, N. A. C. and Capel, P. J. A. (1991). A single amino acid in the second immunoglobulin-like domain of the human Fcγ receptor II is critical for human IgG$_2$ binding. *Journal of Immunology*, **147**, 1338-1343.

Wasz-Höckert, O., Wager, O., Hautala, T. and Widholm, O. (1956). Transmission of antibodies from mother to foetus. A study of diphtheria level in the newborn with oesophageal atresia. *Annales Medicinae Experimentalis Biologiae Fenniae*, **34**, 444-446.

Wehland, J., Willingham, M. C., Dickson, R. and Pastan, I. (1981). Microinjection of anticlathrin antibodies into fibroblasts does not interfere with the receptor-mediated endocytosis of α2 macroglobulin. *Cell*, **25**, 105-119.

Weibull, C., Christiansson, A. and Carlemalm, E. (1983a). Extraction of membrane lipids during fixation, dehydration and embedding of *Acholeplasma laidawii* cells for electron microscopy. *Journal of Microscopy*, **129**, 201-207.

Weibull, C., Villiger, W. and Carlemalm, E. (1983b). Extraction of lipids during freeze-substitution of *Acholeplasma laidawii* for electron microscopy. *Journal of Microscopy*, **134**, 213-216.

West, M. A., Lucocq, J. M. and Watts, C. (1994). Antigen processing and class II MHC peptide-loading compartments in human B-lymphoblastoid cells. *Nature*, **369**, 147-151.

White, J. G. and Amos, W. B. (1987). Confocal microscopy comes of age. *Nature*, **328**, 183-184.

Wilchek, M. and Bayer, E. A. (1984). The avidin-biotin complex in immunology. *Immunology Today*, **5**, 39-43.

Wild, A. E. (1960). Proteins of the liquor amnii. *British Medical Journal*, **1**, 802.

Wild, A. E. (1976). Mechanism of protein transport across the rabbit yolk sac endoderm. In *'Maternofoetal transmission of immunoglobulins'*, (Ed. W. A. Hemmings), pp. 155-167. Cambridge University Press, New York.

Wileman, T., Harding, C. and Stahl, P. (1985). Review article: Receptor mediated endocytosis. *Biochemical Journal*, **232**, 1-14.

Williams, A. F. and Barclay, A. N. (1988). The immunoglobulin superfamily: Domains for cell surface recognition. *Annual Review of Immunology*, **6**, 381-405.

Willingham, M. C. and Pastan, I. (1980). The receptosome an intermediate organelle of receptor-mediated endocytosis in cultured fibroblasts. *Cell*, **21**, 67-77.

Willingham, M. C. and Pastan, I. (1981). The morphologic pathway of receptor mediated endocytosis in cultured fibroblasts. In *'Cellular controls in differentiation'*, (Eds. C. W. Lloyd and D. A. Rees), pp. 59-78. Academic Press, London.

Wislocki, G. B. and Dempsey, E. W. (1965). Electron microscopy of the placenta. *Anatomical Record*, **123**, 133-149.

Wood, G. W., Bjerrum, K. and Johnson, B. (1982). Detection of IgG bound within human trophoblast. *Journal of Immunology*, **129**, 1479-1484.

Wood, G. W., Johnson, B., Halsey, J. F. and King, C. R. (1983). Expression of Fc gamma binding sites on human extraplacental membranes. *American Journal of Reproductive Immunology*, **4**, 21-26.

Wynn, R. M. (1967). Derivation and ultrastructure of the so-called Hofbauer cells. *American Journal of Obstetrics and Gynaecology*, **97**, 235-248.

Wynn, R. M. and French, G. L. (1968). Comparative ultrastructure of the mammalian amnion. *Obstetrics and Gynaecology*, **31**, 759-774.

Wynn, R. M. (1975). Fine structure of the placenta. In *'The placenta and its maternal supply line'* (Ed. P. Gruenwald), pp. 56-79. Medical and technical publishing Co. Ltd., Lancaster.

Yoshida, Y. (1964). Ultrastructural and secretory function of the syncytial trophoblast of human placenta in early pregnancy. *Experimental Cell Research*, **34**, 305-317.

Zaccheo, D., Pistoia, V., Castellucci, M. and Martinoli, C. (1989). Isolation and characterisation of Hofbauer cells from human placental villi. *Archives of Gynaecology and Obstetrics*, **246**, 189-200.

Zak, S. J. and Good, R. A. (1959). Immunochemical studies of human serum gamma-globulin. *Journal of Clinical Investigation*. 38, 579-586.

Zander, J. (1964). Progesterone in human blood and tissues. *Nature*, 174, 406-407.

Publications submitted in support of the thesis:

Abstracts.

1) Abdel-Malak, T. M., Ockleford, C. D., Hubbard, A., Bright, N., Bell, S. C., Mulholland, G., Dalgleish, R. and Macvicar, J. (1992). Confocal immunofluorescent and ultrastructural study of extracellular matrix collagens of human fetal amniochorionic membranes. *Proceedings of the 5th international congress on cell biology,* 182.

2) Bright, N. A., Ockleford, C. D. and Anwar M. (1992). Immunocytochemical localisation of endogenous IgG and 3 subtypes of Fcγ receptor in the chorionic villi of term and immature human placentae. *Proceedings of the 5th international congress on cell biology,* 142.

3) Bright, N., Ockleford, C. and Anwar, M. (1992). The localisation of Fcγ receptors and immunoglobulin G in human chorionic villi. *Placenta,* 13, A7.

4) Ockleford, C. D., Abdel-Malak, T., Hubbard, A., Braken, K., Burton, S. -A., Bright, N. and d'Lacey, C. (1992). Localisation of cytoskeletal components of amnion and chorion in human fetal membranes at full term. *Proceedings of the 5th international congress on cell biology,* 298.

5) Bright, N. A. and Ockleford, C. D. (1993). Fcγ receptor-bearing cells in human term amniochorion. *Journal of Anatomy,* 183, 187-188.

6) Bright, N. A. and Ockleford, C. D. (1993). Expression of Fcγ receptors by cells of the human amniochorion. *Placenta,* 14, A7.

7) Ockleford, C. D., McCracken, S. A., Rimmington, L. A., Hubbard, A. R. D., Bright, N. A., Jefferson, T. B. and d'Lacey, C. (1993). Vertical integration of amnion layers by type VII collagen rivets. *Journal of Pathology,* 170 (Suppl), 44.

8) Ockleford, C. D., Abdel-Malak, T., Hubbard, A., Braken, K., Burton, S.-A., Bright, N., Blakey, G., Goodliffe, J., Garrod, D. and d'Lacey, C. (1993). Human amniochorion cytoskeletons at term. *Placenta,* 14, A56.

9) Ockleford, C. D., McCracken, S. A., Rimmington, L. A., Hubbard, A. R. D., Bright, N. A., Jefferson, T. B. and d'Lacey, C. (1994). Type IV collagen may integrate amnion layers by association with type VII collagen rivets. *Journal of Anatomy,* 184, 191.

10) Byrd, N. A., Bright, N. A. and Ockleford, C. D. (1994). Dual channel localisation of α6β4 integrin and type VII collagen in human term amniochorion. *Journal of Anatomy,* In the press.

Refereed papers in primary journals.

1) Malak, T. M., Ockleford, C. D., Bell, S. C., Dalgleish, R., Bright, N. and Macvicar, J. (1993). Confocal immunofluorescence localisation of collagen types I, III, IV, V and VI and their ultrastructural organisation in human fetal membranes. *Placenta,* 14, 385-406.

2) Ockleford, C., Malak, T., Hubbard, A., Braken, K., Burton, S. -A., Bright, N., Blakey, G., Goodliffe, J., Garrod, D. and d'Lacey, C. (1993). Confocal and conventional immunofluorescence and ultrastructural localisation of intracellular strength giving components of human amniochorion. *Journal of Anatomy,* 183, 483-505.

3) Ockleford, C., Bright, N., Hubbard, A., d'Lacey, C., Smith, J., Gardiner, L., Sheikh, T., Albentosa, M. and Turtle, K. (1993). Micro-trabeculae, macroplaques or mini-basement membranes in human term fetal membranes? *Philosophical Transactions of the Royal Society of London Series B, Biological Sciences*, 342, 121-136.

4) Bright, N. A., Ockleford, C. D. and Anwar, M. (1994). Ontogeny and distribution of Fcγ receptors in the human placenta. Transport or immune surveillance? *Journal of Anatomy*, 184, 297-308.

5) Bright, N. A. and Ockleford, C. D. (1994). Heterogeneity of Fcγ receptor bearing cells in human term amniochorion. *Placenta*, 15, 247-255.

6) Bright, N. A. and Ockleford, C. D. (1994). Cytotrophoblast cells. A barrier to maternofetal transmission of passive immunity? *Journal of Histochemistry and Cytochemistry*, submitted for publication.

7) Ockleford, C. D., Bright, N. A., Hubbard, A. R. D., McCracken, S. A., Rimmington, L. A., Byrd, N. A., Byrne, S., Cockcroft, N., Jefferson, T. B. and d'Lacey, C. (1994). Type VII collagen associated with the basement membrane of a simple epithelium produces giant anchoring rivets which penetrate a massive lamina reticularis. In revision.

8) Bright, N. A. and Ockleford, C. D. Immunogold localisation of endogenous IgG in ultrathin frozen sections of human term amniochorion. In preparation.